Advances in High Energy Physics

Dark Atoms and Dark Radiation

Guest Editors: Maxim Khlopov, Konstantin Belotsky, Jean-René Cudell, and Chris Kouvaris

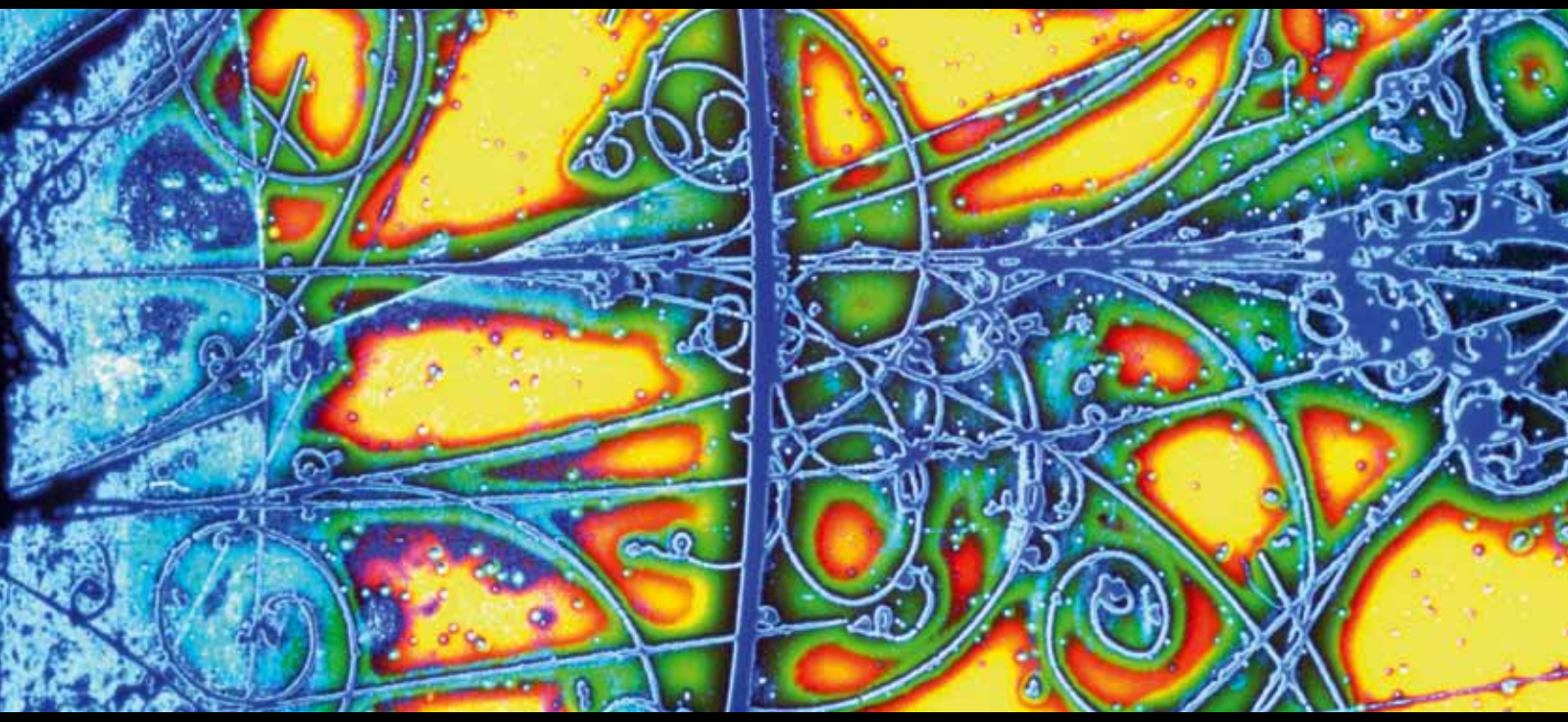

Dark Atoms and Dark Radiation

Advances in High Energy Physics

Dark Atoms and Dark Radiation

Guest Editor: Maxim Khlopov, Konstantin Belotsky, Jean-René Cudell, and Chris Kouvaris

Editorial Board

Contents

Hindawi Publishing Corporation
Advances in High Energy Physics
Volume 2014, Article ID 913856, 2 pages
http://dx.doi.org/10.1155/2014/913856

Editorial

Dark Atoms and Dark Radiation

Maxim Khlopov,[1,2,3] Konstantin Belotsky,[1,2] Jean-René Cudell,[4] and Chris Kouvaris[5]

[1] *National Research Nuclear University MEPHI (Moscow Engineering Physics Institute), Moscow 115409, Russia*
[2] *Centre for Cosmoparticle Physics "Cosmion", Moscow 115409, Russia*
[3] *APC Laboratory, 10 rue Alice Domon et Léonie Duquet, 75205 Paris Cedex 13, France*
[4] *IFPA, Département AGO, Université de Liège, Sart-Tilman, 4000 Liège, Belgium*
[5] *CP[3]-Origins, University of Southern Denmark, Campusvej 55, 5230 Odense, Denmark*

Correspondence should be addressed to Maxim Khlopov; khlopov@apc.univ-paris7.fr

Received 5 May 2014; Accepted 5 May 2014; Published 4 June 2014

Modern astronomical observations prove that dark matter and dark energy are the bedrocks of the modern theory of the universe. These phenomena cannot be grounded in the known laws of physics and they call for hypothetical new particles and fields predicted by extensions of the standard model of particle physics. In the context of cosmology, dark matter stems from the processes in the early universe that create this new form of matter, which is then sufficiently stable to survive to the present day. In the context of particle theory, the stability of dark matter implies new conservation laws, resulting from new fundamental symmetries.

The simplest candidates for dark matter, such as neutral weakly interacting massive particles (WIMPs), have difficulty explaining the results of direct and indirect experimental searches for dark matter particles as well as the astronomical observations of dark matter distribution and structure. This is why a wide variety of other solutions for the dark matter problem are being considered and composite dark matter, made of dark atoms, is of special interest among them, challenging both experimental studies and theoretical research.

We have invited investigators to contribute original research and review articles that seek to define the possible physical nature of composite dark matter and its constituents, to stimulate the experimental searches and to suggest astrophysical tests for their effects. The collected papers in this special issue represent only a first small step in the approach to the thorough investigation of the topic of dark atoms and dark radiation, demonstrating the wide but far from complete variety of possible aspects of this problem.

The papers in this volume discuss dark atom candidates from black-hole or mini-black-hole bound systems to atom-like bound states of new stable electrically charged particles. Pending on their type, dark atom constituents may be bound by ordinary Coulomb interaction, mirror electromagnetism, gravitation, or some new forces. Even if dark atoms act on ordinary matter through its gravity only, as is the case for mirror matter or black holes, their presence in the universe can lead to observable consequences. The signatures of their presence can be probed in the studies of cosmic rays and gamma radiation, if these constituents possess electric charge or can decay to ordinary charged particles. In particular, the excessive intensity of the positron annihilation line in the galactic bulge, observed by INTEGRAL, can find explanation by deexcitation of dark atoms, colliding in the central part of the galaxy. Dark atom content may be multicomponent and the existence of even a strongly subdominant dark atom component can be probed in direct and indirect dark matter searches. Moreover, in the present issue, a possibility to explain the excess of cosmic high-energy positrons, observed by PAMELA, FERMI-LAT, and AMS02, via decays of metastable doubly charged dark atom constituents has been proposed. Such a possibility implies a restricted range of masses for (meta) stable doubly charged particles, challenging accelerator searches.

Acknowledgment

We thank all the authors for their contributions to the present issue and express the hope that its publication will stimulate further extensive discussion of this exciting topic.

Maxim Khlopov
Konstantin Belotsky
Jean-René Cudell
Chris Kouvaris

Hindawi Publishing Corporation
Advances in High Energy Physics
Volume 2014, Article ID 651247, 6 pages
http://dx.doi.org/10.1155/2014/651247

Research Article

Gamma-Ray Effects of Dark Forces in Dark Matter Clumps

K. Belotsky,[1,2] M. Khlopov,[1,2,3] and A. Kirillov[1,2]

[1] *National Research Nuclear University "MEPhI", Moscow 115409, Russia*
[2] *Centre for Cosmoparticle Physics "Cosmion", Moscow 115409, Russia*
[3] *APC Laboratory, 10 rue Alice Domon et Léonie Duquet, 75205 Paris Cedex 13, France*

Correspondence should be addressed to A. Kirillov; kirillov-aa@yandex.ru

Received 28 October 2013; Revised 20 December 2013; Accepted 2 April 2014; Published 23 April 2014

Academic Editor: Jean-René Cudell

Existence of new gauge U(1) symmetry possessed by dark matter (DM) particles implies the existence of a new Coulomb-like interaction, which leads to Sommerfeld-Gamow-Sakharov enhancement of dark matter annihilation at low relative velocities. We discuss a possibility to put constraints on such dark forces of dark matter from the observational data on the gamma radiation in our Galaxy. Gamma-rays are supposed to originate from annihilation of DM particles in the small scale clumps, in which annihilation rate is supposed to be enhanced, besides higher density, due to smaller relative velocities v of DM particles. For possible cross sections, mass of annihilating particles, masses of clumps, and the contribution of annihilating particles in the total DM density we constrain the strength of new dark long range forces from comparison of predicted gamma-ray signal with Fermi/LAT data on unidentified point-like gamma-ray sources (PGS) as well as on diffuse γ-radiation. Both data on diffuse radiation and data on PGS put lower constraints on annihilation cross section at any dark interaction constant, where diffuse radiation provides stronger constraint at smaller clump mass. Density of annihilating DM particles is conventionally supposed to be defined by the frozen annihilation processes in early Universe.

1. Introduction

From the first articles revealing the indirect effects of the cold dark matter (CDM) in the form of heavy neutral leptons [1–8] or supersymmetric particles [7, 9, 10], indirect effects of dark matter annihilation had been the subject of intensive studies in the data on the cosmic rays (CR) and gamma radiation. In the CDM scenario DM particles could form the hierarchic structures over a wide range of scales and masses (from small scale clumps to large scale structures) [11–16]. The annihilation rate of DM particles within these clumpy structures, giving rise to cosmic ray signals [4–8, 17–25], should be enhanced due to higher density of DM particles in them, as compared with their averaged density in the Galaxy. The annihilation cross section can be also enhanced at small relative velocities of DM particles, which are especially small in the lightest clumps, which are likely to be the most abundant. Due to these factors the clumps, located in a neighborhood of Solar System, can be observed as discrete (basically point-like) gamma-ray sources [19, 21, 26–33], while the overall effect of such clumps should increase the diffuse gamma background in the Galaxy.

In this paper we address the sensitivity of the given effect [31–33] to the existence of long range dark forces originated from new U(1) gauge charges, which annihilating dark matter particles possess. Coulomb-like interaction (we will refer to it as "y-interaction") of these U(1) charges leads to Sommerfeld-Gamow-Sakharov (SGS) enhancement of particle annihilation at low relative velocities. Since small scale clumps of dark matter have small gravitational potential, the relative velocities of particles, annihilating within these clumps, are much smaller than those of unclumped particles in the galactic halo, which enhances the sensitivity of both the data on the discrete gamma-ray sources and the data on the diffuse γ-radiation to the effects of the dark forces in dark matter annihilation.

One should note that effects of DM annihilation enhancement due to new interaction were first considered in [34, 35] and then in many successive papers, for example, [36–40]. In most of these papers SGS enhancement was mainly

studied for the case of dominant form of DM that possesses new interaction with massive carrier, and the effect of this enhancement for point-like gamma-ray sources, treated in the present work, was not considered.

The existence of new U(1) gauge symmetry implies the existence of the corresponding massless dark photons. They can increase the effective number of relativistic species at the radiation dominated stage. Decoupling of such photons from the plasma in the early Universe takes place in the period of freezing out of the CDM particles, which makes this contribution compatible with the measurements of the effective number of the neutrino species (see, e.g., [41] for review and references).

Note that new interaction can lead to binding of DM particles into atomic-like states with their successive annihilation [41], or stable dark atoms in case of multicomponent (charge asymmetric) DM [41–43]. This effect, going beyond the scope of the present work, deserves separate consideration.

2. Gamma-Ray Signal from y-Interacting DM Clumps

In calculations of gamma-ray signals from the clump in this paper we follow our previous work [31–33]. For density profile inside the clumps we use profile BGZ obtained in [19, 21, 26], which gives the minimal estimation of the γ-flux from the clump [31–33]. Fraction $\xi = 0.002$ from total density of surrounding DM is taken for the clumps that survived until present time. We study γ-radiation effect for only minimal clump mass, formally assuming that all DM clumps are with this mass. According to theoretical estimates consistent with observations, the small mass clumps are predicted to be the most abundant [19, 21, 44]. However, the following merging and formation of the high-mass clumps (subhalos) lead to the transformation of the mass distribution and the subhalos effect can be also noticeable [45], but the picture does not change a lot.

To cover a wide class of models of DM particles, we parametrize their annihilation cross section as follows:

$$\sigma_{\text{ann}} = \frac{\sigma_0}{v} \times C(v, \alpha), \tag{1}$$

with v being relative velocity of annihilating DM particle and antiparticle. Parameter σ_0 is determined by cosmological density of the particles Ω. The factor $C(v, \alpha)$ takes explicitly into account a possible Coulomb-like y-interaction of DM particles, which leads to a Sommerfeld-Gamow-Sakharov enhancement [46–48] and has the form

$$C(v, \alpha) = \frac{2\pi\alpha/v}{1 - \exp(-2\pi\alpha/v)}. \tag{2}$$

Here α is the fine structure constant of additional interaction.

One should note that y-interaction not only implies SGS enhancement of the annihilation cross section but also leads to the existence of new channels that involve y-photons in the final state. The corresponding suppression of the branching ratio for ordinary photon production is effectively taken into account in our calculations by a multiplicity of produced photons, N_γ (see below).

The enhancement (2) of the annihilation cross section may lead to decrease of the frozen out density of DM particles. However in the period of their freezing out in the early Universe the particles were semirelativistic (with typical velocities $v \sim c/5$) so that relic density cannot decrease significantly. Effect of annihilation of DM particles in massless bosons of y-interaction (y-photons) not only needs in general special study in the framework of particular models of DM particles but it also cannot strongly increase the annihilation cross section (and correspondingly decrease the relic abundance) taking into account all the other possible annihilation channels.

In the modern Universe, when the particle velocities are nonrelativistic, factor (2) may significantly enhance the annihilation effects [49–52]. Such effects become noticeable even for a subdominant component with $\Omega \ll \Omega_{\text{CDM}}$ as it takes place in case of heavy stable neutrinos with y-interaction [53]. Therefore we suppose that an active (annihilating) component of DM may be both dominant and subdominant; that is, $\Omega \leq \Omega_{\text{CDM}}$ with $\Omega_{\text{CDM}} \sim 0.2$ being the total relative density of cold dark matter in Universe. In estimation of cosmological density Ω we follow the standard approach [54, 55].

It is worth noting that the given scheme does not take into account possibility of binding pairs of considered particle-antiparticle due to y-interaction. If nonrelativistic DM particles are decoupled from the ambient plasma, their rapid cooling can strongly enhance the rate of such recombination that may exceed the expansion rate due to high recombination cross section. This process leads inevitably to annihilation and it may strongly suppress the abundance of these DM particles [35].

Since the Coulomb-like y-interaction is excluded for Majorana particles (in fact, ordinary Majorana mass term implies violation of U(1) gauge symmetry of y-interaction which is inconsistent with its long range nature (existence of massless dark photons)), it is assumed in our estimations that the considered DM particles are Dirac particles with mass $m \sim 100$ GeV. If annihilating DM particles do not constitute all DM ($\Omega < \Omega_{\text{CDM}}$), then their contribution to density of clumps is assumed to be proportional to $\Omega/\Omega_{\text{CDM}}$ (4). We do not specify annihilation channel of photon production, assuming that their averaged multiplicity for energy $E_\gamma > 100$ MeV is $N_\gamma = 10$. It is quite typical value for high energy processes at respective energy release.

The photon flux at distance l from the clump centre is given by

$$F = \frac{P}{4\pi l^2} = \frac{N_\gamma}{4\pi l^2} \int_V \langle \sigma_{\text{ann}} v \rangle \, n\overline{n} \, dV, \tag{3}$$

where the particles/antiparticles number density is

$$n = \overline{n} = \frac{1}{2} \frac{\rho(r)}{m} \times \frac{\Omega}{\Omega_{\text{CDM}}}. \tag{4}$$

Note that the fraction of subdominant DM particles should be suppressed in the clumps of mass $M < M_{\text{min}}$, where M_{min}

is the minimal mass which could be formed by considered DM particles if they prevailed in density. In our study we do not take into account this. The value $\langle\sigma_{\text{ann}}v\rangle$ is determined by averaging over velocity distribution of DM particles inside the clump, assumed to be Maxwellian one with the "virial" temperature $T_{\text{vir}} = GMm/2R$.

LAT registers γ-radiation with energy $E_\gamma > 100$ MeV [56] and the flux $> F_{\min} \approx 3 \times 10^{-9}\,\text{cm}^{-2}\text{sec}^{-1}$. The value $F_{\min}$ determines the maximal distance $l_{\max}$ at which the clump can be registered as γ-source. It gives for chosen profile $l_{\max} \sim 10^{-5}$ pc for $\sigma_0 = 10^{-35}\,\text{cm}^2$ and $10^{-10}M_\odot$ without y-interaction and $l_{\max} \sim 1$ pc with y-interaction and the same parameters. The last magnitude corresponds to $\alpha \sim 10^{-2}$ and changes as $\propto \sqrt{\alpha}$ for $\alpha \ll 10^{-2}$ and $\propto 1/\sqrt{\alpha}$ for $\alpha \gg 10^{-2}$. All the obtained $l_{\max} \ll$ Galactic size, which justifies assumption that clump number density $n_{\text{cl}} \approx$ const and corresponds to the local one. So

$$n_{\text{cl}} = \frac{\xi\rho_{\text{loc}}}{M} \approx 1.6 \times 10^{-5}\frac{M_\odot}{M}\text{pc}^{-3}, \tag{5}$$

where $\rho_{\text{loc}} = 0.3\,\text{GeV/cm}^3$. The number of clumps which may be detected by LAT is

$$N_{\text{cl}} = n_{\text{cl}} \times \frac{4}{3}\pi l_{\max}^3. \tag{6}$$

Note that the given results turn out to be independent of M. It is not so for other laws of velocity dependence of cross section [31–33].

The analogous results for some other profile models are given in [33].

Since the clumps at distance $l < l_{\max}$ are expected to be distributed homogeneously, we can try to explain by them only isotropic component of unidentified PGS registered by Fermi LAT [57]. It includes ~100 sources. From this, respective regions of the parameters α and σ_0 for the typical clump masses $10^{-10} \div 10^{-6}M_\odot$ [22] are obtained. The results are shown at Figure 1. Note that unidentified PGS data also allow another application to the exotic physics [58, 59].

The distant clumps situated at $l > l_{\max}$ should contribute to the diffuse γ-radiation. γ-flux from them per given solid angle can be expressed as

$$\Phi = \int_{l_{\max}}^{l_{\text{halo}}} Fn_{\text{cl}}l^2 dl = \frac{Pn_{\text{cl}}l_{\text{halo}}^{\text{eff}}}{4\pi}, \tag{7}$$

where F and P are introduced in (3), l_{halo} is the distance to the edge of halo along line of sight, and $l_{\text{halo}}^{\text{eff}} \approx 10\,\text{kpc}$ is its effective value (typical for many halo density profiles (for direction opposite Galactic center (where flux is more relevant to be compared with extracted by Fermi/LAT isotropic component of gamma background) this value varies from 6 to 11 kpc depending on profile and is almost insensitive to $l_{\max}$)); $l_{\max}$ is negligible with respect to l_{halo}. One requires that

$$\Phi < \Phi_{\text{exp}} \approx 1.5 \times 10^{-5}\,\text{cm}^{-2}\text{s}^{-1}\text{sr}^{-1}, \tag{8}$$

where Φ_{exp} is the diffuse γ-background measured by LAT [60]. It puts, as in the case of PGS, the lower constraint

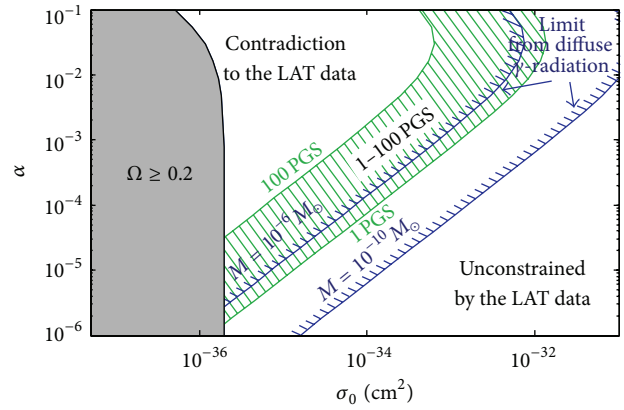

Figure 1: Allowed and forbidden regions of parameters α and σ_0 are shown as they are obtained on the base of Fermi LAT data on PGS and diffuse γ-radiation.

on cross section parameter σ_0 and upper constraint on parameter α, which are also plotted on Figure 1. It follows from these constraints that the possibility to have PGS for clump mass $M = 10^{-10}M_\odot$ is completely ruled out, while such possibility for $M = 10^{-6}M_\odot$ is constrained but up to ~10 PGS is still possible. Higher masses of clumps avoid these restrictions.

As to the parameters σ_0 and α, the ranges $3 \times 10^{-36} \lesssim \sigma_0 \lesssim 10^{-32}\,\text{cm}^2$ and $10^{-6} \lesssim \alpha \lesssim 10^{-1}$ are found to be the most interesting (Figure 1). Note that given range virtually excludes considerable contribution into σ_0 of the annihilation channel into y-photons. In fact if DM particles are $s = 1/2$ Dirac particles, then this contribution is $\pi\alpha^2/m^2$ being much less than the obtained region of σ_0.

The obtained results can be generalized for a case of arbitrary values of the used parameters by multiplying σ_0 on Figure 1 by ζ:

$$\zeta = \left(\frac{m}{100\,\text{GeV}}\right)^2\left(\frac{\Omega_{\text{CDM}}}{0.2}\right)^2\left(\frac{10}{N_\gamma}\right) \times \left(\frac{F_{\min}}{3 \times 10^{-9}\,\text{cm}^{-2}\text{sec}^{-1}}\right)\left(\frac{0.002}{\xi}\right)^{2/3}. \tag{9}$$

Effects of DM annihilation during period of the recombination of hydrogen can put constraints on the parameters of y-interaction. However, this question should be considered along with effects of DM recombination which might help to escape these constraints, which is out of the scope of the present paper.

It is interesting to note that one of the subdominant dark matter candidates, heavy neutrinos ν_4 with y-interaction, can explain a part of unidentified point-like LAT sources due to $\nu_4\overline{\nu}_4$-annihilation with mass $m_{\nu_4} \sim 46$–49 GeV [31–33]. At Figure 2 a typical γ-spectrum from 47 GeV neutrinos annihilation is shown in comparison with measured spectrum of one of the nonidentified PGS (annihilation spectrum was obtained with the help of Monte-Carlo generator Pythia

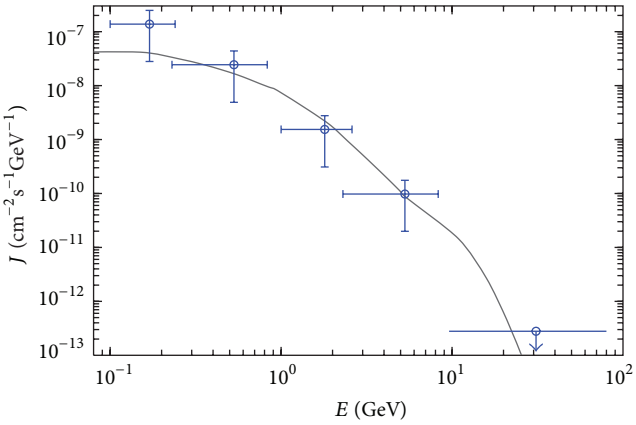

FIGURE 2: Expected spectrum from $\nu_4\bar{\nu}_4$-annihilation is shown for $m_{\nu_4} = 47$ GeV in comparison with the observed spectrum of unidentified source 2FGL J1653.6-0159.

6.4 [61]). However, one should take into account that the heavy neutrino parameters are strongly restricted by underground experiments [53, 62], and the predicted ν_4 relic density suffers with an uncertainty related with their possible annihilation due to recombination of the γ-interacting neutrinos and antineutrinos after their freezing out in the early Universe [53].

3. Conclusion

In this paper we apply the approach developed earlier in our analysis of γ-radiation from annihilation of dark matter in clumps [31–33] to the case of new U(1) symmetry and put constraints on the parameters of the corresponding dark force from the data on discrete gamma sources and gamma background. We have shown that DM clumps in vicinity of the Solar System could be observed as point-like sources of the γ-radiation and they can partially explain unidentified γ-sources, registered by LAT. Effects of DM annihilation in more distant clumps contribute to the diffuse gamma background and this contribution strongly depends on the minimal mass of the clumps. The smaller the mass of clumps the stronger the effect of Sommerfeld-Gamow-Sakharov enhancement of the annihilation rate so that the observational data on γ-background and on the unidentified point-like γ-sources provide constraints on the strength of the Coulomb-like dark force.

These constraints are highly sensitive to the choice of a density profile inside the clump and are obtained for the most "conservative" BGZ [21] model. It should be also noted that the suppression of the subdominant fraction of DM particles in clumps of mass $M < M_{\min}$ has not been taken into account and requires special study. In addition the extragalactic clumps should give contribution in diffuse radiation, strengthening the constraint somewhat [63], while observational limits on γ-flux from separate galaxies or their clusters may become evaded [64].

Conflict of Interests

The authors declare that there is no conflict of interests regarding the publication of this paper.

Acknowledgments

The authors express gratitude to V. Dokuchaev and Yu. Eroshenko for useful discussion of clump evolution. The work of A. Kirillov was supported by Grant of RFBR no. 14-02-31417.

References

[1] B. W. Lee and S. Weinberg, "Cosmological lower bound on heavy-neutrino masses," *Physical Review Letters*, vol. 39, no. 4, pp. 165–168, 1977.

[2] D. A. Dicus, E. W. Kolb, and V. L. Teplitz, "Cosmological upper bound on heavy-neutrino lifetimes," *Physical Review Letters*, vol. 39, no. 4, pp. 168–171, 1977.

[3] D. A. Dicus, E. W. Kolb, and V. L. Teplitz, "Cosmological implications of massive, unstable neutrinos," *The Astrophysical Journal*, vol. 221, pp. 327–341, 1978.

[4] J. E. Gunn, B. W. Lee, I. Lerche, D. N. Schramm, and G. Steigman, "Some astrophysical consequences of the existence of a heavy stable neutral lepton," *The Astrophysical Journal*, vol. 223, pp. 1015–1031, 1978.

[5] F. W. Stecker, "The cosmic gamma-ray background from the annihilation of primordial stable neutral heavy leptons," *The Astrophysical Journal*, vol. 223, pp. 1032–1036, 1978.

[6] Ya. B. Zeldovich, A. A. Klypin, M. Yu. Khlopov, and V. M. Chechetkin, "Astrophysical restrictions of the heavy stable neutral leptons mass," *Yadernaya Fizika*, vol. 31, pp. 1286–1294, 1980.

[7] J. Silk and M. Srednicki, "Cosmic-ray antiprotons as a probe of a photino-dominated universe," *Physical Review Letters*, vol. 53, no. 6, pp. 624–627, 1984.

[8] R. V. Konoplich and M. Yu. Khlopov, "Astrophysical constraints on the mass of very heavy stable neutrinos," *Physics of Atomic Nuclei*, vol. 57, pp. 425–431, 1994.

[9] F. W. Stecker, S. Rudaz, and T. F. Walsh, "Galactic antiprotons from photinos," *Physical Review Letters*, vol. 55, no. 23, pp. 2622–2625, 1985.

[10] S. Rudaz and F. W. Stecker, "Cosmic-ray antiprotons, positrons, and gamma rays from halo dark matter annihilation," *The Astrophysical Journal*, vol. 325, pp. 16–25, 1988.

[11] J. E. Gunn, "Massive galactic halos. I—formation and evolution," *The Astrophysical Journal*, vol. 218, pp. 592–598, 1977.

[12] S. D. M. White and M. J. Rees, "Core condensation in heavy halos: a two-stage theory for Galaxy formation and clustering," *Monthly Notices of the Royal Astronomical Society*, vol. 183, pp. 341–358, 1978.

[13] P. J. E. Peebles, "Large-scale background temperature and mass uctuations due to scale-invariant primeval perturbations," *The Astrophysical Journal*, vol. 263, pp. L1–L5, 1982.

[14] G. R. Blumenthal, H. Pagels, and J. R. Primack, "Galaxy formation by dissipationless particles heavier than neutrinos," *Nature*, vol. 299, no. 5878, pp. 37–38, 1982.

[15] G. R. Blumenthal, S. M. Faber, J. R. Primack, and M. J. Rees, "Formation of galaxies and large-scale structure with cold dark matter," *Nature*, vol. 311, no. 5986, pp. 517–525, 1984.

[16] A. V. Gurevich and K. P. Zybin, "Large-scale structure of the Universe. Analytic theory," *Physics-Uspekhi*, vol. 38, no. 7, pp. 687–722, 1995.

[17] J. Ellis, R. A. Flores, K. Freese, S. Ritz, D. Seckel, and J. Silk, "Cosmic ray constraints on the annihilations of relic particles in the galactic halo," *Physics Letters B*, vol. 214, no. 3, pp. 403–412, 1988.

[18] M. Kamionkowski and M. S. Turner, "Distinctive positron feature from particle dark-matter annihilations in the galatic halo," *Physical Review D*, vol. 43, no. 6, pp. 1774–1780, 1991.

[19] V. S. Berezinsky, A. V. Gurevich, and K. P. Zybin, "Distribution of dark matter in the galaxy and the lower limits for the masses of supersymmetric particles," *Physics Letters B*, vol. 294, no. 2, pp. 221–228, 1992.

[20] A. V. Gurevich and K. P. Zybin, "The mass of cold dark matter particles and microlensing," *Physics Letters A*, vol. 208, no. 4–6, pp. 276–280, 1995.

[21] V. Berezinsky, V. Dokuchaev, and Y. Eroshenko, "Small-scale clumps in the galactic halo and dark matter annihilation," *Physical Review D*, vol. 68, no. 10, Article ID 103003, 19 pages, 2003.

[22] J. Diemand, B. Moore, and J. Stadel, "Earth-mass dark-matter haloes as the first structures in the early Universe," *Nature*, vol. 433, no. 7024, pp. 389–391, 2005.

[23] L. Pieri, E. Branchini, and S. Hofmann, "Difficulty of detecting minihalos via γ rays from dark matter annihilation," *Physical Review Letters*, vol. 95, no. 21, Article ID 211301, 2005.

[24] J. Diemand, M. Kuhlen, and P. Madau, "Early supersymmetric cold dark matter substructure," *Astrophysical Journal Letters*, vol. 649, no. 1, pp. 1–13, 2006.

[25] L. Pieri, G. Bertone, and E. Branchini, "Dark matter annihilation in substructures revised," *Monthly Notices of the Royal Astronomical Society*, vol. 384, no. 4, pp. 1627–1637, 2008.

[26] A. V. Gurevich, K. P. Zybin, and V. A. Sirota, "Small-scale structure of dark matter and microlensing," *Physics-Uspekhi*, vol. 40, no. 9, pp. 869–898, 1997.

[27] S. M. Koushiappas, "Proper motion of gamma rays from microhalo sources," *Physical Review Letters*, vol. 97, no. 19, Article ID 191301, 2006.

[28] M. R. Buckley and D. Hooper, "Dark matter subhalos in the Fermi first source catalog," *Physical Review D*, vol. 82, no. 6, Article ID 063501, 2010.

[29] A. V. Belikov, M. R. Buckley, and D. Hooper, "Searching for dark matter subhalos in the Fermi-LAT second source catalog," *Physical Review D*, vol. 86, no. 4, Article ID 043504, 2012.

[30] H.-S. Zechlin and D. Horns, "Unidentified sources in the Fermi-LAT second source catalog: the case for DM subhalos," *Journal of Cosmology and Astroparticle Physics*, vol. 11, p. 50, 2012.

[31] K. M. Belotsky, A. A. Kirillov, and M. Yu. Khlopov, "Astrophysical manifestations of clumps of cold dark matter," *Physics of Atomic Nuclei*, vol. 76, no. 4, pp. 469–475, 2013.

[32] K. M. Belotsky, A. A. Kirillov, and M. Y. Khlopov, "Astrophysical manifestations of clumps of cold dark matter," *Yadernaya Fizika*, vol. 76, pp. 506–512, 2013.

[33] K. M. Belotsky, A. A. Kirillov, and M. Y. Khlopov, "Gamma-ray evidences of the dark matter clumps," *Gravitation and Cosmology*, vol. 20, pp. 47–54, 2014.

[34] K. M. Belotsky, M. Yu. Khlopov, and K. I. Shibaev, "Sakharov's enhancement in the effect of 4th generation neutrino," *Gravitation and Cosmology*, vol. 6, supplement 6, pp. 140–143, 2000.

[35] M. B. Konstantin, M. Yu. Khlopov, S. V. Legonkov, and K. I. Shibaev, "Effects of a new long-range interaction: recombination of relic heavy neutrinos and antineutrinos," *Gravitation and Cosmology*, vol. 11, pp. 27–33, 2005.

[36] K. N. Abazajian and J. P. Harding, "Constraints on WIMP and Sommerfeld-enhanced dark matter annihilation from HESS observations of the galactic center," *Journal of Cosmology and Astroparticle Physics*, vol. 2012, no. 1, article 041, 2012.

[37] T. R. Slatyer, N. Toro, and N. Weiner, "Sommerfeld-enhanced annihilation in dark matter substructure: consequences for constraints on cosmic-ray excesses," *Physical Review D*, vol. 86, no. 8, Article ID 083534, 18 pages, 2012.

[38] L. G. van den Aarssen, T. Bringmann, and Y. C. Goedecke, "Thermal decoupling and the smallest subhalo mass in dark matter models with Sommerfeld-enhanced annihilation rates," *Physical Review D*, vol. 85, no. 12, Article ID 123512, 20 pages, 2012.

[39] C. Armendariz-Picon and J. T. Neelakanta, "Structure formation constraints on Sommerfeld-enhanced dark matter annihilation," *Journal of Cosmology and Astroparticle Physics*, vol. 2012, no. 12, article 9, 2012.

[40] J. Chen and Y.-F. Zhou, "The 130 GeV gamma-ray line and Sommerfeld enhancements," *Journal of Cosmology and Astroparticle Physics*, vol. 2013, no. 4, article 17, 2013.

[41] K. M. Belotsky, M. Yu. Khlopov, and K. I. Shibaev, "Composite dark matter and its charged constituents," *Gravitation and Cosmology*, vol. 12, pp. 93–99, 2006.

[42] D. E. Kaplan, G. Z. Krnjaic, K. R. Rehermann, and C. M. Wells, "Atomic dark matter," *Journal of Cosmology and Astroparticle Physics*, vol. 2010, no. 5, article 21, 2010.

[43] F.-Y. Cyr-Racine and K. Sigurdson, "Cosmology of atomic dark matter," *Physical Review D*, vol. 87, no. 10, Article ID 103515, 39 pages, 2013.

[44] T. Ishiyama, J. Makino, and T. Ebisuzaki, "Gamma-ray signal from Earth-mass dark matter microhalos," *Astrophysical Journal Letters*, vol. 723, no. 2, pp. L195–L200, 2010.

[45] M. Ackermann, A. Albert, L. Baldini et al., "Search for dark matter satellites using *Fermi*-LAT," *The Astrophysical Journal*, vol. 747, no. 2, article 121, 2012.

[46] G. Gamow, "Zur Quantentheorie des Atomkernes," *Zeitschrift für Physik*, vol. 51, no. 3-4, pp. 204–212, 1928.

[47] A. Sommerfeld, "Über die beugung und bremsung der elektronen," *Annalen der Physik*, vol. 403, no. 3, pp. 257–330, 1931.

[48] A. D. Sakharov, "Interaction of the electron and positron in pair production," *Zhurnal Èksperimental'noi i Teoreticheskoi Fiziki*, vol. 18, pp. 631–635, 1948.

[49] J. B. Dent, S. Dutta, and R. J. Scherrer, "Thermal relic abundances of particles with velocity-dependent interactions," *Physics Letters B*, vol. 687, no. 4-5, pp. 275–279, 2010.

[50] J. Zavala, M. Vogelsberger, and S. D. M. White, "Relic density and CMB constraints on dark matter annihilation with Sommerfeld enhancement," *Physical Review D*, vol. 81, no. 8, Article ID 083502, 2010.

[51] J. L. Feng, M. Kaplinghat, and H.-B. Yu, "Sommerfeld enhancements for thermal relic dark matter," *Physical Review D*, vol. 82, no. 8, Article ID 083525, 2010.

[52] J. Zavala, M. Vogelsberger, T. R. Slatyer, A. Loeb, and V. Springel, "Cosmic X-ray and gamma-ray background from dark matter annihilation," *Physical Review D*, vol. 83, no. 12, Article ID 123513, 19 pages, 2011.

[53] K. M. Belotsky, D. Fargion, M. Y. Khlopov, and R. V. Konoplich, "May heavy neutrinos solve underground and cosmic-ray puzzles?" *Physics of Atomic Nuclei*, vol. 71, no. 1, pp. 147–161, 2008.

[54] A. D. Dolgov and Y. B. Zeldovich, "Cosmology and elementary particles," *Reviews of Modern Physics*, vol. 53, no. 1, pp. 1–41, 1981.

[55] R. J. Scherrer and M. S. Turner, "On the relic, cosmic abundance of stable, weakly interacting massive particles," *Physical Review D*, vol. 33, no. 6, pp. 1585–1589, 1986.

[56] W. B. Atwood, A. A. Abdo, M. Ackermann et al., "The large area telescope on the *Fermi Gamma-Ray Space Telescope* mission," *The Astrophysical Journal*, vol. 697, no. 2, pp. 1071–1102, 2009.

[57] P. L. Nolan, A. A. Abdo, M. Ackermann et al., "Fermi large area telescope second source catalog," *The Astrophysical Journal Supplement Series*, vol. 199, no. 2, article 31, 2012.

[58] K. M. Belotsky, A. V. Berkov, A. A. Kirillov, and S. G. Rubin, "Black hole clusters in our Galaxy," *Gravitation and Cosmology*, vol. 17, no. 1, pp. 27–30, 2011.

[59] K. M. Belotsky, A. V. Berkov, A. A. Kirillov, and S. G. Rubin, "Clusters of black holes as point-like gamma-ray sources," *Astroparticle Physics*, vol. 35, no. 1, pp. 28–32, 2011.

[60] A. A. Abdo, M. Ackermann, M. Ajello et al., "Fermi large area telescope measurements of the diffuse gamma-ray emission at intermediate galactic latitudes," *Physical Review Letters*, vol. 103, no. 25, Article ID 251101, 6 pages, 2009.

[61] http://home.thep.lu.se/~torbjorn/Pythia.html.

[62] Z. Ahmed, D. S. Akerib, S. Arrenberg et al., "Search for weakly interacting massive particles with the first five-tower data from the cryogenic dark matter search at the soudan underground laboratory," *Physical Review Letters*, vol. 102, no. 1, Article ID 011301, 5 pages, 2009.

[63] K. C. Y. Ng, R. Laha, S. Campbell et al., "Resolving small-scale dark matter structures using multi-source indirect detection," http://arxiv.org/abs/1310.1915.

[64] M. A. Sanchez-Conde and F. Prada, "The attening of the concentration-mass relation towards low halo masses and its implications for the annihilation signal boost," http://arxiv.org/abs/1312.1729.

Hindawi Publishing Corporation
Advances in High Energy Physics
Volume 2014, Article ID 214258, 10 pages
http://dx.doi.org/10.1155/2014/214258

Research Article

Decaying Dark Atom Constituents and Cosmic Positron Excess

K. Belotsky,[1,2] M. Khlopov,[1,2,3] C. Kouvaris,[4] and M. Laletin[1]

[1] *National Research Nuclear University "Moscow Engineering Physics Institute", Moscow 115409, Russia*
[2] *Centre for Cosmoparticle Physics "Cosmion", Moscow 115409, Russia*
[3] *APC laboratory 10, rue Alice Domon et Léonie Duquet, 75205 Paris Cedex 13, France*
[4] *CP[3]-Origins, University of Southern Denmark, Campusvej 55, 5230 Odense, Denmark*

Correspondence should be addressed to M. Laletin; mnlaletin@mail.ru

Received 30 November 2013; Revised 3 March 2014; Accepted 20 March 2014; Published 16 April 2014

Academic Editor: Jean-René Cudell

We present a scenario where dark matter is in the form of dark atoms that can accommodate the experimentally observed excess of positrons in PAMELA and AMS-02 while being compatible with the constraints imposed on the gamma-ray ux from Fermi/LAT. This scenario assumes that the dominant component of dark matter is in the form of a bound state between a helium nucleus and a −2 particle and a small component is in the form of a WIMP-like dark atom compatible with direct searches in underground detectors. One of the constituents of this WIMP-like state is a +2 metastable particle with a mass of 1 TeV or slightly below that by decaying to e^+e^+, $\mu^+\mu^+$ and $\tau^+\tau^+$ produces the observed positron excess. These decays can naturally take place via GUT interactions. If it exists, such a metastable particle can be found in the next run of LHC. The model predicts also the ratio of leptons over baryons in the universe to be close to −3.

1. Introduction

The possibility of dark matter being in the form of "dark atoms" has been studied extensively [1–21]. In this scenario, new stable particles are bound by new dark forces (like mirror partners of ordinary particles bound by mirror electromagnetism [22–26]). However, it turns out that even stable electrically charged particles can exist hidden in dark atoms, bound by ordinary Coulomb interactions (see [27–30] and references therein). Stable particles with charge −1 (and corresponding antiparticles as tera-particles [31]) are excluded due to overproduction of anomalous isotopes. However, negatively doubly charged particles are not constrained by anomalous isotope searches as much as −1 charged particles [32]. There exist several types of particle models where heavy stable −2 charged species, O^{--}, are predicted:

(a) AC-leptons, predicted as an extension of the Standard Model, based on the approach of almost-commutative geometry [33–36];

(b) technileptons and antitechnibaryons in the framework of Walking Technicolor (WTC) [37–43].

All these models also predict corresponding +2 charge particles. If these positively charged particles remain free in the early universe, they can recombine with ordinary electrons in anomalous helium, which is strongly constrained in terrestrial matter. Therefore a cosmological scenario should provide a mechanism which suppresses anomalous helium. There are two possible mechanisms that can provide a suppression.

(i) The abundance of anomalous helium in the galaxy may be significant, but in terrestrial matter a recombination mechanism could suppress this abundance below experimental upper limits [33, 35]. The existence of a new $U(1)$ gauge symmetry, causing new Coulomb-like long range interactions between charged dark matter particles, is crucial for this mechanism. This leads inevitably to the existence of dark radiation in the form of hidden photons.

(ii) Free positively charged particles are already suppressed in the early universe and the abundance of anomalous helium in the galaxy is negligible [29, 44].

These two possibilities correspond to two different cosmological scenarios of dark atoms. The first one is realized in the scenario with AC leptons, forming neutral AC atoms [35]. The second assumes a charge asymmetry of the O^{--} which forms the atom-like states with primordial helium [29, 44].

If new stable species belong to nontrivial representations of the SU(2) electroweak group, sphaleron transitions at high temperatures can provide the relation between baryon asymmetry and excess of −2 charge stable species, as it was demonstrated in the case of WTC [37, 45–47].

After formation in the Big Bang Nucleosynthesis (BBN), ^{4}He screens the O^{--} charged particles in composite $(^4\mathrm{He}^{++}O^{--})$ *O*He "atoms" [44]. In all the models of *O*He, O^{--} behaves either as a lepton or as a specific "heavy quark cluster" with strongly suppressed hadronic interactions. Therefore *O*He interactions with matter are determined by the nuclear interactions of He. These neutral primordial nuclear interacting objects can explain the modern dark matter density and represent a nontrivial form of strongly interacting dark matter [48–56].

The cosmological scenario of the *O*He universe can explain many results of experimental searches for dark matter [29]. Such a scenario is insensitive to the properties of O^{--}, since the main features of the *O*He dark atoms are determined by their nuclear interacting helium shell. In terrestrial matter such dark matter species are slowed down and cannot cause significant nuclear recoil in the underground detectors, making them elusive in direct WIMP search experiments (where detection is based on nuclear recoil) such as CDMS, XENON100, and LUX [57–61]. The positive results of DAMA and possibly CRESST and CoGeNT experiments [62–66] can find in this scenario a nontrivial explanation due to a low energy radiative capture of *O*He by intermediate mass nuclei [29, 30].

It has been also shown [37, 45–47] that a two-component dark atom scenario is also possible. Along with the dominant O^{--} abundance, a much smaller excess of positively doubly charged techniparticles can be created. These positively charged particles are hidden in WIMP-like atoms, being bound to O^{--}. In the framework of WTC such positively charged techniparticles can be metastable, with a dominant decay channel to a pair of positively charged leptons. In this paper we show that even a 10^{-6} fraction of such positively charged techniparticles with a mass of 1 TeV or less and a lifetime of 10^{20} s, decaying to e^+e^+, $\mu^+\mu^+$, and $\tau^+\tau^+$, can explain the observed excess of cosmic ray positrons, being compatible with the observed gamma-ray background.

One should note that, as it was shown in [35, 37, 44, 45] (for a review, see [29, 33] and references therein), the case of −2 charged stable particles is significantly different from the case of stable or metastable particles with charge −1, avoiding severe constraints on charged particles from anomalous isotope searches and BBN due to their catalytic effects (see, e.g., [67–69]). In essence this difference comes from the fact that primordial He formed in BBN captures −2 charged particles in neutral *O*He states, while −1 charged particles are captured by He in +1 charged ions, which either (if stable) form anomalous isotopes of hydrogen or (if long-lived, but metastable) catalyze processes of light element production and influence their abundance. Nuclear physics of *O*He is in the course of development, but a qualitative analysis has shown [46] that the *O*He interactions with matter should not lead to overproduction of anomalous isotopes, while *O*He catalytic effects in BBN can lead to primordial heavy element production, but not to overproduction of light elements.

The paper is organized as follows. In Section 2 we give a brief review of dark atoms made of stable charged techniparticles. In Section 3 we present the constraints and the predictions of the scenario with respect to the parameters of the Technicolor model we use, as well as how the ratio of lepton over baryon number is deduced. In Section 4 we show what GUT operators can implement the decay of the doubly charged particle to leptons. In Section 5, we show how the scenario of decaying dark matter can be realized, and how it can explain the PAMELA and AMS-02 results while satisfying the Fermi/LAT constraints. We conclude in Section 6.

2. Dark Atoms from Techniparticles

Technicolor theories that do not violate the electroweak precision tests, while not introducing large flavor changing currents, have been extensively studied lately (see [70] and references therein). Old models where fermions transformed under the fundamental representation of the gauge group required a large number of flavors (for a given number of colors) in order to be close to the conformal window and thus to suppress the flavor changing neutral currents. The need for many flavors coupled to the electroweak sector (that violates the electroweak precision measurements) disfavored Technicolor in the past. However, it has been demonstrated that once one allows fermions to transform under higher representations of the gauge group, quasi-conformality can be achieved even with a small number of colors and flavors [38–40]. This means that there is a set of Technicolor models that evade the strict constraints of the electroweak tests, making Technicolor a viable candidate for the TeV energy scale. Apart from the perturbative calculation of the oblique parameters [41] in this type of models, nonperturbative calculations based on holographic descriptions [71–73] showed that indeed the oblique S parameter can be small. Note that the oblique parameters (e.g., S, T, and U) measure the modifications of the Standard Model gauge boson vacuum polarization amplitudes caused by contributions of new physics. These parameters are severely constrained by electroweak precision tests. Extra flavors that couple with the electroweak sector contribute to these parameters and can potentially exclude a model.

One of the simplest models that possesses the features described above, is the so-called Minimal Walking Technicolor [38, 42, 74]. The theory consists of two techniquarks transforming under the adjoint representation of an SU(2) gauge group, and an extra family of leptons ν' and ζ coupled to the electroweak in order to cancel the global Witten anomaly. The hypercharge assignment can be chosen consistently (without introducing gauge anomalies) such that one of the techniquarks has zero electric charge. Such a simple theory can have a variety of dark matter candidates, ranging from

dark matter particles that are Goldstone bosons of the theory (with nonzero technibaryon number) [43, 75, 76] or Majorana WIMPs [77–82]. Apart from these possibilities, there is another intriguing scenario that is of an electromagnetic bound state between a +2 charged helium nucleus and a −2 charged techniparticle [37, 45]. More specifically in [37], we examined the possibility where the dark matter bound state is He$\overline{U}\,\overline{U}$ or Heζ. Recall that U and D are the two techniquarks of the theory and ν' and ζ are the extra leptons. There is a gauge anomalous free hypercharge assignment where the charges of U, D, ν', and ζ are, respectively, +1, 0, −1, and −2. We should also emphasize that, due to the fact that techniquarks transform under the adjoint representation of the gauge group, some of the Goldstone bosons are colorless diquarks (carrying technibaryon number). Apparently $\overline{UU}$ and ζ have charges −2. This candidate HeA (with A being $\overline{U}\,\overline{U}$ or ζ) is a Strongly Interacting Massive Particle (SIMP) rather than a WIMP due to the large geometric cross section of the helium component. Despite the large cross section, this candidate has not been ruled out by any experiment so far. Amazingly enough, although such a candidate interacts strongly with matter, it cannot be detected in earth based detectors (based on measuring the recoil energy) like CDMS, Xenon, or LUX. By the time such a particle reaches the detector, and it has lost most of its kinetic energy making it impossible to produce recoil energies above the detection threshold. In [45], we examined a generalized version of the aforementioned scenario, where although the majority of dark matter is He$\overline{U}\,\overline{U}$ (or Heζ), a small component can be of the WIMP form $\overline{\zeta}\overline{U}\,\overline{U}$ (or $UU\zeta$). Such a WIMP component must be small since it is constrained by direct detection experiments.

In [37, 45], we had assumed that techniparticles are stable. In particular with respect to the technibaryons, the symmetry associated with the technibaryon number protected the lightest diquark Goldstone boson from decaying. Here we reexamine the scenario of [45] allowing decays of the techniparticles. It has been demonstrated that decaying dark matter can provide a possible explanation of the unexpected positron excess seen in PAMELA [83, 84]. Decaying of dark matter particles through a dimension-6 operator gives a lifetime

$$\tau \sim 8\pi \frac{M_{\mathrm{GUT}}^4}{m^5} = 5\times 10^{20}\,\mathrm{s}\left(\frac{2\,\mathrm{TeV}}{m}\right)^5\left(\frac{M_{\mathrm{GUT}}}{10^{15}\,\mathrm{GeV}}\right)^4, \quad (1)$$

where m is the mass of the dark matter particle. Note that we have normalized the lifetime with respect to a GUT scale by an order of magnitude lower than the typical value of 2×10^{16} GeV suggested by supersymmetry. As we are going to argue a small component of dark matter with a mass of ~TeV or less and a lifetime of 10^{20} s can accommodate nicely the positron excess seen in PAMELA and AMS-02 data. In addition such a lifetime is sufficiently large in order not to deplete the density of this component of dark matter by today since it is a few orders of magnitude larger than the age of the universe. As it was stressed in [83], dimension-6 operators are very natural objects in Technicolor, and therefore such a framework becomes very appealing.

3. Techniparticle Excess

We already mentioned that the MWT has two techniquarks U and D in the adjoint representation of the Technicolor SU(2) with charges +1 and 0 and two new leptons ν' and ζ with charges −1 and −2, respectively. The theory possesses a global SU(4) symmetry that breaks spontaneously to an SO(4). Out of the 9 Goldstone bosons, three of them (with the quantum numbers of the usual pions) are eaten by the W and Z bosons, while the rest 6 are the colorless diquarks UU, UD, and DD and their antiparticles [43].

We are going to consider two possibilities. The first one is to have an excess of −2 charge $\overline{U}\,\overline{U}$ and a little of +2 $\overline{\zeta}$. The main component of dark matter is the SIMP He$\overline{U}\,\overline{U}$. There is also a small WIMP component of $\overline{\zeta}\overline{U}\,\overline{U}$. The second scenario is to have an excess of ζ and a little of UU, in such a way that the main SIMP component of dark matter is Heζ and the small WIMP one is $UU\zeta$. In both cases we have assumed that UU is the lightest among the technibaryons and similarly ζ is the lightest of the new leptons. The calculation of the relic density of the technibaryons taking into account sphaleron violating processes, weak equilibration, and overall charge neutrality gives similarly to [43]

$$\frac{\mathrm{TB}}{B} = -\sigma_{UU}\left(\frac{L'}{B}\frac{1}{3\sigma_\zeta} + 1 + \frac{L}{3B}\right), \quad (2)$$

where TB, B, L, and L' are the technibaryon, baryon, lepton, and new lepton family number, respectively. σ_i are statistical factors for the specific particle i given by

$$\sigma_i = \begin{cases} 6f\left(\dfrac{m_i}{T^*}\right) & \text{for fermions,} \\ 6g\left(\dfrac{m_i}{T^*}\right) & \text{for bosons,} \end{cases} \quad (3)$$

where the functions f and g are defined as follows:

$$f(z) = \frac{1}{4\pi^2}\int_0^\infty dx x^2 \cosh^{-2}\left(\frac{1}{2}\sqrt{x^2+z^2}\right),$$
$$g(z) = \frac{1}{4\pi^2}\int_0^\infty dx x^2 \sinh^{-2}\left(\frac{1}{2}\sqrt{x^2+z^2}\right). \quad (4)$$

T^* is the freeze-out temperature for the sphaleron process, usually taken somewhere between 150 and 250 GeV. In the first aforementioned possibility, the dark matter density is

$$\frac{\Omega_d}{\Omega_B} = \frac{\Omega_{\overline{\zeta}\overline{U}\,\overline{U}}}{\Omega_B} + \frac{\Omega_{\mathrm{He}\overline{U}\,\overline{U}}}{\Omega_B} = \left|\frac{L'}{B}\right|\frac{m_d}{m_p} + \left(\frac{3}{2}\left|\frac{\mathrm{TB}}{B}\right| - \left|\frac{L'}{B}\right|\right)\frac{m_s}{m_p} = 5.47, \quad (5)$$

where m_d, m_s, and m_p are the masses of $UU\zeta$, He$\overline{U}\,\overline{U}$, and proton, respectively. We have taken the ratio of dark matter to baryonic matter to be ~5.47. If ξ denotes the fraction of the WIMP component ($\overline{\zeta}\overline{U}\,\overline{U}$) of dark matter, then the ratio of leptons over baryons is given by

$$\frac{L}{B} = -3 + 5.47 m_p\left[\frac{\xi}{m_d\sigma_\zeta} + \frac{2\xi}{m_d\sigma_{UU}} + \frac{2(1-\xi)}{m_s\sigma_{UU}}\right]. \quad (6)$$

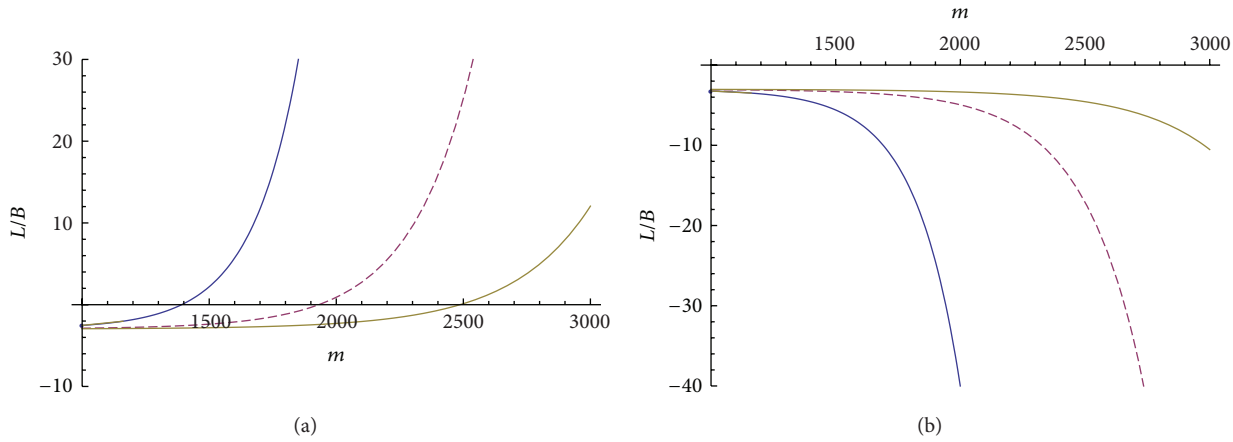

FIGURE 1: The ratio L/B for the two scenarios explained in the text: (6) and (8), respectively, for $m = m_{UU} = m_\zeta$ (in GeV) and $\xi = 10^{-6}$. The three different lines, that is, thin solid, dashed, and thick solid, correspond to freeze-out temperature for the sphalerons T^* of 150, 200, and 250 GeV, respectively.

In the second scenario (that of Heζ and $UU\zeta$),

$$\frac{\Omega_d}{\Omega_B} = \frac{\Omega_{UU\zeta}}{\Omega_B} + \frac{\Omega_{\mathrm{He}\zeta}}{\Omega_B} = \frac{3}{2}\frac{TB}{B}\frac{m_d}{m_p} + \left(\frac{L'}{B} - \frac{3}{2}\frac{TB}{B}\right)\frac{m_{s'}}{m_p}, \tag{7}$$

where m_s' is the mass of Heζ. The ratio L/B is

$$\frac{L}{B} = -3 - 5.47 m_p \left(\frac{\xi}{m_d \sigma_\zeta} + \frac{2\xi}{m_d \sigma_{UU}} + \frac{1-\xi}{m_{s'}\sigma_\zeta}\right). \tag{8}$$

ξ here is again the fraction of the WIMP-like component of dark matter. There are two points we would like to emphasize. The first one is that both possibilities give a ratio of lepton over baryon numbers very close to -3 if the masses of UU and ζ remain around 1 TeV. In fact the first scenario gives a ratio slightly above -3 and the second gives a ratio slightly below. L/B starts deviating (exponentially) as a function of the mass of UU and/or ζ once we go to masses much higher than 1.5 to 2 TeV (see Figure 1). The second point we would like to stress is that ξ is constrained by earth based direct detection search experiments. In [45] we found that the WIMP component of this dark matter scenario cannot be more than 1% (or $\xi < 0.01$). Since then, the constraint from the CDMS and Xenon experiments has improved significantly and more severe constraints from LUX appeared. The cross section of $UU\zeta$ (or its antiparticle) with a proton is [85]

$$\sigma_p = \frac{G_F^2}{2\pi}\mu^2 \overline{Y}^2 F^2 \simeq 1.8 \times 10^{-39}\ \mathrm{cm}^2, \tag{9}$$

where $\overline{Y} = Y_L + Y_R$, that is, the sum of the hypercharge of left and right components. It is easy to check that in our case $\overline{Y} = -1/2$. This is because UU has $Y_L = 1$ and $Y_R = 2$ and ζ has $Y_L = -3/2$ and $Y_R = -2$. The total sum is $-1/2$. In addition since both UU and ζ are much heavier than the proton, the reduced mass μ is approximately the mass of the proton. The form factor F depends on the target nucleus and the recoil energy. For example, for Ge detector with recoil energies between 20 and 50 keV, the form factor ranges from 0.43 to 0.72 [43]. Here in this estimate of the WIMP-proton cross section we have set $F = 1$. The results of the LUX experiment [61] exclude WIMPs with a cross section $10^{-45}\,\mathrm{cm}^2$ for a typical WIMP mass of 1 TeV. This means that WIMPs with the cross section of $UU\zeta$ can make up only a component of $\sim 10^{-6}$ or smaller of the total dark matter. Here we are going to use a typical value of $\xi = 10^{-6}$.

4. Decaying Dark Matter

As we mentioned in the previous section, we might have a $\sim 10^{-6}$ (or less) WIMP component in our dark matter framework. This comes in the form of $\overline{\zeta}\,\overline{U}\,\overline{U}$ (first scenario) or $UU\zeta$ (second scenario). Our goal is to consider decay processes that can produce the excess of positrons seen in PAMELA and AMS-02. For this, it is generically better if the +2 objects decay accordingly.

In the first considered scenario we assume that $\overline{U}\,\overline{U}$ is stable, and therefore the SIMP component which consists the overwhelming part of dark matter is unaffected. On the other hand, we assume that $\overline{\zeta}^{++}$ can decay to leptons. By construction since ζ and ν' belong to the same electroweak doublet, ζ couples to ν' and W^-. Since ν' is a lepton with an electric charge -1, it can in principle slightly mix with the usual -1 leptons, that is, electrons, muons, and taus. The tiny WIMP component of dark matter made of $\overline{\zeta}\overline{U}\,\overline{U}$ decays due to the fact that $\overline{\zeta}$ can decay to a W^+ and (via $\overline{\nu}'$) to positrons, antimuons, and antitaus. We assume that ν' is heavier than ζ, and therefore the decay is suppressed. In order not to get very fast decays of $\overline{\zeta}$, the mixing of $\overline{\nu}'$ with positrons and so forth has to be extremely small. However, this is something expected due to experimental constraints as well as due to the fact that ν' is much heavier than the leptons. It is also expected that the mixing between ν' and τ would be larger than ν' and μ or ν' and positrons. The decay in this scenario can be accommodated via a dimension-5 operator. However,

decays of $\bar{\zeta}$ to positrons, $\mu^+\mu^+$, or $\tau^+\tau^+$ can lead to unwanted production of hadrons via decays of W^+. Therefore we focus on the second case.

In the second scenario the small WIMP component is made of $UU\zeta$. In this case we assume that ζ is stable (and no mixing with other leptons exists), but the UU Goldstone boson decays via a GUT interaction. A natural dimension-6 operator that can accommodate the decay can be of the form

$$\mathcal{O} = \frac{U^T C U \psi^T C' \psi}{\Lambda^2_{\mathrm{GUT}}}, \tag{10}$$

where ψ is an electron, muon, or tau. Notice that, due to the transpose instead of the bar, such an operator violates both the lepton and the technibaryon number. It allows a possible decay of UU to two positrons (or two antimuons or antitaus (in principle we can have an even more general operator where UU decays to different species of antileptons, i.e., a positron, an antimuon, etc)):

$$UU \longrightarrow e^+ + e^+. \tag{11}$$

It is understood that although C and C' can be generic Dirac matrices, C has to be the charge conjugate matrix in order for $U^T C U$ to be the pseudo-Goldstone boson UU. If we require that parity is not violated by the interaction, C' must also be the charge conjugate matrix. In case parity is violated, C' can be $C\gamma_5$ (as it is a well-known fact that $\psi^T C\gamma_5 \psi$ is a scalar). Of course nothing forbids a similar decay of UU to two quarks or even a quark and a lepton, as it would depend on the details of the GUT interaction. However, here we do not want to speculate regarding the GUT interactions but simply to demonstrate that such a realization can in fact produce the positron spectrum seen by experiments. As we already mentioned, a dimension-6 operator of the above form would give according to (1) a lifetime of the order of 10^{20} s for a mass of UU of the order of TeV. If UU does not decay to hadrons, this scenario is more appropriate for explaining the positron excess compared to the first scenario we mentioned because in the first scenario the decay of $\bar{\zeta}$ will always be accompanied by hadronic decays that are not seen by PAMELA.

5. Positron Excess and Fit to the PAMELA and AMS-02 Data

Here we show the impact of decaying UU particles on the cosmic positron flux and diffuse gamma radiation. The so-called "PAMELA anomaly" in the cosmic positron spectrum [86] has been recently confirmed also by AMS-02 [87]. This anomaly cannot be explained by positrons of only secondary origin, and therefore primary positron sources are needed to explain the data. There are attempts to realize it based on decaying or annihilating dark matter models. Any scenario that provides positron excess is constrained by other observational data mainly from the data on cosmic antiprotons, gamma-radiation from our halo (diffuse gamma-background), and other galaxies and clusters [88–95]. If dark matter does not produce antiprotons, then the diffuse gamma-ray background gives the most stringent and model-independent constraints.

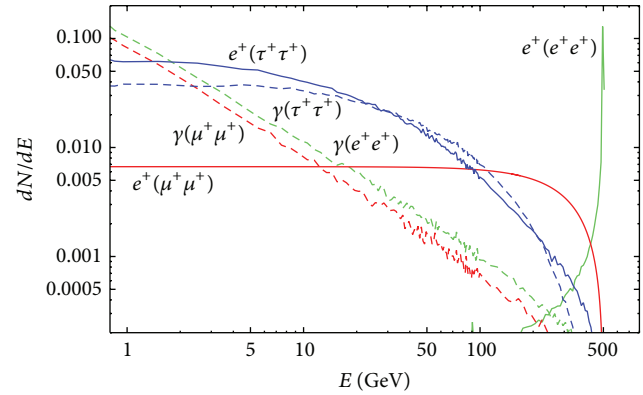

FIGURE 2: Spectra of gamma-rays and positrons from decays $UU \to e^+e^+, \mu^+\mu^+, \tau^+\tau^+$. We used Pythia 6.4 [97].

In our scenario the UU component of a tiny $UU\zeta$ WIMP component of dark matter decays as $UU \to e^+e^+, \mu^+\mu^+, \tau^+\tau^+$ in principle with different branching ratios. All decay modes give directly or through intermediate particle decays the positrons and photons, which are hereafter referred as final state radiation (FSR). In Figure 2 we show the produced positron and gamma spectra for each decay mode individually. Note that, unlike PAMELA, the AMS-02 disfavors decays purely to e^+ and μ^+ (although it does not exclude them).

In the context of indirect dark matter searches from cosmic rays (CR), the leptonic decay modes have been studied extensively (see, e.g., [88–95]), using a variety of different approaches in estimating the CR signals. For our estimate, we adopt the following model of positron propagation in the galaxy. Due to energy losses, positrons have a finite diffusion length at given energy E

$$\lambda \sim \sqrt{\int D dt} = \sqrt{\int D \frac{dE}{b}} \sim 10\,\mathrm{kpc} \sqrt{E^{-0.7} - E_0^{-0.7}}, \tag{12}$$

where $D \approx 4 \cdot 10^{28}\,\mathrm{cm^2\,s^{-1}} E^{0.3}$ is a typical value for the diffusion coefficient [96], $b = \beta E^2$ is the rate of energy losses with $\beta \sim 10^{-16}\,\mathrm{s^{-1}\,GeV^{-1}}$, and E_0 is the initial energy. All energies are measured in GeV. The effect of the diffusion in the propagation can be estimated by assuming a homogeneous distribution of the sources. In fact, the result of diffusion is not sensitive to the effects of inhomogeities, because it depends on the averaged density within the diffusion length. Since we are interested in positron energies above ~ 10 GeV, which corresponds to $\lambda \lesssim 5$ kpc (see (12)) over which no essential inhomogeneity effects are expected, this simple approximation we make here is good. At $E \lesssim 10$ GeV, secondary positrons dominate the spectrum. If λ exceeds the size of the magnetic halo (MH) ($h \sim 4$ kpc in height and $R \sim 15$ kpc in width), the leakage of particles from the halo should be taken into account. We consider this effect

by introducing a suppression factor, which is equal to the ratio of the volume of MH contained within the sphere of radius λ:

$$Q = 1 - \frac{(\lambda - h)^2 (2\lambda + 4)}{2\lambda^3}\eta(\lambda - h) - \frac{2h\left(\lambda^2 - r^2\right)}{3\lambda^3}\eta(\lambda - R), \tag{13}$$

where η is the step function. If dN/dE_0 is the number of positrons produced in a single decay (see Figure 2), the positron flux near the Earth can be estimated as

$$F(E) = \frac{c}{4\pi}\frac{n_{\text{loc}}}{\tau}\frac{1}{\beta E^2}\int_E^{m/2}\frac{dN}{dE_0}Q\left(\lambda\left(E_0, E\right)\right)dE_0, \tag{14}$$

where $n_{\text{loc}} = \xi \cdot (0.3\,\text{GeV/cm}^3)m_{UU}^{-1}$ is the local number density of UU particles with $\xi = 10^{-6}\xi_{-6}$. Recall that ξ is the fraction of dark matter in the WIMP $UU\zeta$ component.

The effect of solar modulation becomes important at the less interesting low energy part of the positron spectrum. To account for this effect, we have adopted the forced field model [98] with two different ϕ parameters for positrons and electrons. They are easily adjusted so they can fit the data points at low energy. The positron and electron background components were taken from [99]. In Figure 3 we present the positron excess due to UU decays for two values of the mass of UU, $m_{UU} = 0.7$ TeV and $m_{UU} = 1$ TeV. We also show the lifetime of $UU\tau$ and the branching ratios that fit the experimental data optimally for each choice of m_{UU}. They evade the existing constraints of [88–95].

The gamma-ray flux from UU decays has two main contributions: one from FSR (shown in Figure 2) and another one from Inverse Compton (IC) scattering of positrons on background photons (star light, infrared background, and CMB).

For the FSR photons produced by UU decays in our galaxy, the flux arriving in the Earth is given by

$$F_{\text{FSR}} = \frac{n_{\text{loc}}}{\tau}\frac{1}{4\pi\Delta\Omega_{\text{obs}}}\int_{\Delta\Omega_{\text{obs}}}\frac{n(r)}{n_{\text{loc}}}dld\Omega \cdot \frac{dN_\gamma}{dE}, \tag{15}$$

where we use an isothermal profile $n(r)/n_{\text{loc}} = ((5\,\text{kpc})^2 + (8.5\,\text{kpc})^2)/((5\,\text{kpc})^2 + r^2)$, r and l are the distances from the Galactic center and the Earth, respectively. We obtain the averaged flux over the solid angle $\Delta\Omega_{\text{obs}}$ corresponding to $|b| > 10^\circ$, $0 < l < 360^\circ$. For the IC photons from our galaxy, we have estimated the contribution following [100]. In Figure 4 we show both contributions in the gamma-ray flux for the same parameters as in Figure 3.

Decays of UU, which are outside our Galaxy being homogeneously distributed over the Universe, should also contribute to the observed gamma-ray flux. For FSR photons this contribution can be estimated as

$$F_{\text{FSR}}^{(U)}(E) = \frac{c}{4\pi}\frac{\langle n_{\text{mod}}\rangle}{\tau}\int\frac{dN}{dE}dt = \frac{c\langle n_{\text{mod}}\rangle}{4\pi\tau} \times \int_0^{\min(1100,(m/2E)+1)}\frac{dN}{dE_0}\left(E_0 = E(z+1)\right) \times \frac{H_{\text{mod}}^{-1}\,dz}{\sqrt{\Omega_\Lambda + \Omega_m(z+1)^3}}, \tag{16}$$

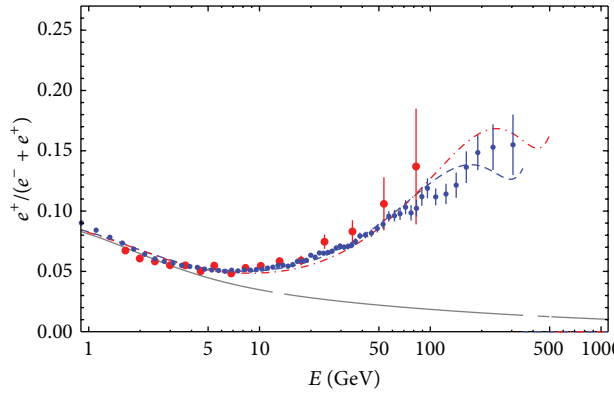

Figure 3: Positron excess due to $UU \to e^+e^+, \mu^+\mu^+, \tau^+\tau^+$ decays compared to PAMELA and AMS-02 data.

where $z = 1100$ corresponds to the recombination epoch, $\langle n_{\text{mod}}\rangle$ is the current cosmological number density of UU, $H_{\text{mod}}^{-1} = (3/2)t_{\text{mod}}\sqrt{\Omega_\Lambda}\ln((1 + \sqrt{\Omega_\Lambda})/\sqrt{\Omega_m})$ is the inverse value of the Hubble parameter with t_{mod} being the age of the universe, and Ω_Λ and $\Omega_m = 1 - \Omega_\Lambda$ are, respectively, the current vacuum and matter relative densities. Note in (16) the transition between distributions at different z, $dN/dE \to (dN/dE_0)(z + 1)$. This extragalactic contribution to FSR increases significantly the total gamma-ray flux as shown in Figure 4 by dot-dashed lines.

It is not expected that extragalactic IC photons can contribute significantly to the spectrum. Indeed, mainly only low energetic CMB photons are present in the medium outside the galaxy (or before the galactic stage). After the scattering of electrons with energy $E_0 \lesssim 500$ GeV off CMB photons with energy $\omega_{\text{CMB}} \lesssim 10^{-3}(z + 1)$ eV, the recoiled photons acquire at redshift z energy $\omega \sim (E_0/m_e)^2\omega_{\text{CMB}} \lesssim (z + 1)$ GeV, which is below 1 GeV in the modern epoch. It makes therefore this contribution indifferent for the energy range of Fermi/LAT.

To conclude, on the basis of Figure 4, one may assert that the considered scenarios of UU decays satisfy the Fermi/LAT constraints. In addition, although we used the best fit values for the branching ratios, we have found that some small variation of the branching ratios is possible. If one chooses $m_{UU} > 1$ TeV, a possible satisfaction of the constraints is possible at the expense of the positron spectrum fit.

6. Conclusions

Dark matter can potentially be in the form of neutral OHe dark atoms made of stable heavy doubly charged particles and primordial He nuclei bound by ordinary Coulomb interactions. This scenario sheds new light on the nature of dark matter and offers a nontrivial solution for the puzzles

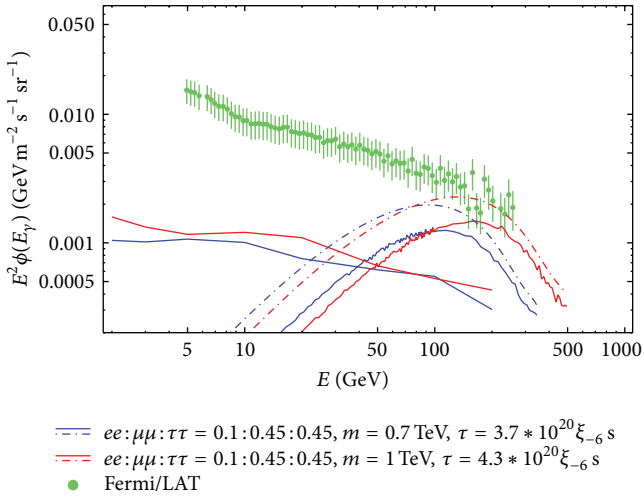

FIGURE 4: Gamma-ray flux from UU decays in the galaxy ($|b| \geq 10^0$) in comparison to the Fermi/LAT data on diffuse background [101]. Two contributions are shown: IC (left curves) and FSR (right curves). Dot-dashed curves take into account FSR photons of both galactic and extragalactic origin.

of direct dark matter searches. It can be realized in the framework of Minimal Walking Technicolor, in which an exact relation between the dark matter density and baryon asymmetry can be naturally obtained predicting also the ratio of leptons over baryons in the universe. In the context of this scenario a sparse component of WIMP-like dark atoms of charged techniparticles can also appear. Direct searches for WIMPs put severe constraints on the presence of this component. However, we demonstrated in this paper that the existence of a metastable positively doubly charged techniparticle, forming this tiny subdominant WIMP-like dark atom component and satisfying the direct WIMP searches constraints, can play an important role in the indirect effects of dark matter. We found that decays of such positively charged constituents of WIMP-like dark atoms to the leptons e^+e^+, $\mu^+\mu^+$, and $\tau^+\tau^+$ can explain the observed excess of high energy cosmic ray positrons, while being compatible with the observed gamma-ray background. These decays are naturally facilitated by GUT scale interactions. This scenario makes a prediction about the ratio of leptons over baryons in the universe to be close to -3. The best fit of the data takes place for a mass of this doubly charged particle of 1 TeV or below making it accessible in the next run of LHC.

Conflict of Interests

The authors declare that there is no conflict of interests regarding the publication of this paper.

Acknowledgment

C. Kouvaris is supported by the Danish National Research Foundation, Grant no. DNRF90.

References

[1] S. I. Blinnikov and M. Yu. Khlopov, "On possible effects of mirror particles," *Soviet Journal of Nuclear Physics*, vol. 36, p. 472, 1982.

[2] S. I. Blinnikov and M. Y. Khlopov, "Excitation of the solar oscillations by objects consisting of y-matter," *Solar Physics*, vol. 82, no. 1-2, pp. 383–385, 1983.

[3] M. Yu. Khlopov, G. M. Beskin, N. E. Bochkarev, L. A. Pustylnik, and S. A. Pustylnik, "Observational physics of mirror world," *Soviet Astronomy*, vol. 35, no. 21, 1991.

[4] H. M. Hodges, "Mirror baryons as the dark matter," *Physical Review D*, vol. 47, no. 2, pp. 456–459, 1993.

[5] H. Goldberg and L. J. Hall, "A new candidate for dark matter," *Physics Letters B*, vol. 174, no. 2, pp. 151–155, 1986.

[6] Z. G. Berezhiani and R. N. Mohapatra, "Reconciling present neutrino puzzles: sterile neutrinos as mirror neutrinos," *Physical Review D*, vol. 52, no. 11, pp. 6607–6611, 1995.

[7] Z. G. Berezhiani, A. D. Dolgov, and R. N. Mohapatra, "Asymmetric inflationary reheating and the nature of mirror universe," *Physics Letters B*, vol. 375, no. 1–4, pp. 26–36, 1996.

[8] R. Foot and R. R. Volkas, "Neutrino physics and the mirror world: how exact parity symmetry explains the solar neutrino deficit, the atmospheric neutrino anomaly, and the LSND experiment," *Physical Review D*, vol. 52, no. 11, pp. 6595–6606, 1995.

[9] R. N. Mohapatra and V. L. Teplitz, "Mirror dark matter and galaxy core densities," *Physical Review D*, vol. 62, no. 6, Article ID 063506, 5 pages, 2000.

[10] R. Foot, "Mirror matter-type dark matter," *International Journal of Modern Physics D*, vol. 13, no. 10, pp. 2161–2192, 2004.

[11] M. J. Strassler and K. M. Zurek, "Echoes of a hidden valley at hadron colliders," *Physics Letters B*, vol. 651, no. 5-6, pp. 374–379, 2007.

[12] N. Arkani-Hamed, D. P. Finkbeiner, T. R. Slatyer, and N. Weiner, "A theory of dark matter," *Physical Review D*, vol. 79, no. 1, Article ID 015014, 2009.

[13] D. E. Kaplan, G. Z. Krnjaic, K. R. Rehermann, and C. M. Wells, "Atomic dark matter," *Journal of Cosmology and Astroparticle Physics*, vol. 2010, p. 021, 2010.

[14] J. G. Wacker, S. R. Behbahani, M. Jankowiak, and T. Rube, "Nearly supersymmetric dark atoms," *Advances in High Energy Physics*, vol. 2011, Article ID 709492, 2011.

[15] D. E. Kaplan, G. Z. Krnjaic, K. R. Rehermannc, and C. M. Wells, "Dark atoms: asymmetry and direct detection," *Journal of Cosmology and Astroparticle Physics*, vol. 2011, p. 011, 2011.

[16] J. M. Cline, Z. Liu, and W. Xue, "Millicharged atomic dark matter," *Physical Review D*, vol. 85, Article ID 101302(R), 2012.

[17] J. M. Cline, Z. Liu, and W. Xue, "Optimistic CoGeNT analysis," *Physical Review D*, vol. 87, Article ID 015001, 2013.

[18] F.-Y. Cyr-Racine and K. Sigurdson, "Cosmology of atomic dark matter," *Physical Review D*, vol. 87, Article ID 103515, 2013.

[19] F.-Y. Cyr-Racine, R. de Putter, A. Raccanelli, and K. Sigurdson, "Constraints on large-scale dark acoustic oscillations from cosmology," *Physical Review D*, vol. 89, Article ID 063517, 2014.

[20] D. H. Weinberg, J. S. Bullock, F. Governato, R. Kuzio de Naray, and A. H. G. Peter, "Cold dark matter: controversies on small scales," submitted to *Proceedings of the National Academy of Sciences of the United States of America*, http://arxiv.org/abs/1306.0913.

[21] J. M. Cline, Z. Liu, G. D. Moore, and W. Xue, "Scattering properties of dark atoms and molecules," *Physical Review D*, vol. 89, Article ID 043514, 2014.

[22] T. D. Lee and C. N. Yang, "Question of parity conservation in weak interactions," *Physical Review*, vol. 104, no. 1, pp. 254–258, 1956.

[23] I. Yu. Kobzarev, L. B. Okun, and I. Ya. Pomeranchuk, *Soviet Journal of Nuclear Physics*, vol. 3, p. 837, 1966.

[24] B. Ya. Zel'dovich and M. Yu. Khlopov, "The neutrino mass in elementary-particle physics and in big bang cosmology," *Soviet Physics Uspekhi*, vol. 24, p. 755, 1981.

[25] L. B. Okun, "Mirror particles and mirror matter: 50 years of speculation and searching," *Physics-Uspekhi*, vol. 50, no. 4, pp. 380–389, 2007.

[26] P. Ciarcelluti, "Cosmology with mirror dark matter," *International Journal of Modern Physics D*, vol. 19, no. 14, pp. 2151–2230, 2010.

[27] M. Y. Khlopov, A. G. Mayorov, and E. Y. Soldatov, "Puzzles of dark matter in the light of dark atoms," *Journal of Physics: Conference Series*, vol. 309, no. 1, Article ID 012013, 2011.

[28] M. Y. Khlopov, A. G. Mayorov, and E. Y. Soldatov, *Bled Workshops in Physics*, vol. 11, p. 73, 2010.

[29] M. Y. Khlopov, "Physics of dark matter in the light of dark atoms," *Modern Physics Letters A*, vol. 26, no. 38, pp. 2823–2839, 2011.

[30] M. Yu. Khlopov, "Fundamental particle structure in the cosmological dark matter," *International Journal of Modern Physics A*, vol. 28, no. 29, Article ID 1330042, 2013.

[31] S. L. Glashow, "A sinister extension of the standard model to $SU(3)XSU(2)XSU(2)XU(1)$," http://arxiv.org/abs/hep-ph/0504287.

[32] D. Fargion and M. Yu. Khlopov, "Tera-leptons' shadows over Sinister universe," *Gravitation and Cosmology*, vol. 19, pp. 219–231, 2013.

[33] M. Y. Khlopov, "New symmetries in microphysics, new stable forms of matter around us," *Annales de la Fondation Louis de Broglie*, vol. 31, no. 2-3, pp. 257–272, 2006.

[34] C. A. Stephan, "Almost-commutative geometries beyond the standard model," *Journal of Physics A*, vol. 39, p. 9657, 2006.

[35] M. Y. Khlopov, C. A. Stephan, and D. Fargion, "Dark matter with invisible light from heavy double charged leptons of almost-commutative geometry?" *Classical and Quantum Gravity*, vol. 23, no. 24, pp. 7305–7354, 2006.

[36] A. Connes, *Noncommutative Geometry*, Academic Press, San Diego, Calif, USA, 1994.

[37] M. Y. Khlopov and C. Kouvaris, "Strong interactive massive particles from a strong coupled theory," *Physical Review D*, vol. 77, no. 6, Article ID 065002, 2008.

[38] F. Sannino and K. Tuominen, "Orientifold theory dynamics and symmetry breaking," *Physical Review D*, vol. 71, no. 5, pp. 1–4, 2005.

[39] D. K. Hong, S. D. H. Hsu, and F. Sannino, "Composite Higgs from higher representations," *Physics Letters B*, vol. 597, no. 1, pp. 89–93, 2004.

[40] D. D. Dietrich, F. Sannino, and K. Tuominen, "Light composite Higgs boson from higher representations versus electroweak precision measurements: predictions for CERN LHC," *Physical Review D*, vol. 72, no. 5, Article ID 055001, 2005.

[41] D. D. Dietrich, F. Sannino, and K. Tuominen, "Light composite Higgs and precision electroweak measurements on the Z resonance: an update," *Physical Review D*, vol. 73, no. 3, Article ID 037701, 2006.

[42] S. B. Gudnason, C. Kouvaris, and F. Sannino, "Towards working technicolor: effective theories and dark matter," *Physical Review D*, vol. 73, no. 11, Article ID 115003, 2006.

[43] S. B. Gudnason, C. Kouvaris, and F. Sannino, "Dark matter from new technicolor theories," *Physical Review D*, vol. 74, no. 9, Article ID 095008, 2006.

[44] M. Y. Khlopov, "Composite dark matter from the fourth generation," *JETP Letters*, vol. 83, no. 1, pp. 1–4, 2006.

[45] M. Y. Khlopov and C. Kouvaris, "Composite dark matter from a model with composite Higgs boson," *Physical Review D*, vol. 78, no. 6, Article ID 065040, 2008.

[46] M. Y. Khlopov, "The puzzles of dark matter searches," in *Invisible Universe International Conference*, vol. 1241 of *AIP Conference Proceedings*, pp. 388–397, July 2009.

[47] M. Y. Khlopov, A. G. Mayorov, and E. Y. Soldatov, "Composite dark matter and puzzles of dark matter searches," *International Journal of Modern Physics D*, vol. 19, no. 8-10, pp. 1385–1395, 2010.

[48] B. D. Wandelt, R. Dave, G. R. Farrar, P. C. McGuire, D. N. Spergel, and P. J. Steinhardt, "Self-Interacting dark matter," in *Proceedings of the 4th International Symposium on Sources and Dete Conference*, pp. 263–274, 2000.

[49] P. C. McGuire and P. J. Steinhardt, "Cracking open the window for strongly interacting massive particles as the halo dark matter," in *Proceedings of the International Cosmic Ray Conference*, p. 1566, Hamburg, Germany, 2001.

[50] G. Zaharijas and G. R. Farrar, "Window in the dark matter exclusion limits," *Physical Review D*, vol. 72, no. 8, Article ID 083502, 2005.

[51] C. B. Dover, T. K. Gaisser, and G. Steigman, "Cosmological constraints on new stable hadrons," *Physical Review Letters*, vol. 42, no. 17, pp. 1117–1120, 1979.

[52] S. Wolfram, "Abundances of new stable particles produced in the early universe," *Physics Letters B*, vol. 82, no. 1, pp. 65–68, 1979.

[53] G. D. Starkman, A. Gould, R. Esmailzadeh, and S. Dimopoulos, "Opening the window on strongly interacting dark matter," *Physical Review D*, vol. 41, no. 12, pp. 3594–3603, 1990.

[54] D. Javorsek II, D. Elmore, E. Fischbach et al., "New experimental limits on strongly interacting massive particles at the TeV scale," *Physical Review Letters*, vol. 87, no. 23, Article ID 231804, 4 pages, 2001.

[55] S. Mitra, "Uranus's anomalously low excess heat constrains strongly interacting dark matter," *Physical Review D*, vol. 70, no. 10, Article ID 103517, 6 pages, 2004.

[56] G. D. Mack, J. F. Beacom, and G. Bertone, "Towards closing the window on strongly interacting dark matter: far-reaching constraints from Earth's heat flow," *Physical Review D*, vol. 76, no. 4, Article ID 043523, 2007.

[57] D. Abrams, D. S. Akerib, M. S. Armel-Funkhouser et al., "Exclusion limits on the WIMP-nucleon cross section from the Cryogenic Dark Matter Search," *Physical Review D*, vol. 66, Article ID 122003, 2002.

[58] D. S. Akerib, M. S. Armel-Funkhouser, M. J. Attisha et al., "Exclusion limits on the WIMP-nucleon cross section from the first run of the Cryogenic Dark Matter Search in the Soudan Underground Laboratory," *Physical Review D*, vol. 72, Article ID 052009, 2005.

[59] Z. Ahmed, D. S. Akerib, S. Arrenberg et al., "Search for weakly interacting massive particles with the first five-tower data from the cryogenic dark matter search at the Soudan underground laboratory," *Physical Review Letters*, vol. 102, Article ID 011301, 2009.

[60] E. Aprile, K. Arisaka, F. Arneodo et al., "First dark matter results from the XENON100 experiment," *Physical Review Letters*, vol. 105, Article ID 131302, 2010.

[61] D. S. Akerib, H. M. Araujo, X. Bai et al., "First results from the LUX dark matter experiment at the Sanford Underground Research Facility," *Physical Review Letters*, vol. 112, Article ID 091303, 2014.

[62] R. Bernabei, P. Belli, R. Cerulli et al., "Search for WIMP annual modulation signature: results from DAMA/NaI-3 and DAMA/NaI-4 and the global combined analysis," *Physics Letters B*, vol. 480, pp. 23–31, 2000.

[63] R. Bernabei, P. Belli, F. Cappella et al., "Dark Matter search," *Rivista del Nuovo Cimento*, vol. 26, no. 1, 2003.

[64] R. Bernabei, P. Belli, F. Cappella et al., "First results from DAMA/LIBRA and the combined results with DAMA/NaI," *European Physical Journal C*, vol. 56, no. 3, pp. 333–355, 2008.

[65] G. Angloher, M. Bauer, I. Bavykina et al., "Results from 730 kg days of the CRESST-II Dark Matter Search," *The European Physical Journal C*, vol. 72, p. 1971, 2012.

[66] C. E. Aalseth, P. S. Barbeau, J. Colaresi et al., "Search for an annual modulation in a p-type point contact germanium dark matter detector," *Physical Review Letters*, vol. 107, Article ID 141301, 2011.

[67] M. Taoso, G. Bertone, and A. Masiero, "Dark matter candidates: a ten-point test," *Journal of Cosmology and Astroparticle Physics*, vol. 2008, no. 3, article 022, 2008.

[68] K. Kohri and T. Takahashi, "Cosmology with long-lived charged massive particles," *Physics Letters B*, vol. 682, pp. 337–341, 2010.

[69] M. Pospelov and J. Pradler, "Big bang nucleosynthesis as a probe of new physics," *Annual Review of Nuclear and Particle Science*, vol. 60, pp. 539–568, 2010.

[70] F. Sannino, "Conformal dynamics for TeV physics and cosmology," *Acta Physica Polonica B*, vol. 40, pp. 3533–3745, 2009.

[71] D. D. Dietrich and C. Kouvaris, "Constraining vectors and axial-vectors in walking technicolor by a holographic principle," *Physical Review D*, vol. 78, Article ID 055005, 2008.

[72] D. D. Dietrich and C. Kouvaris, "Generalized bottom-up holography and walking technicolor," *Physical Review D*, vol. 79, Article ID 075004, 2009.

[73] D. D. Dietrich, M. Jarvinen, and C. Kouvaris, "Linear confinement without dilaton in bottom-up holography for walking technicolour," *Journal of High Energy Physics*, vol. 2010, p. 23, 2010.

[74] R. Foadi, M. T. Frandsen, T. A. Ryttov, and F. Sannino, "Minimal walking technicolor: setup for collider physics," *Physical Review D*, vol. 76, no. 5, Article ID 055005, 2007.

[75] T. A. Ryttov and F. Sannino, "Ultraminimal technicolor and its dark matter technicolor interacting massive particles," *Physical Review D*, vol. 78, Article ID 115010, 2008.

[76] M. T. Frandsen and F. Sannino, "iTIMP: isotriplet technicolor interacting massive particle as dark matter," *Physical Review D*, vol. 81, Article ID 097704, 2010.

[77] C. Kouvaris, "Dark Majorana particles from the minimal walking technicolor theory," *Physical Review D*, vol. 76, Article ID 015011, 2007.

[78] K. Kainulainen, K. Tuominen, and J. Virkajarvi, "Weakly interacting dark matter particle of a minimal technicolor theory," *Physical Review D*, vol. 75, Article ID 085003, 2007.

[79] C. Kouvaris, "Dark side of strongly coupled theories," *Physical Review D*, vol. 78, Article ID 075024, 2008.

[80] K. Belotsky, M. Khlopov, and C. Kouvaris, "Muon flux limits for Majorana dark matter from strong coupling theories," *Physical Review D*, vol. 79, Article ID 083520, 2009.

[81] O. Antipin, M. Heikinheimo, and K. Tuominen, "Natural fourth generation of leptons," *Journal of High Energy Physics*, vol. 2009, p. 018, 2009.

[82] T. Hapola, M. Jarvinen, C. Kouvaris, P. Panci, and J. Virkajarvi, "Constraints on Majorana dark matter from a fourth lepton family," *Journal of Cosmology and Astroparticle Physics*, vol. 1402, p. 050, 2014.

[83] E. Nardi, F. Sannino, and A. Strumia, "Decaying dark matter can explain the $e^{\pm}$ excesses," *Journal of Cosmology and Astroparticle Physics*, vol. 2009, p. 043, 2009.

[84] A. Arvanitaki, S. Dimopoulos, S. Dubovsky, P. W. Graham, R. Harnik, and S. Rajendran, "Astrophysical probes of unification," *Physical Review D*, vol. 79, no. 10, Article ID 105022, 2009.

[85] M. W. Goodman and E. Witten, "Detectability of certain dark-matter candidates," *Physical Review D*, vol. 31, no. 12, pp. 3059–3063, 1985.

[86] PAMELA collaboration.

[87] M. Aguilar, G. Alberti, B. Alpat et al., "First result from the alpha magnetic spectrometer on the international space station: precision measurement of the positron fraction in primary cosmic rays of 0.5–350 GeV," *Physical Review Letters*, vol. 110, Article ID 141102, 2013.

[88] M. Ackermann, A. Albert, B. Anderson et al., "Dark matter constraints from observations of 25 Milky Way satellite galaxies with the fermi large area telescope," *Physical Review D*, vol. 89, Article ID 042001, 2014.

[89] M. Ackermann, M. Ajello, W. B. Atwood et al., "Constraints on the galactic halo dark matter from Fermi-LAT diffuse measurements," *The Astrophysical Journal*, vol. 761, p. 91, 2012.

[90] J. Buckley, D. F. Cowen, S. Profumo et al., "Cosmic Frontier indirect dark matter detection working group summary," http://arxiv.org/abs/1310.7040.

[91] A. Ibarra, D. Tran, and C. Weniger, "Indirect searches for decaying dark matter," *International Journal of Modern Physics A*, vol. 28, no. 27, Article ID 1330040, 2013.

[92] M. Tavakoli, I. Cholis, C. Evoli, and P. Ullio, "Constraints on dark matter annihilations from diffuse gamma-ray emission in the Galaxy," *Journal of Cosmology and Astroparticle Physics*, vol. 2014, p. 017, 2014.

[93] J. Conrad, "Indirect detection of dark matter with gamma-rays—status and perspectives," p. 048.

[94] L. Dugger, T. E. Jeltema, and S. Profumo, "Constraints on decaying dark matter from Fermi observations of nearby galaxies and clusters," *Journal of Cosmology and Astroparticle Physics*, vol. 2010, no. 12, article 015, 2010.

[95] A. Ibarra, A. S. Lamperstorfer, and J. Silk, "Dark matter annihilations and decays after the AMS-02 positron measurements," http://arxiv.org/abs/1309.2570.

[96] A. Strong and I. Moskalenko, "Propagation of cosmic-ray nucleons in the Galaxy," *The Astrophysical Journal*, vol. 509, no. 1, p. 212, 1998.

[97] T. Sjöstrand, S. Mrenna, and P. Skands, "PYTHIA 6.4 physics and manual," *Journal of High Energy Physics*, vol. 0605, p. 026, 2006.

[98] L. J. Gleeson and W. I. Axford, "Solar modulation of galactic cosmic rays," *Astrophysical Journal*, vol. 154, p. 1011, 1968.

[99] E. A. Baltz and J. Edsjo, "Positron propagation and fluxes from neutralino annihilation in the halo," *Physical Review D*, vol. 59, no. 2, Article ID 023511, 1998.

[100] M. Cirelli and P. Panci, "Inverse Compton constraints on the Dark Matter $e^{\pm}$ excesses," *Nuclear Physics B*, vol. 821, no. 1-2, pp. 399–416, 2009.

[101] M. Ackermann, M. Ajello, A. Albert et al., "Fermi LAT search for dark matter in gamma-ray lines and the inclusive photon spectrum," *Physical Review D*, vol. 86, Article ID 022002, 2012.

Hindawi Publishing Corporation
Advances in High Energy Physics
Volume 2014, Article ID 319218, 6 pages
http://dx.doi.org/10.1155/2014/319218

Research Article

Black Component of Dark Matter

A. V. Grobov, S. G. Rubin, and V. Yu. Shalamova

Particle Physics Department, National Research Nuclear University "MEPhI", Moscow 115409, Russia

Correspondence should be addressed to S. G. Rubin; sergeirubin@list.ru

Received 30 November 2013; Accepted 20 January 2014; Published 30 March 2014

Academic Editor: Konstantin Belotsky

A mechanism of primordial black hole formation with specific mass spectrum is discussed. It is shown that these black holes could contribute to the energy density of dark matter. Our approach is elaborated in the framework of universal extra dimensions.

1. Introduction

After discovery of the Higgs boson, dark matter remains the most challenging unsolved problem. A nature of this dominant component of matter density is so far unknown. Extensions of standard model propose a number of possible candidates for the dark matter particle, so-called WIMPs (Weakly Interacting Massive Particles). Most popular candidates—neutralino, sneutrino, or gravitino—come from the SUSY models. Axions represent another way to describe the dark matter phenomenon by means of particle physics [1, 2]. The third widely discussed method is various extra dimensional models producing different sorts of Kaluza-Klein particles that can be considered as the dark matter particles [3].

There are many experiments aimed to clarifying the essence of dark matter. One of the most known Fermi LAT experiments is searching for the dark matter footprints in gamma rays since 2008. According to the recent Fermi LAT data [4] there is some signature of a gamma-ray line at the energy about 130 GeV in the direction of the Galactic Center. Unfortunately, in spite of continual efforts it is not clear yet if this is a real line. Up to now, there are no signatures of dark matter in the existing spectra of cosmic rays. The successor of Fermi LAT, Russian-Italian satellite GAMMA-400, was announced to have an unprecedented energy and angular resolution and believed to be more effective.

Another explanation for dark matter content is the existence of massive compact halo objects (MACHOs) [5–7]. Brown dwarfs, interstellar gas, comets, cosmic dust, neutron stars, and black holes of stellar origin may be considered as MACHOs. All of these constituents are made from baryons which drastically reduces their possible contribution to the energy density of dark matter [8].

Primordial black holes (PBH) with a wide range of masses provide additional contribution to an invisible part of the average energy density of the universe. There are several models describing PBH formation soon after the end of inflation. Starting from the first articles [5–7], various models of such kind have appeared during last decades; see substantial review [9]. In contrast to the black holes originating from stars for PBHs there is no lower mass limit (actually [10] there is black hole minimum mass $\simeq 0.04\sqrt{g_*}M_{\mathrm{pl}}$).

Mechanism of PBH formation as a result of phase transitions during the inflationary stage was developed in [11–13]. The basic of this mechanism is quantum fluctuations of scalar field with a potential possessing at least two minima. Constraints on a PBH abundance associated with cosmological nucleosynthesis are not applicable because the formation of PBHs is a result of first order phase transitions of some scalar field.

The origin of the scalar field remains uncertain in this model. Meantime, extra dimensions provide a wide range of such potentials which can influence the evolution of the universe; see also [14, 15].

In this paper we elaborate the model of PBH formation based on universal extra dimensions. Mass distribution and number of PBH do not contradict observational limits and could contribute substantially to dark matter content.

The rest of the paper is organized as follows. In Section 2 we describe the mechanism of primordial black holes formation. In Section 3 we discuss initial conditions and modern limits on PBHs. In Section 4 we conclude.

2. Primordial Black Holes Formation and Extra Space

As was mentioned above our study is based on the mechanism of PBH formation revealed in [11]. Its necessary ingredient is a potential of scalar field with two minima which is postulated from the beginning. In the framework of multidimensional gravity, metric components of extra space are perceived as scalar fields acting in 4-dim space. In this connection we shortly remind some effective way to reduce a D-dim theory to 4-dim low energy effective theory [16].

Consider a $D = 4 + d$ dimensional manifold with the metric

$$ds^2 = g_{MN}dx^M dx^N = g_{\mu\nu}dx^\mu dx^\nu + e^{2\beta(x)}b_{ab}dx^a dx^b, \quad (1)$$

where $M, N = 1, 2, \ldots, d + 4$ and the extra dimensional metric components b_{ab} are independent of x^μ, the observable space-time coordinates. In the framework of this metric let us consider the curvature-nonlinear theory of gravity with the action which has various nontrivial consequences:

$$S = \frac{1}{2}m_D^{D-2}\int \sqrt{{}^D g}d^D x\left(F(R) + c_1 R^{AB}R_{AB} + c_2\mathcal{K}\right), \quad (2)$$

where m_D is a D-dimensional analogue of the Planck mass. For example, action (2) was used [17] to develop the model describing both primary and secondary inflations. Action (2) contains an arbitrary smooth function $F(R)$, c_1 and c_2 are arbitrary constants, R^{AB} and $\mathcal{K} = R^{ABCD}R_{ABCD}$ are Ricci tensor and Kretschmann scalar, and ${}^D g = |\det(g_{MN})|$.

Let us express all quantities in terms of 4-dimensional variables and $\beta(x)$; notice that now

$$R = R_4 + \phi + f_1,$$
$$f_1 = 2d\beta + d(d+1)(\partial\beta)^2; \quad (3)$$

here we introduce scalar field

$$\phi(x) = \pm m_D^2 d(d-1)e^{-2\beta(x)}. \quad (4)$$

We suppose that all quantities are slowly varying; that is, consider each derivative ∂_μ (including those in the definition of R_4 (Ricci scalar corresponding to $g_{\mu\nu}$)) as an expression containing a small parameter ε, and neglect all quantities of orders higher than $O(\varepsilon^2)$. Then we have the following decompositions:

$$F(R) = F(\phi + R_4 + f_1) \simeq F(\phi) + F'(\phi)\cdot(R_4 + f_1) + \ldots, \quad (5)$$

where $F'(\phi) \equiv dF/d\phi$. For detailed analysis we refer to [16, 18, 19].

We implement the conformal mapping leading to the Einstein frame:

$$g_{\mu\nu} \longmapsto \widetilde{g}_{\mu\nu} = |f(\phi)|\, g_{\mu\nu}, \qquad f(\phi) = e^{d\beta}F'(\phi). \quad (6)$$

After reduction to 4 dimensions the dynamics of the model is defined by the following action:

$$S = \frac{\nu[d]\, m_D^2}{2}\int d^4x\sqrt{{}^4 g}\left(\operatorname{sign} F'\right)L, \quad (7)$$

where $\nu[d] = \int d^d x\sqrt{{}^d g}$ is the volume of a compact hyperbolic d-dimensional extra space of a unit curvature. The volume of such a space could be arbitrary large without contradiction to observations [20–22].

The Lagrangian in the Einstein frame has the form

$$L = \widetilde{R}_4 + \frac{1}{2}K_{\text{Ein}}(\phi)(\partial\phi)^2 - V_{\text{Ein}}(\phi), \quad (8)$$

$$K_{\text{Ein}}(\phi) = \frac{1}{2\phi^2}\left(6\phi^2\left[\frac{F''}{F'}\right]^2 - 2d\phi\frac{F''}{F'} + \frac{1}{2}d(d+2)\right) + \frac{2(c_1 + c_2)}{F'\phi}, \quad (9)$$

$$V_{\text{Ein}}(\phi) = -\frac{\operatorname{sign}(F')}{F'^2}\left[\frac{|\phi|\, m_D^{-2}}{d(d-1)}\right]^{d/2}\left(F(\phi) + c_V\frac{\phi^2}{d}\right),$$
$$c_V = c_1 + \frac{2c_2}{d-1}, \quad (10)$$

$$F(\phi) = \phi + c\phi^2 + b_1\phi^3 + b_2\phi^4 - 2\Lambda. \quad (11)$$

$F(\phi)$ is the function introduced in (2), b_1, b_2 are initial parameters of the model, d is a dimension of extra space, and $\widetilde{R}_4$ is the Ricci scalar constructed from the conformal metric $\widetilde{g}_{\mu\nu}$ of the Einstein frame.

The action acquires the standard form after the renormalization of the kinetic and potential terms

$$K(\phi) = \frac{M_{\text{pl}}^2}{2}K_{\text{Ein}}, \qquad V(\phi) = \frac{M_{\text{pl}}^2}{2}V_{\text{Ein}}, \quad (12)$$

where the Planck mass M_{pl} is expressed in terms of the initial parameters as follows:

$$\nu[d]\, m_D^2 \simeq M_{\text{pl}}^2. \quad (13)$$

In what follows we will use Hubble units ($H = 1$), where H is the value of Hubble parameter at the inflationary stage (we assume $H = 10^{-6}M_{\text{pl}}$).

The potential (10) possesses one maximum; see Figure 2 with some parameter values represented in captions of Figure 3. The observable cosmological constant is small comparing to the energy density at early stages and corresponding conditions

$$V(\phi_{\min}) = 0, \qquad V'_\phi(\phi_{\min}) = 0 \quad (14)$$

give two constraints to parameters of our model.

To simplify the further analysis we will consider the kinetic term in the form (see Figure 1)

$$K(\phi) \approx \frac{c_5}{\phi^2} \quad (15)$$

valid at small ϕ (see Figure 2).

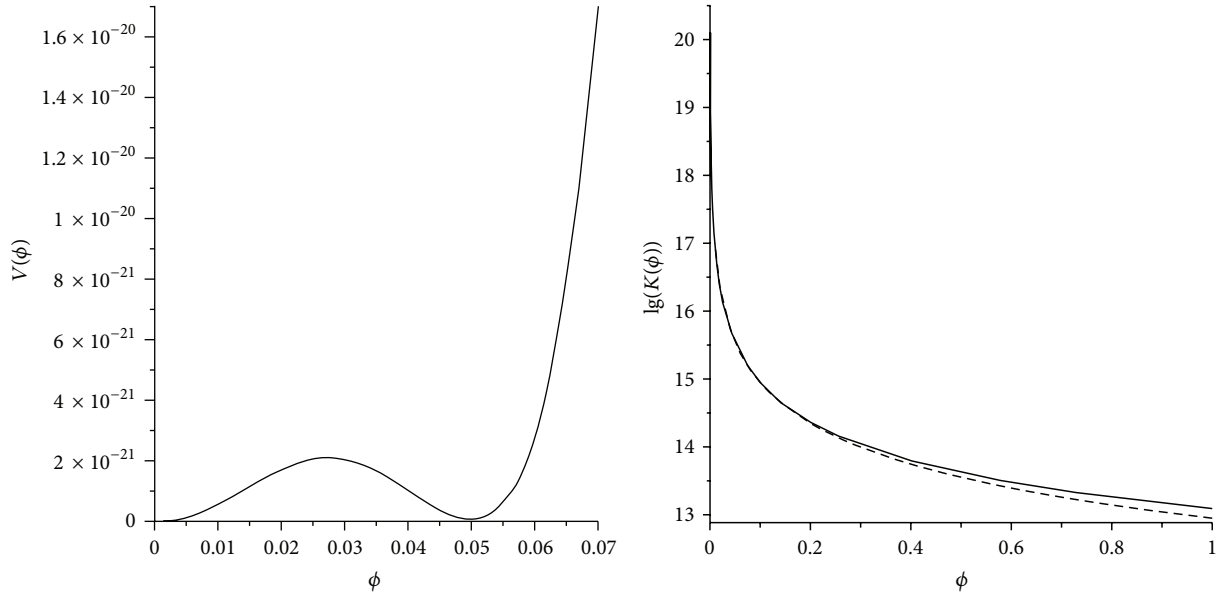

Figure 1: Right panel: Solid line: $\lg K(\phi)$ function; dotted line: approximation of $\lg K(\phi)$; see (15). One can see that this approximation is valid for the small values of ϕ where a dynamic is developed; see Left panel: Potential $V(\phi)$. Numerical values of the parameters are listed in the caption of Figure 3.

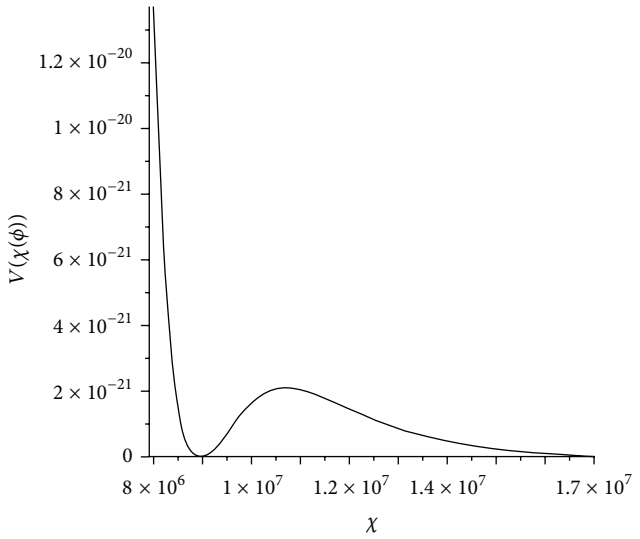

Figure 2: Potential possesses one maximum at $\chi = \chi_{\text{crit}}$ and one minimum at $\chi = \chi_{\text{min}}$. When the field in some region reaches the value $\chi = \chi_{\text{crit}}$ some part of causally independent domains can flip to the other side of the potential with the field value $\chi > \chi_{\text{crit}}$.

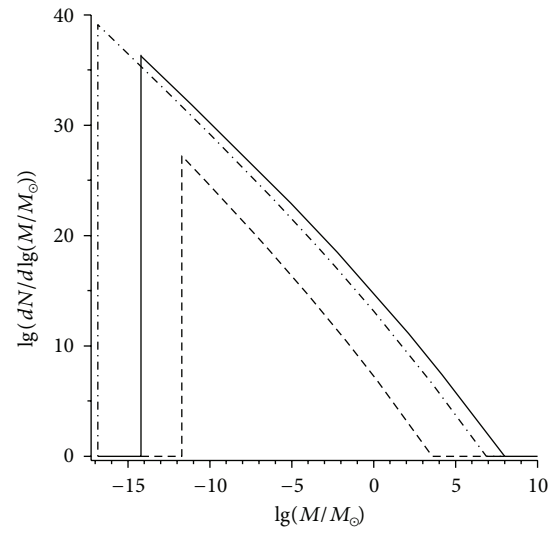

Figure 3: Solid line: mass spectrum of primordial BHs for the parameter values: $c_5 = 8.9 \cdot 10^{12}$, $c = 5.6 \cdot 10^{-6}H^{-2}$, $d = 5$, $b_1 = 12.89 \cdot 10^{-6}H^{-4}$, $b_2 = -8 \cdot 10^{-8}H^6$, $c_1 = 2H^{-2}$, $c_V = -50H^{-2}$, $\Lambda = 0.0125H^2$, $\chi_0 = 1.069 \cdot 10^7 H$, $\nu[d] = 10^3$, and $m_D = 4.4 \cdot 10^4 H$. The spectrum of the PBHs is very sensitive to the initial conditions, so that slight change of χ (in order of $10^{-5}H$) drastically changes the picture (dashed and dot-dashed lines).

In terms of a new field $\chi = -\sqrt{c_5}\ln\phi$ the Lagrangian takes the standard form:

$$L = \frac{1}{2}(\partial\chi)^2 - V(\phi(\chi)). \tag{16}$$

Quantum fluctuations during inflation lead to the appearance of lots of causally independent space regions. Due to quantum fluctuations, each of these regions is characterized by specific value of the field. Eventually field value reaches the maximum at $\chi = \chi_{\text{crit}}$ (see Figure 2) in some region and some part of causally independent domains can flip to the other side of the potential with the field value $\chi > \chi_{\text{crit}}$. In the following the field in such domains moves classically from the maximum to $\chi \to \infty$. After the end of inflation the universe

is filled with the phase $\chi = \chi_{\min}$ except some set of regions filled with the phase $\chi \to \infty$.

As was established [11] domain walls are formed between the regions characterized by different phase. These walls are expanding along with the rest of the space. When the inflationary period is over and the universe stops expanding exponentially, domain walls begin to collapse. In the case when domain wall collapses down to its Schwarzschild radius, the black hole forms.

The detailed description of quantum fluctuations during the inflationary stage can be found in [23, 24]. The corresponding mathematical tool was developed in [25, 26]. An amplitude of quantum fluctuations obeys the Gauss distribution with the average value $\phi(N)$ equal to the classical component of the field at the e-fold number N:

$$dP\left(\chi_{\text{crit}}\right) = \frac{1}{\sqrt{2\pi\left(N_u - N\right)}} \exp\left(-\frac{\left(\chi_{\text{crit}} - \chi\left(N\right)\right)^2}{2\delta\chi^2\left(N_u - N\right)}\right). \quad (17)$$

Here $\delta\chi = H/(2\pi)$ is the average value of the amplitude of the field fluctuation and $N_u = 60$ is a duration of the inflationary period.

Number of regions filled with the phase $\chi > \chi_{\text{crit}}$ that appear during one e-fold and N e-folds before the end of inflation and that lead to the formation of BHs is defined by the probability (17). The volume filled with the false vacuum can be calculated using the iterative procedure. Let $v(t)$ be a volume with new phase. This volume is expanding in e^3 times during one e-fold. Besides, new volume $\Delta v(t)$ will be filled with the new phase due to quantum transitions. Finally we obtain the connection

$$\begin{aligned} v\left(t+1\right) &\simeq v\left(t\right)e^3 + \Delta v\left(t\right), \\ \Delta v\left(t\right) &\equiv \left[v_U\left(t+1\right) - e^3 v\left(t\right)\right] dP\left(t\right); \end{aligned} \quad (18)$$

here we substitute $t = 60 - N$, where N is a number of e-folds before the end of inflation and $v_U = e^{3(N_U - N)}H^{-3}$ is the volume of the universe. We also put $N_U = 60$ followed from observations. Number of closed walls is estimated as

$$N_{\text{walls}} = H^3 \Delta v\left(t\right). \quad (19)$$

After the end of the inflationary period these regions are surrounded by closed domain walls. Due to the collapse of such a domain wall its energy is concentrated in a small volume inside the Schwarzschild radius—fulfilling the necessary condition for the formation of PBH. To calculate the amount of energy concentrated during the collapse of a domain wall we should estimate the surface energy density of the wall σ that depends on the parameters of the potential (10).

To simplify the analysis let us approximate the potential term of our model in the vicinity of its maximum by Higgs-like potential; see Figure 2. In this case the soliton solution is well known [27] together with its width d_w and surface energy density σ.

The radius R of the region that is formed N e-folds before the end of inflation was found in [11]

$$R = \left(2^8\pi\sigma\right)^{-1/3}\left(\frac{M_{\text{pl}}}{H}\right)^{2/3} N^{-2/3} \exp\left(\frac{4N}{3}\right). \quad (20)$$

Thereby we get the total amount of energy of the black hole as $E \sim 4\pi R^2\sigma$. Masses of the forming BHs depend on the typical size of the closed wall. This size is the bigger; the earlier space region surrounded by the domain wall starts to form.

3. Primordial Black Holes as MACHO Objects

Discrete spectrum $N_{\text{PBH}}(M)$ of specific masses M of PBH can be easily obtained by iterative procedure (18). It will be used later (see (25)) for an estimation of PBH density. Much more informative is the differential spectrum of the PBHs presented in Figure 3. It is obtained approximately on the basis of numerical solution $N_{\text{PBH}}(M)$.

We presented three different spectra, to show the dependence of spectra on the initial conditions and parameters of the Lagrangian. Since PBHs are forming during the phase transitions when the domain wall collapses inside the Schwarzschild radius r_{Sch} there exists a natural requirement

$$r_{\text{Sch}} < d_w \quad (21)$$

that cuts off PBHs of smaller masses. If the width d_w of the domain wall is bigger than r_{Sch} then PBHs of that mass cannot form.

There exist strong constraints on the PBHs of the mass about 10^{15} g, so the fact that PBHs with masses $<10^{16}$ g do not appear under certain choice of the parameters allows us to avoid the constraints related to the evaporations of PBHs during Big Bang nucleosynthesis.

According to [9] the current PBHs density is limited from above by parameter

$$\begin{aligned} \Omega_{\text{PBH}} &= \frac{M n_{\text{PBH}}\left(t_0\right)}{\rho_c} \\ &\approx \left(\frac{\beta\left(M\right)}{1.15\times10^{-8}}\right)\left(\frac{h}{0.72}\right)^{-2}\gamma^{1/2}\left(\frac{g_{*i}}{106.75}\right)^{-1/4} \\ &\quad\times\left(\frac{M}{M_\odot}\right)^{-1/2} \end{aligned} \quad (22)$$

for PBHs which have not been evaporated yet. Here M is the PBHs mass, $n_{\mathrm{PBH}}(t_0)$ is their concentration, ρ_c is the critical density, $\beta(M) = \rho_{\mathrm{PBH}}(t_i)/\rho(t_i)$ and t_i indicates an epoch of PBH formation, $h = 0.72$ is the Hubble parameter, γ is a numerical factor of order unity related to the gravitational collapse details, and g_{*i} is the number of relativistic degrees of freedom.

It is convenient to define a new parameter $\beta'(M)$:

$$\beta'(M) = \gamma^{1/2}\left(\frac{g_{*i}}{106.75}\right)^{-1/4}\beta(M) \tag{23}$$

so that (22) gives

$$\beta'(M) = 1.15\times 10^{-8}\Omega_{\mathrm{PBH}}\left(\frac{M}{M_\odot}\right)^{1/2}. \tag{24}$$

Contribution of PBH into the average energy density Ω_{PBH} may be estimated as follows:

$$\Omega_{\mathrm{PBH}}(t_0) = \frac{M\cdot N_{\mathrm{PBH}}(M)}{\rho_c v_U}, \tag{25}$$

where uniform space distribution of PBH is supposed. Here $N_{\mathrm{PBH}}(M)$ is the number of PBHs of mass M discussed in the beginning of this section, and $v_U \approx l_U^3$ is the volume of the universe with $l_U \approx 6000$ Mpc.

To satisfy the constraints (see [9]), we should have

$$\begin{aligned}\beta'(M) &< 10^{-21} \quad \text{for } M \approx 10^{16} g\left(\approx 10^{-17} M_\odot\right),\\ \beta'(M) &< 10^{-18} \quad \text{for } M \approx 10^{17} g\left(\approx 10^{-16} M_\odot\right).\end{aligned} \tag{26}$$

They are true for the solid and dashed lines while the dot-dashed line does not satisfy these conditions. According to the chaotic inflation, a lot of universes with different initial conditions are formed due to quantum fluctuations. In our context it means that there are a lot of universes filled be various number of PBH and we live in one of them. Comparison of solid and dashed distribution reveals strong dependence on initial conditions.

The differential spectrum represented by solid line in Figure 3 gives total mass of all PBHs $M_{\mathrm{total}} \approx 2\times 10^{22} M_\odot$, what could explain most of the hidden mass of the universe.

The mass of the particles corresponding to the field χ is about 10 KeV that is small enough for them to remain unseen. Axions and gravitino in GMSB model are other examples of very light particles that have not been detected yet [28–30].

4. Conclusion

In this paper, we propose a way to explain the hidden mass of the universe. Our approach is based on the scalar fields that appear in frame of the multidimensional gravity. Components of extra space metric are perceived as scalar fields. Appropriate Lagrangian in low energy limit is obtained from the initial pure gravitational Lagrangian in $d + 4$ dimensions.

Closed domain walls formed during the inflationary phase of the universe begin to collapse immediately after the end of inflation. If due to the collapse of domain wall its energy is concentrated within the gravitational radius, one can expect the formation of a primordial black hole.

Primordial black holes with wide range of masses are uniformly dispersed in the early universe. Their mass spectrum satisfies the observational constraints on the density of primordial black holes. Their total mass is large enough to explain substantial of the dark matter in the universe. This approach is an alternative to the WIMP-explanation of dark matter. Nevertheless, there is a room for particles beyond the standard model.

Conflict of Interests

The authors declare that there is no conflict of interests regarding the publication of this paper.

Acknowledgments

The authors are grateful to K. Belotsky, A. Kirillov, and I. Svadkovsky for their interest and helpful remarks.

References

[1] J. E. Kim and G. Carosi, "Axions and the strong CP problem," *Reviews of Modern Physics*, vol. 82, no. 1, pp. 557–601, 2010.

[2] M. Yu. Khlopov, A. S. Sakharov, and D. D. Sokoloff, "The nonlinear modulation of the density distribution in standard axionic CDM and its cosmological impact," *Nuclear Physics B*, vol. 72, no. 1–3, pp. 105–109, 1999.

[3] H.-C. Cheng, J. L. Feng, and K. T. Matchev, "Kaluza-Klein dark matter," *Physical Review Letters*, vol. 89, no. 21, Article ID 211301, 4 pages, 2002.

[4] C. Weniger, "A tentative gamma-ray line from dark matter annihilation at the Fermi large area telescope," *Journal of Cosmology and Astroparticle Physics*, vol. 1208, article 007, 2012.

[5] M. Y. Khlopov and A. G. Polnarev, "Primordial black holes as a cosmological test of grand unification," *Physics Letters B*, vol. 97, no. 3-4, pp. 383–387, 1980.

[6] I. D. Novikov, A. G. Polnarev, A. A. Starobinsky, and B. Ya. Zeldovich, "Primordial black holes," *Astronomy & Astrophysics*, vol. 80, pp. 104–109, 1979.

[7] A. G. Polnarev and M. Y. Khlopov, "Cosmology, primordial black holes, and supermassive particles," *Soviet Physics Uspekhi*, vol. 28, no. 3, pp. 213–232, 1985.

[8] W. Sutherland, "Gravitational microlensing—a report on the MACHO project," *Reviews of Modern Physics*, vol. 71, no. 1, pp. 421–434, 1999.

[9] B. J. Carr, K. Kohri, Y. Sendouda, and J. Yokoyama, "New cosmological constraints on primordial black holes," *Physical Review D*, vol. 81, no. 10, Article ID 104019, 2010.

[10] T. Harada, "Is there a black hole minimum mass?" *Physical Review D*, vol. 74, no. 8, Article ID 084004, 4 pages, 2006.

[11] S. G. Rubin, M. Yu. Khlopov, and A. S. Sakharov, "Primordial black holes from nonequilibrium second order phase transition," *Gravitation and Cosmology*, supplement 6, pp. 51–58, 2000.

[12] A. V. Grobov, S. G. Rubin, D. A. Samarchenko, and E. D. Zhizhin, "A mechanism of supermassive primordial black hole

formation," *Gravitation and Cosmology*, vol. 17, no. 2, pp. 181–184, 2011.

[13] S. G. Rubin, A. S. Sakharov, and M. Y. Khlopov, "The formation of primary galactic nuclei during phase transitions in the early Universe," *Journal of Experimental and Theoretical Physics*, vol. 92, no. 6, pp. 921–929, 2001.

[14] S. V. Chervon, V. M. Zhuravlev, and V. K. Shchigolev, "New exact solutions in standard inflationary models," *Physics Letters B*, vol. 398, no. 3-4, pp. 269–273, 1997.

[15] M. A. Skugoreva, S. V. Sushkov, and A. V. Toporensky, "Cosmology with nonminimal kinetic coupling and a power-law potential," *Physical Review D*, vol. 88, no. 8, Article ID 083539, 10 pages, 2013.

[16] K. A. Bronnikov and S. G. Rubin, "Self-stabilization of extra dimensions," *Physical Review D*, vol. 73, no. 12, Article ID 124019, 10 pages, 2006.

[17] K. A. Bronnikov, S. G. Rubin, and I. V. Svadkovsky, "Multidimensional world, inflation, and modern acceleration," *Physical Review D*, vol. 81, no. 8, Article ID 084010, 2010.

[18] K. A. Bronnikov and S. G. Rubin, "Abilities of multidimensional gravity," *Gravitation & Cosmology*, vol. 13, no. 4, pp. 253–258, 2007.

[19] K. A. Bronnikov, R. V. Konoplich, and S. G. Rubin, "The diversity of universes created by pure gravity," *Classical and Quantum Gravity*, vol. 24, no. 5, pp. 1261–1278, 2007.

[20] M. Trodden, "Diluting gravity with compact hyperboloids," in *proceedings of the COSMO-2000 Fourth International Workshop on Particle Physics and the Early Universe*, Cheju Island, Republic of Korea, September 2000.

[21] Y. Kim and S. C. Park, "Hyperbolic inflation," *Physical Review D*, vol. 83, no. 6, Article ID 066009, 5 pages, 2011.

[22] D. Orlando and S. C. Park, "Compact hyperbolic extra dimension: a M-theory solution and its implications for the LHC," *Journal of High Energy Physics*, vol. 2010, no. 8, article 006, 2010.

[23] K. A. Bronnikov and S. G. Rubin, *Black Holes, Cosmology and Extra Dimensions*, World Scientific Publishing, River Edge, NJ, USA, 2012.

[24] V. I. Dokuchaev, Yu. N. Eroshenko, S. G. Rubin, and D. A. Samarchenko, "Mechanism for the suppression of intermediate-mass black holes," *Astronomy Letters*, vol. 36, no. 11, pp. 773–779, 2010.

[25] A. A. Starobinsky, "Stochastic de sitter (inflationary) stage in the early universe," in *Field Theory, Quantum Gravity and Strings: Proceedings of a Seminar Series Held at DAPHE*, H. J. de Vega and N. Sanchez, Eds., vol. 246 of *Lecture Notes in Physics*, pp. 107–126, Springer, Berlin, Germany, 1986.

[26] S.-J. Rey, "Dynamics of inflationary phase transition," *Nuclear Physics B*, vol. 284, pp. 706–728, 1987.

[27] R. Rajaraman, *Solitons and Instantons*, North-Holland, New York, NY, USA, 1982.

[28] J. Kandaswamy, P. Salomonson, and J. Schechter, "Mass of the axion," *Physical Review D*, vol. 17, no. 11, pp. 3051–3054, 1978.

[29] G. G. Raffelt, J. Redondo, and N. V. Maira, "The meV mass frontier of axion physics," *Physical Review D*, vol. 84, no. 10, Article ID 103008, 2011.

[30] Particle Data Group, C. Amsler, M. Doser et al., "Review of particle physics," *Physics Letters B*, vol. 667, no. 1–5, pp. 1–6, 2008.

Hindawi Publishing Corporation
Advances in High Energy Physics
Volume 2014, Article ID 891820, 8 pages
http://dx.doi.org/10.1155/2014/891820

Research Article

Dark Photon Searches Using Displaced Vertices at Low Energy e^+e^- Colliders

Fabio Bossi

Laboratori Nazionali dell'INFN, Via E. Fermi 40, 00044 Frascati, Rome, Italy

Correspondence should be addressed to Fabio Bossi; fabio.bossi@lnf.infn.it

Received 26 November 2013; Accepted 29 January 2014; Published 11 March 2014

Academic Editor: Jean-René Cudell

The existence of a new, photon-like, massive particle, the γ' or dark photon, is postulated in several extensions of the Standard Model. These models are often advocated to explain some recent puzzling astrophysical observations, as well as to solve the so far unexplained deviation between the measured and calculated values of the muon anomaly. Dark photons can be produced at e^+e^- colliders both in continuum events and in vector meson transitions and can eventually decay into an electron-positron pair. For a proper choice of the parameters of the theory, a γ' can have a relatively long lifetime and can therefore be observed as an e^+e^- vertex well separated by the primary interaction point. This case is discussed in reference to very high luminosity e^+e^- colliders either in construction or under study in several laboratories in the world. It is shown that a search strategy based on the detection of displaced vertices can be in principle very effective in covering a rather wide and to date unexplored region of the theoretical parameters space.

1. Introduction

In the Standard Model (SM), interactions among elementary particles are mediated by the vector bosons of the strong, weak, and electromagnetic forces. Experimental evidence for the existence of those bosons is compelling and precise measurements of their properties have been accumulated in the past decades. New forces can have escaped detection so far, either if their associated bosons are very heavy or if their couplings to ordinary matter are weak enough. The latter case has been advocated, among others, in models which try to explain and reconcile among them several puzzling astrophysical observations performed in recent years [1–4]. They are sometimes also used to reconcile the measured value of the muon anomaly to the SM prediction, which differ by approximately by 3.5σ (see, e.g., [5]).

If new, light, neutral bosons (which from now on will be called γ' or *dark photons*) exist and if they are measurably, albeit weakly, coupled with SM particles, they can be produced and observed at colliding-beams and fixed target experiments [6–12]. In fact, there have been several attempts to observe evidence for such particles, using data from running facilities [13–19] or data mining old experiments [7, 20–23]. Since no evidence for their existence was found, limits have been set as a function of the γ' mass and of its coupling to ordinary matter.

In the near future, new experiments under construction are expected to extend those limits in a region of couplings and/or masses so far unexplored. All of them are designed to exploit the radiative production of the γ' by a very intense electron or positron beam on a properly built high-Z target [24–29]. The purpose of the present letter is to show that comparable results can be obtained by high luminosity and low energy electron-positron colliders, such as those under construction or under study in several laboratories in the world [30–32]. These facilities will take advantage of two main construction features which coherently conspire to enhance their discovery potential: their very high goal luminosity and the usage of very compact beams (these two features are in fact strongly correlated). Actually, high luminosity translates into the possibility of probing lower production cross sections, that is, lower effective couplings between the γ' and ordinary matter. On the other hand, low couplings translate into longer γ' decay paths, especially for low γ'

masses. Thus, the usage of beams of very small dimensions allows one to obtain a clear γ' signal by observing secondary vertices of a well-defined invariant mass, well separated by the beams interaction point.

In the paper, this case will be discussed for three different possible choices of the machine center-of-mass energy, corresponding, respectively, to the mass of the $\phi(1020)$, the $J/\psi(1S)$, and the $\Upsilon(4S)$ mesons. This choice is motivated by the projects mentioned above. It will be shown that higher energy machines are favoured, not only because they are expected to deliver larger data sets, but also because the γ' therein produced have longer decay paths, ceteris paribus. Instrumental effects play however a relevant role in the actual detection strategy and can in some cases dramatically reduce the discovery potential of the method. Still, in particular for the case of a high luminosity τ-charm factory, it remains high enough to be competitive to the fixed target experiments mentioned above.

The paper is organized as follows. Firstly, the theoretical framework of the paper is discussed, together with a short presentation of the experimental limits on the existence of dark photons obtained so far. The case for the searches at low energy, high luminosity e^+e^- colliders is discussed in Section 3, followed by some considerations on the actual implementation of the proposed method to existing, or planned, facilities. Radiative vector meson decays are discussed in Section 5. Conclusions are given in Section 6.

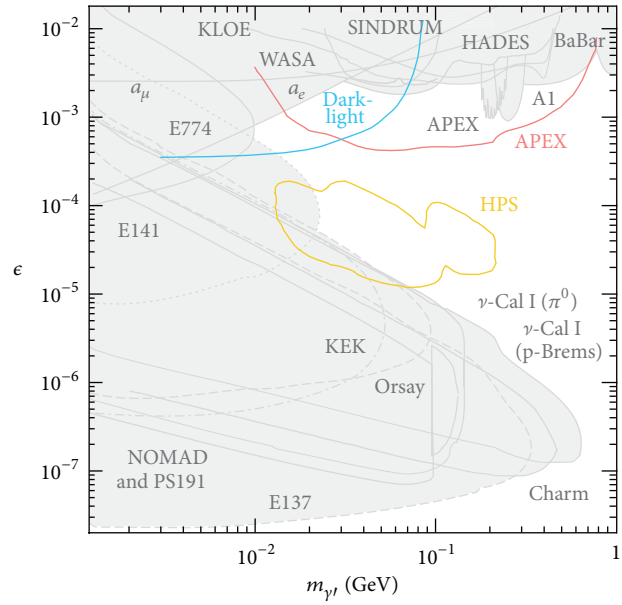

Figure 1: Excluded region in the plane ϵ-$m_{\gamma'}$ resulting from presently available data. Electron beam dump experiment covers the region of low masses and very low couplings, down to $\epsilon \sim 10^{-7}$. For higher masses and lower couplings limits come mainly from meson decays and electron-nucleon scattering experiments and to B-factories data (plot courtesy of S. Andreas). The plot reports also the projections for the experiments presently under construction. For details on single experiments see [39].

2. Physics Case

In many new physics scenarios, the SM is extended by simply adding an additional $U(1)_D$ symmetry, under which SM particles are uncharged at first order [5, 33, 34]. The gauge boson associated to the new symmetry, the γ', can still interact with ordinary matter via kinetic mixing described by an effective interaction Lagrangian. Consider

$$L_{\text{kin-mix}} = i\epsilon e \overline{\psi}_{\text{SM}} \gamma^\mu \psi_{\text{SM}} A_\mu, \tag{1}$$

where A denotes the γ' field. The kinetic mixing factor ϵ parametrizes the coupling strength relative to the electric charge and is predicted in various models to be in the range 10^{-12}–10^{-2}. The mass of the dark photon ($m_{\gamma'}$) rests unpredicted. On phenomenological grounds, however, masses in the MeV–GeV range, which are of interest for the present work, are favoured.

There might exist non-SM matter particles which are sensitive to the new $U(1)_D$ interaction. Often they are postulated to be the main constituent of the yet undiscovered dark matter component of the universe (DM) and must therefore be electrically neutral and stable. If kinematically allowed, the γ' will decay preferably into pairs of these particles; thus its decay becomes "invisible." The case for detecting invisible decays is discussed, for instance, in [28, 35–38]. On the other hand, if the dark photon is lighter than DM, it is forced to decay into a pair of SM particles, with a width regulated by (1). In this case, its proper time is approximately given by [39]

$$c\tau\,(\text{mm}) = \frac{0.08}{N_f} \cdot \left(\frac{10^{-4}}{\epsilon}\right)^2 \cdot \frac{100}{m_{\gamma'}\,(\text{MeV})}, \tag{2}$$

where N_f is the number of SM decay channels allowed by kinematics.

There have been several attempts to experimentally observe a γ' signal, using many different techniques. Figure 1, taken from reference [39], shows the exclusion plot in the plane $m_{\gamma'}$-ϵ, resulting from the above mentioned searches. Electron beam dump experiment covers the region of low masses and very low couplings, down to $\epsilon \sim 10^{-7}$. For higher masses and lower couplings, limits come mainly from meson decays and electron-nucleon scattering experiments and to B-factories data. Important information, not shown in Figure 1, can also be deduced by astrophysical observations (see for instance [40] and references therein). For $m_{\gamma'} > 10$–20 MeV, the region with $\epsilon < 10^{-3}$ remains largely unexplored.

There are currently various experiments either running or under construction aiming at probing part of this region. All of them are designed to exploit the radiative production of the γ' by a very intense electron or positron beam on a properly built high-Z target. In particular, the HPS experiment at Thomas Jefferson Laboratory (USA) is designed to cover the region $\epsilon = (10^{-4}, 10^{-5})$, $m_{\gamma'} = (20, 300)$ MeV [25] (see Figure 1).

In the following, the case for the search for dark photons in the same parameters space region at a very high luminosity e^+e^- collider will be discussed.

3. Searches at e^+e^- Colliders

In the last decades, large amount of data have been collected at high luminosity e^+e^- flavour factories operating at different center of mass energies. These data range from the ~2 fb^{-1} delivered at the $\phi(1020)$ peak by the Italian collider DAΦNE to the 0.5–1 ab^{-1} produced by the B-factories at PEP-II (USA) and KEK-B (Japan). In the near future, a consistent increase of the above statistics is expected both at DAΦNE and at KEK-B which aims at increasing their data sample by factors of 10 and 50, respectively. An option to increase the center of mass energy of DAΦNE up to 2.5 GeV has been taken into consideration [41]. Finally, studies for the construction of a collider capable of delivering ~1 ab^{-1} around the charm threshold are under consideration in Italy, Russia, and China (see for instance [31]).

As of today, searches for dark photons at e^+e^- colliders have been pursued mainly by studying the process $e^+e^- \to \gamma\gamma'$ with the subsequent decay of the γ' into a $\mu^+\mu^-$ pair. This limits the search to $m_{\gamma'} > 2m_\mu$, which, as a consequence of (2), results in its lifetime being unmeasurably short. Therefore, the signal can be separated by the more copious and otherwise indistinguishable QED background, only by observing a sharp peak in the invariant mass distribution of the final state lepton pair.

The question arises whether it would be possible to extend the search also to the region with $m_{\gamma'} < 2m_\mu$ and in particular with $\epsilon < 10^{-3}$. The main message of the present paper is that the foreseen increase of the potentially available data sample allows one to give a positive answer to the above question, not only because of the increased statistical sensitivity but also because it opens the doors to the possibility of observing a clear signal for a long-lived γ', which is only marginal with the presently available data.

Here and in what follows, for the sake of simplicity, only the case of symmetric machines is considered. Also, since we are interested in the case with $m_{\gamma'} < 2m_\mu$, the dark photon can decay only into a e^+e^- pair.

The differential cross section for radiative γ' production in e^+e^- collisions is given by [11]

$$\frac{d\sigma}{d\cos\theta} = \frac{2\pi\alpha^2\epsilon^2}{{E_{\text{c.m.}}}^2} \cdot \frac{1+\cos^2\theta}{\sin^2\theta}, \tag{3}$$

where θ is the angle between the incoming positron and the outcoming photon and $E_{\text{c.m.}}$ denotes the center of mass energy of the event. By integrating the above equation between $\cos(\theta) = \pm 0.8$, one obtains a total cross section of approximately $0.9 \times \epsilon^2\ \mu$b, $0.1 \times \epsilon^2\ \mu$b, and $3.6 \times \epsilon^2$ nb for $E_{\text{c.m.}} = 1.02$, 3.1, and 10.5 GeV, respectively. Thus, in the presently available data samples, for $\epsilon = 10^{-4}$ a few dozens γ' can be found.

Due to the two body kinematics, the dark photon is boosted in the laboratory frame by a factor $E_{\text{c.m.}}/m_{\gamma'}$. Therefore, for small kinetic mixings and for low enough dark photon masses, its lifetime in the laboratory frame becomes sizeable. For instance, for $\epsilon = 10^{-4}$ and $m_{\gamma'} = 20$ MeV, the mean decay path of a dark photon is ~1, 3, and 10 cm for $E_{\text{c.m.}} = 1.02$, 3.1, and 10.5 GeV, respectively.

Can these long decay paths be exploited to separate a potential γ' signal from the QED background? Clearly, although the secondary vertex can be determined with standard vertexing techniques, cannot be, on an event by event basis. On the other hand, the actual position and size of the collision envelope can be determined on a statistical basis using known processes, such as Bhabha scattering or muon pair production. Interestingly, at all of the e^+e^- facilities under consideration, one of the strategies used to maximize luminosity is to keep the transverse beam dimensions at the interaction point as small as possible, typically ≤1 mm. Therefore, assuming a perfectly Gaussian distribution of the beam spot, with a maximum transverse dimension of 1 mm, the probability for observing an e^+e^- vertex from standard QED processes at a transverse distance of 1 cm or more from the center of the collision spot is practically zero. On the other hand, the number of γ' decay events with transverse decay path larger than 1 cm, $N_{1\,\text{cm}}$ can be as large as several thousands, depending on the actual value of ϵ, $m_{\gamma'}$, and $E_{\text{c.m.}}$ and of the luminosity integrated by the machine, L_{int}.

Figure 2 shows the variation of $N_{1\,\text{cm}}$ as a function of ϵ, for different values of $m_{\gamma'}$ and for three different experimental conditions: (a) $E_{\text{c.m.}} = 1.02$ GeV, $L_{\text{int}} = 20$ fb^{-1}; (b) $E_{\text{c.m.}} = 3.1$ GeV, $L_{\text{int}} = 1$ ab^{-1}; (c) $E_{\text{c.m.}} = 10.5$ GeV, $L_{\text{int}} = 50$ ab^{-1}. The chosen values for L_{int} correspond to the target performance for the facilities under construction or under study mentioned above. The behaviour of the curves is easily explained. For $\epsilon \ll 10^{-4}$ the mean decay path of a dark photon is much larger than 1 cm, and therefore $N_{1\,\text{cm}}$ increases with ϵ^2, independently of $m_{\gamma'}$. It eventually reaches a peak and drops rapidly towards zero, as long as, with increasing ϵ, the lifetime becomes shorter and shorter. The position of the peak is determined by the proper balance between the effect of the production cross section, which increases with ϵ^2, and that of the lifetime which decreases with it. It depends also on the value of $m_{\gamma'}$, the decay path decreasing again quadratically with it. It is seen that, despite the lower production cross section, the largest expected integrated luminosity combined with the higher boost factors favours the B-factory option (case (c)). In this case, however, the peak of the distribution, especially for lower masses, is obtained for values of the kinetic mixing ~10^{-3}. It can be noted also that in case (a) the number of observable dark photons with masses greater than ~30 MeV becomes hopelessly small. This is not only due to the lower luminosity but also to the reduced Lorentz boost, consequence of the lower center of mass energy of the collision.

Although the results obtained so far look very encouraging on general grounds, there are two main limitations coming from the implementation of the above search strategy into a real experiment. On the one hand, for specific values of the parameters, the γ' lifetime becomes so long that a relevant part of the decays would escape detection of an apparatus of realistic dimensions. For instance,

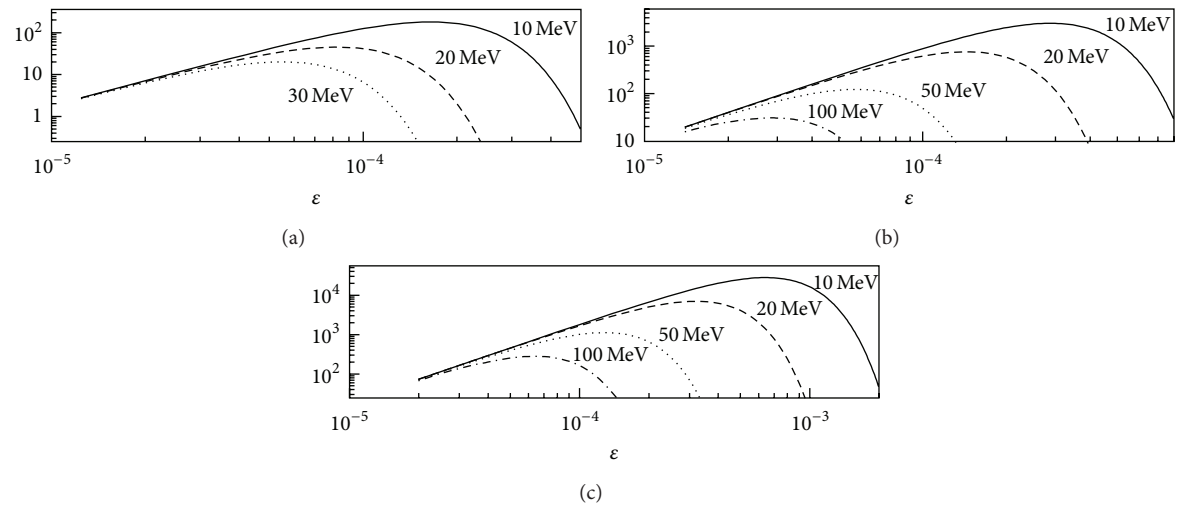

FIGURE 2: Number of γ' decay events with transverse decay path larger than 1 cm, as a function of ϵ, for different values of $m_{\gamma'}$. Three different experimental conditions are taken into consideration: (a) $E_{\text{c.m.}} = 1.02\,\text{GeV}$, $L_{\text{int}} = 20\,\text{fb}^{-1}$; (b) $E_{\text{c.m.}} = 3.1\,\text{GeV}$, $L_{\text{int}} = 1\,\text{ab}^{-1}$; (c) $E_{\text{c.m.}} = 10.5\,\text{GeV}$, $L_{\text{int}} = 50\,\text{ab}^{-1}$. Note that the horizontal scale is slightly different for the three plots.

for $E_{\text{c.m.}} = 10.5\,\text{GeV}$, $\epsilon = 5 \times 10^{-5}$, and $m_{\gamma'} = 10\,\text{MeV}$, the γ' mean decay path is about 1.5 m. More importantly, a very dangerous instrumental background comes into operation, namely, photon conversions on the detector material induced by $e^+e^- \to \gamma\gamma$ events. This is particularly relevant since experiments are often designed to have beam pipes with very small radii at the interaction point. Although one can try to minimize the conversion probability on the detector elements, by properly choosing type and dimensions of the materials, the cross section of the $e^+e^- \to \gamma\gamma$ process is so much larger than the signal one (in fact, it is larger by a factor ϵ^{-2}) that this background rapidly becomes unbeatable.

The simplest way to cope with this problem is to allow for a large enough empty region around the interaction point, where photons cannot interact with matter and dark photons can at least partly undergo their decay. It would then be reasonable to accept only events with decay vertices occurring before the beam pipe but still far (1 cm) from the nominal beam spot center. Assuming a beam pipe of 5 cm radius, such as that presently used by the KLOE-2 experiment at DAΦNE, the number of events thus obtained within acceptance, n_{acc}, is shown in Figure 3 for the three cases under consideration.

For high values of ϵ, this acceptance cut does not observably affect the previous distributions. In fact, in this case, the lifetime is so short that almost all of the dark photons decay much before 5 cm. For lower values of ϵ, instead, the consequence of the cut in acceptance is more visible and can decrease the number of accepted events by an order of magnitude, especially for very low γ' masses. However, and this is one of the main messages of this paper, the number of potentially observable events remains still considerable for a wide region of the parameter space, especially for the higher energy machine options. In particular, also allowing for some further detection inefficiency, it can be seen that kinetic mixings down to few times 10^{-5} and masses up to ~200 MeV can be probed.

Based only on signal statistics (i.e., without taking into consideration possible detector resolution effects and other possible instrumental backgrounds), this translates into the explorable regions shown in Figure 4, for the three cases under consideration. While case (a) covers almost entirely a region already excluded by previous beam-dump experiments, cases (b) and (c) can potentially probe a relatively wide unexplored region (see Figure 1). On the other hand, it has also to be underlined that this same region is expected to be covered by the aforementioned future fixed target experiments (see again Figure 1).

It is worthwhile stressing once more that the requirement for observing a cm-scale decay path ideally rejects every possible physical background to our signal. Still, other instrumental effects need to be taken carefully into account, as discussed in the following section.

4. Implementation at Current and Future Facilities

It is of interest understanding how difficult it would be to practically implement on real experimental facilities the ideas discussed so far. This requires a detailed knowledge of the actual machine and detector's design and expected (or measured) performance. Only specific studies based on these figures can in the end determine whether the method is applicable or not, to which extent, and on which machine. An obvious difference between our simplified models and reality can be found for instance in case (c); both the old and the future B-factories are in fact asymmetric machines, the electron beam being of higher energy with respect to the positron one. Although this might somewhat change the specific acceptance requirements with respect to the symmetric

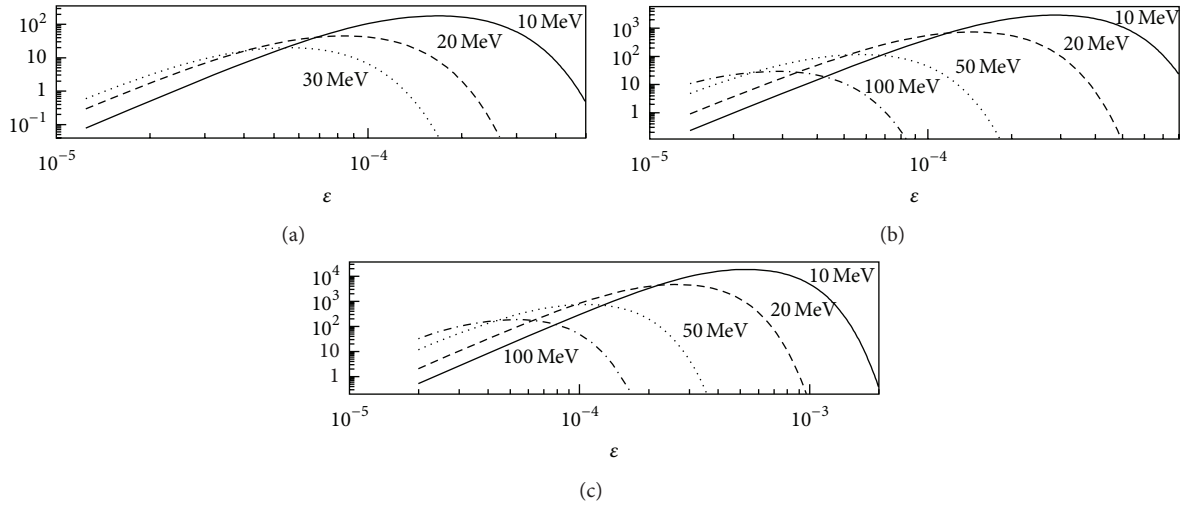

Figure 3: Same as Figure 2, with the further request that the transverse decay path is lower than 5 cm.

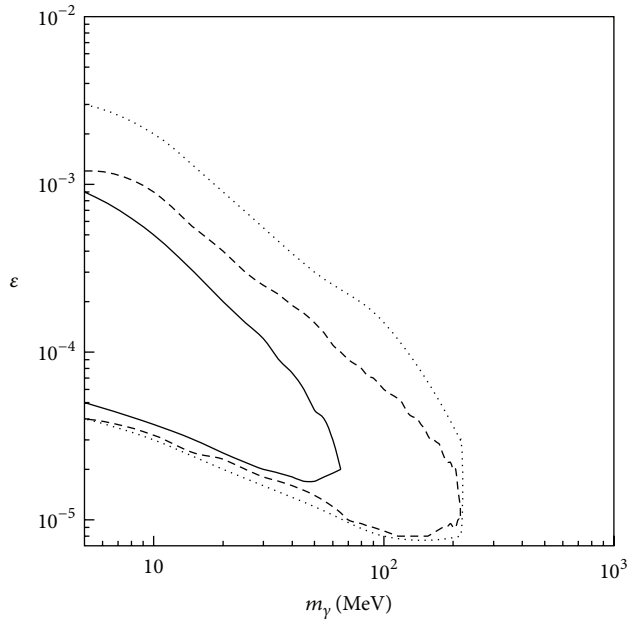

Figure 4: Explorable region for cases (a) solid, (b) dashed, and (c) dotted in the plane ϵ-$m_{\gamma'}$. No instrumental backgrounds are taken into consideration, as well as potential efficiency and resolution effects for the detector. Above ~210 MeV, the opening of the 2-muon channel drastically reduces the effectiveness of the method.

option discussed in this paper, it is however reasonable to assume that similar conclusions can still be drawn.

On general grounds, there are four parameters that have to be taken into consideration: the primary γ' production rate, the dimensions of the beams, those of the beam pipe, and the vertexing capabilities of the detector.

As for the first point, despite the higher production cross section, the ϕ-factory option (case (a)) is less performing than the other two, not only because of the much lower integrated luminosity, but also, as noted before, because of the intrinsic limitation due to the lower Lorentz boost factors. The proposal for running DAΦNE at higher energies is, under this respect, particularly interesting because this would allow increasing the decay paths proportionally to $E_{\text{c.m.}}$.

As previously remarked, for all of the machines under consideration, the dimensions of the beams are kept very small in the transverse direction. For instance, at DAΦNE, the beams have σ_X~1.5 mm, σ_y~0.02 mm, and much lower dimensions at the other machines. Note that both Figures 2 and 3, on which we base our search strategy, refer to transverse decay paths, so the beam dimensions in the longitudinal direction are irrelevant for our conclusions. Obviously, non-Gaussian tails of the collision envelope can to some extent increase the background contamination. However, if not completely suppressed, they can still be studied using other known processes, as for the Gaussian part.

A real concern is the actual beam-pipe dimensions. Among the existing facilities, KLOE-2 at DAΦNE is the only one having a beam pipe radius at the interaction point of 5 cm. As for the machines running at the charm threshold, the only one presently in operation, the Chinese collider BEPC, has a beam pipe at the interaction point of 3.5 cm in radius; however, its present luminosity is about a factor 100 lower than that required by our arguments at that energy. For the B-factories, the beam pipe radii range from the 2.5 cm for the BaBar detector to 1 cm for the future SuperBelle.

While a reconsideration of the inner region of SuperBelle is probably very unlikely, in the case of a future high luminosity τ-charm factory, it is conceivable that the interaction region can be designed so as to maximise the sensitivity for the dark photon search under consideration. It is worth noticing here that the request for minimizing the beam pipe dimensions comes to first order from the experiment more than from the machine. In fact, they are somehow anticorrelated with the detector's vertexing capabilities. Actually, the resolution of a decay length measurement for a generic detector is approximately proportional to the single point resolution of the most internal tracking device and inversely proportional to its distance from the decay point. Under

this respect the less favourable situation is that of KLOE-2, whose first tracking device, a triple-GEM cylindrical detector, has an internal radius of 12 cm and single point resolution of ~200 μm. Still, its estimated vertex resolution for $K^0 \to \pi^+\pi^-$ events is of 1-2 mm [42]. The use of silicon detectors, which can have single point resolution of order 10 μm, would definitely improve with respect to the KLOE-2 case. Noticeably, all the LEP experiments, which had beam pipes of 5.5 cm, could reach typical decay length resolution of ~250 μm for B decay events, thanks to the use of silicon detectors [43]. This implies that, considering the cm scale decay length we have been interested in so far, vertexing resolution should not be a major issue. On the other hand, it can play a relevant role in the considerations discussed in the following section.

5. Meson Decays

Electron-positron colliders provide a useful γ' production mechanism via radiative vector meson decays, too. Actually, for each observed $V \to P\gamma$ decay (V and P being a vector and a pseudoscalar meson, resp.), there could be a $V \to P\gamma'$ process, suppressed by a factor ϵ^2 with respect to the former one [9]. This fact has actually been exploited by the KLOE-2 collaboration which has searched for the dark photon using the $\phi \to \eta e^+e^-$ process in [17, 18]. As for the searches in the $e^+e^- \to \mu^+\mu^-\gamma$ channel, the signal is separated by the SM (Dalitz decay) background by looking for a peak in the invariant mass distribution of the final state lepton pair. However, once the γ' lifetime becomes sizeable, these events are characterised as well by the presence of e^+e^- vertices clearly separated by the collision point, thus allowing the usage of the search strategy described in the previous sections.

The number of produced γ' is given by

$$N_{\gamma'} = N_V \cdot \mathrm{BR}_{VP\gamma} \cdot \epsilon^2, \tag{4}$$

where N_V is the number of produced vector mesons, and $\mathrm{BR}_{VP\gamma}$ is the branching ratio for the corresponding standard radiative decay.

Let us firstly consider the above mentioned $\phi \to \eta\gamma'$ process. At a ϕ-factory, $\sim 3 \cdot 10^9 \phi$ mesons are produced every fb^{-1} delivered by the machine. Since $\mathrm{BR}_{\phi \to \eta\gamma} \simeq 1.3 \cdot 10^{-2}$ [44], it is easily seen that the number of produced signal events, assuming $L_{\mathrm{int}} = 20\,\mathrm{fb}^{-1}$, becomes negligible for $\epsilon \leq 10^{-4}$. On the other hand, for higher values of ϵ, the γ' mean decay path becomes unmeasurably (as compared with millimeter scale vertex resolutions) short, but for very low masses. For instance, for $\epsilon = 2 \cdot 10^{-4}$ it is already 0.8(0.2) cm, for $m_{\gamma'} = 10(20)$ MeV. Unless, therefore, one integrates luminosities largely exceeding those expected from the presently considered machine, the method is hardly applicable to this decay channel.

Let us now turn our attention to the $J/\psi \to \eta'\gamma'$ transition. This process has been already studied in [45], where, however, the case for short lived dark photons only is considered. As before, one has $N_{J/\psi} \simeq 3 \cdot 10^9/\mathrm{fb}^{-1}$, running at the J/ψ peak. Considering that $\mathrm{BR}_{J/\psi \to \eta'\gamma} \simeq 5 \cdot 10^{-3}$ [44], one obtains ~150 events for $\epsilon = 10^{-4}$ and $L_{\mathrm{int}} = 1\,\mathrm{ab}^{-1}$. On the other hand, for this value of kinetic mixing, the γ' mean decay path is of the right order of magnitude only for a limited range of mass values. It is, for instance, 11.2, 2.8, and 0.45 cm for $m_{\gamma'} = 10$, 20, and 50 MeV, respectively. The effect of this is seen in Figure 5 where the number of γ' decays occurring at a distance between 1 and 5 cm from the interaction point is plotted as a function of ϵ, for different values of $m_{\gamma'}$. Differently from the $e^+e^- \gamma$ case, here, it is the effect of the lifetime being short to be dominant, at least for the kinetic mixing values of interest, because for higher dark photon masses and low enough ϵ, almost all of the γ' survive for less than 1 cm. Note, also, that some further reduction in the number of observable events must be considered due to geometrical acceptance considerations. Still, there remains a small region of the parameter space for which one can hope to observe a reasonable number of γ' decays within acceptance.

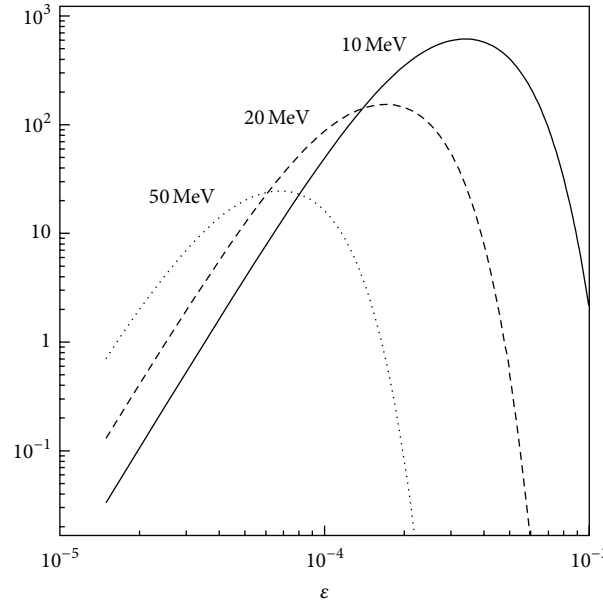

Figure 5: Number of dark photons from the process $J/\psi \to \eta'\gamma'$ with decay paths larger than 1 cm and lower than 5 cm, as a function of ϵ and for various values of $m_{\gamma'}$. An integrated luminosity of 1 ab^{-1} is considered.

There is however a further benefit specific of $V \to Pe^+e^-$ events; these processes can in fact be used also to measure on an event-by-event basis the actual dark photon decay path, provided that the final state meson decays into at least a pair of charged particles. In this case, the position of the latter particles determines the *primary production* vertex, while the γ' decay position is determined, as usual, by the e^+e^- one.

For instance, for $J/\psi \to \eta'\gamma'$ events, one can use the process $\eta' \to \eta\pi^+\pi^-$, where the $\pi^+\pi^-$ pair allows determining exactly the collision point, at the price of reducing the total amount of useful events by a factor ~0.43 [44]. Since we are interested in millimeter scale decay paths, the photon conversion background should not be a problem

anymore. However, there is a physical background to be kept now into consideration, namely, the Dalitz decay of the $J\psi$, $J/\psi \rightarrow \eta' e^+ e^-$. Its branching ratio can be estimated to be approximately BR($J/\psi \rightarrow \eta' e^+ e^-$)~BR($J/\psi \rightarrow \eta'\gamma$) $\times$ 0.01, so that the process is ~10^6 times more frequent than the signal, if $\epsilon = 10^{-4}$. However, in this case, the e^+e^- and $\pi^+\pi^-$ vertices must coincide within the detector's resolution, σ_{res}. Therefore, a reduction of the background by a factor 10^4 can be achieved by accepting only events with measured decay paths larger than $4\sigma_{\text{res}}$. Moreover, background events are expected to have a broad e^+e^- invariant mass distribution, while γ' decays are a narrow resonance in such channel. Not considering form factor effects, the number of background events, N_B, in a window of δm around $m_{e^+e^-} = m_{\gamma'}$ is given approximately by [9]

$$N_B = N_{J/\psi \rightarrow \eta' e^+ e^-} \times B\left(\eta' \longrightarrow \eta\pi^+\pi^-\right) \times \frac{\delta m}{m_{\gamma'}} \times \frac{1}{\ln\left(\left(m_{J/\psi} - m_{\eta'}\right)/2m_e\right)}. \quad (5)$$

Note that the $1/m_{\gamma'}$ dependence on (5) favours the observation of higher mass dark photons. On the other hand, since the decay path scales as $1/m_{\gamma'}^2$, the effect of a finite vertex resolution favours the observation of lower mass particles.

In a given experiment, therefore, two parameters should ideally be kept as small as possible, σ_{res} and δm. Take, for instance, $\epsilon = 10^{-4}$, $m_{\gamma'} = 50$ MeV. According to (5), the number of background events in the interesting mass bin would in this case be ~2×10^5 for $\delta_m = 1$ MeV. By applying the $4\sigma_{\text{res}}$ cut discussed above, this number reduces to ~20. Therefore, for $\sigma_{\text{res}} = 1(0.5)$ mm, the signal significance (i.e., the number of signal events divided by the square root of the background) would be ~4(6). It is important to underline that in this case the dimensions of the beam pipe are to first order irrelevant, since we are dealing with relatively short decay lengths. On the other hand, it has also to be noted, that we are here assuming full detection efficiency which might reveal an overoptimistic assumption. As for the continuum events, only detailed studies based on realistic detector parameters can finally assess the potentials of the method.

6. Conclusions

Experimental searches for a new, light, neutral boson, the "dark photon" or γ', are being pursued in many laboratories in the world, using different detection techniques. If the γ' is light enough and if its couplings with SM particles are suppressed by a factor $\leq 10^{-3}$ with respect to those of the ordinary photon, it can acquire a relatively long lifetime. This fact can be exploited at e^+e^- colliders by searching a $\gamma' \rightarrow e^+e^-$ decay vertex well separated by the *primary production* one, in $e^+e^- \rightarrow \gamma'\gamma$ events. The paper shows that new generation e^+e^- colliders have the potentials to fully exploit this technique and can explore effective couplings down to few times 10^{-5} and γ' masses in the range 10–100 MeV approximately. In general, higher energy machines are favoured, because the higher Lorentz boost of the produced (light) bosons allows a better separation of the secondary vertices. It is also seen, however, that the implementation of this method to real facilities requires a proper design of the interaction region and a wise choice of the tracking detector. To our knowledge, unfortunately, the beam pipe dimensions of SuperBelle are far from being optimal under this respect. On the other hand, since all of the future high luminosity τ-charm factories are still in a preliminary design study phase, it is conceivable that in this case the interaction region can be designed so as to maximise the sensitivity for the proposed γ' search technique. Such a machine can also provide a complementary search method by the observation of displaced e^+e^- vertices in fully reconstructed $J/\psi \rightarrow \eta'\gamma'$ events, therefore, enhancing the interest for the construction of such a facility.

Conflict of Interests

The author declares that there is no conflict of interests regarding the publication of this paper.

Acnowledgments

The author would like to thank S. Andreas and D. Babusci for help and useful discussions.

References

[1] N. Arkani-Hamed, D. P. Finkbeiner, T. R. Slatyer, and N. Weiner, "A theory of dark matter," *Physical Review D*, vol. 79, no. 1, Article ID 015014, 2009.

[2] M. Pospelov and A. Ritz, "Astrophysical signatures of secluded dark matter," *Physics Letters B*, vol. 671, no. 3, pp. 391–397, 2009.

[3] C. Boehm and P. Fayet, "Scalar dark matter candidates," *Nuclear Physics B*, vol. 683, no. 1-2, pp. 219–263, 2004.

[4] N. Borodatchenkova, D. Choudhury, and M. Drees, "Probing MeV dark matter at low-energy e^+e^- colliders," *Physical Review Letters*, vol. 96, no. 14, Article ID 141802, 2006.

[5] M. Pospelov, "Secluded U(1) below the weak scale," *Physical Review D*, vol. 80, no. 9, Article ID 095002, 2009.

[6] P. Fayet, "U-boson production in e^+e^- annihilations, ψ and γ decays, and light dark matter," *Physical Review D*, vol. 75, no. 11, Article ID 115017, 2007.

[7] J. D. Bjorken, R. Essig, P. Schuster, and N. Toro, "New fixed-target experiments to search for dark gauge forces," *Physical Review D*, vol. 80, no. 7, Article ID 075018, 2009.

[8] B. Batell, M. Pospelov, and A. Ritz, "Probing a secluded U(1) at B factories," *Physical Review D*, vol. 79, no. 11, Article ID 115008, 2009.

[9] M. Reece and L. T. Wang, "Searching for the light dark gauge boson in GeV-scale experiments," *Journal of High Energy Physics*, vol. 0907, p. 051, 2009.

[10] B. Batell, M. Pospelov, and A. Ritz, "Exploring portals to a hidden sector through fixed targets," *Physical Review D*, vol. 80, no. 9, Article ID 095024, 2009.

[11] R. Essig, P. Schuster, and N. Toro, "Probing dark forces and light hidden sectors at low-energy e^+e^- colliders," *Physical Review D*, vol. 80, no. 1, Article ID 015003, 2009.

[12] L. Barzè, G. Balossini, C. Bignamini et al., "Radiative events as a probe of dark forces at GeV-scale e^+e^- colliders ," *The European Physical Journal C*, vol. 71, p. 1680, 2011.

[13] H. Merkel, P. Achenbach, C. A. Gayoso et al., "Search for light Gauge Boson of the dark sector at the mainz microtron," *Physical Review Letters*, vol. 106, no. 25, Article ID 251802, 2011.

[14] S. Abrahamyan, Z. Ahmed, K. Allada et al., "Search for a new Gauge Boson in electron-nucleus fixed-target scattering by the APEX experiment," *Physical Review Letters*, vol. 107, no. 19, Article ID 191804, 2011.

[15] J. P. Lees, V. Poireau, V. Tisserand et al., "Search for low-mass dark-sector Higgs Bosons," *Physical Review Letters*, vol. 108, no. 21, Article ID 211801, 2012.

[16] B. Echenard, "Search for low-mass dark matter at BABAR," *Modern Physics Letters A*, vol. 27, no. 18, Article ID 1230016, 2012.

[17] F. Archilli, D. Babusci, D. Badoni et al., "Search for a vector gauge boson in ϕ meson decays with the KLOE detector," *Physics Letters B*, vol. 706, no. 4-5, pp. 251–255, 2012.

[18] D. Babusci, D. Badoni, I. Balwierz-Pytko et al., "Limit on the production of a light vector gauge boson in ϕ meson decays with the KLOE detector," *Physics Letters B*, vol. 720, no. 1–3, pp. 111–115, 2013.

[19] P. Adlarson, W. Augustyniak, W. Bardan et al., "Search for a dark photon in the $\pi^0 \to e^+e^-\gamma$ decay," *Physics Letters B*, vol. 726, no. 1–3, pp. 187–193, 2013.

[20] S. Andreas, C. Niebuhr, and A. Ringwald, "New limits on hidden photons from past electron beam dumps," *Physical Review D*, vol. 86, no. 9, Article ID 095019, 2012.

[21] J. Blumlein and J. Brunner, "New exclusion limits for dark gauge forces from beam-dump data ," *Physics Letters B*, vol. 701, no. 2, pp. 155–159, 2011.

[22] S. N. Gninienko, "Stringent limits on the $\pi^0 \to \gamma X, X \to e^+e^-$ decay from neutrino experiments and constraints on new light gauge bosons ," *Physical Review D*, vol. 85, no. 5, Article ID 055027, 2012.

[23] S. N. Gninienko, "Constraints on sub-GeV hidden sector gauge bosons from a search for heavy neutrino decays ," *Physics Letters B*, vol. 713, no. 3, pp. 244–248, 2012.

[24] R. Essig, P. Schuster, N. Toro, and B. Wojtsekhwski, "An electron fixed target experiment to search for a new vector Boson A' Decaying to e^+e^-," *Journal of High Energy Physics*, vol. 1102, p. 009, 2011.

[25] P. Hansson Adrian et al., [HPS Collaboration], https://confluence.slac.stanford.edu/display/hpsg/HPS+Proposals.

[26] T. Beranek, H. Merkel, and M. Vanderhaeghen, "Theoretical framework to analyze searches for hidden light gauge bosons in electron scattering fixed target experiments," *Physical Review D*, vol. 88, Article ID 015032, 2013.

[27] M. Freytsis, G. Ovanesyan, and J. Thaler, "Dark force detection in low energy *e-p* collisions," *Journal of High Energy Physics*, vol. 2010, p. 111, 2010.

[28] B. Wojtsekhowski, D. Nikolenko, and I. Racheck, "Searching for a new force at VEPP-3," 2012, http://arxiv.org/abs/1207.5089.

[29] S. N. Gninienko, "Search for MeV dark photons in a light-shining-through-walls experiment at CERN," http://arxiv.org/abs/1308.6521.

[30] D. Alesini, D. Babusci, M. E. Biagini et al., "DaØne upgrade for Siddharta run," LNF-06/33(IR), 2006.

[31] M. E. Biagini, S. Bini, R. Boni et al., "Tau/Charm factory accelerator report," Tech. Rep. INFN-13-13(CLAB), 2013.

[32] Y. Ohnishi, T. Abe, T. Adachi et al., "Accelerator design at Super KEKB," *Progress of Theoretical and Experimental Physics*, vol. 2013, Article ID 03A011, 2013.

[33] P. Fayet, "Extra U(1)'s and new forces," *Nuclear Physics B*, vol. 347, no. 3, pp. 743–768, 1990.

[34] B. Holdom, "Two U(1)'s and ϵ charge shifts," *Physics Letters B*, vol. 166, no. 2, pp. 196–198, 1986.

[35] Y. Kahn and J. Thalerm, "Searching for an invisible A' vector boson with DarkLight," *Physical Review D*, vol. 86, no. 11, Article ID 115012, 2012.

[36] P. de Niverville, M. Pospelov, and A. Ritz, "Observing a light dark matter beam with neutrino experiments," *Physical Review D*, vol. 84, no. 7, Article ID 075020, 2011.

[37] E. Izaguirre, G. Krnjaic, P. Schuster, and N. Toro, "New electron beam-dump experiments to search for MeV to few-GeV dark matter," *Physical Review D*, vol. 88, no. 11, Article ID 114015, 2013.

[38] R. Essig, J. Mardon, M. Papucci, T. Volansky, and Y.-M. Zhong, "Constraining light dark matter with low-energy e^+e^- colliders," 2013, http://arxiv.org/abs/1309.5084.

[39] S. Andreas, "Light weakly interacting particles: constraints and connection to dark matter," DESY Report DESY-THESIS-2013-024, 2013.

[40] H. K. Dreiner, J. F. Fortin, C. Hanhart, and L. Ubaldi, "Supernova constraints on MeV dark sectors from e^+e^- annihilations," http://arxiv.org/abs/1310.3826.

[41] D. Babusci, G. Bencivenni, C. Bloise et al., "KLOE," LNF-10/17(P), 2010.

[42] F. Archilli, D. Badoni, F. Gonnella et al., "Technical design report of the inner tracker for the KLOE-2 experiment," Tech. Rep. LNF-10/3(P), 2010.

[43] P. Coyle and O. Schneider, "High spatial resolution detectors and particle lifetime measurements at LEP," *Comptes Rendus Physique*, vol. 3, no. 9, pp. 1143–1154, 2002.

[44] J. Beringer, J.-F. Arguin, R. M. Barnett et al., "Review of particle physics," *Physical Review D*, vol. 86, no. 1, Article ID 010001, 2012.

[45] J. Fu, H. B. Li, X. Qin, and M. Z. Yang, "Study of the electromagnetic transitions $J/\psi \to PI^+I^-$ and probe dark photon," *Modern Physics Letters A*, vol. 27, no. 38, Article ID 1250223, 2012.

Hindawi Publishing Corporation
Advances in High Energy Physics
Volume 2014, Article ID 434539, 5 pages
http://dx.doi.org/10.1155/2014/434539

Research Article

Black Hole Atom as a Dark Matter Particle Candidate

V. I. Dokuchaev and Yu. N. Eroshenko

Institute for Nuclear Research of the Russian Academy of Sciences, 60th October Anniversary Prospect 7a, Moscow 117312, Russia

Correspondence should be addressed to Yu. N. Eroshenko; eroshenko@ms2.inr.ac.ru

Received 29 November 2013; Revised 28 January 2014; Accepted 28 January 2014; Published 5 March 2014

Academic Editor: Maxim Khlopov

We propose the new dark matter particle candidate—the "black hole atom," which is an atom with the charged black hole as an atomic nucleus and electrons in the bound internal quantum states. As a simplified model we consider the the central Reissner-Nordström black hole with the electric charge neutralized by the internal electrons in bound quantum states. For the external observers these objects would look like the electrically neutral Schwarzschild black holes. We suppose the prolific production of black hole atoms under specific conditions in the early universe.

1. Introduction

The idea of "black hole atoms" goes back a long way in several variations. Markov et al. proposed and studied in detail the model of maximons (or friedmons) [1–3]. These objects are the particle-like gravitating systems (semiclosed worlds) with mass close to the Planck mass $M_{\mathrm{Pl}} = \sqrt{\hbar c/G} \approx 10^{-5}$ g. They may have in principle a large gravitational mass defect. Maximons are interesting for cosmological applications, in particular, because they have the particle-like properties and may be the enigmatic dark matter particles. The idea of micro black hole carrying the electric charge and having the orbiting electrons or protons at the outer (outside the horizon) orbits was discussed by Hawking in [4]. He firstly proposed that the charged black holes may play a role similar to the atomic nuclei. Later the idea of black hole atoms was investigated in [5–7]. The possible origin of such Planck mass black hole is the final stable state of the evaporated primordial black holes (PBH); see, for example, [2, 3, 8]. The remnants of the evaporated black holes can be stable and also can serve as the dark matter candidates [9–15].

In this paper we discuss the black hole atoms, which are the atoms with the charged black hole as atomic nuclei and with electrons in the bound *internal* quantum states. The quantum bound states of electrons may exist in principle not only outside the event horizon but also inside the Cauchy horizon of the charged black hole. So, the main new idea is that there can be configurations in which the orbiting electrons are *inside* the black hole Cauchy horizon. We propose these black hole atoms as the possible origin of dark matter particles.

The quantum levels in the gravitational field of black holes outside the event horizon were studied in [16–27]. The resulting black hole atoms can be the dark matter particles in the case of uncompensated charge (electrons at outer levels) as it was proposed in [26]. The similar idea but for the zero total charge $q = -Q$ and for the electrons inside a black hole was proposed in [28]. In the latter case, the total charge of all the electrons at the inner orbits is equal to the charge of the black hole, which appears at Reissner-Nordström metric. In the case of compensated charge these systems look for the external observer as having the Schwarzschild metric. Neutral systems interact weakly with other particles, it makes them the good candidates for the dark matter particles.

The stationary quantum levels of fermions in the gravitational field of the charged black holes have been found in the work [28] by solving the corresponding Dirac equation. The Dirac equation in the Riemann geometry was first derived in the paper [29]. The using of only the covariant generalization is not enough for derivation of the corresponding Dirac equation. It is needed the determination of the parallel spinor transport. As it was shown in [28], a self-consistent steady-state solution with a finite normalization integral can exist only in the case of extreme black hole, whose charge in the appropriate units is equal to its mass $M = |Q|$.

2. Electrons inside the Black Holes

Let us briefly describe the method of quantum level calculations (for more details see [28]). The Dirac equation in the general metric has the following form [30]:

$$\left(i\gamma^{\mu}D_{\mu} - m\right)\psi = 0, \tag{1}$$

where $\gamma^{\mu} = e_{(a)}{}^{\mu}\gamma^{(a)}$, $\gamma^{(a)}$ are the standard Dirac matrices, and $e_{(a)}{}^{\mu}$ are tetrads. The elongated derivative has the form $D_{\mu} = \partial_{\mu} + iqA_{\mu} + \Gamma_{\mu}$, where $\Gamma_{\mu} = (1/4)\gamma^{(a)}\gamma^{(b)}e_{(a)}{}^{\mu}e_{(b)\nu;\mu}$, and A_{μ} is the electromagnetic 4-potential. We consider a charged Reissner-Nordström black hole with the metric $ds^2 = fdt^2 - f^{-1}dr^2 - r^2(d\theta^2 + \sin^2\theta\, d\phi^2)$, where $f = 1 - 2M/r + Q^2/r^2$, M is the black hole mass, and Q is its charge. Following the method of [30] we separate the variables by the following way:

$$\psi = e^{-iEt}Z(\theta,\phi)\, f^{-1/4}r^{-1}(\sin\theta)^{-1/2}\begin{bmatrix} g(r)\, I_2 \\ ih(r)\, I_2 \end{bmatrix}, \tag{2}$$

where $I_2 = (1,1)^T$, and $Z(\theta,\phi)$ is the angular part of the wave function. After substitution in (1), we obtain the next system of equations:

$$\begin{aligned} \frac{dg}{dr} - \frac{gk}{rf^{1/2}} + \frac{h}{f^{1/2}}\left[\frac{1}{f^{1/2}}\left(E - \frac{qQ}{r}\right) + m\right] = 0, \\ \frac{dh}{dr} + \frac{hk}{rf^{1/2}} - \frac{g}{f^{1/2}}\left[\frac{1}{f^{1/2}}\left(E - \frac{qQ}{r}\right) - m\right] = 0, \end{aligned} \tag{3}$$

where $k = 0, \pm1, \pm2, \ldots$. The condition for the physically acceptable solution is the finiteness of the normalization integral

$$2\int_0^{r_-}\left(|g|^2 + |h|^2\right) f^{-1}(r)\, dr = 1, \tag{4}$$

which was derived from the zero component of the fermion current $j^{\mu} = \overline{\psi}\gamma^{\mu}\psi$. This integral is finite only in the case of extremal black hole $M = |Q|$. Such a black hole has equal horizons radii $r_- = r_+ = M$. Consider the internal solution for extreme black hole near the Cauchy horizon $r \to r_-$. Let us denote $\mu = mM/M_{\mathrm{Pl}}^2$ and $\nu = qQ/(\hbar c)$. As can be shown [28], (3) in this case have the regular solution

$$g = C\left(\frac{M}{r} - 1\right)^{\varkappa}, \qquad h = C\left(\frac{M}{r} - 1\right)^{\varkappa}\frac{k + \varkappa}{\mu - \nu}, \tag{5}$$

where $C = \mathrm{const}$, $\varkappa = \sqrt{k^2 + \mu^2 - \nu^2}$, and (4) is finite in the case $k^2 + \mu^2 - \nu^2 > 1/4$. This solution corresponds to the energy level

$$E = \frac{qQ}{M}. \tag{6}$$

Electron has the same energy of (6) for the regular external solution outside the event horizon. Equation (3) can be solved numerically far away from the horizons [28]. In the case of the nonextreme black hole, $M \neq |Q|$, the integral (4) diverges at the horizons [28].

We suppose that quantum levels in the black hole interiors are stable. These means, additionally, the supposition of the internal universes inside the charged black holes, like in the idealized eternal black holes. The other possibility is the dynamical formation of the internal universes in the gravitational collapse [31]. For the quantum formation of black holes at the particle accelerators the specific extra dimensions are needed [13]. The classical bound stable orbits inside black holes are considered, for example, in [32–34].

The basic condition of existence of an atom as a quantum system in the quasiclassical approximation in flat space is the geometrical condition for Compton wavelength $\lambda \leq a$, where a is the characteristic scale of the potential hole. Strong space-tame curvature, especially near the horizons, changes this criterion drastically. A physical reason for the geometrical criterion breakdown is the infinite stretching of the physical distance $dl^2 = (-g_{\alpha\beta} + g_{0\alpha}g_{0\beta}/g_{00})dx^{\alpha}dx^{\beta}$ at the Cauchy horizon r_-. Really, the physical distance from the centre $r = 0$ of the extremal Reissner-Nordström black hole ($r_- = r_+ = M$) to some r is

$$l = \int_0^r f^{-1/2}\, dr = r + M\ln\left(1 - \frac{r}{M}\right). \tag{7}$$

It diverges for $r \to M$. Therefore, there is enough space under the Cauchy horizon for particles with any wavelength. As seen from the exact solution of the Dirac equation, the wave function of the electron just localised under the horizon, and it occurs far from quasiclassical regime. A question about capture of particle with large $\lambda \gg r_g$ wavelength by a black hole can arise. But we do not consider here the capture of the electron inside the black hole. Instead, we propose the formation of black hole with the electron already inside due to single quantum jump.

3. Black Hole Atoms Formation

PBHs can be formed at the cosmological stage of radiation dominance from the adiabatic density perturbations [4, 35, 36] and in the early dust-like stages [37, 38]. Although the primordial black hole is formed by the classical gravitational collapse, its final stage of evaporation is mainly the quantum process. Sakharov discussed the possibility of the superheavy particles emission by the black hole at the last stage of its evaporation [39]. The emitted particles could have even the masses up to the Planck mass although the probability of such emission is not clear. One can imagine the last stage of a black hole evaporation not as a gradual radiation but as the quantum jump into a new state. We assume that black hole atoms can result from such quantum jumps. The discussion about the final stage of evaporation can be found in [40, 41]. In the case of the jump the charged black holes with electrons on internal quantum orbits could be born effectively just after the evaporation of the PBHs population.

Note that the Hawking temperature for the extremal black hole is equal to zero and, so, the extremal black holes do not experience the quantum evaporation (see [14, 15, 40, 41]), and

they are stable dark matter candidates in this sense. Really the Hawking temperature of the charged black hole

$$T_H \propto \sqrt{M^2 - Q^2} \tag{8}$$

equals zero if $Q = M$. Nevertheless, the stability of the extremal black hole atoms with respect to quantum decay remains questionable.

Let us consider in more details the formation mechanism of PBH from the adiabatic density perturbations. Such perturbations can arise at inflationary stage, and the necessary condition for the effective PBH formation is the excess of perturbations' power at some small scale because the simplest near flat spectrum cannot produce the sufficient amount of PBHs. But in the case of some peak in the spectrum, the PBHs can form just in the required cosmological abundance. Now we consider the modification of the required peak's height by taking into account the mass loss of the BPHs during their evaporation from the initial mass M_{PBH} at the formation moment $t_f \simeq GM_{\mathrm{PBH}}/c^2$ till the Plank mass remnants after evaporation. With this mass loss the contemporary cosmological parameter of the PBHs can be expressed as [8]

$$\Omega_m \simeq \beta \frac{a\left(t_{\mathrm{eq}}\right)}{a\left(t_f\right)} \frac{M_{\mathrm{Pl}}}{M_{\mathrm{PBH}}}, \tag{9}$$

where Δ_h is the r.m.s. perturbation at the mass scale M_{PBH}, $\delta_c = 1/3$ according to the analytical estimation of [36] or $\delta_c \simeq 0.7$ as was obtained in the models of critical collapse, $a(t)$ is the scale factor, t_{eq} is the matter radiation equality moment, and

$$\beta = \int_{\delta_c}^{1} \frac{d\delta}{\sqrt{2\pi}\Delta_h} e^{-\delta^2/(2\Delta_h^2)} \simeq \frac{\Delta_h}{\delta_c \sqrt{2\pi}} e^{-\delta_c^2/(2\Delta_h^2)}. \tag{10}$$

By solving iteratively the system of (9) and (10) with $\Omega_m = 0.3$ we find the dependence of Δ_h on M_{PBH}, which is shown at Figure 1. For $M_{\mathrm{PBH}} \geq 10^{13}$ g there are no solutions of (9) and (10), and the scenario is limited only by smaller M_{PBH}. Therefore, to produce the cosmological abundance of PBHs' Plank mass remnants $\Omega_m \approx 0.3$ as is required for dark matter, one needs the density perturbations spectrum with the r.m.s. values shown at Figure 1.

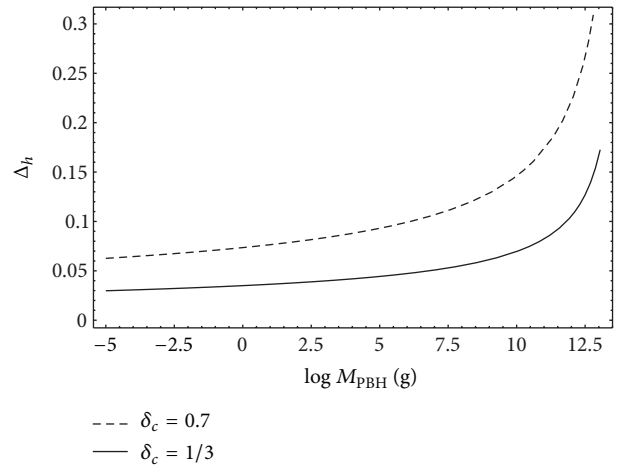

Figure 1: The dependence of the r.m.s. perturbation Δ_h at the mass scale M_{PBH} required for the explanations of dark matter as PBHs remnants in dependence on the initial PBH's mass M_{PBH} for value of the collapse threshold $\delta_c = 1/3$ (solid curve) and $\delta_c \simeq 0.7$ (dashed curve).

4. Interactions of the Black Hole Atoms

The interaction of the neutral black hole atoms with ordinary matter via the gravitational dynamical friction effect is extremely weak, as it was first shown in [4]. This is due to the extremely small cross-section $\sim \pi r_g^2 (c/v)^2 \sim 3 \times 10^{-66} (c/v)^2\ \mathrm{sm}^2$, where v is the relative velocity, $(c/v)^2 \sim 10^6$ in the galactic halo. One can compare it with the neutrino-nucleons interaction cross-sections $\sim 10^{-43}$–$10^{-34}\ \mathrm{sm}^2$.

The black hole can be born charged even in the classical collapse. But the neutralization by the accretion could reduce the initial charge till the value $Z \simeq 30$ [4]. The remaining charge can interact with the ordinary matter in the universe like heavy atomic nuclei [4]. So, the charged black hole atoms experience strong collisions and dissipations. This creates some difficulties for these systems as dark matter particles. Although, the solution of this problem may be in the formation of molecular-like systems with ordinary charged particles as in the composite-dark-matter scenario [42]. Possible detection method of charged black hole atoms was also proposed in the seminal paper [4]. These systems can draw straight tracks in the chambers almost without the deflection by the magnetic field due to their large masses.

Although in the case of a nonextreme black hole the normalization integral diverges, the irregular quasistationary solutions can exist [43, 44]. In addition, the regular internal (under the Cauchy horizon) and external solutions are possible [28]. Regular internal solutions have only single energy levels inside and outside the black hole. The internal level has the energy $E = qQ/r_-$, and the energy for the outer one is $E = qQ/r_+$. If electron jumps or tunnels from the external to the internal level, the energy

$$\Delta E = qQ\left(\frac{1}{r_-} - \frac{1}{r_+}\right) = \frac{2Mc^2 q}{Q}\sqrt{1 - \frac{Q^2}{GM^2}} \tag{11}$$

can be radiated in the form of photons. This energy could reach the very high value up to the energy corresponding to the ultrahigh energy cosmic rays. Note that the radiation from the bound system of two friedmons was considered in [2]. The released energy is supplied by the gravitational energy of the black hole and by the energy of the electrostatic interaction of electrons with a charged black hole. The gravitational factor is due to the fact that gravity is responsible for the localization of electrons near horizons at the quasistationary regular quantum orbits. In the case of the extreme black hole one has $r_+ = r_-$. In this case the energy release during the electron transition is absent. For this reason the extreme black holes with $q = -Q$ are the very

"quiet," dark, and noninteracting objects. These properties are just one needs for the dark matter candidates.

5. Conclusions

In this paper we discuss the new kind of "black hole atom" system: the Reissner-Nordström black holes with the electrons at quantum levels under the Cauchy horizon. If the electric charge of the black hole is neutralized by the internal electrons in bound quantum states, these objects would look like the electrically neutral Schwarzschild black holes for the external observers. Due to extremely small interaction cross-section, these neutral systems are almost noninteracting with baryons and behave as collisionless and dissipationless gas. This property makes them the good dark matter candidates.

The black hole atoms under consideration could form at the final stages of PBHs evaporation at early universe. The PBH itself may form in different scenarios: from adiabatic perturbations, during cosmological phase transitions, or at the early dust-like stages [37]. The extremal black holes do not evaporate in the Hawking process, and they are stable in this sense. But the existence of the internal and external quantum levels gives the possibility of the quantum transitions between the levels with radiation of the photons, and this effect makes the "black hole atoms" observable in principle.

Conflict of Interests

The authors declare that there is no conflict of interests regarding the publication of this paper.

Acknowledgments

This study was supported by the Grants RFBR 13-02-00257-a and OFN-17.

References

[1] M. A. Markov, "Elementary particles of maximally large masses (Quarks and Maximons)," *Soviet Physics (Journal of Experimental and Theoretical Physics)*, vol. 24, p. 584, 1967.

[2] V. I. Man'ko and M. A. Markov, "Properties of fridmons and the early stage of evolution of the universe," *Theoretical and Mathematical Physics*, vol. 17, no. 2, pp. 1060–1063, 1973.

[3] M. A. Markov, "The maximon and minimon in light of a possible formulation of the concept of an 'elementary particle'," *JETP Letters*, vol. 45, pp. 141–144, 1987.

[4] S. Hawking, "Gravitationally collapsed objects of very low mass," *Monthly Notices of the Royal Astronomical Society*, vol. 15, p. 75, 1971.

[5] V. V. Flambaum and J. C. Berengut, "Atom made from charged elementary black hole," *Physical Review D*, vol. 63, no. 8, Article ID 084010, 2001.

[6] E. G. Floratos, G. K. Leontaris, and N. D. Vlachos, "Gravitational atom in compactified extra dimensions," *Physics Letters B*, vol. 694, no. 4-5, pp. 410–416, 2011.

[7] M. L. Fil'Chenkov and P. Yu. Laptev, "Graviatom dipole radiation," *Gravitation and Cosmology*, vol. 12, p. 65, 2006.

[8] B. J. Carr, J. H. Gilbert, and J. E. Lidsey, "Black hole relics and inflation: limits on blue perturbation spectra," *Physical Review D*, vol. 50, no. 8, pp. 4853–4867, 1994.

[9] J. H. Macgibbon, "Can Planck-mass relics of evaporating black holes close the Universe?" *Nature D*, vol. 329, no. 6137, pp. 308–309, 1987.

[10] A. D. Dolgov, P. D. Naselsky, and I. D. Novikov, "Gravitational waves, baryogenesis, and dark matter from primordial black holes," http://arxiv.org/abs/astro-ph/0009407 .

[11] R. J. Adler, P. Chen, and D. I. Santiago, "The generalized uncertainty principle and black hole remnants," *General Relativity and Gravitation*, vol. 33, no. 12, pp. 2101–2108, 2001.

[12] P. Chen and R. J. Adler, "Black hole remnants and dark matter," *Nuclear Physics B*, vol. 124, pp. 103–106, 2003.

[13] B. J. Carr, "Primordial black holes as a probe of cosmology and high energy physics," *Lecture Notes in Physics*, vol. 631, pp. 301–321, 2003.

[14] I. Dymnikova and E. Galaktionov, "Vacuum dark fluid," *Physics Letters B*, vol. 645, no. 4, pp. 358–364, 2007.

[15] I. Dymnikova and M. Korpusik, "Regular black hole remnants in de Sitter space," *Physics Letters B*, vol. 685, no. 1, pp. 12–18, 2010.

[16] N. Deruelle and R. Ruffini, "Quantum and classical relativistic energy states in stationary geometries," *Physics Letters B*, vol. 52, no. 4, pp. 437–441, 1974.

[17] I. M. Ternov, V. R. Khalilov, G. A. Chizhov, and A. B. Gaina, "Finite motion of massive particles in the Kerr and Schwarzschild fields," *Soviet Physics Journal*, vol. 21, pp. 1200–1204, 1978.

[18] L. A. Kofman, "Bound states in quantum evaporation of black holes," *Physics Letters A*, vol. 87, no. 6, pp. 281–284, 1982.

[19] M. Soffel, B. Muller, and W. Greiner, "Particles in a stationary spherically symmetric gravitational field," *Journal of Physics A*, vol. 10, no. 4, pp. 551–560, 1977.

[20] I. M. Ternov, A. B. Gaina, and G. A. Chizhov, "Finite motion of electrons in the field of microscopic black holes," *Soviet Physics Journal*, vol. 23, no. 8, pp. 695–700, 1980.

[21] D. V. Gal'tsov, G. V. Pomerantseva, and G. A. Chizhov, "Filling of quasibound states by electrons in a schwarzchild field," *Soviet Physics Journal*, vol. 26, no. 8, pp. 743–745, 1983.

[22] I. M. Ternov and A. B. Gaina, "Energy spectrum of the Dirac equation in the Schwarzschild and Kerr fields," *Izvestiya Vysshikh Uchebnykh Zavedenii. Fizika*, vol. 31, no. 2, pp. 86–92, 1988.

[23] A. B. Gaina and O. B. Zaslavskiĭ, "On quasilevels in the gravitational field of a black hole," *Classical and Quantum Gravity*, vol. 9, no. 3, pp. 667–676, 1992.

[24] A. Lasenby, C. Doran, J. Pritchard, A. Caceres, and S. Dolan, "Bound states and decay times of fermions in a Schwarzschild black hole background," *Physical Review D*, vol. 72, no. 10, Article ID 105014, 2005.

[25] M. V. Gorbatenko and V. P. Neznamov, "Stationary bound states of dirac particles in collapsar fields," http://arxiv.org/abs/1205.4348 .

[26] M. A. Vronsky, M. V. Gorbatenko, N. S. Kolesnikov, V. P. Neznamov, E. Yu. Popov, and I. I. Safronov, "Stationary bound states of dirac particles in the schwarzschild gravitational field," http://arxiv.org/abs/1301.7595.

[27] V. Dzhunushaliev, "Canonical conjugated Dirac equation in a curved space," http://arxiv.org/abs/1202.5100.

[28] V. I. Dokuchaev and Yu. N. Eroshenko, "Stationary solutions of the dirac equation in the gravitational field of a charged black hole," *Journal of Experimental and Theoretical Physics*, vol. 117, pp. 72–77, 2013.

[29] V. Fock, "Geometrisierung der diracschen theorie des elektrons," *Zeitschrift fur Physik*, vol. 57, pp. 261–277, 1929.

[30] D. R. Brill and J. A. Wheeler, "Interaction of neutrinos and gravitational fields," *Reviews of Modern Physics*, vol. 29, pp. 465–479, 1957.

[31] V. P. Frolov, M. A. Markov, and V. F. Mukhanov, "Black holes as possible sources of closed and semiclosed worlds," *Physical Review D*, vol. 41, no. 2, pp. 383–394, 1990.

[32] J. Bičák, Z. Stuchlík, and V. Balek, "The motion of charged particles in the field of rotating charged black holes and naked singularities," *Bulletin of the Astronomical Institutes of Czechoslovakia*, vol. 40, pp. 65–92, 1989.

[33] S. Grunau and V. Kagramanova, "Geodesics of electrically and magnetically charged test particles in the Reissner-Nordström space-time: Analytical solutions," *Physical Review D*, vol. 83, no. 4, Article ID 044009, 2011.

[34] V. I. Dokuchaev, "Is there life inside black holes?" *Classical and Quantum Gravity*, vol. 28, no. 23, Article ID 235015, 2011.

[35] Ya. B. Zel'dovich and I. D. Novikov, "The hypothesis of cores retarded during expansion and the hot cosmological model," *Soviet Astronomy*, vol. 10, p. 602, 1967.

[36] B. J. Carr, "The primordial black hole mass spectrum," *The Astrophysical Journal*, vol. 201, pp. 1–19, 1975.

[37] A. G. Polnarev and M. Yu. Khlopov, "Cosmology, primordial black holes, and supermassive particles," *Soviet Physics Uspekhi*, vol. 28, p. 213, 1985.

[38] N. A. Zabotin, P. D. Naselskii, and A. G. Polnarev, "High-amplitude peaks of density disturbances and the formation of primordial black-holes in the dust like universe," *Soviet Astronomy*, vol. 31, p. 353, 1987.

[39] A. D. Sakharov, "Evaporation of black miniholes, highenergy physics," *Soviet Journal of Experimental and Theoretical Physics Letters*, vol. 44, p. 379, 1986.

[40] I. G. Dymnikova, "De Sitter-Schwarzschild black hole: its particlelike core and thermodynamical properties," *International Journal of Modern Physics D*, vol. 5, no. 5, pp. 529–540, 1996.

[41] Y. S. Myung, Y.-W. Kim, and Y.-J. Park, "Quantum cooling evaporation process in regular black holes," *Physics Letters B*, vol. 656, no. 4-5, pp. 221–225, 2007.

[42] N. Mankoc Borstnik, H. B. Nielsen, C. D. Froggatt, and D. Lukman, Eds., "Proceedings of the 14th International Workshop, 'What Comes Beyond the Standard Model'," vol. 12, pp. 94–102, Bled, Slovenia, 2011.

[43] M. V. Gorbatenko and V. P. Neznamov, "Stationary bound states of spin-half particles in the Reissner-Nordstroem gravitational field," http://arxiv.org/abs/1302.2557.

[44] M. V. Gorbatenko and V. P. Neznamov, "Stationary bound states of spin-half particles in the Kerr and Kerr-Newman gravitational fields," http://arxiv.org/abs/1303.1127.

Hindawi Publishing Corporation
Advances in High Energy Physics
Volume 2014, Article ID 702343, 7 pages
http://dx.doi.org/10.1155/2014/702343

Research Article

Big Bang Nucleosynthesis in Visible and Hidden-Mirror Sectors

Paolo Ciarcelluti

Web Institute of Physics, Via Fortore 3, 65015 Montesilvano, Italy

Correspondence should be addressed to Paolo Ciarcelluti; paolo.ciarcelluti@gmail.com

Received 31 October 2013; Accepted 7 January 2014; Published 26 February 2014

Academic Editor: Maxim Khlopov

One of the still viable candidates for the dark matter is the so-called mirror matter. Its cosmological and astrophysical implications were widely studied, pointing out the importance to go further with research. In particular, the Big Bang nucleosynthesis provides a strong test for every dark matter candidate, since it is well studied and involves relatively few free parameters. The necessity of accurate studies of primordial nucleosynthesis with mirror matter has then emerged. I present here the results of accurate numerical simulations of the primordial production of both ordinary nuclides and nuclides made of mirror baryons, in presence of a hidden mirror sector with unbroken parity symmetry and with gravitational interactions only. These elements are the building blocks of all the structures forming in the Universe; therefore, their chemical composition is a key ingredient for astrophysics with mirror dark matter. The production of ordinary nuclides shows differences from the standard model for a ratio of the temperatures between mirror and ordinary sectors $x = T'/T \gtrsim 0.3$, and they present an interesting decrease of the abundance of ^{7}Li. For the mirror nuclides, instead, one observes an enhanced production of ^{4}He, which becomes the dominant element for $x \lesssim 0.5$, and much larger abundances of heavier elements.

1. Introduction

The nature of the dark matter of the Universe is still completely unknown, and mirror matter represents one of the possible promising candidates. Its postulation derives theoretically from the necessity to restore the parity symmetry of the physical laws and phenomenologically from the need of describing the physics at any scale, from the whole cosmos to the elementary particles. In its basic theory, mirror matter is formed by baryons with exactly the same properties as our ordinary baryons, but with opposite handedness (right) of weak interactions so that globally the system of all particles together (ordinary and mirror) is parity symmetric. All the particles and the coupling constants are the same; then the physical laws of mirror matter are the same as that of ordinary matter, but the only interaction between the two kinds of particles is gravitational, while the other fundamental interactions act separately in each sector. This is valid also for electromagnetic interactions, meaning that a mirror photon would interact with mirror baryons but not with the ordinary ones, making mirror matter invisible to us and detectable just via their gravitational effects. To this basic model of interactions, it is possible to add other interactions involving mixings between ordinary and mirror particles. The most important of them is, at the present, the kinetic mixing of photons that in the mirror paradigm would be responsible of the positive results of the dark matter direct detection experiments. Extensive reviews on mirror matter at astro- and particle physics levels can be found, for example, in [1–4]. The original idea and the first applications of mirror matter are present in [5–8].

One of the key points in the macroscopic mirror theory is that, even if the physical laws are the same as ordinary matter, the initial conditions can be different. This means that the densities of particles and their temperatures can be different, leading to the need of only two free parameters that describe the basic mirror model defined as

$$x \equiv \left(\frac{s'}{s}\right)^{1/3} \approx \left(\frac{T'}{T}\right), \qquad \beta \equiv \frac{\Omega_b'}{\Omega_b}, \tag{1}$$

where $s(s')$, $T(T')$, and $\Omega_b(\Omega_b')$ are, respectively, the ordinary (mirror) entropy density, photon temperature, and cosmological baryon density.

Different cosmological parameters for initial temperatures and densities mean different cosmological evolutions for the two kinds of particles, in particular concerning the key phenomena of Big Bang nucleosynthesis (BBN), recombination, cosmic microwave background (CMB), large scale structure (LSS) formation, and the following evolution at lower scales, as galactic and stellar formation and evolution. The CMB and LSS were well studied [3, 9–13], and a recent work [14] has even shown that mirror matter can fit the observations with the same level of accuracy as generic cold dark matter (CDM). Primordial nucleosynthesis was studied in the past in several works [1, 6, 7, 15–17], obtaining historically the first bound on mirror matter parameters [18]. In fact, if, for example, the temperature of the mirror particles would be the same as that of ordinary ones, the contribution of mirror relativistic species to the Hubble expansion rate at BBN epoch would be equivalent to that of an effective number of extra- (massless) neutrino families $\Delta N_\nu \simeq 6.14$. This would be in conflict with any estimate, even the most conservative one. Then, considering the weak bound $\Delta N_\nu \lesssim 1$ and just applying the approximate relation $\Delta N_\nu \approx 6.14x^4$, one obtains $x \lesssim 0.7$ [15, 18]. The 4th power of x gives a mild dependence on this parameter. In view of the definition 1 of x, this simply means that the mirror particles should have a lower temperature than the ordinary ones in the early Universe.

One of the peculiarities of mirror matter is that not only it influences the ordinary BBN but also it has its own mirror BBN. This is a parallel primordial nucleosynthesis that is influenced by the ordinary baryonic matter, in an analogous way and for the same reason as mirror matter influences ordinary BBN. The big difference is that, while ordinary BBN receives very low influence by the mirror matter, since $\Delta N_\nu \propto x^4$ and $x < 1$, the opposite happens for the mirror BBN, since instead for it $\Delta N_\nu \propto x^{-4}$!

As the mirror particles have a lower temperature than the ordinary ones, the conditions required to start the nucleosynthesis are reached at earlier cosmological times, which mean different conditions, and in particular a larger cosmic expansion rate. This effect was studied in previous works, obtaining as a main result an increased production of mirror helium He' in comparison with the ordinary one. This last effect was studied also in the presence of the photon-mirror photon kinetic mixing, obtaining similar results [19, 20]. The primordial abundance Y' of He' is dependent on the inverse of the parameter x and can reach very high values, up to $Y' = 0.8\text{-}0.9$ for low values $x \sim 0.1$. All these studies considered the approximate relation $x \simeq T'/T$ expressed in (1) to be valid. Indeed this relation is valid along most of the history of the Universe, but not at the period of BBN, since at this time the electron-positron annihilations in both ordinary and mirror sectors heat the respective photons at different times, inducing large differences between x and T'/T, up to 30–40%. This effect and the thermodynamics of the early Universe were studied in detail in [21]. Here we use the results of that work for the degrees of freedom and temperatures in the two particle sectors, in order to obtain a more detailed numerical description of the ordinary and mirror primordial nucleosynthesis processes, and more carefully predict the primordial abundances. Some preliminary results of this analysis were previously presented in [1, 16, 17].

An accurate study of BBN in ordinary and mirror particle sectors is important for the following reasons.

(i) At the present status of knowledge, the standard theory of BBN is essentially dependent on just one parameter, the baryonic asymmetry $\eta = n_b/n_\gamma$. If compared with other cosmological tools, as, for example, CMB, which have much more free parameters, one can easily understand its importance as a key test for any dark matter candidate.

(ii) In standard BBN there is the still open "lithium problem," related to the discrepancy between observations and predictions of the primordial abundance of this nuclide. This suggests the need for new physics beyond the standard model; then it is important to understand if mirror matter can alleviate this problem.

(iii) The interpretation of DAMA and other direct detection experiments in terms of mirror matter is dependent on the abundance of mirror helium He' and heavier elements (so-called "metals"); then a correct estimate of their abundances is crucial in order to verify this hypothesis [22, 23].

(iv) The mirror BBN furnishes the primordial chemical composition of dark matter, which sets the initial conditions for the formation and evolution of structures at cosmic, galactic, and subgalactic scales. The effect of the enhanced abundance of He' on the evolution of mirror stars has already been studied, showing a large effect [24]. It is fundamental to estimate also the abundances of metals, which are responsible for many opacity processes of matter, involved in fragmentation processes forming galaxies and stars.

2. Models

I consider models in which the dark matter is made of mirror matter and there are no interactions between ordinary and mirror particles except for the gravitation that links the two sectors. Each set of particles is assumed to be in thermodynamical equilibrium (as usual in primordial nucleosynthesis studies) independently of the other one. This implies that there are no entropy exchanges between the two sectors then the entropy densities are separately conserved, and the parameter x is constant by definition. Using the definition of the entropy density [25], the parameter x is

$$x \equiv \left(\frac{s'}{s}\right)^{1/3} = \left[\frac{q'(T')}{q(T)}\right]^{1/3} \frac{T'}{T}, \tag{2}$$

where $q(T)$ and $q'(T')$ are the ordinary and mirror entropic degrees of freedom. The ratio of entropic degrees of freedom

in the two sectors determines the mirror temperature as a function of the ordinary one, once the parameter x is fixed. This ratio is not constant at the times of primordial nucleosynthesis, since the e^+-e^- annihilations heat the photons of each sectors independently, and they happen at different times in the early Universe. This and related aspects were studied in detail in [21]. Here we use the same treatment, valid for the ranges of temperatures which we are interested in (below ~10 MeV). It is based on the numerical solution of the equations for the conservations of ordinary and mirror entropies and the absence of entropy exchanges (constancy of x):

$$\frac{(7/8)\, q_e(T) + q_\gamma}{(7/8)\, q_\nu}\left(\frac{T}{T_\nu}\right)^3 = \frac{22}{21},$$

$$\frac{(7/8)\, q_e\left(T'\right) + q_\gamma}{(7/8)\, q_\nu}\left(\frac{T'}{T'_\nu}\right)^3 = \frac{22}{21}, \tag{3}$$

$$\frac{\left[(7/8)\, q_e\left(T'\right) + q_\gamma\right] T'^3 + (7/8)\, q_\nu T'^3_\nu}{\left[(7/8)\, q_e(T) + q_\gamma\right] T^3 + (7/8)\, q_\nu T^3_\nu} = x^3,$$

where q_i is the entropic degrees of freedom of species i, T_ν and T'_ν are the temperatures of the ordinary and mirror neutrinos.

Since ordinary and mirror particles have the same microphysics, I assume that the neutrino decoupling temperature is the same in each sector, which means, due to the initial difference of temperatures, that the decouplings of ordinary and mirror neutrinos take place at different times in the early Universe. This simplification is justified by the fact that, despite being the mirror sector colder, the final value of the neutrino to photon temperature ratio is the same in both sectors.

Together with x, the second free parameter for the mirror BBN is the mirror baryon to photon ratio (or baryonic asymmetry) $\eta' = n'_b/n'_\gamma$, which can be expressed in terms of the ordinary baryon to photon ratio $\eta = n_b/n_\gamma$ and the mirror parameters x and β:

$$\eta' = \beta x^{-3} \eta > \eta, \tag{4}$$

where the inequality is due to the bounds on x and the expected values for $\beta > 1$.

Since the nuclear physics is the same for ordinary and mirror matter, it is possible to use and modify a preexisting code for primordial nucleosynthesis that numerically solves the equations governing the production and evolution of nuclides. The choice is the well-tested and fast Wagoner-Kawano code [26, 27], which has enough accuracy for the purposes of this analysis. The numerical code has been doubled to include the mirror sector and modified in order to take into account the evolution of the temperature of the mirror particles and the degrees of freedom of both sectors, according to the aforementioned treatment [21]. For the neutron lifetime we consider the value $\tau = 885.7$ s, while for the final baryon to photon the ratio $\eta = 6.14 \cdot 10^{-10}$. We consider the usual standard number of neutrino families for ordinary matter $N_\nu = 3.04$. Then, the only two free parameters of the code are the mirror ones, x and β. Several models are computed for x ranging from 0.1 to 0.7 and β from 1 to 5, which are the values of cosmological interests.

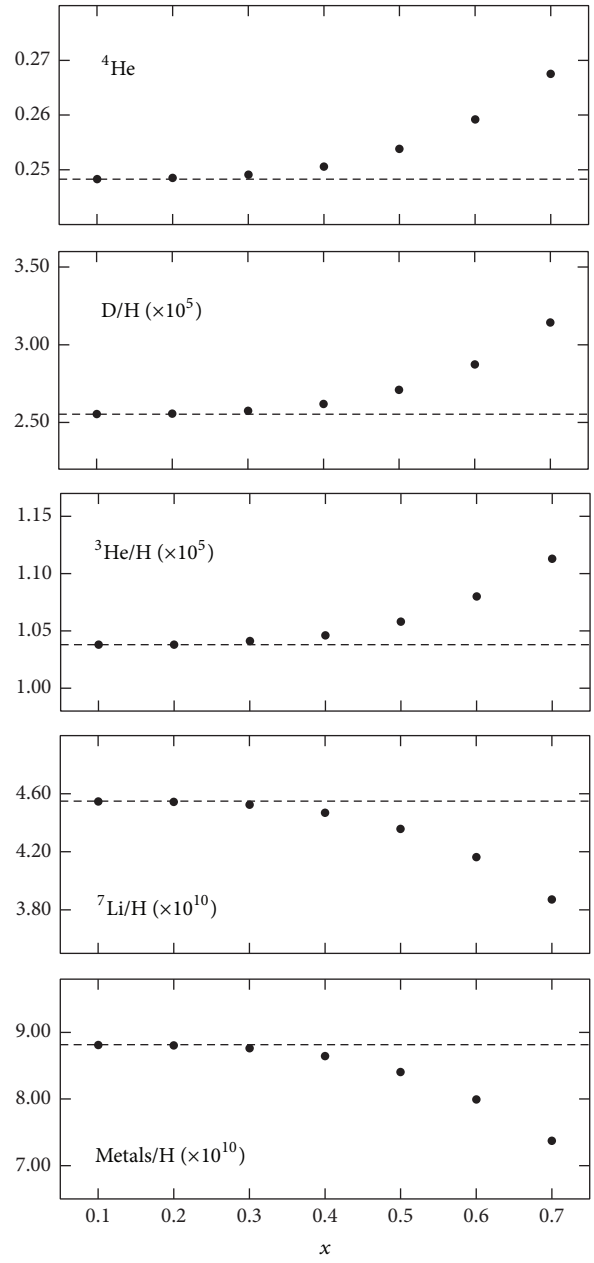

Figure 1: Primordial abundances of ordinary ^{4}He, D, ^{3}He, ^{7}Li, and metals (elements heavier than ^{4}He) for several values of x and compared with the predictions of the standard model (dashed lines).

3. Results

For each couple of mirror parameters (x, β) the primordial abundances of both ordinary and mirror elements are derived. The ordinary BBN, as expected, is independent on the density of mirror baryons (mirror baryonic asymmetry); then it depends, once fixed the microphysical parameters and the ordinary baryonic asymmetry, on just one parameter, the ratio of entropies x. The mirror BBN, instead, is clearly dependent on both x and the cosmic mirror baryonic density, expressed by the parameter β.

Table 1: Elements produced in the ordinary sector. The last row includes all elements with atomic mass larger than 7.

	Standard	$x = 0.1$	$x = 0.2$	$x = 0.3$	$x = 0.4$	$x = 0.5$	$x = 0.6$	$x = 0.7$
n/H (10^{-16})	1.161	1.161	1.160	1.159	1.510	1.505	1.527	2.044
p	0.7518	0.7518	0.7516	0.7511	0.7495	0.7463	0.7409	0.7326
D/H (10^{-5})	2.554	2.555	2.558	2.575	2.618	2.709	2.874	3.144
T/H (10^{-8})	8.064	8.065	8.076	8.132	8.280	8.588	9.146	10.07
^{3}He/H (10^{-5})	1.038	1.038	1.038	1.041	1.046	1.058	1.080	1.113
^{4}He	0.2483	0.2483	0.2485	0.2491	0.2506	0.2538	0.2592	0.2675
^{6}Li/H (10^{-14})	1.111	1.111	1.113	1.124	1.151	1.210	1.318	1.499
^{7}Li/H (10^{-10})	4.549	4.548	4.543	4.523	4.468	4.356	4.162	3.871
^{7}Be/H (10^{-10})	4.266	4.266	4.260	4.238	4.177	4.051	3.832	3.502
^{8}Li+/H (10^{-15})	1.242	1.242	1.243	1.251	1.269	1.306	1.370	1.464

Table 2: Elements produced in the mirror sector. The last row includes all elements with atomic mass larger than 7.

	$x = 0.1$ ($\beta = 5$)	$x = 0.2$ ($\beta = 5$)	$x = 0.3$ ($\beta = 5$)	$x = 0.4$ ($\beta = 5$)	$x = 0.5$ ($\beta = 5$)	$x = 0.6$ ($\beta = 5$)	$x = 0.7$ ($\beta = 5$)
n/H	$5.762 \cdot 10^{-25}$	$2.953 \cdot 10^{-24}$	$2.590 \cdot 10^{-22}$	$2.908 \cdot 10^{-21}$	$1.840 \cdot 10^{-20}$	$6.858 \cdot 10^{-20}$	$1.726 \cdot 10^{-19}$
p	0.1735	0.2840	0.3646	0.4357	0.4966	0.5488	0.5924
D/H	$1.003 \cdot 10^{-12}$	$3.090 \cdot 10^{-10}$	$4.838 \cdot 10^{-9}$	$2.240 \cdot 10^{-8}$	$6.587 \cdot 10^{-8}$	$1.553 \cdot 10^{-7}$	$3.279 \cdot 10^{-7}$
T/H	$9.679 \cdot 10^{-21}$	$4.999 \cdot 10^{-16}$	$1.238 \cdot 10^{-13}$	$2.603 \cdot 10^{-12}$	$2.108 \cdot 10^{-11}$	$1.030 \cdot 10^{-10}$	$3.722 \cdot 10^{-10}$
^{3}He/H	$3.282 \cdot 10^{-6}$	$3.522 \cdot 10^{-06}$	$3.740 \cdot 10^{-6}$	$3.949 \cdot 10^{-6}$	$4.172 \cdot 10^{-6}$	$4.415 \cdot 10^{-6}$	$4.691 \cdot 10^{-6}$
^{4}He	0.8051	0.7233	0.6351	0.5648	0.5035	0.4514	0.4077
^{6}Li/H	$7.478 \cdot 10^{-21}$	$1.241 \cdot 10^{-18}$	$1.309 \cdot 10^{-17}$	$4.460 \cdot 10^{-17}$	$1.016 \cdot 10^{-16}$	$1.923 \cdot 10^{-16}$	$3.361 \cdot 10^{-16}$
^{7}Li/H	$1.996 \cdot 10^{-7}$	$7.162 \cdot 10^{-8}$	$3.720 \cdot 10^{-8}$	$2.289 \cdot 10^{-8}$	$1.535 \cdot 10^{-8}$	$1.086 \cdot 10^{-8}$	$7.962 \cdot 10^{-9}$
^{7}Be/H	$1.995 \cdot 10^{-7}$	$7.159 \cdot 10^{-8}$	$3.675 \cdot 10^{-8}$	$2.236 \cdot 10^{-8}$	$1.489 \cdot 10^{-8}$	$1.041 \cdot 10^{-8}$	$7.885 \cdot 10^{-9}$
^{8}Li+/H	$4.354 \cdot 10^{-9}$	$3.458 \cdot 10^{-10}$	$5.926 \cdot 10^{-11}$	$1.396 \cdot 10^{-11}$	$3.827 \cdot 10^{-12}$	$1.168 \cdot 10^{-12}$	$3.949 \cdot 10^{-13}$
	$x = 0.1$ ($\beta = 1$)	$x = 0.2$ ($\beta = 1$)	$x = 0.3$ ($\beta = 1$)	$x = 0.4$ ($\beta = 1$)	$x = 0.5$ ($\beta = 1$)	$x = 0.6$ ($\beta = 1$)	$x = 0.7$ ($\beta = 1$)
n/H	$8.888 \cdot 10^{-17}$	$1.110 \cdot 10^{-16}$	$1.915 \cdot 10^{-16}$	$1.620 \cdot 10^{-16}$	$2.058 \cdot 10^{-16}$	$1.399 \cdot 10^{-16}$	$2.076 \cdot 10^{-16}$
p	0.1772	0.2831	0.3675	0.4400	0.5028	0.5566	0.6017
D/H	$1.331 \cdot 10^{-6}$	$4.086 \cdot 10^{-6}$	$7.094 \cdot 10^{-6}$	$1.018 \cdot 10^{-5}$	$1.352 \cdot 10^{-5}$	$1.743 \cdot 10^{-5}$	$2.235 \cdot 10^{-5}$
T/H	$3.068 \cdot 10^{-9}$	$1.192 \cdot 10^{-8}$	$2.190 \cdot 10^{-8}$	$3.228 \cdot 10^{-8}$	$4.358 \cdot 10^{-8}$	$5.675 \cdot 10^{-8}$	$7.328 \cdot 10^{-8}$
^{3}He/H	$5.228 \cdot 10^{-6}$	$6.119 \cdot 10^{-6}$	$6.880 \cdot 10^{-6}$	$7.566 \cdot 10^{-6}$	$8.232 \cdot 10^{-6}$	$8.931 \cdot 10^{-6}$	$9.719 \cdot 10^{-6}$
^{4}He	0.8226	0.7168	0.6326	0.5602	0.4974	0.4436	0.3984
^{6}Li/H	$8.638 \cdot 10^{-15}$	$1.422 \cdot 10^{-14}$	$1.660 \cdot 10^{-14}$	$1.747 \cdot 10^{-14}$	$1.790 \cdot 10^{-14}$	$1.845 \cdot 10^{-14}$	$1.951 \cdot 10^{-14}$
^{7}Li/H	$5.712 \cdot 10^{-8}$	$1.867 \cdot 10^{-8}$	$8.930 \cdot 10^{-9}$	$4.953 \cdot 10^{-9}$	$2.948 \cdot 10^{-9}$	$1.811 \cdot 10^{-9}$	$1.120 \cdot 10^{-9}$
^{7}Be/H	$5.711 \cdot 10^{-8}$	$1.863 \cdot 10^{-8}$	$8.878 \cdot 10^{-9}$	$4.896 \cdot 10^{-9}$	$2.891 \cdot 10^{-9}$	$1.755 \cdot 10^{-9}$	$1.064 \cdot 10^{-9}$
^{8}Li+/H	$2.036 \cdot 10^{-10}$	$1.468 \cdot 10^{-11}$	$2.514 \cdot 10^{-12}$	$5.944 \cdot 10^{-13}$	$1.657 \cdot 10^{-13}$	$5.184 \cdot 10^{-14}$	$1.814 \cdot 10^{-14}$

In Table 1 the primordial abundances of elements produced by ordinary nucleosynthesis, for different values of x compared with the standard model of nucleosynthesis (absence of dark matter), are reported. Protons and ^{4}He are expressed in mass fraction, all the other nuclei in ratios to the proton abundance. In the last row, indicated with ^{8}Li+, the contributions of the elements with atomic mass larger than 7 are included all together. The evolution of the abundances has been followed until the end of BBN process (at $T \sim 8 \cdot 10^{-4}$ MeV). It is evident that the differences with the standard BBN appear only for $x > 0.1$ (for $x = 0.1$ they are of order 10^{-4} or less), and for $x = 0.3$ they are limited to below 1%, but they increase for increasing values of x. The abundances of most elements (D, T, ^{3}He, ^{4}He, ^{6}Li, and ^{8}Li+) increase with x, while those of ^{7}Li and ^{7}Be decrease. This predicted decrease for ^{7}Li is an interesting result, since it goes exactly in the direction required to solve the still open "lithium problem." At first sight, the entity of the decrease should not be sufficient to solve this problem of standard BBN, but could certainly alleviate it. A dedicated statistical analysis will help to better evaluate this interesting possibility carried by the mirror matter. The trends of the observable primordial abundances, namely, ^{4}He, D, ^{3}He, ^{7}Li, and metals (the sum of the abundances of all elements heavier than ^{4}He), are plotted in Figure 1 as functions of x and compared with the standard model. As expected, the trend with x is not linear, since it is (indirectly) dependent on the ordinary degrees of freedom that scale as x^4. This dependence is the reason of the negligible effects predicted at lower x.

The results of the models for mirror nuclei are shown in Table 2, which is the analogous of Table 1. Since in this case the models depend on both the ratio of entropies and

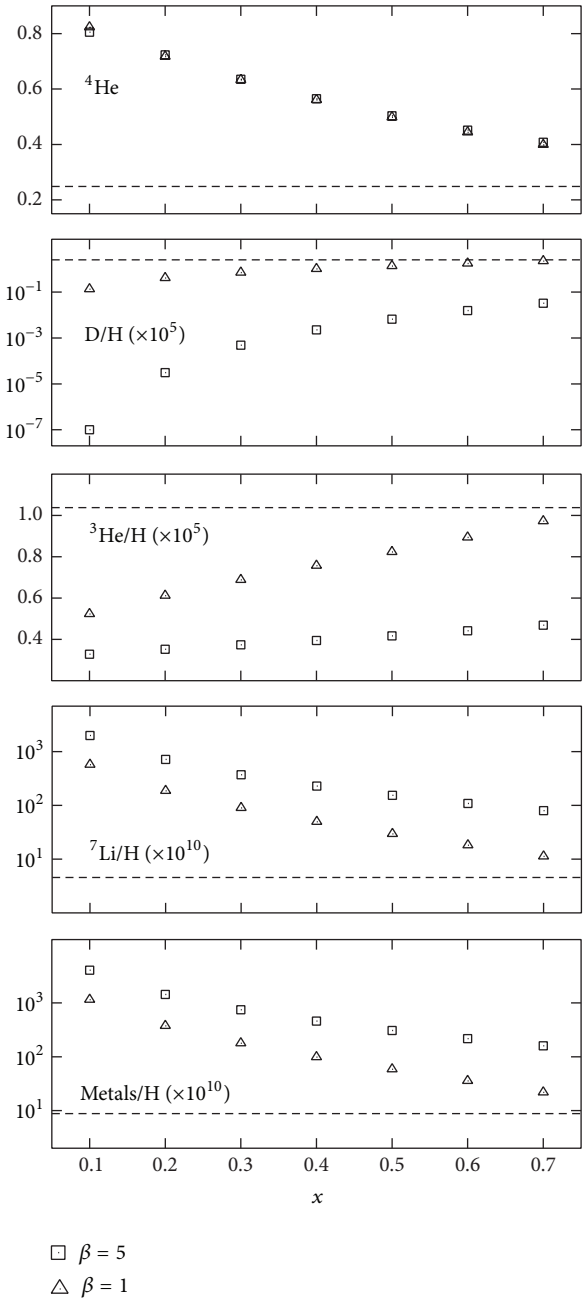

Figure 2: Primordial abundances of mirror ^{4}He, D, ^{3}He, ^{7}Li, and metals (elements heavier than ^{4}He) for several values of x and two different β and compared with the predictions of the standard model (dashed lines).

the ratio of baryonic densities, they are computed for the same different values of x as for the ordinary BBN, and for two different values of β, chosen at the extremes of the range (1 and 5) in order to maximize the effects of their change. One immediately sees that the mirror BBN is very different from the ordinary one. This is what in fact one expects; since the contribution of the ordinary particles to the mirror degrees of freedom has a dependence as x^{-4}, then it is significant and becomes higher for lower x. As expected, for higher values of x, the primordial abundances of mirror nuclides become less different from the ordinary ones, since the temperature of the mirror particles becomes higher, and then similar to that of the ordinary ones, in view of the approximate relation $T' \sim xT$. In addition, the same general trend is observed for lower values of β that means baryonic densities similar to the ordinary ones. It is not simple to describe the trends of the mass fractions by changing sectors and parameters, as the final abundances depend on many physical processes acting together, but one can try to summarize some results. Comparing the mirror nuclei with the ordinary ones, one observes the following: much less residual neutrons and considerably less protons that essentially went to build ^{4}He nuclei; much more ^{4}He (clearly the dependence on x is the opposite as for the protons); several orders of magnitude less D, T, ^{3}He; much less ^{6}Li for $\beta = 5$ and similar abundances for $\beta = 1$; much more ^{7}Li, ^{7}Be, and ^{8}Li+. Considering the trends with x, mirror abundances of n, p, ^{4}He, and ^{8}Li+ have opposite trends than the corresponding ordinary elements. Comparing the predictions obtained for the different values of β, one observes the following: the trends with x are the same for each element; the abundances of ^{4}He are very similar; the abundances of ^{3}He become almost double going from $\beta = 5$ to $\beta = 1$; for the lower β there is much more D, T, and ^{6}Li (some orders of magnitude) and much less ^{7}Li, ^{7}Be, and ^{8}Li+ (around one order). Analogously to what was done for the ordinary matter, in Figure 2 I plot the abundances of mirror ^{4}He, D, ^{3}He, ^{7}Li, and metals, as functions of x and for the two values of β. The previously mentioned trends, namely, the growing similarity with the standard model abundances for higher x and lower β, are evident. Differently from the ordinary nuclei, the mirror ones are not directly observable, but their primordial abundances are a key ingredient for studies of the following evolution of the Universe at all scales and for the aforementioned interpretation of the dark matter direct detection experiments. The computed mass fraction for mirror ^{4}He is in qualitative agreement with what predicted by previous analytical studies [1, 15], confirming that it is larger than the ordinary one for every x and becomes the dominant mass contribution for $x \lesssim 0.5$, meaning that dark matter would be dominated by mirror helium. Another important result of the simulations is the prediction of a much larger abundance of metals produced by mirror nucleosynthesis. These elements have a large influence on the opacity of mirror matter, which has an important role in many astrophysical processes, as, for example, the fragmentation of primordial gas during the phase of contraction.

In order to complete the analysis, I show in Figure 3 the evolution of the abundances of ordinary and mirror D, ^{3}He, ^{4}He, and metals. The models used have the parameters $x = 0.4$ and $\beta = 5$. The evolutions of standard and ordinary abundances are very similar (and for this reason the standard ones are not shown in the figure), while the mirror ones have a similar shape, but different values. In particular, they appear shifted towards earlier times, as a consequence of the smaller temperature of the primordial mirror plasma.

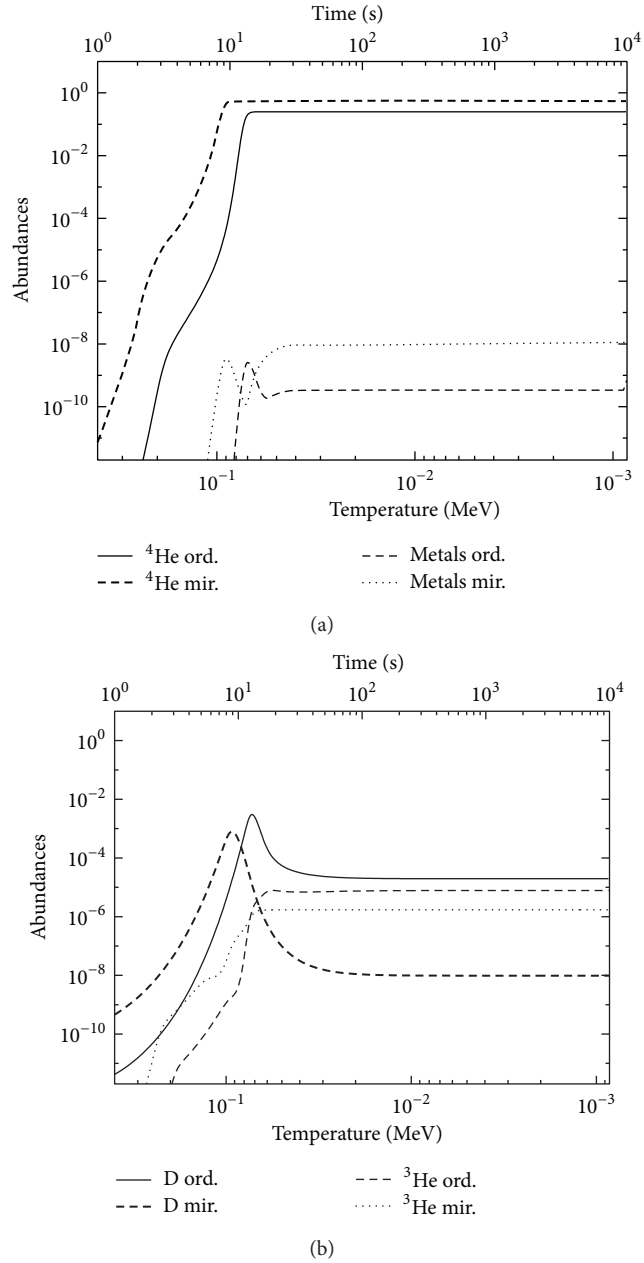

Figure 3: Time/temperature evolution of nuclides during ordinary and mirror primordial nucleosynthesis. The models have the mirror parameters $x = 0.4$ and $\beta = 5$.

4. Conclusions

In this paper I present the detailed study of the primordial nucleosynthesis in presence of mirror dark matter in its basic model with only gravitational interactions between ordinary and mirror particles. The BBN is studied for both kinds of matter, using an accurate treatment of the thermodynamics of the early Universe, based on the work done in [21], which considers the changes in the radiation temperatures due to the two e^+-e^- annihilations. The present analysis shows the results of accurate numerical simulations and updates all the previous works. Fixing the cosmological parameters to their standard values, only the two free mirror parameters are considered, namely, the ratio of entropies x and the ratio of baryonic densities β. Both ordinary and mirror nucleosynthesis are followed until their ends, obtaining the evolution and final abundances of primordial elements in every sector. For the ordinary nuclides, they depend only on the parameter x, while for the mirror ones they are dependent also on β. As expected, the upper bound $x < 0.7$ limits the effect of mirror particles on ordinary nucleosynthesis that is negligible for $x = 0.1$ and starts to be around few percent for $x = 0.3$, with a dependence growing with x. An interesting unexpected result is the prediction of a lower abundance of ^{7}Li. This effect

could help to alleviate the "lithium problem," but it requires a future dedicated statistical analysis. In the mirror sector, the Big Bang nucleosynthesis produces in a similar way mirror nuclides, but with different abundances as a consequence of its different initial conditions. In particular, as previously analytically predicted, there is an enhanced production of mirror ^{4}He that becomes the dominant nuclide for $x \lesssim 0.5$ and arrives at more than 80% for the lowest values of x. This effect has a very small dependence on β. In addition, there is a much larger (few orders of magnitude) production of mirror metals (elements heavier that ^{4}He). Even if their abundances are anyway very low, they could have consequences on the opacity of dark matter and on its many related astrophysical phenomena. This work provides the primordial chemical composition of the mirror dark matter, which has to be used in studies of the evolution of the Universe at all scales and in the analyses of the dark matter direct detection experiments.

Conflict of Interests

The author declares that there is no conflict of interests regarding the publication of this paper.

References

[1] P. Ciarcelluti, "Cosmology with mirror dark matter," *International Journal of Modern Physics D*, vol. 19, no. 14, pp. 2151–2230, 2010.

[2] L. B. Okun, "Mirror particles and mirror matter: 50 years of speculation and search," *Physics-Uspekhi*, vol. 50, no. 4, pp. 380–389, 2007.

[3] P. Ciarcelluti, *Cosmology of the mirror universe [Ph.D. thesis]*, 2003.

[4] R. Foot, "Experimental implications of mirror matter-type dark matter," *International Journal of Modern Physics A*, vol. 19, no. 23, pp. 3807–3818, 2004.

[5] T. D. Lee and C. N. Yang, "Question of parity conservation in weak interactions," *Physical Review*, vol. 104, no. 1, pp. 254–258, 1956.

[6] S. Blinnikov and M. Khlopov, "Possible astronomical effects of mirror particles," *Soviet Astronomy*, vol. 27, pp. 371–375, 1983.

[7] M. Y. Khlopov, G. Beskin, N. Bochkarev, L. Pustylnik, and S. Pustylnik, "Observational physics of mirror word," *Soviet Astronomy*, vol. 35, p. 21, 1991.

[8] R. Foot, H. Lew, and R. R. Volkas, "A model with fundamental improper spacetime symmetries," *Physics Letters B*, vol. 272, no. 1-2, pp. 67–70, 1991.

[9] P. Ciarcelluti, "Cosmology with mirror dark matter II: cosmic microwave background and large scale structure," *International Journal of Modern Physics D*, vol. 14, no. 2, pp. 223–256, 2005.

[10] P. Ciarcelluti, "Cosmology with mirror dark matter I: linear evolution of perturbations," *International Journal of Modern Physics D*, vol. 14, no. 2, pp. 187–222, 2005.

[11] Z. Berezhiani, P. Ciarcelluti, D. Comelli, and F. L. Villante, "Structure formation with mirror dark matter: CMB and LSS," *International Journal of Modern Physics D*, vol. 14, no. 1, pp. 107–120, 2005.

[12] P. Ciarcelluti, "Structure formation, CMB and LSS in a mirror dark matter scenario," *Frascati Physics Series*, vol. 555, p. 1, 2004, http://arxiv.org/abs/astro-ph/0409629.

[13] A. Y. Ignatiev and R. R. Volkas, "Mirror dark matter and large scale structure," *Physical Review D*, vol. 68, no. 2, Article ID 023518, 11 pages, 2003.

[14] P. Ciarcelluti and Q. Wallemacq, "Is dark matter made of mirror matter? Evidence from cosmological data," *Physics Letters B*, vol. 729, pp. 62–66, 2014.

[15] Z. Berezhiani, D. Comelli, and F. L. Villante, "The early mirror universe: inflation, baryogenesis, nucleosynthesis and dark matter," *Physics Letters B*, vol. 503, no. 3-4, pp. 362–375, 2001.

[16] P. Ciarcelluti, "Astrophysical tests of mirror dark matter," *AIP Conference Proceedings*, vol. 1038, pp. 202–210, 2008.

[17] P. Ciarcelluti, "Early universe cosmology with mirror dark matter," *AIP Conference Proceedings*, vol. 1241, p. 351, 2010, http://arxiv.org/abs/0911.3592.

[18] Z. G. Berezhiani, A. D. Dolgov, and R. N. Mohapatra, "Asymmetric inflationary reheating and the nature of mirror universe," *Physics Letters B*, vol. 375, no. 1–4, pp. 26–36, 1996.

[19] P. Ciarcelluti and R. Foot, "Early universe cosmology in the light of the mirror dark matter interpretation of the DAMA/Libra signal," *Physics Letters B*, vol. 679, no. 3, pp. 278–281, 2009.

[20] P. Ciarcelluti and R. Foot, "Primordial He' abundance implied by the mirror dark matter interpretation of the DAMA/Libra signal," *Physics Letters B*, vol. 690, no. 5, pp. 462–465, 2010.

[21] P. Ciarcelluti and A. Lepidi, "Thermodynamics of the early universe with mirror dark matter," *Physical Review D*, vol. 78, no. 12, Article ID 123003, 7 pages, 2008.

[22] R. Foot, "Mirror dark matter and the new DAMA/LIBRA results: a simple explanation for a beautiful experiment," *Physical Review D*, vol. 78, no. 4, Article ID 043529, 10 pages, 2008.

[23] R. Foot, "Mirror dark matter interpretations of the DAMA, CoGeNT and CRESST-II data," *Physical Review D*, vol. 86, no. 2, Article ID 023524, 10 pages, 2012.

[24] Z. Berezhiani, P. Ciarcelluti, S. Cassisi, and A. Pietrinferni, "Evolutionary and structural properties of mirror star MACHOs," *Astroparticle Physics*, vol. 24, no. 6, pp. 495–510, 2006.

[25] E. W. Kolb and M. S. Turner, *The Early Universe*, Frontiers of Physics 69, Addison-Wesley, New York, NY, USA, 1990.

[26] R. V. Wagoner, "Big-Bang nucleosynthesis revisited," *The Astrophysical Journal*, vol. 179, pp. 343–360, 1973.

[27] L. Kawano, "Let's go: early universe. 2. Primordial nucleosynthesis: the computer way," FERMILAB-PUB-92-004-A, 1992.

Hindawi Publishing Corporation
Advances in High Energy Physics
Volume 2014, Article ID 148319, 7 pages
http://dx.doi.org/10.1155/2014/148319

Research Article

Cosmological Constraints on Mirror Matter Parameters

Paolo Ciarcelluti[1] and Quentin Wallemacq[2]

[1] *Web Institute of Physics, 65015 Montesilvano, Italy*
[2] *IFPA, Département AGO, Université de Liège, 4000 Liège, Belgium*

Correspondence should be addressed to Paolo Ciarcelluti; paolo.ciarcelluti@gmail.com

Received 28 November 2013; Accepted 17 January 2014; Published 26 February 2014

Academic Editor: Maxim Khlopov

Up-to-date estimates of the cosmological parameters are presented as a result of numerical simulations of cosmic microwave background and large scale structure, considering a flat Universe in which the dark matter is made entirely or partly of mirror matter, and the primordial perturbations are scalar adiabatic and in linear regime. A statistical analysis using the Markov Chain Monte Carlo method allows to obtain constraints of the cosmological parameters. As a result, we show that a Universe with pure mirror dark matter is statistically equivalent to the case of an admixture with cold dark matter. The upper limits for the ratio of the temperatures of ordinary and mirror sectors are around 0.3 for both the cosmological models, which show the presence of a dominant fraction of mirror matter, $0.06 \lesssim \Omega_{\text{mirror}} h^2 \lesssim 0.12$.

1. Introduction

Since a missing mass in the Universe was pointed out in the 1930s, astrophysical evidences for dark matter have been accumulating, increasingly confirming its presence at all cosmological scales. But even if the processes of structure formation can draw a picture of its main features, the elementary nature of dark matter remains unknown.

Modern cosmology provides powerful tools for testing dark matter: Big Bang Nucleosynthesis (BBN), the Cosmic Microwave Background (CMB), and the large scale structure (LSS) power spectra can be reproduced in numerical simulations to better discriminate between the different classes of candidates, one of them giving good agreements with all these observations being known as cold dark matter (CDM). Similarly, mirror dark matter can also account for the cosmological observations, and it is of primary interest to determine whether or not it gives a better agreement than CDM, or if it is equivalent.

Mirror matter was originally proposed by Lee and Yang [1] and further considered by several authors [2–5], in order to restore the parity symmetry of the Lagrangian of the standard model. The most natural way to do so is to add to the existing Lagrangian its parity-symmetric counterpart, so that the whole Lagrangian is invariant under the parity transformation, each part transforming into the other. This corresponds to reintroduce all the known fields with the same coupling constants but with opposite parities. We therefore end up with a new sector of particles, called mirror sector, which is an exact duplicate of the ordinary sector, but where ordinary particles have left-handed interactions, mirror particles have right-handed interactions [5].

As a consequence, the three-gauge interactions act separately in each sector, the only link between them being gravity. Because mirror baryons, just like their ordinary counterparts, are stable and can be felt only through their gravitational effects, the mirror matter scenario provides an ideal interpretation of dark matter. Its particularity is that it is a self-interacting candidate (astrophysical constraints on self-interactions of dark matter present in literature are valid only for homogeneous distributions of dark matter particles and are therefore not directly applicable to the mirror matter case) but without any new parameter at the level of particle physics.

Since it was introduced, mirror matter has been widely studied and its compatibility with experimental and observational constraints has been verified [6–11]. Some potential

indications of its existence came not only from the observation of neutron stars [12, 13], but also from the direct-search experiments, for which mirror matter gives one of the few possible explanations [14, 15]. Previous analytical and numerical studies on CMB and LSS power spectra [8, 16–20] have given encouraging results, but have only limited the parameter space of mirror dark matter. Here, we explore it in detail using the fast numerical code CAMB, in order to quantify the compatibility of mirror matter with cosmological observations and to obtain constraints on its parameters.

In Section 2, we recall the important cosmological quantities and epochs in presence of mirror matter. We describe briefly how we modified the numerical codes CAMB and cosmoMC in order to incorporate the mirror components into the evolution of the Universe in Section 3. We then present, in Section 4, the $1-\sigma$ constraints on the cosmological parameters coming from the CMB and LSS data for different dark matter compositions, that is, pure CDM, mixed CDM and mirror matter, and pure mirror matter, and we compare the corresponding best-fit models. We show also the temporal evolution of the density perturbations for the different components of the Universe.

2. Basic Cosmology with Mirror Matter

Even if the ordinary and mirror sectors are characterized by identical Lagrangians and obey therefore the same physical laws, their macroscopic realizations are not necessarily the same. The differences between the evolutions of the two sectors are parametrized by two cosmological free parameters: the ratio x of the temperatures of the ordinary and mirror cosmic background radiations and the relative amount β of mirror baryons compared to the ordinary ones:

$$x \equiv \left(\frac{S'}{S}\right)^{1/3} \simeq \frac{T'}{T}, \qquad \beta \equiv \frac{\Omega_b'}{\Omega_b}, \tag{1}$$

where T (T'), Ω_b (Ω_b'), and S (S') are, respectively, the ordinary (mirror) photon temperature, cosmological baryon density (normalized to the critical density of the Universe), and entropy per comoving volume [6].

There are several components that contribute to the total present energy density $\Omega_{\rm tot}$: the energy density of relativistic species (radiation) Ω_r, the energy density of nonrelativistic species (matter) Ω_m, and the energy density of the vacuum (cosmological constant or dark energy) Ω_Λ. According to the observations of the CMB anisotropies, $\Omega_{\rm tot} = \Omega_m + \Omega_r + \Omega_\Lambda \approx 1$, meaning that the Universe today is almost flat. In presence of mirror matter, mirror components are present in both radiation and matter energy densities, and the latter is expressed by

$$\Omega_m = \Omega_b + \Omega_b' + \Omega_{\rm DM} = \Omega_b\left(1+\beta\right) + \Omega_{\rm DM}, \tag{2}$$

where the term $\Omega_{\rm DM}$ includes the contributions of any other possible dark matter particles but mirror baryons.

It can be shown that during BBN, the mirror species γ', $e^{\pm\prime}$, and $\nu'_{e,\mu,\tau}$, respectively, for mirror photon, electrons, positrons, and neutrinos, bring a contribution to the relativistic degrees of freedom equivalent to an effective number of extra neutrino families $\Delta N_\nu \simeq 6.14x^4$. In view of the current bounds on ΔN_ν [21], this corresponds to an upper limit $x \lesssim 0.7$, which means that the temperature of the mirror sector was smaller than that of the ordinary one at the epoch of nucleosynthesis, $T' < T$.

Due to the separate conservation of entropies in the two sectors, this initial temperature difference holds throughout the expansion of the Universe, so that the cosmological key epochs take place at different redshifts in the two sectors, happening earlier in the mirror sector than in the ordinary one [6, 17]. The relevant epochs for structure formation are the matter-radiation equality (MRE), the matter-radiation decouplings (MRD) in the ordinary and mirror sectors, and the photon-baryon equipartitions in each sector, occurring, respectively, at the redshifts $z_{\rm eq}$, $z_{\rm dec}$, $z'_{\rm dec}$, $z_{b\gamma}$ and $z'_{b\gamma}$.

The MRE is common to both sectors and, in presence of mirror matter, happens at the redshift:

$$1 + z_{\rm eq} = \frac{\Omega_m}{\Omega_r} \approx 2.4 \cdot 10^4 \frac{\Omega_m h^2}{1+x^4}, \tag{3}$$

while the MRDs and photon-baryon equipartitions in each sector are, respectively, related by

$$1 + z'_{\rm dec} \simeq x^{-1}\left(1 + z_{\rm dec}\right), \tag{4}$$

$$1 + z'_{b\gamma} = \frac{\Omega_b'}{\Omega_\gamma'} \simeq \frac{\Omega_b \beta}{\Omega_\gamma x^4} = \left(1 + z_{b\gamma}\right)\frac{\beta}{x^4} > 1 + z_{b\gamma}, \tag{5}$$

since $T'_{\rm dec} \simeq T_{\rm dec}$ up to small corrections to (4). Because $x > 0$, the value of $z_{\rm eq}$ obtained in the mirror scenario is always smaller than in the standard case, while the upper bound $x \lesssim 0.7$ ensures that $z'_{\rm dec} > z_{\rm dec}$ and $z'_{b\gamma} > z_{b\gamma}$, showing that the MRD and the photon-baryon equipartition occur earlier in the mirror sector.

By identifying $z_{\rm eq}$ and $z'_{\rm dec}$ from (3) and (4), one obtains a reference value $x_{\rm eq}$ [6, 17] under which the mirror photons decouple during the radiation-dominated era, with the consequence that the primordial perturbations evolve, in the linear regime, in a way that is very similar to the standard CDM case. Also, analytical and numerical studies on CMB and LSS power spectra [8, 16–20, 22] have already shown, by comparing qualitatively the results with the observations, that for relatively cold mirror sectors ($x \lesssim 0.3$), the dark matter of the Universe can be fully realized by mirror baryons, while for higher x ($x \gtrsim 0.3$) mirror baryons and CDM would form an admixture.

3. The Modified Numerical Tools CAMB and cosmoMC

We modified the publicly available code CAMB [23] for the simulation of the anisotropies of the microwave background and the large scale structure of the Universe, together with its Markov Chain Monte Carlo sampling tool cosmoMC [24], in order to include the mirror components. CAMB is used in its

Table 1: Adopted flat priors for the parameters.

Parameter	Lower limit	Upper limit
$\Omega_b h^2$	0.01	0.1
$\Omega_{\rm CDM} h^2$	0.01	0.8
x	0.05	0.7
β	0.5	9.0
$100\theta_s$	0.1	10
τ	0.01	0.8
n_s	0.7	1.3
$\ln(10^{10} A_s)$	2.7	4

most standard mode, that is, with adiabatic initial conditions for the perturbations, in linear regime, in a flat Universe ($\Omega_{\rm tot} = 1$), with an equation of state of vacuum $p_\Lambda = -\rho_\Lambda$ ($w_\Lambda = -1$), without any massive neutrinos and with the standard number of neutrino families $N_{\rm eff} = 3.046$.

We defined the necessary mirror variables and included them into the calculations of all the relevant quantities related to the evolution of the background. In particular, we considered both ordinary and mirror matter when describing the gravitational interactions. As the mirror particles obey the same physical laws as ordinary ones, we doubled the equations related to the evolution of the perturbations of the background, adding the corresponding variables for the perturbations of mirror energy densities and peculiar velocities.

The recombinations are calculated separately in each sector, using two times per model the same code RECFAST [25] present in CAMB. This considerably increases the computational time of a model, especially for small values of x. Indeed, the recombination of mirror hydrogen (as well as of mirror helium) scales as x^{-1}, as stated by (4), so that the integration of the equations giving the ionized fractions of mirror hydrogen and helium has to be performed over a wider range of redshifts. However, the program is still fast enough to calculate the huge number of models required for a Monte Carlo analysis of the parameter space.

Compared with previous numerical studies [8, 16–19], we have used here an updated estimate of the primordial composition of mirror particles from [6, 26–29], checking that the models obtained using CAMB with this more accurate treatment of mirror BBN are consistent with the previous ones.

We performed Markov Chain Monte Carlo (MCMC) analyses of the parameter space constituted by the standard cosmological parameters plus the two mirror ones using cosmoMC. To this aim, we added the mirror parameters to the parameter list of cosmoMC and linked them to the equivalent ones in CAMB. We end up with an eight-dimensional set of cosmological parameters for which we adopt flat priors and broad distributions, as summarized in Table 1. $\Omega_b h^2$ and $\Omega_{\rm CDM} h^2$ are, respectively, the baryon and cold dark matter densities, x and β are the mirror photon temperature and mirror baryon density relative to the corresponding ordinary quantities, θ_s is the ratio of the sound horizon to the angular diameter distance at decoupling, τ is the reionization optical depth, n_s is the scalar spectral index, and A_s is the scalar fluctuation amplitude.

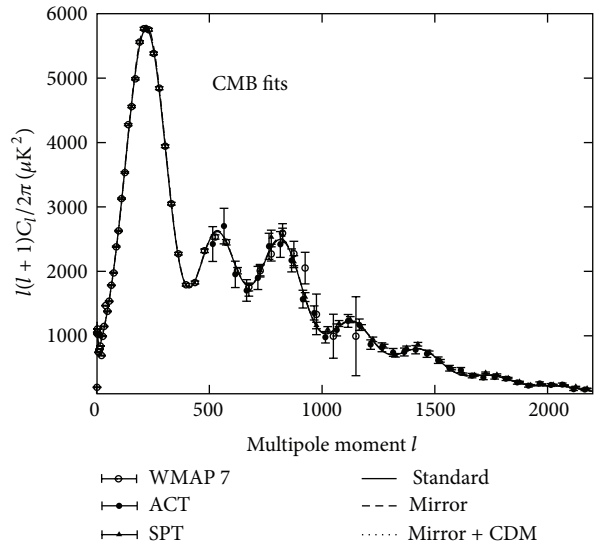

Figure 1: CMB power spectrum for best-fit models with baryons and mirror matter (dashed line), or baryons, mirror matter, and cold dark matter (dotted line) obtained using CMB only data. For comparison we show also the standard model fit (solid line).

The upper limit on x is set by the BBN limit mentioned in Section 2. CAMB also calculates derived parameters such as the matter and dark energy densities Ω_m and Ω_Λ, the redshift of reionization $z_{\rm re}$, the Hubble parameter h, the age of the Universe in Gyr, and the density fluctuation amplitude σ_8 at $8h^{-1}$ Mpc. The runs include, as in the standard version of CAMB, weak priors on the Hubble parameter, $0.4 \le h \le 1.0$, and on the age of the Universe, $10 \le \text{age(Gyr)} \le 20$.

4. Results

This modified version of CAMB can be used in three configurations of dark matter: standard CDM, pure mirror matter, and mixed mirror-CDM matter. We considered all these three cases and performed for each of them two analyses, one using the CMB data only and the other using the CMB data combined with the LSS ones. The standard CDM case, with the same assumptions and priors, serves as a reference model.

The CMB datasets come from the WMAP7 team [30], together with the APT [31] and SPT [32] observations. The former provides the acoustic oscillations of the Cosmic Microwave Background on degree scales with limited cosmic-variance precision, while the other two give accurate power spectra at higher l's. For the LSS, we included the power spectrum from the SDSS-DR7 luminous red galaxy sample [33] limited to $k \lesssim 0.2h\,\text{Mpc}^{-1}$, corresponding to sufficiently large length scales, where nonlinear clustering and scale-dependent galaxy biasing do not have to be taken into account.

In Table 2, we show the $1-\sigma$ constraints on the parameters obtained from the different dark matter compositions and cosmological tests. The density probability of the parameter

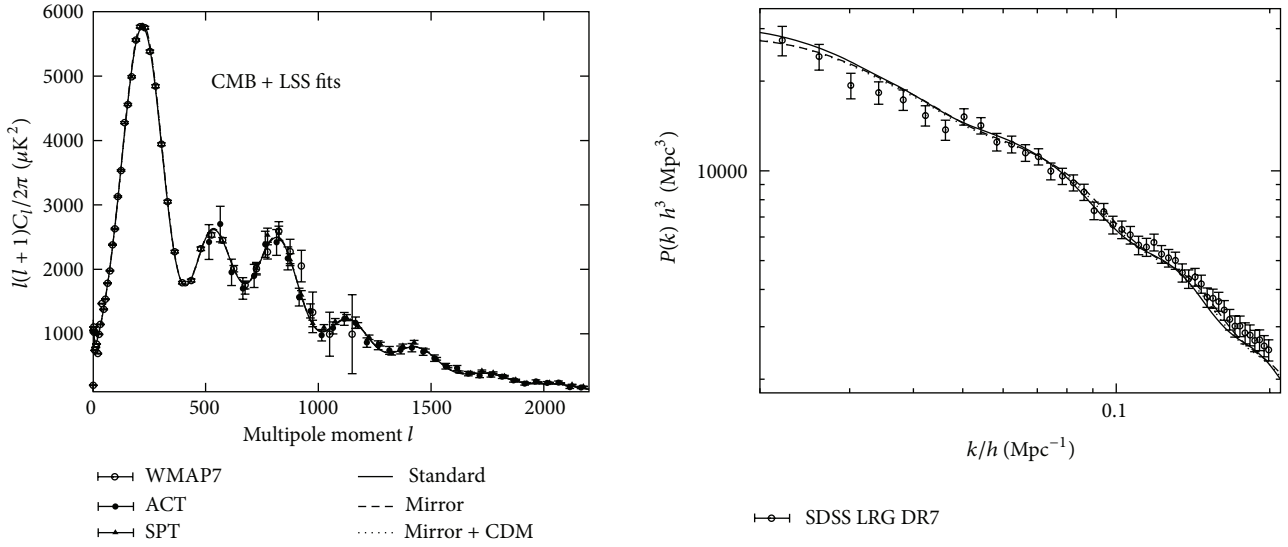

Figure 2: CMB and LSS power spectra for best-fit models with baryons and mirror matter (dashed line), or baryons, mirror matter, and cold dark matter (dotted line) obtained using both CMB and LSS datasets. For comparison we show also the standard model fit (solid line).

Table 2: $1-\sigma$ constraints on the parameters obtained using different dark matter compositions and cosmological tests. For the parameter x we reported the upper limit computed at the 95% c.l.

Parameter	Standard CMB	Standard CMB + LSS	Mirror CMB	Mirror CMB + LSS	Mirror + CDM CMB	Mirror + CDM CMB + LSS
Primary						
$\Omega_b h^2$	0.02213 ± 0.00041	0.02205 ± 0.00034	0.02213 ± 0.00040	0.02215 ± 0.00045	0.02225 ± 0.00044	0.02201 ± 0.00034
$\Omega_{\rm CDM} h^2$	0.1113 ± 0.0046	0.1161 ± 0.0031	—	—	0.026 ± 0.012	0.036 ± 0.010
n_s	0.9616 ± 0.0097	0.9578 ± 0.0081	0.966 ± 0.011	0.961 ± 0.013	0.964 ± 0.012	0.9558 ± 0.0061
$\ln(10^{10} A_s)$	3.051 ± 0.024	3.074 ± 0.021	3.082 ± 0.034	3.090 ± 0.032	3.100 ± 0.038	3.072 ± 0.018
$100\theta_s$	1.0406 ± 0.0017	1.0404 ± 0.0015	1.0413 ± 0.0016	1.0403 ± 0.0016	1.0408 ± 0.0017	1.0400 ± 0.0014
τ	0.073 ± 0.012	0.075 ± 0.011	0.083 ± 0.014	0.085 ± 0.016	0.089 ± 0.016	0.0755 ± 0.0085
Mirror						
x	—	—	<0.456	<0.297	<0.479	<0.315
β	—	—	5.13 ± 0.30	5.21 ± 0.21	4.03 ± 0.50	3.64 ± 0.46
Derived						
Ω_m	0.267 ± 0.025	0.292 ± 0.017	0.273 ± 0.031	0.285 ± 0.020	0.285 ± 0.030	0.291 ± 0.017
Ω_Λ	0.733 ± 0.025	0.708 ± 0.017	0.727 ± 0.031	0.715 ± 0.020	0.715 ± 0.030	0.709 ± 0.017
$z_{\rm re}$	9.3 ± 1.0	9.70 ± 0.95	10.3 ± 1.2	10.5 ± 1.3	10.8 ± 1.4	9.73 ± 0.77
h	0.710 ± 0.022	0.690 ± 0.013	0.708 ± 0.024	0.695 ± 0.017	0.698 ± 0.023	0.690 ± 0.014
Age (Gyr)	13.750 ± 0.092	13.793 ± 0.066	13.687 ± 0.093	13.759 ± 0.088	13.71 ± 0.10	13.782 ± 0.067
σ_8	—	0.824 ± 0.015	—	0.767 ± 0.021	—	0.746 ± 0.018

x was found to be almost flat in the low-x region and sharply decreasing at higher x. For that reason, we chose to give the upper limits on that parameter at the 95% confidence level. The best-fit models obtained by using the CMB data only and both CMB and LSS data are shown in Figures 1 and 2, respectively.

From Table 2, we directly note that the primary cosmological parameters, except the CDM energy density, do not vary significantly from one kind of model to the other and for both analyses (CMB and CMB + LSS). On the other hand, some derived parameters are more perturbed, as the total matter density, which increases at the expenses of the dark energy density in models using CMB data only. This is coupled to the decrease of the Hubble parameter, which still falls within the current constraints. The nonbaryonic matter density is in all cases 5 or 6 times larger than the baryonic density, as usually derived from standard analyses. Turning to the mirror parameters, the 95% c.l. upper limits on x are found to be $x < 0.456$ for a pure mirror Universe and $x < 0.479$ for the mixed mirror-CDM scenario, in case of the CMB only analysis. Adding the LSS constraints in the computations significantly lowers these upper limits, since we

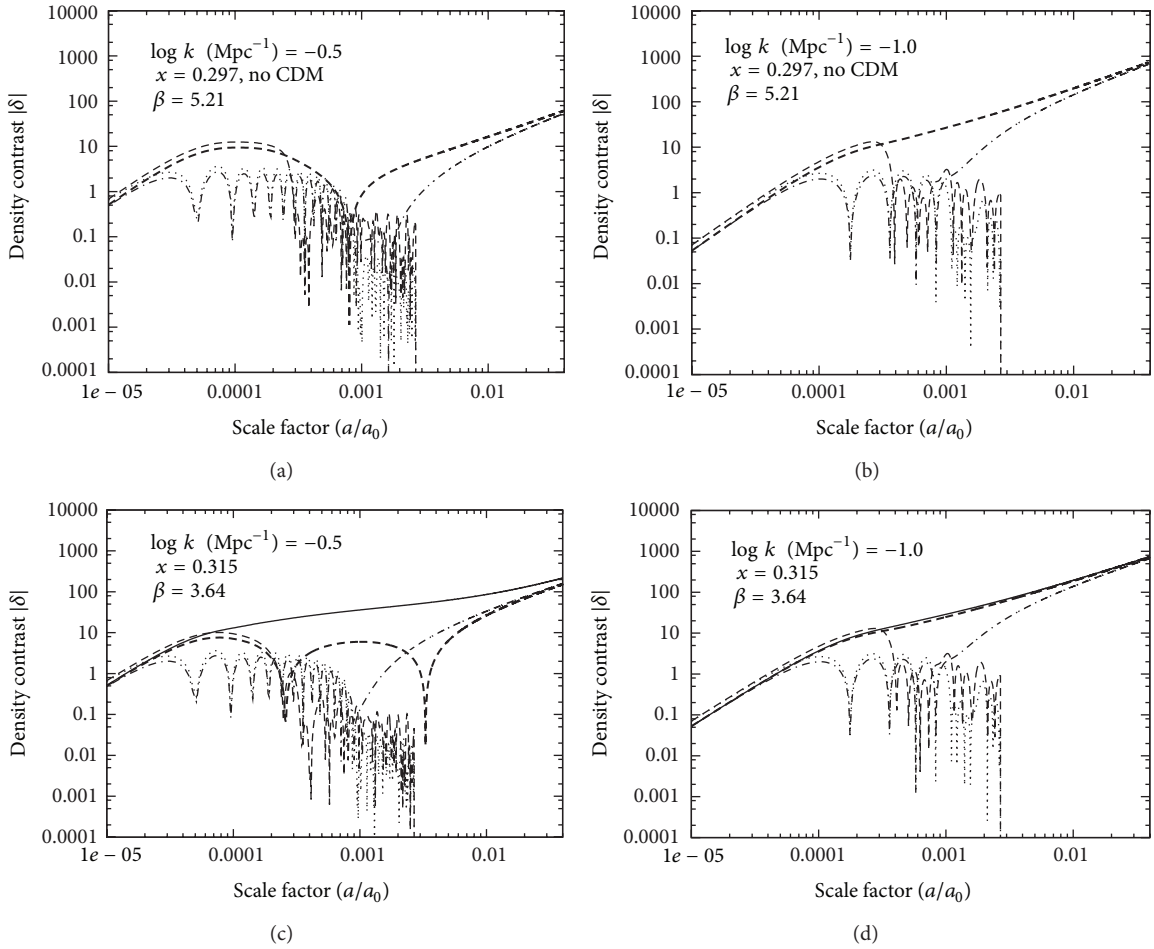

Figure 3: Evolution of the density perturbations of the different components of a mirror Universe: cold dark matter (solid), ordinary baryons (dot-dashed), ordinary photons (dotted), mirror baryons (long dashed), and mirror photons (dashed). The models correspond to the parameters of Table 2 obtained with the CMB and LSS data. (a) Pure mirror case at the scale $\log k\,(\mathrm{Mpc}^{-1}) = -0.5$. (b) Pure mirror case at the scale $\log k\,(\mathrm{Mpc}^{-1}) = -1.0$. (c) Mixed mirror-CDM case at the scale $\log k\,(\mathrm{Mpc}^{-1}) = -0.5$. (d) Mixed mirror-CDM case at the scale $\log k\,(\mathrm{Mpc}^{-1}) = -1.0$.

obtain $x < 0.297$ and $x < 0.315$ at 95% c.l., respectively, for the pure mirror and mixed mirror-CDM cases. This confirms the higher sensitivity on x of the formation of the large scale structure of the Universe already highlighted in previous studies [6, 16]. Note that all these allowed intervals for x contain the values that make possible the interpretation of the direct-dark-matter-search experiments by mirror matter [14, 15]. Finally, the parameter β, quantifying the presence of mirror matter in the Universe, has similar values with CMB only and CMB combined with LSS. In the pure mirror case, β lies between 5 and 5.5, indicating that mirror models require consistent amounts of mirror matter in order to reproduce the observables. In the mixed mirror-CDM case, we find mirror matter densities that are between 2 and 4 times larger than those of CDM. This suggests that, in a Universe with a dark matter composed of several components, the mirror one would be the dominant part.

The likelihoods of the best-fit models for the three compositions of dark matter have, for each analysis (CMB and CMB + LSS), very close values. For pure CDM, pure mirror, and mixed mirror-CDM, they are, respectively, $-\ln(\mathscr{L}) = 3772$, $-\ln(\mathscr{L}) = 3771$, and $-\ln(\mathscr{L}) = 3771$ in case of the CMB only analysis and 3795, 3794, and 3795 in the other case. In view of the difference of one or two degrees of freedom between the models, these values do not show any statistical preference.

In Figure 3 we show the temporal evolution of density perturbations for CDM, ordinary and mirror baryons, and ordinary and mirror photons, computed at two different scales and for our estimated values of the parameters (for x we considered the upper limits) in the two configurations of pure mirror (upper figures) and mixed mirror-CDM (lower figures). In every plot it is visible that the decoupling of mirror baryons and photons happens before the one of the ordinary species, and this is more evident in the right plots. In particular, comparing the top and bottom right plots, one can see the equivalence between CDM and mirror matter for this scale of perturbations and this region of x. The left panels are for the perturbations at a smaller scale. The mentioned CDM-mirror equivalence is at first sight less

evident, but considering the final temporal effect (that gives the distribution of the cosmological matter structures that we see today), again the mirror baryons have a role comparable to the CDM, driving the evolutions of the structures and providing the gravitational seeds where ordinary baryons can fall and accrete.

The fact that we can access only an upper limit on x, together with the equivalence of the different best fits, could suggest a mirror matter with a CDM-like behavior. Indeed, as announced by (4) and further confirmed by [6, 16, 17], the smaller the x, the earlier the decoupling of mirror baryons, and the more they behave like cold dark matter at linear scales, the case $x \to 0$ being equivalent to CDM. If such a trend is verified, CDM could find a possible interpretation through mirror matter. Future data on LSS, especially in nonlinear regimes where mirror matter shows more marked differences with CDM at nonzero x, should help to discriminate between mirror and CDM models, or confirm their equivalence.

5. Conclusion

In summary, we presented up-to-date estimates of the cosmological mirror parameters x and β coming from the observations of the anisotropies of the Cosmic Microwave Background and of the large scale structure of the Universe. The most stringent constraints were obtained by using both the CMB and LSS data, for which we determined that $x < 0.297$ (95% c.l.) and $\beta = 5.21 \pm 0.21$ (1σ) in the pure mirror case, and $x < 0.315$ (95% c.l.) and $\beta = 3.64 \pm 0.46$ (1σ) in the mixed mirror-CDM case. These parameter ranges contain the values favored by the direct searches for dark matter. On the other hand, we have seen that cosmological models with dark sectors constituted by pure CDM, pure mirror matter, and both CDM and mirror matter are equivalent concerning the CMB and LSS power spectra. The upper limits on x together with the equivalence of the different compositions of dark matter may indicate that, if present, mirror matter could behave like CDM. Future data on LSS at nonlinear length scales should help to discriminate between CDM and mirror matter or confirm their equivalence, in which case the latter would be an interpretation of the former.

Conflict of Interests

The authors declare that there is no conflict of interests regarding the publication of this paper.

Acknowledgments

The authors are grateful to Jean-Réné Cudell for useful discussions. Paolo Ciarcelluti acknowledges the hospitality of the IFPA group and the financial support of the Belgian Science Policy during part of this work. Quentin Wallemacq is supported by the Belgian Fund FRS-FNRS as a Research Fellow.

References

[1] T. D. Lee and C. N. Yang, "Question of parity conservation in weak interactions," *Physical Review*, vol. 104, no. 1, pp. 254–258, 1956.

[2] S. Blinnikov and M. Khlopov, "Possible astronomical effects of mirror particles," *Soviet Astronomy*, vol. 27, pp. 371–375, 1983.

[3] E. W. Kolb, D. Seckel, and M. S. Turner, "The shadow world of superstring theories," *Nature*, vol. 314, no. 6010, pp. 415–419, 1985.

[4] M. Y. Khlopov, G. M. Beskin, N. E. Bochkarev, L. A. Pustylnik, and S. A. Pustylnik, "Observational physics of mirror world," *Soviet Astronomy*, vol. 35, p. 21, 1991.

[5] R. Foot, H. Lew, and R. R. Volkas, "A model with fundamental improper spacetime symmetries," *Physics Letters B*, vol. 272, no. 1-2, pp. 67–70, 1991.

[6] P. Ciarcelluti, "Cosmology with mirror dark matter," *International Journal of Modern Physics D*, vol. 19, no. 14, p. 2151, 2010.

[7] L. B. Okun, "Mirror particles and mirror matter: 50 years of speculation and searching," *Physics-Uspekhi*, vol. 50, no. 4, p. 380, 2007.

[8] P. Ciarcelluti, "Cosmology ofthe mirror universe," http://arxiv.org/abs/astro-ph/0312607.

[9] R. Foot, "Experimental implications of mirror matter-type dark matter," *International Journal of Modern Physics A*, vol. 19, no. 23, p. 3807, 2004.

[10] P. Ciarcelluti and R. Foot, "Early Universe cosmology in the light of the mirror dark matter interpretation of the DAMA/Libra signal," *Physics Letters B*, vol. 679, no. 3, pp. 278–281, 2009.

[11] P. Ciarcelluti and R. Foot, "Primordial He' abundance implied by the mirror dark matter interpretation of the DAMA/LIBRA signal," *Physics Letters B*, vol. 690, no. 5, pp. 462–465, 2010.

[12] F. Sandin and P. Ciarcelluti, "Effects of mirror dark matter on neutron stars," *Astroparticle Physics*, vol. 32, no. 5, pp. 278–284, 2009.

[13] P. Ciarcelluti and F. Sandin, "Have neutron stars a dark matter core?" *Physics Letters B*, vol. 695, no. 1–4, pp. 19–21, 2011.

[14] R. Foot, "Mirror dark matter and the new DAMA/LIBRA results: a simple explanation for a beautiful experiment," *Physical Review D*, vol. 78, no. 4, Article ID 043529, 10 pages, 2008.

[15] R. Foot, "Mirror dark matter interpretations of the DAMA, CoGeNT, and CRESST-II data," *Physical Review D*, vol. 86, no. 2, Article ID 023524, 10 pages, 2012.

[16] P. Ciarcelluti, "Cosmology with mirror dark matter II: cosmic microwave background and large scale structure," *International Journal of Modern Physics D*, vol. 14, no. 2, p. 223, 2005.

[17] P. Ciarcelluti, "Cosmology with mirror dark matter I: linear evolution of perturbations," *International Journal of Modern Physics D*, vol. 14, no. 2, p. 187, 2005.

[18] Z. Berezhiani, P. Ciarcelluti, D. Comelli, and F. L. Villante, "Structure formation with mirror dark matter: CMB and LSS," *International Journal of Modern Physics D*, vol. 14, no. 1, p. 107, 2005.

[19] P. Ciarcelluti, "Structure formation, CMB and LSS in a mirror dark matter scenario," *Frascati Physics Series*, vol. 555, p. 1, 2004.

[20] A. Y. Ignatiev and R. R. Volkas, "Mirror dark matter and large scale structure," *Physical Review D*, vol. 68, no. 2, Article ID 023518, 11 pages, 2003.

[21] Y. Izotov and T. Thuan, "The primordial abundance of ^{4}He: evidence for non-standard big bang nucleosynthesis," *The Astrophysical Journal Letters*, vol. 710, no. 1, p. L67, 2010.

[22] R. Foot, "Implications of mirror dark matter kinetic mixing for CMB anisotropies," *Physics Letters B*, vol. 718, no. 3, pp. 745–751, 2012.

[23] A. Lewis, A. Challinor, and A. Lasenby, "Efficient computation of cosmic microwave background anisotropies in closed Friedmann-Robertson-Walker models," *The Astrophysical Journal*, vol. 538, no. 2, p. 473, 2000.

[24] A. Lewis and S. Bridle, "Cosmological parameters from CMB and other data: a Monte Carlo approach," *Physical Review D*, vol. 66, no. 10, Article ID 103511, 16 pages, 2002.

[25] S. Seager, D. D. Sasselov, and D. Scott, "A new calculation of the recombination epoch," *The Astrophysical Journal Letters*, vol. 523, no. 1, p. L1, 1999.

[26] P. Ciarcelluti, "Astrophysical tests of mirror dark matter," *AIP Conference Proceedings*, vol. 1038, pp. 202–210, 2008.

[27] P. Ciarcelluti and A. Lepidi, "Thermodynamics of the early Universe with mirror dark matter," *Physical Review D*, vol. 78, no. 12, Article ID 123003, 7 pages, 2008.

[28] P. Ciarcelluti, "Early Universe cosmology with mirror dark matter," *AIP Conference Proceedings*, vol. 1241, p. 351, 2010.

[29] P. Ciarcelluti, "Big Bang nucleosynthesis in visible and hidden-mirror sectors," *Advances in High Energy Physics*. In Press.

[30] D. Larson, J. Dunkley, G. Hinshaw et al., "Seven-year Wilkinson Microwave Anisotropy Probe (WMAP) observations: power spectra and WMAP-derived parameters," *The Astrophysical Journal Supplement Series*, vol. 192, no. 2, p. 16, 2011.

[31] J. L. Sievers, R. A. Hlozek, M. R. Nolta et al., "The Atacama Cosmology Telescope: cosmological parameters from three seasons of data," *Journal of Cosmology and Astroparticle Physics*, vol. 1310, article 60S, 2013.

[32] R. Keisler, C. Reichardt, K. Aird et al., "A measurement of the damping tail of the cosmic microwave background power spectrum with the south pole telescope," *The Astrophysical Journal*, vol. 743, no. 1, p. 28, 2011.

[33] B. A. Reid, W. J. Percival, D. J. Eisenstein et al., "Cosmological constraints from the clustering of the Sloan Digital Sky Survey DR7 luminous red galaxies," *Monthly Notices of the Royal Astronomical Society*, vol. 404, no. 1, pp. 60–85, 2010.

Hindawi Publishing Corporation
Advances in High Energy Physics
Volume 2014, Article ID 869425, 5 pages
http://dx.doi.org/10.1155/2014/869425

Research Article

Dark Atoms and the Positron-Annihilation-Line Excess in the Galactic Bulge

J.-R. Cudell,[1] M. Yu. Khlopov,[2,3,4] and Q. Wallemacq[1]

[1] *IFPA, "Département d'AGO", Université de Liège, Sart Tilman, 4000 Liège, Belgium*
[2] *National Research Nuclear University "Moscow Engineering Physics Institute," Moscow 115409, Russia*
[3] *Centre for Cosmoparticle Physics "Cosmion," 115409 Moscow, Russia*
[4] *APC Laboratory 10, rue Alice Domon et Léonie Duquet, 75205 Paris Cedex 13, France*

Correspondence should be addressed to Q. Wallemacq; quentin.wallemacq@ulg.ac.be

Received 25 November 2013; Accepted 13 January 2014; Published 25 February 2014

Academic Editor: Chris Kouvaris

It was recently proposed that stable particles of charge −2, O^{--}, can exist and constitute dark matter after they bind with primordial helium in O-helium (OHe) atoms. We study here in detail the possibility that this model provides an explanation for the excess of gamma radiation in the positron-annihilation line from the galactic bulge observed by INTEGRAL. This explanation assumes that OHe, excited to a 2s state through collisions in the central part of the Galaxy, deexcites to its ground state via an $E0$ transition, emitting an electron-positron pair. The cross-section for OHe collisions with excitation to 2s level is calculated and it is shown that the rate of such excitations in the galactic bulge strongly depends not only on the mass of O-helium, which is determined by the mass of O^{--}, but also on the density and velocity distribution of dark matter. Given the astrophysical uncertainties on these distributions, this mechanism constrains the O^{--} mass to lie in two possible regions. One of these is reachable in the experimental searches for stable multicharged particles at the LHC.

1. Introduction

According to modern cosmology, dark matter corresponds to 25% of the total cosmological density, is nonbaryonic, and consists of new stable particles. Such particles (see [1–6] for reviews and references) should be stable, provide the measured dark-matter density, and be decoupled from plasma and radiation at least before the beginning of the matter-dominated era. It was recently shown that heavy stable particles of charge −2, O^{--}, bound to primordial helium in OHe atoms, can provide an interesting explanation for cosmological dark matter [6, 7]. It should also be noted that the nuclear cross-section of the O-helium interaction with matter escapes the severe constraints [8–10] on strongly interacting dark-matter particles (SIMPs) [8–16] imposed by the XQC experiment [17, 18].

The hypothesis of composite O-helium dark matter, first considered to provide a solution to the puzzles of direct dark-matter searches, can offer an explanation for another puzzle of modern astrophysics [6, 7, 19]: this composite dark-matter model can explain the excess of gamma radiation in the electron-positron-annihilation line, observed by INTEGRAL in the galactic bulge (see [20] for a review and references). The explanation assumes that OHe provides all the galactic dark matter and that its collisions in the central part of the Galaxy result in 2s-level excitations of OHe which are deexcited to the ground state by an $E0$ transition, in which an electron-positron pair is emitted. If the 2s level is excited, pair production dominates over the two-photon channel in the deexcitation, because electrons are much lighter than helium nuclei, and positron production is not accompanied by a strong gamma-ray signal.

According to [21] the rate of positron production $3 \cdot 10^{42}\ s^{-1}$ is sufficient to explain the excess in the positron-annihilation line from the bulge measured by INTEGRAL. In the present paper we study the process of 2s-level excitation of OHe from collisions in the galactic bulge and determine the conditions under which such collisions can provide

the observed excess. Inelastic interactions of O-helium with matter in interstellar space and subsequent deexcitation can give rise to radiation in the range from a few keV to a few MeV. In the galactic bulge with radius $r_b \sim 1\,\mathrm{kpc}$ the number density of O-helium can be of the order of $n_o \approx 3 \cdot 10^{-3}/S_3\,\mathrm{cm}^{-3}$ or larger, and the collision rate of O-helium in this central region was estimated in [19]: $dN/dt = n_o^2 \sigma v_h 4\pi r_b^3/3 \approx 3 \cdot 10^{42} S_3^{-2}\,\mathrm{s}^{-1}$, with $S_3 = m_{\mathrm{OHe}}/1\,\mathrm{TeV}$. At the velocity of $v_h \sim 3 \cdot 10^7$ cm/s energy transfer in such collisions is $\Delta E \sim 1\,\mathrm{MeV} S_3$. These collisions can lead to excitation of O-helium. If OHe levels with nonzero angular momentum are excited, gamma lines should be observed from transitions $(n > m)$ $E_{nm} = 1.598\,\mathrm{MeV}(1/m^2 - 1/n^2)$ (or from similar transitions corresponding to the case $I_o = 1.287\,\mathrm{MeV}$) at the level $3 \cdot 10^{-4} S_3^{-2} (\mathrm{cm}^2\,\mathrm{s\,MeV\,ster})^{-1}$.

2. Collisional Excitation Cross-Section

The studied reaction is the collision between two OHe atoms, both being initially in their ground state $|1s\rangle$, giving rise to the excitation of one of them to a $|ns\rangle$ state while the other remains in its ground state:

$$\mathrm{OHe}\,(1s) + \mathrm{OHe}\,(1s) \longrightarrow \mathrm{OHe}\,(1s) + \mathrm{OHe}\,(ns)\,. \quad (1)$$

If we work in the rest frame of the OHe that gets excited and if we neglect its recoil after the collision, the differential cross-section of the process is given by

$$d\sigma\,(1s \longrightarrow ns) = 2\pi \left| \left\langle ns, \vec{p}\,' | U | 1s, \vec{p} \right\rangle \right|^2 \times \delta\left(\frac{p'^2}{2M} + E_{ns} - \frac{p^2}{2M} - E_{1s} \right) \frac{d^3 p'}{(2\pi)^3}, \quad (2)$$

where M is the mass of OHe, $\vec{p}$ and $\vec{p}\,'$ are the momenta of the incident OHe before and after the collision, E_{1s} and E_{ns} are the ground-state and excited-state energies of the target OHe, and U is the interaction potential between the incident and the target OHe's.

We will neglect the internal structure of the incident OHe, so that its wave functions are plane waves. $\psi_{\vec{p}}$ is normalized to obtain a unit incident current density and the normalisation of $\psi_{\vec{p}'}$ is chosen for it to be pointlike, that is, the Fourier transform of $\delta^{(3)}(\vec{r})$ [22]:

$$\psi_{\vec{p}} = \sqrt{\frac{M}{p}} e^{i\vec{p}\cdot\vec{r}}, \qquad \psi_{\vec{p}'} = e^{i\vec{p}'\cdot\vec{r}}, \quad (3)$$

where $\vec{r}$ is the position vector of the incident OHe and $p = |\vec{p}|$.

In the following, we will be led to consider O^{--} masses which are much larger than the mass of helium or the bound-state energies. Therefore, the origin of the rest frame of the target OHe coincides with the position of its O^{--} component and its reduced mass μ can be taken as the mass of helium M_{He}.

The OHe that gets excited is described as a hydrogen-like atom, with energy levels $E_{ns} = -0.5 M_{\mathrm{He}} (Z_{\mathrm{He}} Z_{\mathrm{O}} \alpha)^2/n^2$ and initial and final bound-state wave functions ψ_{1s} and ψ_{ns} of a hydrogenoid atom with a Bohr radius $a_0 = (M_{\mathrm{He}} Z_{\mathrm{He}} Z_{\mathrm{O}} \alpha)^{-1}$.

The incident OHe interacts with the O^{--} and helium components in the target OHe, so that the interaction potential U is the sum of the two contributions U_{O} and U_{He}:

$$U(\vec{r}) = U_{\mathrm{O}}(\vec{r}) + U_{\mathrm{He}}(\vec{r} - \vec{r}_{\mathrm{He}})\,, \quad (4)$$

where $\vec{r}_{\mathrm{He}}$ is the position vector of the helium component.

The first term U_{O} gives a zero contribution to the integral of expression (2) since the states ψ_{1s} and ψ_{ns} are orthogonal. For the second term, we treat the incident OHe as a heavy neutron colliding on a helium nucleus through short-range nuclear forces. The interaction potential can then be written in the form of a contact term:

$$U_{\mathrm{He}}(\vec{r} - \vec{r}_{\mathrm{He}}) = -\frac{2\pi}{M_{\mathrm{He}}} a_0 \delta(\vec{r} - \vec{r}_{\mathrm{He}})\,, \quad (5)$$

where we have normalised the delta function to obtain an OHe-helium elastic cross-section equal to $4\pi a_0^2$.

Going to spherical coordinates for $\vec{p}\,'$ and integrating over $p' = |\vec{p}\,'|$ in the differential cross-section (2), together with the previous expressions (3), (4), and (5), we get

$$d\sigma\,(1s \longrightarrow ns) = \left(\frac{M}{M_{\mathrm{He}}} \right)^2 a_0^2 \left(\frac{p'}{p} \right) \times \left| \int e^{-i\vec{q}\cdot\vec{r}_{\mathrm{He}}} \psi_{ns}^* \psi_{1s} d^3 r_{\mathrm{He}} \right|^2 d\Omega, \quad (6)$$

where $\vec{q} = \vec{p}\,' - \vec{p}$ is the transferred momentum and $d\Omega$ is the solid angle. From the integration over the delta function in (2), we have obtained the conservation of energy during the process:

$$p'^2 = p^2 + 2M(E_{1s} - E_{ns})\,. \quad (7)$$

It leads to the threshold energy corresponding to $p'^2 = 0$ and to a minimum incident velocity $v_{\min} = \sqrt{2(E_{ns} - E_{1s})/M}$. The previous expression for p' allows us to express the squared modulus of $\vec{q}$ as

$$q^2 = 2\left(p^2 + M(E_{1s} - E_{ns}) - p\sqrt{p^2 + 2M(E_{1s} - E_{ns})\cos\theta} \right), \quad (8)$$

where θ is the deviation angle of the incident OHe with respect to the collision axis in the rest frame of the target OHe.

e^+e^- pairs will be dominantly produced if OHe is excited to a 2s state, since the only deexcitation channel is in this case from 2s to 1s. As e^+e^- pair production is the only possible channel, the differential pair-production cross-section $d\sigma_{ee}$ is equal to the differential collisional excitation cross-section. By particularizing expression (6) to the case $n = 2$, one finally gets

$$\frac{d\sigma_{ee}}{d\cos\theta} = 512^2 \left(\frac{2\pi M^2}{M_{\mathrm{He}}^2} \right) a_0^6 \left(\frac{p'}{p} \right) \frac{q^4}{2\left(4a_0^2 q^2 + 9\right)^6}. \quad (9)$$

3. The e^+e^- Pair-Production Rate in the Galactic Bulge

The total e^+e^- pair-production rate in the galactic bulge is given by

$$\left.\frac{dN}{dt}\right|_{ee} = \int_{V_b} \frac{\rho_{\rm DM}^2\left(\vec{R}\right)}{M^2}\left\langle\sigma_{ee}v\right\rangle\left(\vec{R}\right)d\vec{R}, \tag{10}$$

where V_b is the volume of the galactic bulge, which is a sphere of radius $R_b = 1.5$ kpc, $\rho_{\rm DM}$ is the energy density distribution of dark matter in the galactic halo, and $\langle\sigma_{ee}v\rangle$ is the pair-production cross-section σ_{ee} times relative velocity v averaged over the velocity distribution of dark-matter particles. The total pair-production cross-section σ_{ee} is obtained by integrating (9) over the diffusion angle. Its dependence on the relative velocity v is contained in p, p', and q through $p = Mv$ and the expressions (7) and (8) of p' and q in terms of p.

We use a Burkert [23, 24] flat, cored, dark-matter density profile known to reproduce well the kinematics of disk systems in massive spiral galaxies and supported by recent simulations including supernova feedback and radiation pressure of massive stars [25] in response to the cuspy halo problem:

$$\rho_{\rm DM}(R) = \rho_0\frac{R_0^3}{(R+R_0)\left(R^2+R_0^2\right)}, \tag{11}$$

where R is the distance from the galactic center. The central dark-matter density ρ_0 is left as a free parameter and R_0 is determined by requiring that the local dark-matter density at $R = R_\odot = 8$ kpc is $\rho_\odot = 0.3\,\text{GeV/cm}^3$. The dark-matter mass enclosed in a sphere of radius R is therefore given by

$$M_{\rm DM}(R) = \rho_0\pi R_0^3\left\{\log\left(\frac{R^2+R_0^2}{R_0^2}\right) + 2\log\left(\frac{R+R_0}{R_0}\right) - 2\arctan\left(\frac{R}{R_0}\right)\right\}. \tag{12}$$

For the baryons in the bulge, we use an exponential profile [26] of the form

$$\rho_b(R) = \frac{M_{\rm bulge}}{8\pi R_b^3}e^{-R/R_b}, \tag{13}$$

where $M_{\rm bulge} = 10^{10}M_\odot$ [27] is the mass of the bulge. This gives the baryonic mass distribution in the galactic bulge

$$M_b(R) = M_{\rm bulge}\left\{1 - e^{-R/R_b}\left(1+\frac{R}{R_b}+\frac{R^2}{R_b^2}\right)\right\}. \tag{14}$$

We assume a Maxwell-Boltzmann velocity distribution for the dark-matter particles of the galactic halo, with a velocity dispersion $u(R)$ and a cutoff at the galactic escape velocity $v_{\rm esc}(R)$:

$$f\left(R,\vec{v}_h\right) = \frac{1}{C(R)}e^{-v_h^2/u^2(R)}, \tag{15}$$

where $\vec{v}_h$ is the velocity of the dark-matter particles in the frame of the halo and $C(R) = \pi u^2(\sqrt{\pi}u\,\text{erf}(v_{\rm esc}/u) - 2v_{\rm esc}e^{-v_{\rm esc}^2/u^2})$ is a normalization constant such that $\int_0^{v_{\rm esc}(R)} f(R,\vec{v}_h)d\vec{v}_h = 1$.

The radial dependence of the velocity dispersion is obtained via the virial theorem:

$$u(R) = \sqrt{\frac{GM_{\rm tot}(R)}{R}}, \tag{16}$$

where $M_{\rm tot} = M_{\rm DM} + M_b$, while $v_{\rm esc} = \sqrt{2}u$.

Using the velocity distribution (15), going to center-of-mass and relative velocities $\vec{v}_{\rm CM}$ and $\vec{v}$, and performing the integrals over $\vec{v}_{\rm CM}$, we obtain for the mean pair-production cross-section times relative velocity

$$\left\langle\sigma_{ee}v\right\rangle = \frac{1}{u^2}\frac{\sqrt{2\pi}u\,\text{erf}\left(\sqrt{2}v_{\rm esc}/u\right) - 4v_{\rm esc}e^{-2v_{\rm esc}^2/u^2}}{\left(\sqrt{\pi}u\,\text{erf}\left(v_{\rm esc}/u\right) - 2v_{\rm esc}e^{-v_{\rm esc}^2/u^2}\right)^2} \times \int_0^{2v_{\rm esc}}\sigma_{ee}(v)\,v^3e^{-v^2/2u^2}dv, \tag{17}$$

which is also a function of R through u and $v_{\rm esc}$. Putting (9), (11), (12), (14), (16), and (17) together allows us to compute the pair-production rate in the galactic bulge defined in (10) as a function of ρ_0 and M.

4. Results

The rate of excessive e^+e^- pairs to be generated in the galactic bulge was estimated in [21] to be $dN/dt|_{\rm obs} = 3\times10^{42}\,\text{s}^{-1}$. We computed $dN/dt|_{ee}$ for a large range of central dark-matter densities, going from $0.3\,\text{GeV/cm}^3$ to an ultimate upper limit of $10^4\,\text{GeV/cm}^3$ [28]. For each value of ρ_0, we searched for the mass M of OHe that reproduces the observed rate. The results are shown in Figure 1.

The observed rate can be reproduced from a value of $\rho_0 \simeq 115\,\text{GeV/cm}^3$, corresponding to an OHe mass of $M \simeq 1.25$ TeV. As ρ_0 gets larger, two values of M are possible, with the lower one going from 1.25 TeV to 130 GeV and the upper one going from 1.25 to 130 TeV as ρ_0 goes from 115 to $10^4\,\text{GeV/cm}^3$.

5. Conclusion

The existence of heavy stable particles is one of the most popular solutions for the dark- matter problem. Usually they are considered to be electrically neutral. But dark matter can potentially be made of stable heavy charged particles bound in neutral atom-like states by Coulomb attraction. An analysis of the cosmological data and of the atomic composition of the Universe forces the particle to have charge -2. O^{--} is then trapped by primordial helium in neutral O-helium states and this avoids the problem of overproduction of anomalous isotopes, which are severely constrained by observations. Here we have shown that the cosmological model of O-helium dark matter can explain the puzzle of positron line emission from the center of our Galaxy.

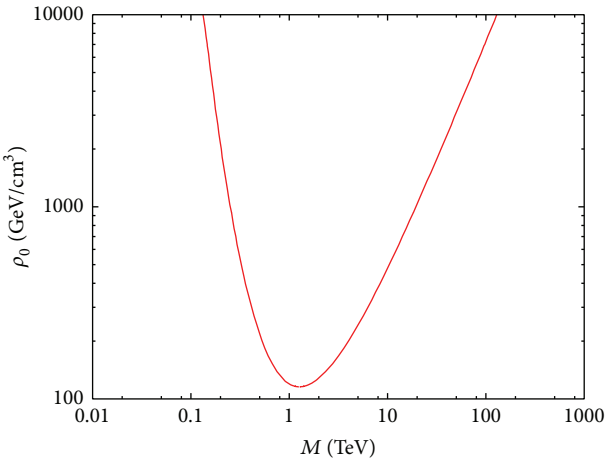

FIGURE 1: Values of the central dark-matter density ρ_0 (GeV/cm^3) and of the OHe mass M (TeV) reproducing the excess of e^+e^- pairs production in the galactic bulge. Below the red curve, the predicted rate is too low.

The proposed explanation is based on the assumption that OHe dominates the dark-matter sector. Its collisions can lead to $E0$ deexcitations of the 2s states excited by the collisions. The estimated luminosity in the electron-positron-annihilation line strongly depends not only on the mass of O^{--} but also on the density profile and velocity distribution of dark matter in the galactic bulge. Note that the density profile we considered is used only to obtain a reasonable estimate for the uncertainties on the density in the bulge. It indeed underestimates the mass of the Galaxy, but it shows that the uncertainties on the astrophysical parameters are large enough to reproduce the observed excess for a rather wide range of masses of O^{--}. For a fixed density profile and a fixed velocity distribution, only two values of the O^{--} mass lead to the necessary rate of positron production. The lower value of this mass, which does not exceed 1.25 TeV, is within the reach of experimental searches for multicharged stable heavy particles at the LHC.

Conflict of Interests

The authors declare that there is no conflict of interests regarding the publication of this paper.

Acknowledgment

The authors express their gratitude to A. S. Romaniouk for discussions.

References

[1] M. Yu. Khlopov, *Cosmoparticle Physics*, World Scientific, Singapore, 1999.

[2] M. Yu. Khlopov, "Cosmoarcheology. Direct and indirect astrophysical effects of hypothetical particles and fields," in *Cosmion-94*, M. Yu. Khlopov, M. E. Prokhorov, A. A. Starobinsky, and J. Tran Thanh Van, Eds., pp. 67–76, Editions Frontières, Quebec, Canada, 1996.

[3] M. Y. Khlopov, "Proceedings to the 9th workshop 'what comes beyond the standard models'," *Bled Workshops in Physics*, vol. 7, no. 2, p. 51, 2006.

[4] M. Y. Khlopov, "Proceedings to the 10th workshop 'what comes beyond the standard models'," *Bled Workshops in Physics*, vol. 8, no. 2, p. 114, 2007.

[5] M. Yu. Khlopov, *Fundamentals of Cosmoparticle Physics*, CISP-Springer, Cambridge, UK, 2012.

[6] M. Yu. Khlopov, "Fundamental particle structure in the cosmological dark matter," *International Journal of Modern Physics A*, vol. 28, no. 29, Article ID 1330042, 60 pages, 2013.

[7] M. Yu. Khlopov, "Physics of dark matter in the light of dark atoms," *Modern Physics Letters A*, vol. 26, no. 38, Article ID 2823, 2011.

[8] B. D. Wandelt, R. Dave, G. R. Farrar, P. C. McGuire, D. N. Spergel, and P. J. Steinhardt, "Self-interacting dark matter," http://arxiv.org/abs/astro-ph/0006344.

[9] P. C. McGuire and P. J. Steinhardt, "Cracking open the window for strongly interacting massive particles as the halo dark matter," http://arxiv.org/abs/astro-ph/0105567.

[10] G. Zaharijas and G. R. Farrar, "Window in the dark matter exclusion limits," *Physical Review D*, vol. 72, no. 8, Article ID 083502, 11 pages, 2005.

[11] C. B. Dover et al., "Cosmological constraints on new stable hadrons," *Physical Review Letters*, vol. 42, no. 17, pp. 1117–1120, 1979.

[12] S. Wolfram, "Abundances of new stable particles produced in the early universe," *Physics Letters B*, vol. 82, no. 1, pp. 65–68, 1979.

[13] G. D. Starkman, A. Gould, R. Esmailzadeh, and S. Dimopoulos, "Opening the window on strongly interacting dark matter," *Physical Review D*, vol. 41, no. 12, pp. 3594–3603, 1990.

[14] D. Javorsek, D. Elmore, E. Fischbach et al., "New experimental limits on strongly interacting massive particles at the TeV scale," *Physical Review Letters*, vol. 87, no. 23, Article ID 231804, 2001.

[15] S. Mitra, "Uranus's anomalously low excess heat constrains strongly interacting dark matter," *Physical Review D*, vol. 70, no. 10, Article ID 103517, 2004.

[16] G. D. Mack, J. F. Beacom, and G. Bertone, "Towards closing the window on strongly interacting dark matter: far-reaching constraints from Earth's heat flow," *Physical Review D*, vol. 76, no. 4, Article ID 043523, 2007.

[17] D. McCammon, R. Almy, S. Deiker et al., "A sounding rocket payload for X-ray astronomy employing high-resolution microcalorimeters," *Nuclear Instruments and Methods in Physics Research Section A*, vol. 370, no. 1, pp. 266–268, 1996.

[18] D. McCammon, R. Almy, E. Apodaca et al., "A high spectral resolution observation of the soft X-ray diffuse background with thermal detectors ," *The Astrophysical Journal*, vol. 576, no. 1, p. 188, 2002.

[19] M. Yu. Khlopov, "Composite dark matter from stable charged constituents," http://arxiv.org/abs/0806.3581.

[20] B. J. Teegarden, K. Watanabe, P. Jean et al., "INTEGRAL SPI limits on electron-positron annihilation radiation from the galactic plane," *The Astrophysical Journal*, vol. 621, no. 1, p. 296, 2005.

[21] D. P. Finkbeiner and N. Weiner, "Exciting dark matter and the INTEGRAL/SPI 511 keV signal," *Physical Review D*, vol. 76, no. 8, Article ID 083519, 2007.

[22] L. D. Landau and E. M. Lifshitz, *Quantum Mechanics*, Pergamon Press, Elmsford, NY, USA, 1965.

[23] A. Burkert, "The structure of dark matter haloes in dwarf galaxies," *IAU Symposia*, vol. 171, p. 175, 1996.

[24] A. Burkert, "The structure of dark matter haloes in dwarf galaxies," *The Astrophysical Journal*, vol. 447, no. 1, p. L25, 1995.

[25] A. V. Maccio, G. Stinson, C. B. Brook et al., "HALO Expansion in cosmological hydro simulations: toward a baryonic solution of the cusp/core problem in massive spirals," *The Astrophysical Journal Letters*, vol. 744, no. 1, p. L9, 2012.

[26] O. Y. Gnedin, A. V. Kravtsov, A. A. Klypin, and D. Nagai, "Response of dark matter halos to condensation of Baryons: cosmological simulations and improved adiabatic contraction model," *The Astrophysical Journal*, vol. 616, no. 1, p. 16, 2004.

[27] H. Mo, F. van den Bosch, and S. White, *Galaxy Formation and Evolution*, Cambridge University Press, Cambridge, UK, 2010.

[28] X. Hernandez and W. H. Lee, "An upper limit to the central density of dark matter haloes from consistency with the presence of massive central black holes," *Monthly Notices of the Royal Astronomical Society*, vol. 404, no. 1, p. L10, 2010.

Hindawi Publishing Corporation
Advances in High Energy Physics
Volume 2014, Article ID 406458, 7 pages
http://dx.doi.org/10.1155/2014/406458

Research Article

Probes for 4th Generation Constituents of Dark Atoms in Higgs Boson Studies at the LHC

M. Yu. Khlopov[1,2,3] and R. M. Shibaev[1]

[1] *National Research Nuclear University "Moscow Engineering Physics Institute", Moscow 115409, Russia*
[2] *Centre for Cosmoparticle Physics "Cosmion" Moscow 115409, Russia*
[3] *APC laboratory 10, rue Alice Domon et Léonie Duquet, 75205 Paris Cedex 13, France*

Correspondence should be addressed to R. M. Shibaev; ratibor.shibaev@list.ru

Received 20 October 2013; Revised 18 December 2013; Accepted 18 December 2013; Published 18 February 2014

Academic Editor: Konstantin Belotsky

The nonbaryonic dark matter of the Universe can consist of new stable charged species, bound in heavy neutral "atoms" by ordinary Coulomb interaction. Stable $\overline{U}$ (anti-U)quarks of 4th generation, bound in stable colorless $(\overline{U}\,\overline{U}\,\overline{U})$ clusters, are captured by the primordial helium, produced in Big Bang Nucleosynthesis, thus forming neutral "atoms" of O-helium (OHe), a specific nuclear interacting dark matter that can provide solution for the puzzles of direct dark matter searches. However, the existence of the 4th generation quarks and leptons should influence the production and decay rates of Higgs boson and is ruled out by the experimental results of the Higgs boson searches at the LHC, if the Higgs boson coupling to 4th generation fermions is not suppressed. Here, we argue that the difference between the three known quark-lepton families and the 4th family can naturally lead to suppression of this coupling, relating the accelerator test for such a composite dark matter scenario to the detailed study of the production and modes of decay of the 125.5 GeV boson, discovered at the LHC.

1. Introduction

The cosmological dark matter can consist of dark atoms, in which new stable charged particles are bound by ordinary Coulomb interaction (see [1–5] for review and references). In order to avoid anomalous isotopes overproduction, stable particles with charge −1 (and corresponding antiparticles as tera-particles [6]) should be absent [7], so that stable negatively charged particles should have charge −2 only.

There exist several types of particle models, in which heavy stable −2 charged species, O^{--}, are predicted as follows:

(a) AC-leptons, predicted in the extension of standard model, based on the approach of almost-commutative geometry [8–11],

(b) technileptons and antitechnibaryons in the framework of walking technicolor models (WTC) [12–18],

(c) finally, stable "heavy quark clusters" $\overline{U}\,\overline{U}\,\overline{U}$ formed by anti-U quark of 4th generation [8, 19–23].

All these models also predict corresponding +2 charge particles. If these positively charged particles remain free in the early Universe, they can recombine with ordinary electrons in anomalous helium, which is strongly constrained in the terrestrial matter. Therefore, cosmological scenario should provide a mechanism, which suppresses anomalous helium. There are two possibilities, requiring two different mechanisms of such suppression.

(i) The abundance of anomalous helium in the Galaxy may be significant, but in the terrestrial matter there exists a recombination mechanism suppressing this abundance below experimental upper limits [8, 10]. The existence of a new strict $U(1)$ gauge symmetry, causing new Coulomb-like long range interaction between charged dark matter particles, is crucial for this mechanism. Therefore, the existence of dark radiation in the form of hidden photons is inevitable in this approach.

(ii) Free positively charged particles are already suppressed in the early Universe and the abundance of anomalous helium in the Galaxy is negligible [3, 4, 20].

These two possibilities correspond to two different cosmological scenarios of dark atoms. The first one is realized in the scenario with AC leptons, forming neutral AC atoms [10]. The second assumes charge asymmetric case with the excess of O^{--}, which form atom-like states with primordial helium [3, 4, 20].

If new stable species belong to nontrivial representations of electroweak SU(2) group, sphaleron transitions at high temperatures can provide the relationship between baryon asymmetry and excess of −2 charge stable species, as it was demonstrated in the case of WTC [12, 24–26].

After it is formed in the Standard Big Bang Nucleosynthesis (SBBN), ^4He screens the O^{--} charged particles in composite ($^4He^{++}O^{--}$) *O-helium* "atoms" [20].

In all the models of O-helium, O^{--} behaves either as lepton or as specific "heavy quark cluster" with strongly suppressed hadronic interaction. Therefore, O-helium interaction with matter is determined by nuclear interaction of He. These neutral primordial nuclear interacting objects can explain the modern dark matter density and represent a nontrivial form of strongly interacting dark matter [27–35].

The cosmological scenario of O-helium Universe allows to explain many results of experimental searches for dark matter [3]. Such scenario is insensitive to the properties of O^{--}, since the main features of OHe dark atoms are determined by their nuclear interacting helium shell. It challenges experimental probes for the new stable charged particles at accelerators and such probes strongly depend on the nature of O^{--}.

Stable −2 charge states (O^{--}) can be elementary like AC-leptons or technileptons or look like elementary as technibaryons. The latter, composed of techniquarks, reveal their structure at much higher energy scale and should be produced at the LHC as elementary species. They can also be composite-like "heavy quark clusters" $\overline{U}\,\overline{U}\,\overline{U}$ formed by anti-U quark in the models of stable fourth generation [19, 20].

In the context of composite dark matter scenario, accelerator probe for new stable quark-lepton generation acquires the meaning of critical test for the existence of charged constituents of cosmological dark matter.

The signature for double charged AC leptons and techniparticles is unique and distinctive what has already allowed to obtain the lower bound on their mass of 430 GeV in the ATLAS experiment [36].

Test for composite O^{--} at the LHC can be only indirect through the search for heavy hadrons, composed of single U or $\overline{U}$ and light quarks (similar to R-hadrons) [5], or by virtual effects of 4th generation fermions in the processes with known particles. Here, we study a possibility for experimental probe of the hypothesis of stable 4th generation in the studies of 125.5 GeV Higgs boson, discovered in the ATLAS [37, 38] and the CMS experiments [39, 40] at the LHC. The results of these studies [37–40] indicate that the number of the detected events, being the production cross section times the decay rate of Higgs boson to two-photon channel, is consistent with the prediction of the Standard model. On the other hand, as it was first revealed in [41], the existence of 4th generation leads to enhancement of the main mechanism of Higgs boson production in pp collisions, what puts constraints on the effect of 4th generation particles and practically excludes the possibility of their full strength coupling to 125.5 GeV Higgs boson.

In the model of stable 4th generation, the difference of these fermions from the quarks and leptons of the three known families is related to some new conserved charge (which can be even a gauge charge) that protects the stability of the lightest quarks and leptons (U-quark and the 4th neutrino-N). The experimental lower limits on the new quarks and leptons make these particles be heavier than the three light families, what can be explained by the existence of an additional mechanism of their mass generation, for example, in the framework of multi-Higgs models. It can naturally lead to suppression of the coupling of 4th generation fermions to the 125.5 GeV Higgs boson, discovered at the LHC. Here, we explore a possibility to make the 4th generation hypothesis consistent with the experimental data on the two gamma decays of Higgs boson, what opens the door to the indirect probes of the charged constituents of composite dark matter in the detailed studies of production and modes of decay of the 125.5 GeV Higgs boson.

2. Effects of 4th Generation in Higgs Boson Production and Decay

2.1. The Stable 4th Generation. The precision data on the parameters of the W and Z bosons of the Standard model do not exclude [42–45] the existence of the 4th generation of quarks and leptons.

The existence of the 4th generation can follow from the heterotic string phenomenology and its difference from the three known light generations can be explained by a new conserved charge, possessed only by its quarks and leptons [19–23, 46–48]. Strict conservation of this charge makes the lightest particle of the 4th family (the 4th neutrino) absolutely stable, but it was shown in [46–48] that this neutrino cannot be the dominant form of the dark matter. The same conservation law requires the lightest quark to be long living [19, 20]. In principle, the lifetime of U can exceed the age of the Universe, if $m_U < m_D$ [19, 20].

Due to their Coulomb-like QCD attraction ($\propto \alpha_c^2 \cdot m_U$, where α_c is the QCD constant) stable double and triple U bound states (UUq), (UUU) can exist [6, 7, 19–23]. The corresponding antiparticles can be formed by heavy antiquark $\overline{U}$. Formation of these double and triple states at accelerators and in cosmic rays is strongly suppressed by phase space constraints, but they can be formed in early Universe and strongly influence cosmological evolution of 4th generation hadrons. As shown in [20], anti-U-triple state called anutium or $\Delta^{--}_{3\overline{U}}$ is of a special interest. This stable anti-Δ-isobar, composed of $\overline{U}$ antiquarks, can be bound with ^4He in atom-like state of O-helium [8].

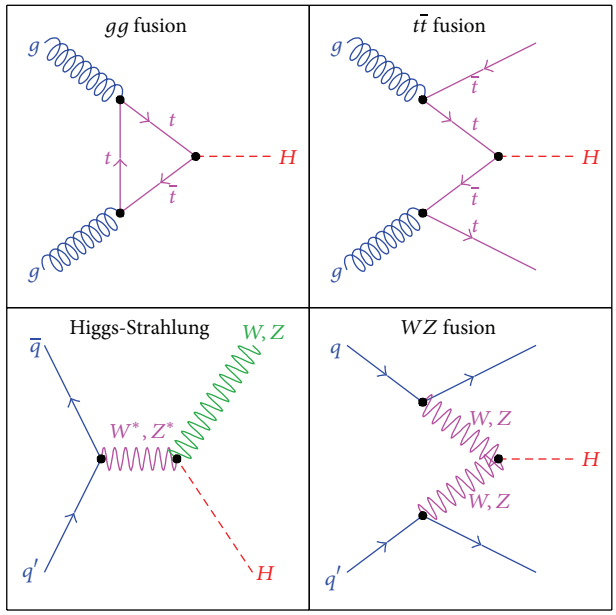

FIGURE 1: Feynman diagrams of the main processes of Higgs boson production in pp collisions (taken from [52]).

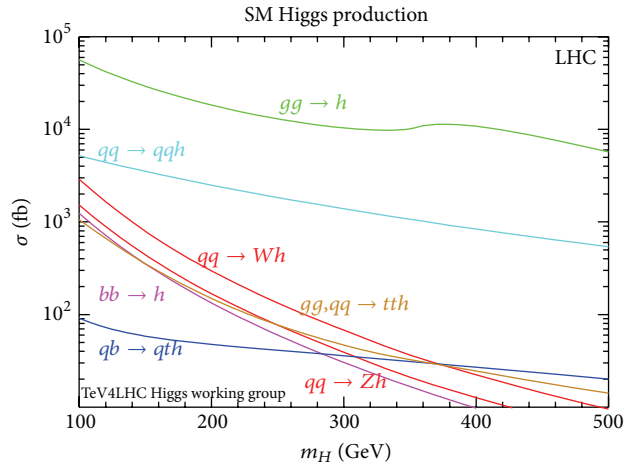

FIGURE 2: The cross section of the main processes of Higgs boson production in pp collisions at LHC (from [49]).

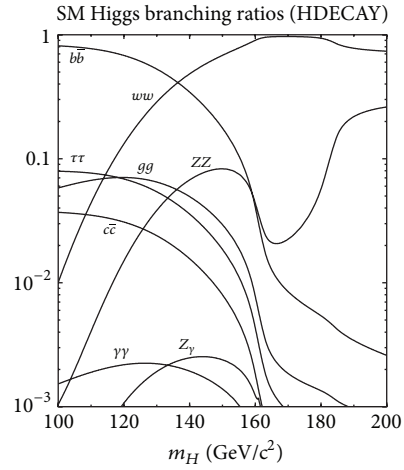

FIGURE 3: The branching ratio of Higgs boson decay modes in the Standard model (from [49]).

Since simultaneous production of three $U\overline{U}$ pairs and their conversion in two doubly charged quark clusters UUU are suppressed, the only possibility to test the models of composite dark matter from 4th generation in the collider experiments is a search for production of stable hadrons containing single U or $\overline{U}$ [5] or for effects of 4th generation quarks and leptons in the processes with known particles. Such effects should influence the production and decay rates of the Higgs boson, so the first step in such analysis is to check the consistency of the 4th generation hypothesis with the experimental data on the 125.5 GeV Higgs boson, discovered at the LHC. In the present paper, we show that the suppression of couplings of this boson to the 4th generation quarks and leptons can make compatible the experimental data on the two-photon decay mode of the Higgs boson with this hypothesis. The precise determination of the range of such couplings implies the account for the two-loop electroweak corrections and for the results of the Higgs searches in other decay channels, what goes beyond the scope of the present paper.

We take for definiteness the masses of the fourth generation U and D quarks to be about 350 GeV, of the lepton E about 100 GeV, and the mass of the 4th neutrino N about 50 GeV (see [4] for the recent review and references) and vary the coupling constants of the fourth generation fermions to the 125.5 GeV Higgs boson taking into account their possible suppression.

2.2. Effects of 4th Generation in Higgs Boson Production. The main channels of Higgs boson production in pp collisions are presented in Figure 1. Their relative contribution was calculated in [49] and presented in Figures 2 and 3.

The dominant mechanism of Higgs production, related to the gluon-gluon fusion, goes through the loop with virtual quarks. Thus, the existence of the quarks of fourth generation should influence the amplitude of this process. The corresponding contribution depends on the mass of these quarks and on their Yukawa coupling to the Higgs boson. The value of this coupling constant can vary due to the fact that the large mass of the fourth generation fermions can result from a combined effect of several Higgs fields so that the coupling to the 125.5 GeV Higgs boson can be suppressed. In the present work, we calculate the cross section of the Higgs boson production with the use of the HIGLU program [50] for different parameters of the model of 4th generation with the account for the QCD corrections.

2.3. Effects of 4th Generation in Two-Photon Higgs Boson Decay. Effects of 4th generation in the decay rates of Higgs boson, calculated in [41], are presented in Figure 4. The two-photon decay, considered here, goes through a loop diagram,

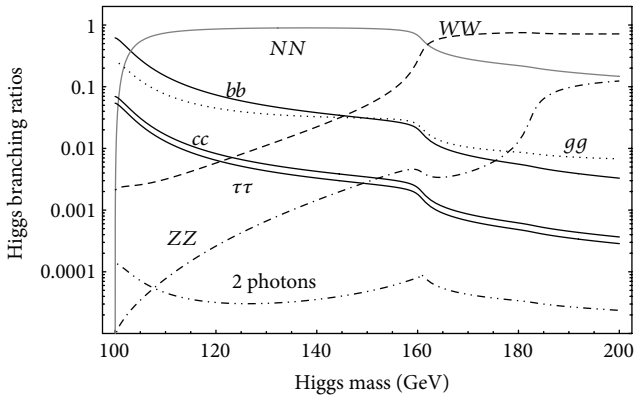

Figure 4: Branching ratios of the main processes of Higgs boson decay in the model of stable 4th generation (from [41]).

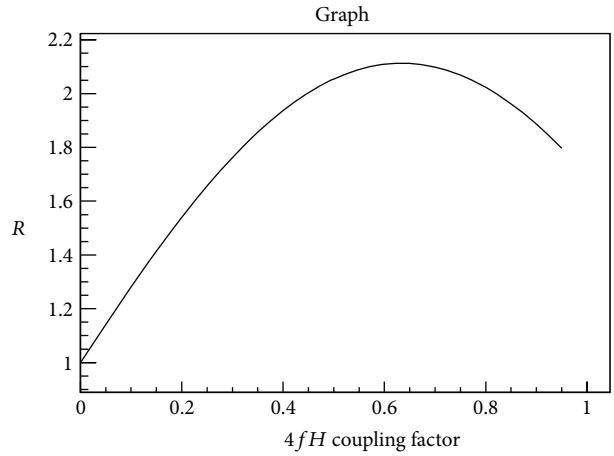

Figure 5: The dependence of the ratio R on the suppression factor, which is the same for all the quarks and leptons of the 4th generation.

which contribute all the charged particles. The width of this decay, calculated as in the Standard model [51] and modified with the account for the suppression of Higgs coupling constants, is given by

$$\Gamma\left(H \longrightarrow \gamma\gamma\right) = \frac{G_F \alpha^2 {m_H}^3}{128\sqrt{2}\pi^3}\left|\sum_{i=W,f} g_i N_c {e_i}^2 F_i\right|^2, \quad (1)$$

where $\alpha_s \approx 0.118$ and $\alpha \approx 1/137$ are the QCD and QED running gauge constants and N_c and e_i are the number of color degrees of freedom and the electric charge of an ith particle, respectively. The loop factor F_i is given by

$$F_{\text{boson}} = 2 + 3\delta + 3\delta\left(2 - \delta\right) f\left(\delta\right) \quad (2)$$

for bosons and

$$F_{\text{fermion}} = -2\delta\left(1 + \left(1 - \delta\right) f\left(\delta\right)\right) \quad (3)$$

for fermions, where

$$f\left(\delta\right) = \begin{cases} \text{arctg}\dfrac{1}{\sqrt{\delta - 1}}, & \delta \geq 1 \\ \dfrac{i}{2}\ln\dfrac{1 + \sqrt{1 - \delta}}{1 - \sqrt{1 - \delta}} + \dfrac{\pi}{2}, & \delta < 1. \end{cases} \quad (4)$$

The parameter δ is defined as

$$\delta = \left(\frac{2m_i}{m_H}\right)^2. \quad (5)$$

In the limit of $m_i \gg m_H$, the loop factor depends very weakly on the mass of an intermediate particle, so that the width equation (1) depends weakly on the mass of the heavy 4th generation fermions. In (1), g_i are the suppression factors of Higgs boson couplings. They are equal to 1 for the fermions of the three known generations and can vary from 0 to 1 for the quarks and charged lepton of the 4th generation.

3. The Results of Calculations

In the present work, we have calculated the ratio

$$R = \frac{\sigma_{\text{SM4}}\left(gg \rightarrow H\right)\Gamma_{\text{SM4}}\left(H \rightarrow \gamma\gamma\right)}{\sigma_{\text{SM}}\left(gg \rightarrow H\right)\Gamma_{\text{SM}}\left(H \rightarrow \gamma\gamma\right)} \quad (6)$$

of the number of events of two-photon decays of Higgs boson in the model of 4th generation and in the Standard model and compared it with the results of ATLAS [37, 38] and CMS experiments [39, 40] at the LHC. These results within the experimental errors are consistent with the prediction of the Standard model ($R = 1$) with the median values $R = 1.1$ in CMS and $R = 1.3$ in ATLAS that may favor some modest excess of the number of events relative to this prediction. One cannot make compatible the prediction of the model of the 4th generation with these results without suppression of Higgs boson coupling to new quarks and leptons.

The following possibilities for the suppression of the Higgs boson couplings were considered.

(a) The suppression factor is the same for all the quarks and leptons of the 4th generation.

(b) The uptype and downtype fermions of the 4th generation have different suppression factors.

(c) Quarks and leptons of the 4th generation have different suppression factors.

(d) All the fermions of the 4th generation have different suppression factors.

The results of calculations are presented in Figures 5, 6, 7, 8, 9, and 10. The predicted number of events is strongly enhanced by the effects of 4th generation quarks in gluon fusion mechanism of Higgs boson production, so that the corresponding suppression of the Higgs couplings is necessary to make the number of events close to the prediction of the Standard model. However, in the case of different suppression factors for different types of 4th generation particles, a nontrivial range of these parameters is possible. One can expect that the analysis of the predictions of the model of the 4th generation for the number of events of other decay modes of the 125.5 GeV Higgs boson will provide an overdetermined system of equations for these parameters, making possible the complete test of this model.

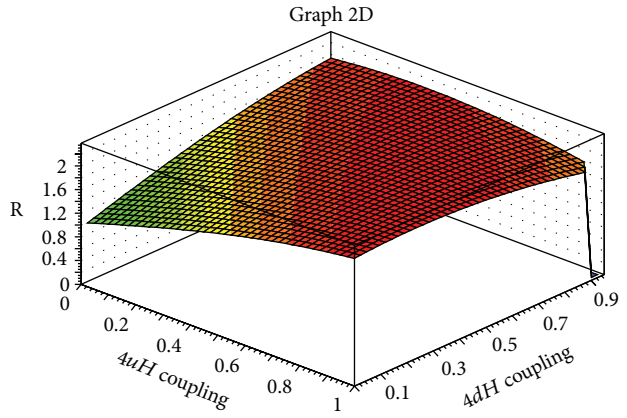

Figure 6: The dependence of the ratio R on the suppression factors $4uH$ and $4dH$ of Higgs coupling to correspondingly up- and downtype fermions of the 4th generation.

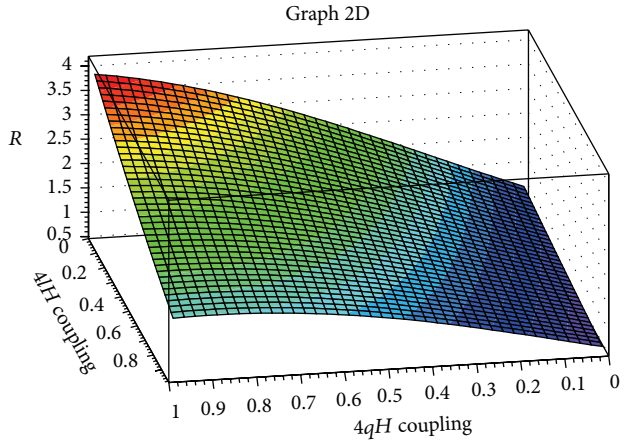

Figure 7: The dependence of the ratio R on the suppression factors $4qH$ and $4lH$ of Higgs coupling to correspondingly quarks and leptons of the 4th generation.

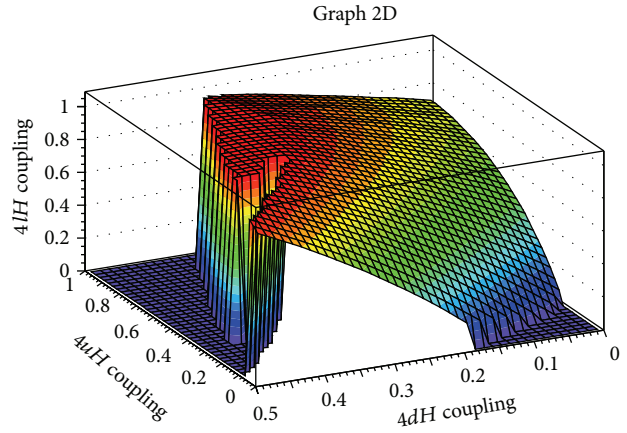

Figure 8: The surface in the space of parameters of the suppression factors $4dH$, $4uH$, and $4lH$ in the Higgs coupling to the quarks and leptons of the 4th generation, at which the median value of ratio $R = 1.3$, measured in the ATLAS experiment at LHC [37], is reproduced.

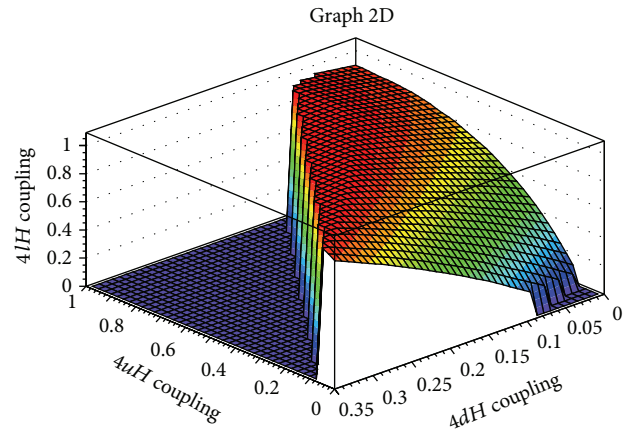

Figure 9: The surface in the space of parameters of the suppression factors $4dH$, $4uH$, and $4lH$ in the Higgs coupling to the quarks and leptons of the 4th generation, at which the median value of ratio $R = 1.1$, measured in the CMS experiment at LHC [40], is reproduced.

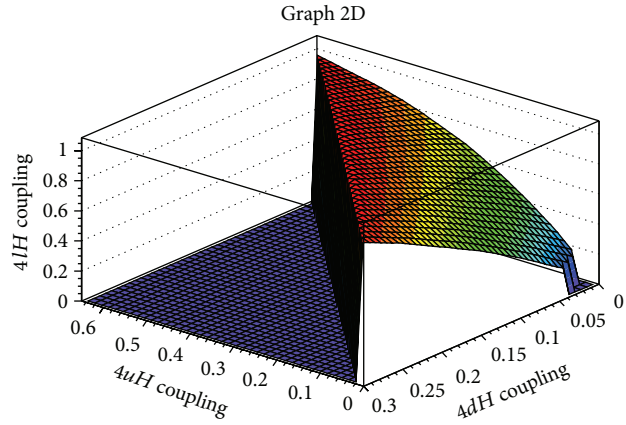

Figure 10: The surface in the space of parameters of the suppression factors $4dH$, $4uH$, and $4lH$ in the Higgs coupling to the quarks and leptons of the 4th generation, at which the value of ratio $R = 1$, corresponding to the Standard model prediction, is reproduced.

4. Conclusions

The cosmological dark matter can be formed by stable heavy double charged particles bound in neutral OHe dark atoms with primordial He nuclei by ordinary Coulomb interaction. This scenario sheds new light on the nature of dark matter and offers nontrivial solution for the puzzles of direct dark matter searches. It can be realized in the model of stable 4th generation and challenges for its experimental probe at accelerators. In the context of this scenario, search for effects of new heavy quarks and leptons acquires the meaning of direct experimental probe for charged constituents of dark atoms of dark matter.

The O^{--} constituents of OHe in the model of stable 4th generation are "heavy antiquark clusters" $\overline{U}\,\overline{U}\,\overline{U}$. Production of such clusters (and their antiparticles) at accelerators is virtually impossible. Therefore experimental test of the hypothesis of stable 4th generation is reduced to the search for

stable or metastable U hadrons, containing only single heavy quark or antiquark, or to the studies of virtual effects of 4th generation quarks and leptons in the processes with known particles.

The discovery of the 125.5 GeV Higgs boson at the LHC opens the new room for such indirect test of the model of stable 4th generation. The number of detected events of decays of this boson to the two-photon channel is consistent within the experimental errors with the prediction of the Standard model, putting severe constraints on the contribution of new quarks and leptons. On the other hand, the existence of heavy quarks of the 4th generation should lead to enhancement of the gluon fusion mechanism of Higgs boson production, which is its dominant production mechanism in pp collisions. Therefore, to be compatible with the experimental data, the model of the stable 4th generation should involve a mechanism of suppression of new quark and lepton couplings to the 125.5 GeV Higgs boson [53]. Taking into account the difference of the 4th generation from the three known families of quarks and leptons and in particular the lower limits on the masses of new quarks and leptons, one can assume some additional mechanisms of their mass generation, what can lead to suppression of their couplings to the 125.5 GeV Higgs boson.

In the present work, we have shown that, indeed, the suppression in the Higgs boson couplings to 4th generation quarks and lepton the can make compatible the existence of this generation with the experimental data on the two-photon decays of the 125.5 GeV Higgs boson. We consider this result as the first step in the thorough investigation of the predictions of the model of stable 4th generation for the whole set of decay channels of Higgs boson. The confrontation of these predictions with the detailed experimental study of the 125.5 GeV Higgs boson will provide the complete test for the composite dark matter scenarios based on the model of the stable 4th generation.

Conflict of Interests

The authors declare that there is no conflict of interests regarding the publication of this paper.

Acknowledgment

The authors would like to thank K. Belotsky for discussions.

References

[1] M. Y. Khlopov, A. G. Mayorov, and E. Y. Soldatov, "Puzzles of dark matter in the light of dark atoms," *Journal of Physics*, vol. 309, Article ID 012013, 2011.

[2] M. Y. Khlopov, A. G. Mayorov, and E. Y. Soldatov, "Dark Atoms of the Universe: towards OHe nuclear physics," *Bled Workshops in Physics*, vol. 11, p. 73, 2010.

[3] M. Y. Khlopov, "Physics of dark matter in the light of dark atoms," *Modern Physics Letters A*, vol. 26, no. 38, pp. 2823–2839, 2011.

[4] M. Yu. Khlopov, "Fundamental particle structure in the cosmological dark matter," *International Journal of Modern Physics A*, vol. 28, Article ID 1330042, 2013.

[5] K. M. Belostky, M. Y. Khlopov, and K. I. Shibaev, "Probes for constituents of composite dark matter," *Gravitation and Cosmology*, vol. 18, pp. 127–131, 2012.

[6] S. L. Glashow, "A sinister extension of the standard model to SU(3)XSU(2)XSU(2)XU(1)," http://arxiv.org/abs/hep-ph/0504287.

[7] D. Fargion and M. Khlopov, "Tera-leptons' shadows over sinister universe," *Gravitation and Cosmology*, vol. 19, no. 4, pp. 219–231, 2013.

[8] M. Y. Khlopov, "New symmetries in microphysics, new stable forms of matter around us," http://arxiv.org/abs/astro-ph/0607048.

[9] C. A. Stephan, "Almost-commutative geometries beyond the standard model," *Journal of Physics A*, vol. 39, Article ID 9657, 2006.

[10] D. Fargion, C. A. Stephan, D. Fargion et al., "Dark matter with invisible light from heavy double charged leptons of almost-commutative geometry?" *Classical and Quantum Gravity*, vol. 23, Article ID 7305, 2006.

[11] A. Connes, *Noncommutative Geometry*, Academic Press, London, UK, 1994.

[12] M. Y. Khlopov and C. Kouvaris, "Strong interactive massive particles from a strong coupled theory," *Physical Review D*, vol. 77, no. 6, Article ID 065002, 2008.

[13] F. Sannino and K. Tuominen, "Orientifold theory dynamics and symmetry breaking," *Physical Review D*, vol. 71, Article ID 051901, 2005.

[14] D. K. Hong, S. D. H. Hsu, and F. Sannino, "Composite Higgs from higher representations," *Physics Letters B*, vol. 597, no. 1-2, pp. 89–93, 2004.

[15] D. D. Dietrich and F. Sannino, "Light composite Higgs boson from higher representations versus electroweak precision measurements: predictions for CERN LHC," *Physical Review D*, vol. 72, Article ID 055001, 2005.

[16] D. D. Dietrich, F. Sannino, and K. Tuominen, "Light composite Higgs and precision electroweak measurements on the resonance: an update," *Physical Review D*, vol. 73, Article ID 037701, 2006.

[17] S. B. Gudnason, C. Kouvaris, and F. Sannino, "Towards working technicolor: effective theories and dark matter," *Physical Review D*, vol. 73, Article ID 115003, 2006.

[18] S. B. Gudnason, C. Kouvaris, and F. Sannino, "Dark matter from new technicolor theories," *Physical Review D*, vol. 74, Article ID 095008, 2006.

[19] K. M. Belotsky, D. Fargion, M. Y. Khlopov, R. V. Konoplich, M. G. Ryskin, and K. I. Shibaev, "Heavy hadrons of 4th family hidden in our Universe and close to detection?" *Gravitation and Cosmology*, vol. 11, pp. 41–42, 2005.

[20] M. Yu. Khlopov, "Composite dark matter from the fourth generation," *Journal of Experimental and Theoretical Physics Letters*, vol. 83, no. 1, pp. 1–4, 2006.

[21] K. Belotsky, M. Khlopov, and K. Shibaev, "Stable matter of 4th generation: hidden in the Universe and close to detection?" http://arxiv.org/abs/astro-ph/0602261.

[22] K. M. Belotsky, M. Y. Khlopov, and K. I. Shibaev, "Composite dark matter and its charged constituents," *Gravitation and Cosmology*, vol. 12, p. 1, 2006.

[23] K. Belotsky, M. Yu. Khlopov, and K. I. Shibaev, "Stable quarks of the 4th family?" in *The Physics of Quarks: New Research*, N. L. Watson and T. M. Grant, Eds., vol. 265 of *Horizons in World Physics*, pp. 19–47, NOVA Publishers, Hauppauge, NY, USA, 2009, http://arxiv.org/abs/0806.1067.

[24] M. Y. Khlopov and C. Kouvaris, "Composite dark matter from a model with composite Higgs boson," *Physical Review D*, vol. 78, no. 6, Article ID 065040, 2008.

[25] M. Y. Khlopov, "The puzzles of dark matter searches," *AIP Conference Proceedings*, vol. 1241, p. 388, 2010.

[26] M. Y. Khlopov, A. G. Mayorov, and E. Y. Soldatov, "Composite dark matter and puzzles of dark matter searches," *International Journal of Modern Physics D*, vol. 19, no. 8–10, pp. 1385–1395, 2010.

[27] B. D. Wandelt, R. Dave, G. R. Farrar et al., "Self-interacting dark matter," http://arxiv.org/abs/astro-ph/0006344.

[28] P. C. McGuire and P. J. Steinhardt, "Cracking open the window for strongly interacting massive particles as the halo dark matter," in *Proceedings of the International Cosmic Ray Conference*, p. 1566, Hamburg, Germany, 2001, http://arxiv.org/abs/astro-ph/0105567.

[29] G. Zaharijas and G. R. Farrar, "Window in the dark matter exclusion limits," *Physical Review D*, vol. 72, no. 8, Article ID 083502, 2005.

[30] C. B. Dover, T. K. Gaisser, and G. Steigman, "Cosmological constraints on new stable hadrons," *Physical Review Letters*, vol. 42, no. 17, pp. 1117–1120, 1979.

[31] S. Wolfram, "Abundances of new stable particles produced in the early universe," *Physics Letters B*, vol. 82, no. 1, pp. 65–68, 1979.

[32] G. D. Starkman, A. Gould, R. Esmailzadeh, and S. Dimopoulos, "Opening the window on strongly interacting dark matter," *Physical Review D*, vol. 41, no. 12, pp. 3594–3603, 1990.

[33] D. Javorsek, D. Elmore, E. Fischbach et al., "New experimental limits on strongly interacting massive particles at the TeV scale," *Physical Review Letters*, vol. 87, Article ID 231804, 2001.

[34] S. Mitra, "Uranus's anomalously low excess heat constrains strongly interacting dark matter," *Physical Review D*, vol. 70, no. 10, Article ID 103517, pp. 1–103517, 2004.

[35] G. D. Mack, J. F. Beacom, G. Bertone et al., "Towards closing the window on strongly interacting dark matter: far-reaching constraints from Earth's heat flow," *Physical Review D*, vol. 76, Article ID 043523, 2007.

[36] G. Aad, T. Abajyan, B. Abbott et al., "Search for long-lived, multi-charged particles in pp collisions at $\sqrt{s} = 7$ TeV using the ATLAS detector," *Physics Letters B*, vol. 722, no. 4-5, pp. 305–323, 2013.

[37] S. M. Consonni, "Higgs search at ATLAS," http://arxiv.org/abs/1305.3315.

[38] G. Aad, T. Abajyan, B. Abbott et al., "Measurements of Higgs boson production and couplings in diboson final states with the ATLAS detector at the LHC," *Physics Letters B*, vol. 726, no. 1–3, pp. 88–119, 2013.

[39] S. Chatrchyan, V. Khachatryan, A. M. Sirunyan et al., "Observation of a new boson with mass near 125 GeV in pp collisions at $\sqrt{s} = 7$ and 8 TeV," *Journal of High Energy Physics*, vol. 6, p. 81, 2013.

[40] C. Palmer and C. M. S. Collaboration, "CMS measurements of the higgs-like boson in the two photon decay channel," http://arxiv.org/abs/1305.3654.

[41] K. M. Belotsky, D. Fargion, M. Khlopov et al., "Invisible Higgs boson decay into massive neutrinos of fourth generation," *Physical Review D*, vol. 68, Article ID 054027, 2003.

[42] M. Maltoni, V. A. Novikov, L. B. Okun, A. N. Rozanov, and M. I. Vysotsky, "Extra quark-lepton generations and precision measurements," *Physics Letters B*, vol. 476, no. 1-2, pp. 107–115, 2000.

[43] V. A. Ilyin, M. Maltoni, V. A. Novikov, L. B. Okun, A. N. Rozanov, and M. I. Vysotsky, "On the search for 50 GeV neutrinos," *Physics Letters B*, vol. 503, no. 1-2, pp. 126–132, 2001.

[44] V. A. Novikov, L. B. Okun, A. N. Rozanov, and M. I. Vysotsky, "Extra generations and discrepancies of electroweak precision data," *Physics Letters B*, vol. 529, no. 1-2, pp. 111–116, 2002.

[45] V. A. Novikov, L. B. Okun, A. N. Rozanov et al., "Mass of the higgs versus fourth generation masses," *Journal of Experimental and Theoretical Physics Letters*, vol. 76, pp. 127–130, 2002.

[46] K. M. Belotsky, M. Yu. Khlopov, and K. I. Shibaev, "Sakharov's enhancement in the effect of 4th generation neutrino," *Gravitation and Cosmology Supplement*, vol. 6, pp. 140–143, 2000.

[47] K. M. Belotsky, D. Fargion, M. Y. Khlopov, R. V. Konoplich, and K. I. Shibaev, "Heavy neutrinos of 4th generation in searches for dark matter," *Gravitation and Cosmology*, vol. 11, p. 16, 2005.

[48] K. M. Belotsky, D. Fargion, M. Y. Khlopov, and R. V. Konoplich, "May heavy neutrinos solve underground and cosmic-ray puzzles?" *Physics of Atomic Nuclei*, vol. 71, no. 1, pp. 147–161, 2008.

[49] S. Bolognesi, G. Bozzi, and A. Di Simone, "Higgs at LHC," *Nuovo Cimento B*, vol. 123, pp. 499–508, 2008.

[50] M. Spira, "HIGLU: a program for the calculation of the total Higgs production cross-section at hadron colliders via gluon fusion including QCDcorrections," http://arxiv.org/abs/hep-ph/9510347.

[51] L. B. Okun, *Leptons and Quarks*, Nauka, Moscow, Russia, 1990.

[52] http://en.wikipedia.org/wiki/ATLAS_experiment.

[53] O. Eberhardt, G. Herbert, H. Lacker et al., "Impact of a Higgs boson at a mass of 126 GeV on the standard model with three and four fermion generations," *Physical Review Letters*, vol. 109, no. 24, Article ID 241802, 5 pages, 2012.

Hindawi Publishing Corporation
Advances in High Energy Physics
Volume 2014, Article ID 525208, 9 pages
http://dx.doi.org/10.1155/2014/525208

Research Article

Milli-Interacting Dark Matter Interpretation of the Direct-Search Experiments

Quentin Wallemacq

IFPA, AGO Department, University of Liège, Sart Tilman, 4000 Liège, Belgium

Correspondence should be addressed to Quentin Wallemacq; quentin.wallemacq@ulg.ac.be

Received 25 November 2013; Accepted 24 December 2013; Published 20 January 2014

Academic Editor: Konstantin Belotsky

 The publication of this article was funded by SCOAP^3.

We reinterpret the results of the direct searches for dark matter in terms of milli-interacting dark particles. The model reproduces the positive results from DAMA/LIBRA and CoGeNT and is consistent with the absence of signal in the XENON100, CDMS-II/Ge, and LUX detectors. Dark atoms, interacting with standard atoms through a kinetic mixing between photons and dark photons and a mass mixing of σ mesons with dark scalars, diffuse elastically in terrestrial matter where they deposit all their energy. Reaching underground detectors through gravity at thermal energies, they form bound states with nuclei of the active medium by radiative capture, which causes the emission of photons that produce the observed signals. The parameter space of the model is explored and regions reproducing the results at the 2σ level are obtained for each experiment.

1. Introduction

Dark matter has been one of the most persistent enigmas in astrophysics since an invisible kind of matter was suggested in 1933 by Zwicky as an explanation to the missing mass between galaxies. Nowadays, the presence of dark matter is known at all cosmological scales and it is mostly believed that it is due to a unique species of collisionless particles, whose nature remains a mystery. One way to solve part of the problem is to observe directly these weakly interacting massive particles (WIMPs) in underground detectors. Such direct searches for dark matter have started in the late 1990 s and have led today to stunning results. The DAMA/LIBRA [1, 2] and CoGeNT [3, 4] experiments both have performed temporal analyses of their signals and confirmed the presence of an annual modulation of the event rates with statistical significances of 9.3σ and 2.8σ, respectively. CRESST-II [5] and recently CDMS-II/Si [6] support these results with the observation of events in their detectors that cannot be due to background. On the other hand, XENON100 [7], CDMS-II/Ge [8], and recently LUX [9] exclude any detection.

The current problem is that these experiments seem to come into conflict when their results are interpreted in terms of WIMPs producing nuclear recoils by colliding on nuclei in the detectors, although a more precise account for theoretical and experimental uncertainties could improve the status of WIMPs in that field. The tensions between experiments with positive results and the apparent incompatibility of the latter with experiments with negative results has led to considering other dark matter models that could provide new frameworks to reinterpret the data. Among these, mirror matter [10], millicharged atomic dark matter [11], O-helium dark atoms [12–14], and exothermic double-disk dark matter [15] propose interesting and varied mechanisms that can reconcile part of the experiments but always keep contradictions with the others. Light-mediator exchange [16] provides a viable mechanism which is able to explain the modulation effects, but its compatibility with the experiments with negative results is still uncertain. One common feature of all these scenarios is the high complexity of their dark sectors with respect to WIMPs, often reaching a phenomenology as rich as that of our ordinary sector.

The model presented here follows this trend and keeps some aspects of the above ones but presents new ingredients which aim at reconciling the experiments with positive results without contradicting those with negative results. The dark sector is composed of two new fermions both coupled to massless dark photons with opposite couplings and neutral

dark scalars to which is coupled one of the two species via a Yukawa coupling. The oppositely charged dark fermions bind to form dark hydrogenoid atoms with standard atomic sizes. Such a dark matter candidate presents self-interactions on which constraints have been established from the Bullet Cluster and from halo shapes [17]. To avoid them, we follow [18] in which the self-interacting part of the dark sector is reduced to at most 5% of the total dark matter mass content of the galaxy, with the rest being realized by conventional collisionless particles presenting too weak interactions with standard particles to produce any recoil in underground detectors. The same kind of kinetic photon-dark photon mixing as in [10, 11] produces small effective couplings of the dark fermions to the standard photon, with the former behaving therefore like electric millicharges interacting with electrically charged standard particles. An additional mass mixing between the standard scalar σ meson and the dark scalar creates an attractive interaction between one of the two dark fermions and the standard nucleons that are coupled to σ in the framework of an effective Yukawa theory. The dark atoms interact sufficiently with terrestrial matter to lose all their energy between the surface and underground detectors, reaching them with thermal energies. There, dark and standard nuclei form bound states by radiative capture, causing the emission of photons that are the sources of the observed signals.

In [19], the model was introduced and a specific set of parameters that reproduced well the results from DAMA/LIBRA and CoGeNT and presenting no contradictions with XENON100 and CDMS-II/Ge was given. Here, the parameter space of the model is explored to determine the regions that reproduce DAMA/LIBRA and CoGeNT at the 2σ level and to put upper and lower limits on the different parameters, always without contradicting the null results from XENON100 and CDMS-II/Ge, as well as the new constraint from LUX.

2. Dark Sector

In this model, the complex part of the dark sector is realized by two kinds of fermions, F and G, of masses m_F and m_G, interacting through a dark $U(1)$ gauge interaction carried out by dark massless photons Γ. In addition, the species F exchanges dark neutral scalars S of mass m_S via a Yukawa coupling, which leads to the dark interaction Lagrangian:

$$\mathscr{L}_{\text{int}}^{\text{dark}} = e'\overline{\psi}_F\gamma^\mu A'_\mu\psi_F - e'\overline{\psi}_G\gamma^\mu A'_\mu\psi_G + g'\phi_S\overline{\psi}_F\psi_F, \quad (1)$$

where ψ_F and ψ_G are the fermionic fields of F and G, A' and ϕ_S are the vectorial and real scalars fields of Γ and S, $+e'$ and $-e'$ are the electric charges of F and G, and g' is the Yukawa coupling of F to S.

In order to produce nongravitational interactions between the standard and dark sectors, we postulate that the dark photons Γ are kinetically mixed with the standard photons γ and that the dark scalars S are mixed with the neutral scalar mesons σ via a mass term, with the mixing Lagrangian:

$$\mathscr{L}_{\text{mix}} = \frac{1}{2}\widetilde{\epsilon}\mathscr{F}^{\mu\nu}\mathscr{F}'_{\mu\nu} + \widetilde{\eta}\left(m_\sigma^2 + m_S^2\right)\phi_\sigma\phi_S, \quad (2)$$

where $\mathscr{F}$ and $\mathscr{F}'$ are the electromagnetic-field-strength tensors of the massless standard and dark photons, ϕ_σ is the real scalar field of the σ meson, and $m_\sigma = 600$ MeV [20] is its mass. $\widetilde{\epsilon}$ and $\widetilde{\eta}$ are the dimensionless parameters of the kinetic $\gamma - \Gamma$ and mass $\sigma - S$ mixings and are assumed to be small compared with unity.

In principle, the model contains seven free parameters, m_F, m_G, m_S, e', g', $\widetilde{\epsilon}$, and $\widetilde{\eta}$, but these can in fact be reduced to four. Indeed, only the products $\widetilde{\epsilon}e'$ and $\widetilde{\eta}g'$ will be directly constrained by the direct-search experiments, which suggests to define them in terms of the charge of the proton e and of the Yukawa coupling constant of the nucleon to the σ meson $g = 14.4$ [21]: $\widetilde{\epsilon}e' \equiv \epsilon e$ and $\widetilde{\eta}g' \equiv \eta g$, where ϵ and η are dimensionless mixing parameters. Moreover, the oppositely charged fermions F and G will bind to form hydrogenoid dark atoms where F and G will, respectively, play the roles of dark nucleus and dark electron, satisfying $m_G \ll m_F$. The Bohr radius of such atoms is given by $a'_0 = 1/m_G\alpha'$, where $\alpha' = e'^2/4\pi$, and gives another parameter that will be fixed to 1 Å so that dark atoms have the same size as standard ones and can thermalize in the Earth before reaching the underground detectors, as will be specified in Section 3.3. As a result, the parameters of the model can be reexpressed as m_F, m_S, ϵ, and η.

The dark particles F will bind to nuclei in underground detectors and have therefore to be sufficiently massive to form bound states. For that reason, we will explore masses of F between 10 GeV and 10 TeV. The mass mixing term in (2) induces an attractive interaction between F and nucleons with a range determined by m_S^{-1}. It cannot be too long ranged but it must allow the existence of nucleus-F bound states of at least the size of the nucleus, so we will seek masses of S between 100 keV and 10 MeV. The model parameters that we will consider are therefore

$$\begin{gathered} 10\,\text{GeV} \le m_F \le 10\,\text{TeV}, \\ 100\,\text{keV} \le m_S \le 10\,\text{MeV}, \\ \epsilon, \eta \ll 1, \\ a'_0 = 1\,\text{Å}. \end{gathered} \quad (3)$$

Note that the galactic dark matter halo could also be populated by dark ions F and G, but [22] ensures that, if $\epsilon > 9\times10^{-12}\,(m_{F,G}/\text{GeV})$, they have been evacuated from the disk by supernovae shock waves while galactic magnetic fields prevent them from reentering. This condition will clearly be satisfied by the parameters used to reproduce the results of the direct-dark-matter-search experiments and we can consider their signals to be fully due to dark atoms.

3. Interaction Potentials with Standard Matter

Because of the mixings present in (2), the dark fermions F and G can interact with our standard particles. The kinetic $\gamma - \Gamma$ mixing induces small effective couplings $\pm\tilde{\epsilon}e' = \pm\epsilon e$ to the standard photon for F and G. The dark species can therefore interact electromagnetically with any charged standard particle with millicharges $\pm\epsilon e$. Similarly, the $\sigma - S$ mass mixing generates an effective coupling between F and σ, making F capable of interacting with any standard particle coupled to σ, that is, the nucleons in the framework of an effective Yukawa theory. In the nonrelativistic limit, these couplings give rise to interaction potentials between the dark and the standard particles.

3.1. Interactions of F and G Fermions with Nucleons and Electrons. At the elementary level, the kinetic $\gamma - \Gamma$ mixing produces a Coulomb interaction potential between the millicharged dark particles and the proton and the electron:

$$V_k = \pm\frac{\epsilon\alpha}{r}, \tag{4}$$

where k refers to kinetic and $\alpha = e^2/4\pi$ is the fine structure constant. The plus and minus signs stand, respectively, for the pairs proton-F or electron-G and proton-G or electron-F.

Since the mass mixing parameter $\tilde{\eta}$ is small, the attractive interaction between F and the nucleons is dominated by one $\sigma + S$ exchange, which gives

$$V_m = -\frac{\eta\left(m_\sigma^2 + m_S^2\right)\beta}{r}\left(\frac{e^{-m_\sigma r} - e^{-m_S r}}{m_S^2 - m_\sigma^2}\right), \tag{5}$$

where m stands for mass and $\beta = g^2/4\pi = 16.5$. Note that because $m_S \ll m_\sigma$, the potential (5) is essentially a Yukawa potential of range m_S^{-1}: $V_m \simeq -(\eta\beta/r)e^{-m_S r}$.

3.2. Interactions of F Fermions with Nuclei. Because of their interactions with nucleons, the dark fermions F interact with atomic nuclei. Assuming that a nucleus of mass number A and atomic number Z is a uniformly charged sphere of radius $R = r_0 A^{1/3}$ and volume $V = (4/3)\pi R^3$, the integrations of the elementary potentials (4) and (5) over its electric and nuclear charge distributions $\rho_k = Ze/V$ and $\rho_m = Ag/V$ give

$$\begin{aligned} V_k^{\text{nucl}}(r) &= \int_V \left(\frac{V_k\left(\left|\vec{r} - \vec{r'}\right|\right)}{e}\right)\rho_k d\vec{r'} \\ &= \frac{\epsilon Z\alpha}{2R}\left(3 - \frac{r^2}{R^2}\right), \quad r < R \\ &= \frac{\epsilon Z\alpha}{r}, \quad r > R \end{aligned} \tag{6}$$

and $V_m^{\text{nucl}}(r) = \int_V (V(|\vec{r} - \vec{r'}|)_m/g)\rho_m d\vec{r'}$; that is,

$$\begin{aligned} &V_m^{\text{nucl}}(r < R) \\ &= -\frac{V_0}{r}\left[2r\left(m_\sigma^{-2} - m_S^{-2}\right)\right. \\ &\qquad + \left(R + m_\sigma^{-1}\right)m_\pi^{-2}\left(e^{-m_\sigma r} - e^{m_\sigma r}\right)e^{-m_\sigma R} \\ &\qquad \left. - \left(R + m_S^{-1}\right)m_S^{-2}\left(e^{-m_S r} - e^{m_S r}\right)e^{-m_S R}\right], \\ &V_m^{\text{nucl}}(r > R) \\ &= -\frac{V_0}{r}\left[m_\sigma^{-2}e^{-m_\sigma r}\left(e^{m_\sigma R}\left(R - m_\sigma^{-1}\right) + e^{-m_\sigma R}\left(R + m_\sigma^{-1}\right)\right)\right. \\ &\qquad - m_S^{-2}e^{-m_S r}\left(e^{m_S R}\left(R - m_S^{-1}\right)\right. \\ &\qquad \left.\left. + e^{-m_S R}\left(R + m_S^{-1}\right)\right)\right], \end{aligned} \tag{7}$$

where nucl indicates nucleus, $\vec{r'}$ is the position vector of a charge element in the nucleus, $V_0 = 3\eta(m_\sigma^2 + m_S^2)\beta/(2r_0^3(m_S^2 - m_\sigma^2))$, and $r_0 = 1.2$ fm.

V_k^{nucl} consists in a repulsive Coulomb potential outside the nucleus and in a harmonic potential, which is concave down, inside. Both are continuously connected at $r = R$ (as well as their first derivatives), with an inflection point at $r = R$ and a maximum reached at $r = 0$, where the first derivative is zero.

V_m^{nucl} corresponds to a finite attractive well, with a size of the order of m_S^{-1}, an inflection point at $r = R$ and tending to zero as $(-1/r)e^{-m_S r}$ outside the nucleus.

The total nucleus-F potential $V_k^{\text{nucl}} + V_m^{\text{nucl}}$ is therefore a negative attractive well at distances $r \lesssim m_S^{-1}$ that is continuously connected, together with its first derivative, to a positive potential barrier, coming from the repulsive Coulomb potential, at larger distances. As $r \to \infty$, V_m^{nucl} rapidly tends to zero and the total potential is dominated by the Coulomb part. In order to reproduce the direct-search experiments, the depth of the well, mainly determined by the parameter η, will be of the order of 10 keV while the barrier, which height depends on m_S and ϵ, will rise up to a few eV.

3.3. Interactions of Dark FG Atoms with Terrestrial Atoms. The galactic dark atoms interact, after hitting the surface of the Earth because of its motion in the dark matter halo, with terrestrial atoms under the surface. Because $m_F \gg m_G$, F plays the role of a dark nucleus while G is spherically distributed around it, so that the mass of the bound state m_{FG} is almost equal to m_F. To model the atom-dark atom interaction, the dark atoms, as well as the terrestrial ones, are seen as uniformly charged spheres of charges $-\epsilon e$ and $-Ze$ and radii a_0' and a_0, respectively, where Z is the atomic number of the terrestrial atom, with opposite point-like charges at their centers. The atomic radii are both fixed to 1 Å to allow sufficient interaction for the dark atoms to lose all their kinetic energy by elastic collisions between the surface

and the underground detectors and hence to reach them with thermal energies.

The atom-dark atom interaction potential is then the sum of the electrostatic interaction V_k^{at} and the $\sigma + S$ echange V_m^{at} between the dark nucleus F and the atomic nucleus. V_k^{at} is obtained by adding the contributions from the four pairs of crossed substructures: nucleus-F (point-like-point-like, pure Coulomb repulsion), nucleus-G distribution (point-like-sphere, attractive of form (6)), electron distribution-F (sphere-point-like, attractive of form (6)), and electron distribution-G distribution (sphere-sphere, obtained by integrating the form (6) over a uniformly charged sphere which center is separated by a distance r from the center of the first one). This gives

$$\begin{aligned} V_k^{\text{at}} &= \frac{\epsilon Z\alpha}{160a_0^6}\left(-r^5+30a_0^2r^3+80a_0^3r^2\right. \\ &\qquad \left.-288a_0^5+\frac{160a_0^6}{r}\right), \quad r<a_0 \\ &= \frac{\epsilon Z\alpha}{160a_0^6}\left(-r^5+30a_0^2r^3-80a_0^3r^2\right. \\ &\qquad \left.+192a_0^5-\frac{160a_0^6}{r}\right), \quad a_0<r<2a_0 \\ &= 0, \quad r>2a_0, \end{aligned} \tag{8}$$

where the upper label at refers to atomic. Because the nucleus is here supposed to be pointlike, V_m^{at} is simply obtained by multiplying (5) by the number A of nucleons in the nucleus:

$$V_m^{\text{at}}(r) = -\frac{\eta\left(m_\sigma^2+m_S^2\right)A\beta}{r}\left(\frac{e^{-m_\sigma r}-e^{-m_S r}}{m_S^2-m_\sigma^2}\right). \tag{9}$$

The atom-dark atom electrostatic potential V_k^{at} shows three parts as a function of the distance r between the two centers. Each sphere appears neutral from outside because the positive charge at the center compensates exactly the negative charge distributed in the sphere, so that there is no interaction when they are completely separated ($r > 2a_0$). As they merge ($a_0 < r < 2a_0$), the electrostatic potential becomes attractive due to the attraction between the nucleus of each sphere and the negatively charged distribution of the other one. When the nuclei enter simultaneously in the approaching spheres ($r = a_0$), an inflection point occurs and the potential reaches then a minimum ($r = 0.88$ Å for $a_0 = 1$ Å). As the centers continue to approach each other ($r < 0.88$ Å for $a_0 = 1$ Å), the potential becomes repulsive due to the Coulomb repulsion between nuclei. The potential well appearing when the two atoms merge will have a depth of the order of 10^{-4}-10^{-3} eV and will therefore not contain any bound state (or if any, not thermally stable), so that it will not contribute in the following to the formation of atom-dark atom bound states.

As $m_S \ll m_\sigma$, $V_m^{\text{at}} \simeq -(\eta A\beta/r)e^{-m_S r}$, which is a pure Yukawa potential. The total atom-dark atom potential $V_k^{\text{at}} + V_m^{\text{at}}$ is therefore essentially equal to its electrostatic part V_k^{at} for $r < m_S^{-1}$, while the attractive part V_m^{at} dominates at smaller distances.

4. From Space to Underground Detectors

4.1. Thermalization in the Terrestrial Crust. Due to its orbital motion around the Sun, which turns around the center of the galaxy, the Earth moves through the galactic dark matter halo. This results in a wind of dark atoms hitting the surface of the Earth throughout the year (however, according to [18], it is expected that the subdominant self-interacting species form a disk rotating around the galactic center, so that the incident flux on Earth might be different than in the halo assumption). A dark atom penetrates the surface and starts interacting with terrestrial atoms via the atomic potentials (8) and (9). As there is no stable bound state in the total atomic potential with the relatively light terrestrial atoms, the diffusions are purely elastic. If the elastic diffusion cross section is sufficiently large, then the dark atom can deposit all its energy in the terrestrial matter, assumed to be mainly made of silicon atoms with $Z_{\text{Si}} = 14$ and $A_{\text{si}} = 28$, before reaching an underground detector typically located at a depth of 1 km.

A differential elastic diffusion cross section $d\sigma/d\Omega$ deriving from a two-body-interaction potential $V(\vec{r})$ can be obtained in the framework of the Born approximation via the Fourier transform of the potential: $d\sigma/d\Omega = (\mu^2/4\pi^2)\left|\int d\vec{r}e^{-i\vec{K}\cdot\vec{r}}V(\vec{r})\right|^2$, where μ is the reduced mass of the two-body system and $\vec{K}$ is the transferred momentum. Here, from potentials (8) and (9) and in the center-of-mass frame of the silicon-F system, we get

$$\begin{aligned} \left(\frac{d\sigma}{d\Omega}\right)^{\text{at}} &= \left(\frac{d\sigma}{d\Omega}\right)_k^{\text{at}} + \left(\frac{d\sigma}{d\Omega}\right)_m^{\text{at}} \\ &\quad - \frac{4\mu^2\epsilon\eta Z_{Si}A_{Si}\alpha\beta}{a_0^6}\left(\frac{m_\sigma^2+m_S^2}{m_S^2-m_\sigma^2}\right)\frac{I}{K^8} \\ &\quad \times\left[\frac{1}{m_\sigma^2+K^2}-\frac{1}{m_S^2+K^2}\right], \end{aligned} \tag{10}$$

with

$$\begin{aligned} \left(\frac{d\sigma}{d\Omega}\right)_k^{\text{at}} &= \frac{\mu^2\epsilon^2Z_{mSi}^2\alpha^2}{a_0^{12}}\frac{1}{K^{16}}I^2, \\ I &= 9\left(K^2a_0^2+1\right)+9\cos\left(2Ka_0\right)\left(K^2a_0^2-1\right) \\ &\quad +12\cos\left(Ka_0\right)K^4a_0^4-18\sin\left(2Ka_0\right)Ka_0 \\ &\quad -12\sin\left(Ka_0\right)K^3a_0^3+2K^6a_0^6 \end{aligned} \tag{11}$$

for the electrostatic interaction and

$$\begin{aligned} \left(\frac{d\sigma}{d\Omega}\right)_m^{\text{at}} &= 4\mu^2\eta^2A_m^2\beta^2\left(\frac{m_\sigma^2+m_S^2}{m_S^2-m_\sigma^2}\right)^2 \\ &\quad \times\left[\frac{1}{m_\sigma^2+K^2}-\frac{1}{m_S^2+K^2}\right]^2 \end{aligned} \tag{12}$$

for the $\sigma + S$ exchange, where $\mu = m_F m_{Si}/(m_F + m_{Si})$, where m_{Si} is the mass of a silicon atom, and $K = 2k \sin\theta/2$, where $k = \sqrt{2\mu E}$ is the initial momentum and θ is the deflection angle with respect to the collision axis.

For a dark atom to thermalize between the surface and an underground detector, we have to ensure that its penetration length does not exceed 1 km. It is estimated by assuming a linear path of the dark atom through terrestrial matter:

$$x = \int_{E_{\text{th}}}^{E_0} \frac{dE}{|dE/dx|} < 1, \tag{13}$$

where dE/dx is the energy loss per unit length in the frame of the Earth:

$$\frac{dE}{dx} = n_{Si} \int_\Omega \Delta K \left(\frac{d\sigma}{d\Omega}\right)^{\text{at}} d\Omega, \tag{14}$$

obtained by integrating over all diffusion angles. In (13), the integration is performed from the initial kinetic energy of the dark atom E_0 to the thermal energy of the medium $E_{\text{th}} = (3/2)T_{\text{med}}$, where $T_{\text{med}} \simeq 300\,\text{K}$. In (14), n_{Si} is the number density of atoms in the terrestrial crust and $\Delta K = p^2(\cos\theta - 1)/m_{Si}$ is the energy lost in the frame of the Earth for each collision with a silicon atom at rest in the terrestrial surface, expressed in terms of the momentum p of each atom in the center-of-mass frame. It is clear that the linear path approximation is valid only when $m_F \gg m_{Si}$, but it gives in the other cases an upper limit on the penetration length of a dark atom through the Earth, which is of interest here.

4.2. Drift Down towards Underground Detectors. Once it has thermalized, a dark atom starts to drift towards the center of the Earth by gravity until it reaches an underground detector. The number density of dark atoms in the detector n_F is determined by the equilibrium between the infalling flux at the surface and the down-drifting thermalized flux: $(n_0/4)|\vec{V}_h + \vec{V}_E| = n_F V_d$, where $n_0\,(\text{cm}^{-3}) = 3 \times 10^{-4}/m_F$ (TeV) is the local number density of dark atoms, $\vec{V}_h + \vec{V}_E$ is the superposition of the orbital velocity of the Sun around the galactic center $\vec{V}_h$ and of the Earth around the sun $\vec{V}_E$, and V_d is the drift velocity of the dark atoms in the terrestrial matter once they have thermalized. Because of the orbital motion of the Earth around the Sun, $|\vec{V}_h + \vec{V}_E|$ is modulated in time: $|\vec{V}_h + \vec{V}_E| = V_h + V_E \cos\gamma \cos(\omega(t - t_0))$, so that n_F can be written as

$$n_F = n_F^0 + n_F^m \cos\left(\omega\left(t - t_0\right)\right), \tag{15}$$

where $\gamma \simeq 60^\circ$ is the inclination angle of the Earth orbital plane with respect to the galactic plane, $\omega = 2\pi/T_{\text{orb}}$ is the angular frequency of the orbital motion of the Earth, $T_{\text{orb}} = 1$ yr is the orbital period, and $t_0 \simeq$ June 2 is the period of the year when the Earth and Sun orbital velocities are aligned. As $V_d = g/n\langle\sigma_k^{\text{at}} v\rangle$, where $g = 980\,\text{cm/s}^2$ is the acceleration of gravity and $n \simeq 5 \times 10^{22}\,\text{cm}^{-3}$ is the number density of atoms in the terrestrial crust, the constant and modulated parts n_F^0 and n_F^m can be expressed as

$$n_F^0 = \frac{n_0 n \left\langle\sigma_k^{\text{at}} v\right\rangle}{4g} V_h, \tag{16}$$

$$n_F^m = \frac{n_0 n \left\langle\sigma_k^{\text{at}} v\right\rangle}{4g} V_E \cos\gamma. \tag{17}$$

In these two expressions, $V_h = 220 \times 10^5$ cm/s, $V_E = 29.5 \times 10^5$ cm/s, and $n\langle\sigma_k^{\text{at}} v\rangle$ is the rate of elastic collisions between a thermalized dark atom FG and terrestrial atoms, averaged over a Maxwellian velocity distribution at temperature $T_{\text{med}} \simeq 300\,\text{K}$. σ_k^{at} is obtained by integrating the differential cross section (11) over all diffusion angles and v is the relative velocity between a dark atom and a terrestrial atom. Note that σ_k^{at} dominates over σ_m^{at} at low energies, so there is no need to consider the total cross section σ^{at} here.

Arriving in the detector at room temperature, a dark atom still has to thermalize at the operating temperature. The latter is always lower than 300 K, except for the DAMA detectors, which operate at room temperature. We will check that this second thermalization at the edge of the detector is realized over a distance much smaller than the typical size of the device and can therefore be considered as instantaneous.

4.3. Bound-State-Formation Events. In the active medium, the dark atoms undergo collisions with the constituent atoms. Because of the Coulomb barrier due to the electric repulsion between nuclei (potential (6)), most of these collisions are elastic, but sometimes tunneling through the barrier can occur and bring a dark nucleus F into the region of the potential well present at smaller distance, due to the exchange of σ and S between F and the nuclei of the detector (potential (7)). There, electric dipole transitions $E1$ produce deexcitation of the system to low-energy bound states by emission of photons that can be detected, causing the observed signal. At this point, only the interaction between nuclei $V_k^{\text{nucl}} + V_m^{\text{nucl}}$ is therefore considered to calculate the capture cross section, since it dominates at small distance ($r \lesssim 1$ Å) and because the long-range part of the atom-dark atom potential $V_k^{\text{at}} + V_m^{\text{at}}$ is negligible and does not affect the initial diffusion eigenstate.

At thermal energies, to order v/c, only the partial s-wave of an incident plane wave on an attractive center is affected by the potential. Due to selection rules, direct $E1$ transitions to final s-bound states are forbidden. It can also be shown that magnetic dipole and electric quadrupole transitions $M1$ and $E2$ to such final levels are not present [23], leaving only the possibility to capture F in two $E1$ transitions, first to a p-bound state and then to an s-bound state, corresponding, respectively, to levels at relative angular momenta $l = 1$ and $l = 0$ in the nucleus-F potential $V_k^{\text{nucl}} + V_m^{\text{nucl}}$. The $E1$ capture cross section of F by a nucleus of charge Ze and mass m is then given by

$$\sigma_{\text{capt}} = \frac{32\pi^2 Z^2 \alpha}{3\sqrt{2}} \left(\frac{m_F}{m_F + m}\right)^2 \frac{1}{\sqrt{\mu}} \frac{\left(E - E_f\right)^3}{E^{3/2}} D^2, \tag{18}$$

where $\mu = m_F m/(m_F + m)$ is the reduced mass of the nucleus-F system, E is the total incident energy in the center-of-mass frame, E_f is the binding energy of the lower bound state at $l = 1$, and $D = \int_0^\infty r R_f(r) R(r) r^2 dr$, where R and R_f are the radial parts of the eigenfunctions of energies E and E_f, with r being the relative distance between F and the nucleus.

It is important to note here that each capture event will give rise to the emission of two photons. For the events to be seen as single-hit events, as stated by DAMA, one will require that the first emitted photon with the greatest possible energy, corresponding to the $E1$ capture from the continuum at $E \sim 10^{-2}$ eV to the lower p-state E_f, has an energy below the threshold $E_{\text{threshold}}$ of the considered experiment. In other words, we will have $|E_f - E| \simeq |E_f| < E_{\text{threshold}}$. The second emitted photon, corresponding to the $E1$ transition from a p-state $E^{l=1}$ to an s-state $E^{l=0}$, will have an energy beyond the threshold; that is, $|E^{l=0} - E^{l=1}| > E_{\text{threshold}}$.

Thermal motion in a detector at temperature T made of nuclei N gives rise to collisions between N and F species and hence to the event counting rate per unit volume:

$$R = n_F n_N \left\langle \sigma_{\text{capt}} v \right\rangle, \tag{19}$$

where n_F and n_N are the number densities of F and N in the detector and $\langle \sigma_{\text{capt}} v \rangle$ is the thermally averaged capture cross section times the relative velocity. Using Maxwellian velocity distributions at temperature T in the frame of the detector, passing to center-of-mass and relative velocities $\vec{v}_{CM}$ and $\vec{v}$ and performing the integral over the center-of-mass variables, we get

$$R = 8\pi n_F n_N \frac{1}{(2\pi T)^{3/2}} \frac{1}{\mu^{1/2}} \int_0^\infty \sigma_{\text{capt}}(E)\, E e^{-E/T} dE. \tag{20}$$

Given the modulated form (15) of the number density of F, one gets a modulated expression for the event rate:

$$R = R^0 + R^m \cos\left(\omega\left(t - t_0\right)\right). \tag{21}$$

The constant and modulated parts R^0 and R^m, when expressed in counts per day and per kilogram (cpd/kg), are given by

$$\begin{aligned} R^0 &= C n_F^0 \int_0^\infty \sigma_{\text{capt}}(E)\, E e^{-E/T} dE, \\ R^m &= C n_F^m \int_0^\infty \sigma_{\text{capt}}(E)\, E e^{-E/T} dE, \end{aligned} \tag{22}$$

with (note that a factor of π was missing in C in [19] and has been corrected here)

$$C = 7.54 \times 10^{11} \frac{Q t N_{Av}}{M_{\text{mol}}} \frac{1}{(2\pi T)^{3/2}} \frac{1}{\mu^{1/2}}, \tag{23}$$

where $Q = 1000\,\text{g}$, $t = 86400\,\text{s}$, $N_{Av} = 6.022 \times 10^{23}$, and M_{mol} is the molar mass of the active medium of the detector in g/mol.

An important feature of the model is its reinterpretation of the results of the direct-search experiments in terms of bound-state-formation events emitting photons that produce the observed signals. This is in opposition to the common scenario where WIMPs colliding on nuclei at velocity $\sim$ 220 km/s produce nuclear recoils: here, the thermal energies in play in the detectors are insufficient to create such recoils, and the emitted photons cause electron recoils. In experiments that do not discriminate between these two kinds of recoils, as DAMA/LIBRA and CoGeNT, the reinterpretation is straightforward. In experiments with a discrimination power, the present dark atoms are good candidates if the results are negative, as it is the case for XENON100, LUX, and CDMS-II/Ge. Indeed, even if the bound-state-formation events cannot be naturally suppressed, the remaining events will be interpreted as backgrounds and rejected. Further studies have to be performed in the case of discriminative experiments with positive results, as CRESST-II and CDMS-II/Si, to find if it is possible that the observed nuclear recoils may be misinterpreted bound-state-formation events occurring near the edge of those detectors.

5. Exploring the Parameter Space

5.1. Reproduction of the Results from DAMA and CoGeNT. The DAMA/LIBRA and CoGeNT experiments observe integrated modulation amplitudes $\widetilde{R}^m_{\text{DAMA}} = (0.0464 \pm 0.0052)$ cpd/kg and $\widetilde{R}^m_{\text{CoGeNT}} = (1.66 \pm 0.38)$ cpd/kg in the energy intervals (2–6) keV and (0.5–2.5) keV, respectively.

As a first approximation and for simplicity, the signal is supposed to be made of one monochromatic line of energy $\Delta E = E_g - E_f$, where E_g is the ground state at $l = 0$, falling within the detection range (it would be interesting to reproduce the observed energy spectra by taking into account the different possible transitions from the p-states to the s-states).

The 4-dimensional parameter space of the model is explored separately for DAMA and CoGeNT in order to reproduce the observed rates and energy intervals at the 2σ level, which gives corresponding regions for each experiment. We use the isotopes ^{127}I and ^{74}Ge, respectively, for DAMA and CoGeNT, as their detectors are made of NaI and Ge crystals. The choice of the iodine component of the DAMA/LIBRA experiment, rather than ^{23}Na, is crucial since it allows getting rid of the formation of bound states with light elements, thus preventing the formation of anomalous heavy isotopes on Earth and during Big Bang nucleosynthesis. A direct consequence is that the collisions in the terrestrial crust are purely elastic.

For each set of parameters and for each experiment, the Schrodinger equation independent of time, with potential $V_k^{\text{nucl}} + V_m^{\text{nucl}}$ applied to the constituent nucleus, is first solved through the WKB approximation. This gives good approximations for the eigenvalues and eigenfunctions of the corresponding nucleus-F systems, the former allowing us to calculate ΔE. The modulated part n_F^m of the number density of F in the detector is then computed using (17) before finally evaluating the modulated part of the event rate R^m from (22), at the operating temperatures $T = 300$ K for DAMA and $T = 77$ K for CoGeNT. To compute the capture cross section σ_{capt},

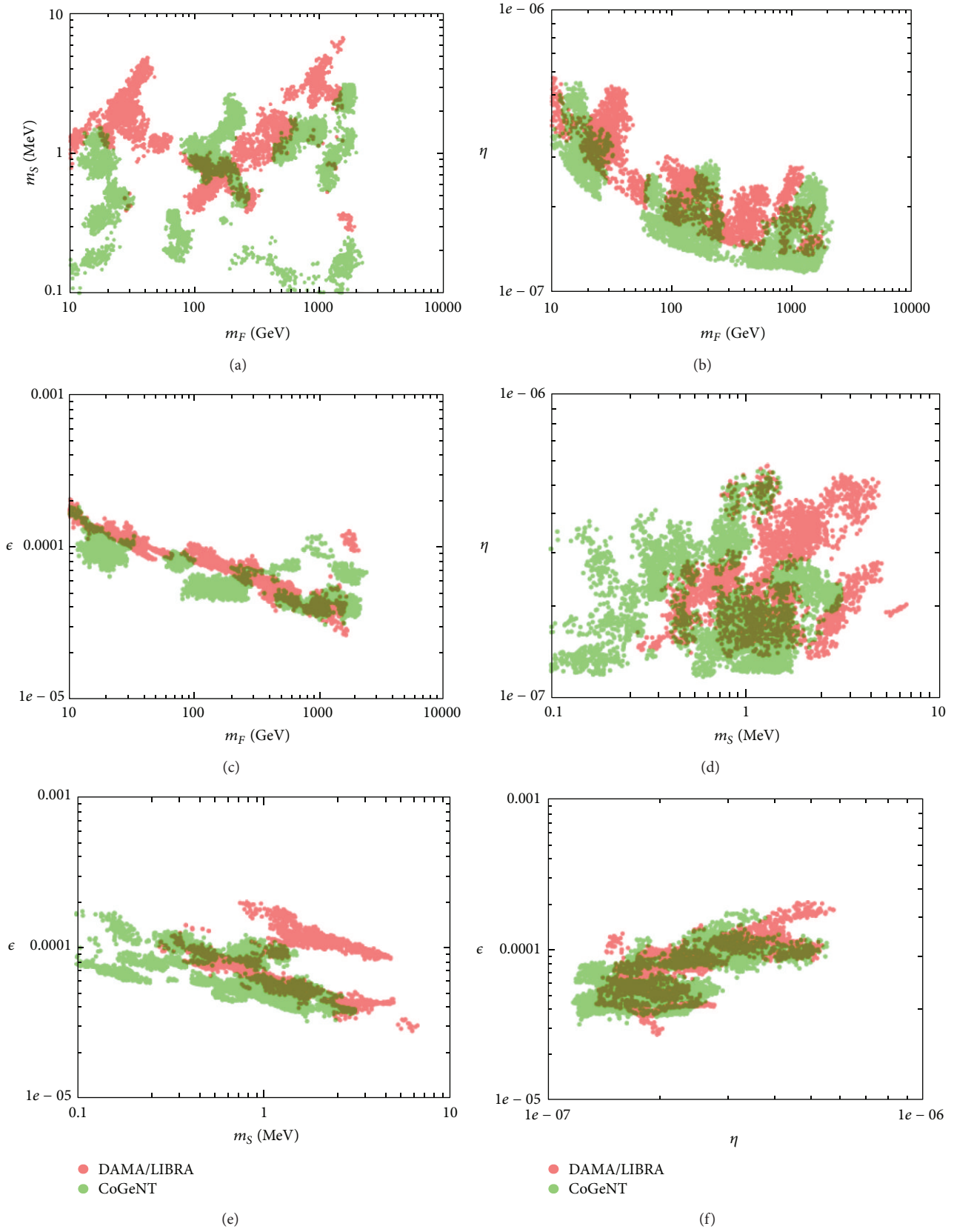

Figure 1: Two-dimensional parameter regions reproducing the DAMA/LIBRA (light red) and CoGeNT (light green) results at the 2σ level. The overlapping regions stand out in dark green. (a) (m_F, m_S) plane. (b) (m_F, η) plane. (c) (m_F, ϵ) plane. (d) (m_S, η) plane. (e) (m_S, ϵ) plane. (f) (η, ϵ) plane.

given by (18), at a given energy E in the center-of-mass frame of the nucleus-F system, one numerically solves the radial Schrodinger equation in the continuum to get the radial part $R(r)$ of the initial diffusion eigenstate and calculate the matrix element D of the electric dipole operator.

The regions are projected in two dimensions by combining all the possible pairs of parameters and are given in Figure 1. For each model, one has ensured that the first emitted photon has an energy below the threshold of the considered experiment while the second one has an energy beyond the threshold, that thermalization occurs before 1 km, that no bound states can form with elements characterized by $Z \leq 14$ ($Z = 14$ being silicon), and that thermalization at the edge of the CoGeNT detector requires a penetration length much shorter than the size of the detector. For the latter point, we have used (13) and (14) with $E_0 = (3/2)T_{\text{room}}$, where $T_{\text{room}} = 300$ K is the initial room temperature, and $E_{\text{th}} = (3/2)T$, where $T = 77$ K is the final temperature.

From the overlapping regions in the projected parameter spaces implying m_F, we see that possible values for that parameter are between 10 GeV and 2 TeV. The upper limit comes from the requirement that the penetration length must be less than 1 km. Analyzing the regions where the parameter m_S is involved indicates that the values reproducing both the DAMA/LIBRA and CoGeNT experiments at the 2σ level must lie within $[0.4, 3]$ MeV. In the same way, we find that η ranges from 1.3×10^{-7} to 5×10^{-7} while ϵ goes from 3×10^{-5} to 2×10^{-4}.

5.2. Considerations about the Constraints on η and ϵ. One has derived, in [19], a constraint on $\widetilde{\eta} = \eta g/g'$ from unseen vector meson disintegrations: $\widetilde{\eta} < 1.2 \times 10^{-4}$. In principle, it is not applicable to η, but a reasonable choice would consist in posing $g' = g$. In this case, the constraint translates directly to η and we see that all the previous models satisfy it easily, by two or three orders of magnitude.

The cosmological and astrophysical constraints on ϵ, generally derived in the framework of models with a single millicharged species realizing the full cosmological dark matter density, cannot be applied directly to this subdominant, atomic, and millicharged scenario and should in any case be somewhat weakened. However, constraints from accelerators can always be used. For masses $m_F \geq 1$ GeV, they let a large allowed window for $\epsilon < 0.1$ [24], which is clearly the case here. Some interesting discussion may arise from the lighter species G, with constraints on ϵ from accelerators being stronger for smaller masses. Similarly to η, m_G is not directly constrained by the previous analysis but only the product of m_G and e'^2 through the Bohr radius a_0' of the dark atoms. However, if we do once again the reasonable assumption $e' \simeq e$, then the adopted value of $a_0' = 1$ Å leads to $m_G \simeq m_e$, where m_e is the mass of the electron. It turns out that for $m_G \sim 1$ MeV, the upper limit on ϵ from accelerators lies just in the interval deduced in the previous section from direct experiments. If it is so, we could therefore be close to a discovery of millicharges in accelerators via the component G.

5.3. Consistency with XENON100, CDMS-II/Ge, and LUX. For the models of Figure 1 to be fully acceptable, we have to ensure that they satisfy the constraints set by the experiments that do not observe any signal, as XENON100, CDMS-II/Ge, and LUX. These are able to discriminate between nuclear and electron recoils and, as already mentioned at the end of Section 4.3, bound-state-formation events producing electron recoils in such detectors will be considered as backgrounds. Therefore, if some events remain, they should still have a smaller rate than the observed background.

XENON100 and LUX have similar detectors, but LUX puts the strongest constraint with expected and observed electron-recoil backgrounds, respectively, of $(2.6 \pm 0.2_{\text{stat}} \pm 0.4_{\text{syst}}) \times 10^{-3}$ and $(3.1 \pm 0.2_{\text{stat}}) \times 10^{-3}$ cpd/kg/keV$_{ee}$ in the $(0.9 - 5.3)$ keV$_{ee}$ range. This leaves the possibility of an additional contribution to the expected background of at most 5.72×10^{-3} cpd/kg in that energy interval. Computing the constant part R^0 of the rate from (22) for ^{132}Xe and at the operating temperature $T = 173$ K, and rejecting the models leading to higher rates, does not change the ranges of parameters previously found from the reproduction of the experiments with positive results.

Finally, this model predicts strongly suppressed event rates in cryogenic detectors, such as CDMS-II, where temperatures ~1 mK give rise to much too low thermal energies for the dark atoms to tunnel through the Coulomb barrier and be captured. The rates computed with ^{74}Ge at $T = 1$ mK are effectively consistent with zero and are therefore in agreement with the negative results from CDMS-II/Ge.

6. Conclusions

We have explored the parameter space of our milli-interacting dark matter model and found, while only one model was given in [19], that regions reproducing the direct-dark-matter-search experiments at the 2σ level can be identified. The overlaps of the regions of DAMA/LIBRA and CoGeNT indicate that the interesting models must lie in the ranges $10\,\text{GeV} \leq m_F \leq 2\,\text{TeV}$, $0.4\,\text{MeV} \leq m_S \leq 3\,\text{MeV}$, $10^{-7} \leq \eta \leq 5 \times 10^{-7}$, and $3 \times 10^{-5} \leq \epsilon \leq 2 \times 10^{-4}$. Within these intervals, models that do not contradict the negative results from XENON100 and LUX exist, and their rates contribute to the expected electron-recoil background. The model naturally prevents any bound-state-formation event in cryogenic detectors ($T \sim 1$ mK), which is in agreement with the Germanium detector of CDMS-II. Some difficulties appear, however, with the CRESST-II and CDMS-II/Si cryogenic experiments, for which the collisions at the edges of the detectors should be studied in detail, when the particles are still at room temperature and can have sufficient energies to be captured and produce a signal.

More than giving constraints on the parameters of a specific model, it has been shown here that it is possible, in the framework of dark matter models containing a sector with a richness and a complexity similar to ours, to reconcile experiments such as DAMA/LIBRA and XENON100 that seem contradictory when interpreted in terms of WIMPs.

Conflict of Interests

The author declares that there is no conflict of interests regarding the publication of this paper.

Acknowledgments

The author thanks J. R. Cudell for useful advice. This work is supported by the Belgian fund F.R.S-FNRS.

References

[1] R. Bernabei, P. Belli, F. Cappella et al., "New results from DAMA/LIBRA," *The European Physical Journal C*, vol. 67, no. 1, pp. 39–49, 2010.

[2] R. Bernabei, P. Belli, F. Cappella et al., "Final model independent result of DAMA/LIBRA–phase1," *The European Physical Journal C* , vol. 73, article 2648, 2013.

[3] C. E. Aalseth, P. S. Barbeau, J. Colaresi et al., "Search for an annual modulation in a *p*-type point contact Germanium dark matter detector," *Physical Review Letters*, vol. 107, no. 14, Article ID 141301, 5 pages, 2011.

[4] J. Collar, "Search for an annual modulation in 3.4 years of CoGeNT data," in *Proceedings of the 13th International Conference on Topics in Astroparticle and Underground Physics (TAUP '13)*, Asilomar, Calif, USA, September 2013.

[5] G. Angloher, M. Bauer, I. Bavykina et al., "Results from 730 kg days of the CRESST-II Dark Matter search," *The European Physical Journal C*, vol. 72, no. 4, article 1971, pp. 1–22, 2012.

[6] R. Agnese, Z. Ahmed, A. J. Anderson et al., "Silicon Detector Dark Matter Results from the Final Exposure of CDMS II," *Physical Review Letters*, vol. 111, no. 25, Article ID 251301, 6 pages, 2013.

[7] E. Aprile, M. Alfonsi, K. Arisaka et al., "Dark matter results from 225 live days of XENON100 data," *Physical Review Letters*, vol. 109, no. 18, Article ID 181301, 6 pages, 2012.

[8] Z. Ahmed, D. S. Akerib, S. Arrenberg et al., "Results from a low-energy analysis of the CDMS II Germanium data," *Physical Review Letters*, vol. 106, no. 13, Article ID 131302, 5 pages, 2011.

[9] D. S. Akerib, H. M. Araujo, X. Bai et al., "First results from the LUX dark matter experiment at the Sanford Underground Research Facility," 2013.

[10] R. Foot, "Mirror dark matter interpretations of the DAMA, CoGeNT and CRESST-II data," *Physical Review D*, vol. 86, no. 2, Article ID 023524, 10 pages, 2012.

[11] J. M. Cline, Z. Liu, and W. Xue, "Millicharged atomic dark matter," *Physical Review D*, vol. 85, no. 10, Article ID 101302, 6 pages, 2012.

[12] M. Y. Khlopov, A. G. Mayorov, and E. Y. Soldatov, "The dark atoms of dark matter," *Prespacetime Journal*, vol. 1, pp. 1403–1417, 2010.

[13] M. Y. Khlopov, A. G. Mayorov, and E. Y. Soldatov, "Towards nuclear physics of OHe dark matter," in *Proceedings of the 14th International Workshop, "What Comes Beyond the Standard Model"*, N. Mankoc Borstnik, H. B. Nielsen, C. D. Froggatt, and D. Lukman, Eds., vol. 12, pp. 94–102, Bled, Slovenia, 2011.

[14] J. R. Cudell, M. Khlopov, and Q. Wallemacq, "The nuclear physics of OHe," in *Proceedings of the 15th International Workshop "What Comes Beyond the Standard Model"*, N. Mankoc Borstnik, H. B. Nielsen, and D. Lukman, Eds., vol. 13, pp. 10–27, Bled, Slovenia, 2012.

[15] M. McCullough and L. Randall, "Exothermic double-disk dark matter," *Journal of Cosmology and Astroparticle Physics*, vol. 2013, 2013.

[16] N. Fornengo, P. Panci, and M. Regis, "Long-range forces in direct dark matter searches," *Physical Review D*, vol. 84, no. 11, Article ID 115002, 20 pages, 2011.

[17] J. Miralda-Escudé, "A test of the collisional dark matterhypothesis from cluster lensing," *The Astrophysical Journal*, vol. 564, no. 1, pp. 60–64, 2002.

[18] J. Fan, A. Katz, L. Randall, and M. Reece, "Double-disk dark matter," *Physics of the Dark Universe*, vol. 2, no. 3, pp. 139–156.

[19] Q. Wallemacq, "Milli-interacting dark matter," *Physical Review D*, vol. 88, no. 6, Article ID 063516, 10 pages, 2013.

[20] C. Amsler, M. Doser, M. Antonelli et al., "Review of particle physics," *Physics Letters B*, vol. 667, no. 1–5, pp. 1–6, 2008.

[21] G. Erkol, R. G. E. Timmermans, and T. A. Rijken, "Nucleon-sigma coupling constant in QCD sum rules," *Physical Review C*, vol. 72, no. 3, Article ID 035209, 7 pages, 2005.

[22] S. D. McDermott, H. B. Yu, and K. M. Zurek, "Turning off the lights: how dark is dark matter?" *Physical Review D*, vol. 83, no. 6, Article ID 063509, 9 pages, 2011.

[23] E. Segre, *Nuclei and Particles*, W. A. Benjamin, New York, NY, USA, 2nd edition, 1977.

[24] J. Jaeckel and A. Ringwald, "The low-energy frontier of particle physics," *Annual Review of Nuclear and Particle Science*, vol. 60, pp. 405–437, 2010.

Hindawi Publishing Corporation
Advances in High Energy Physics
Volume 2013, Article ID 856196, 5 pages
http://dx.doi.org/10.1155/2013/856196

Review Article

The Dark Side of Neutron Stars

Chris Kouvaris

CP^3*-Origins, University of Southern Denmark, Campusvej 55, 5230 Odense, Denmark*

Correspondence should be addressed to Chris Kouvaris; kouvaris@cp3.dias.sdu.dk

Received 19 August 2013; Accepted 12 November 2013

Academic Editor: Konstantin Belotsky

We review severe constraints on asymmetric bosonic dark matter based on observations of old neutron stars. Under certain conditions, dark matter particles in the form of asymmetric bosonic WIMPs can be effectively trapped onto nearby neutron stars, where they can rapidly thermalize and concentrate in the core of the star. If some conditions are met, the WIMP population can collapse gravitationally and form a black hole that can eventually destroy the star. Based on the existence of old nearby neutron stars, we can exclude certain classes of dark matter candidates.

1. Introduction

Compact stars such as neutron stars and white dwarfs can lead in general to two types of constraints regarding dark matter candidates. The first one has to do with annihilating dark matter that changes the thermal evolution of the star. Annihilation of Weakly Interacting Massive Particles (WIMPs) that are trapped inside compact stars can lead to the production of significant amount of heat that can change the temperature of old stars [1–4]. Such a phenomenon can be in principle contrasted to observations. The second type of constraints is related to asymmetric dark matter [5–12]. Asymmetric dark matter is an attractive alternative to thermally produced dark matter especially due to the intriguing possibility of relating its asymmetry to the baryonic one. For recent reviews see [13, 14]. Due to the asymmetry, WIMP annihilation is not significant in this case. If a certain amount of WIMPs is trapped inside the star, the WIMPs can quite rapidly thermalize and concentrate within a tiny radius in the core of the star. If the WIMP population grows significantly, WIMPs might become self-gravitating and they might collapse forming a mini black hole. Under certain conditions, the black hole might consume the rest of the star, thus leading to the ultimate destruction of the star. However, very old (older than a few billion years) nearby neutron stars have been well observed and studied. The simple presence of such verified old stars leads to the conclusion that no black hole has consumed the star and as we will argue, this can lead to very severe constraints on the properties of certain types of asymmetric dark matter. We should also mention that additional constraints on asymmetric dark matter can be imposed on different ways (e.g., from asteroseismology [15–17], from effects on the transport properties of the neutron stars [18], and/or from hybrid dark matter rich compact stars [19, 20]).

One can easily figure out that fermionic WIMPs, due to the fact that they have to overcome Fermi pressure, require a huge number in order to collapse; that is, $N \sim (M_{\rm pl}/m)^3$ where $M_{\rm pl}$ and m are the Planck mass and WIMP mass, respectively. This number of WIMPs is very difficult to accumulate within a few billion years and with dark matter densities similar to the ones of the earth. However, this required number for gravitational collapse is reduced significantly in the case of attractive Yukawa forces among the WIMPs [8].

2. Asymmetric Bosonic Dark Matter

In the case of asymmetric bosonic WIMPs, the necessary WIMP number for collapse is much smaller because there is no Fermi pressure and only the uncertainty principle keeps particles from collapsing. The collapse takes place once the momentum becomes smaller than the self-gravitational potential energy as follows:

$$\frac{\hbar}{r} < \frac{GMm}{r} \Longleftrightarrow M > \frac{M_{\rm pl}^2}{m}, \tag{1}$$

where $M = Nm$ is the total mass of the WIMP cloud. A more accurate and generic estimate that includes the effect of self-interactions gives [21]

$$M_{\rm crit} = \frac{2}{\pi}\frac{M_{\rm pl}^2}{m}\sqrt{1+\frac{\lambda M_{\rm pl}^2}{32\pi m^2}}. \quad (2)$$

Although self-interactions between WIMPs can be quite general in nature, without loss of generality, we can assume that the self-interaction can be approximated well by a $\lambda\phi^4$ interaction term. At the no interaction limit $\lambda = 0$, we trivially get the critical mass mentioned above (up to factors of order one).

The accretion of WIMPs for a typical $1.4M_\odot$ 10 km neutron star taking into account relativistic effects has been calculated in [3]. The total mass of WIMPs accreted is

$$M_{\rm acc} = 1.3\times 10^{43}\left(\frac{\rho_{\rm dm}}{0.3\,{\rm GeV/cm^3}}\right)\left(\frac{t}{\rm Gyr}\right) f\,{\rm GeV}, \quad (3)$$

where $\rho_{\rm dm}$ is the local dark matter density, and the "efficiency" factor $f = 1$ if the WIMP-nucleon cross section satisfies $\sigma > 10^{-45}\,{\rm cm^2}$ and $f = \sigma/(10^{-45}\,{\rm cm^2})$ if $\sigma < 10^{-45}\,{\rm cm^2}$.

One can easily check that $M_{\rm acc}$ can be larger than $M_{\rm crit}$ practically for all masses larger than ~100 keV. To form a black hole, satisfying the condition (2) is necessary but it is not sufficient. One should make sure that, after the WIMPs have been captured, they slow down and thermalize with nuclear matter concentrating within a small thermal radius. Failing to satisfy this condition, even if condition (2) is satisfied, does not necessarily lead to the formation of a black hole, since WIMPs would not be confined in a tiny region. The thermalization time scale has been estimated in [3, 5] as follows:

$$t_{\rm th} = 0.2\,{\rm yr}\left(\frac{m}{\rm TeV}\right)^2\left(\frac{\sigma}{10^{-43}\,{\rm cm^2}}\right)^{-1}\left(\frac{T}{10^5\,{\rm K}}\right)^{-1}. \quad (4)$$

As one can observe, despite the Pauli blocked interactions between WIMPs and nucleons, unless they are very heavy, WIMPs thermalize in less than a year. Having thermalized with nuclear matter, WIMPs concentrate in the center of the star within a thermal radius that can be easily obtained by use of the virial theorem as follows:

$$r_{\rm th} = \left(\frac{9kT_c}{8\pi G\rho_c m}\right)^{1/2} = 220\,{\rm cm}\left(\frac{\rm GeV}{m}\right)^{1/2}\left(\frac{T_c}{10^5\,{\rm K}}\right)^{1/2}, \quad (5)$$

where k is the Boltzmann constant, T_c is the temperature at the core of the star, and $\rho_c = 5\times 10^{38}\,{\rm GeV/cm^3}$ is a typical value for the neutron star core density.

Once the WIMPs are thermalized and if sufficient number is accumulated in the star, there are two different events that take place, the time order of which depends on the WIMP mass. One is the self-gravitation of the WIMP sphere and the second is the formation of a Bose Einstein condensate (BEC). Self-gravitation takes place once the mass of the WIMP sphere inside the thermal radius becomes larger than the mass of the neutron star within the same radius. In other words, this happens once WIMPs start feeling strongly their own gravitational field. For this to happen the WIMP sphere should have a mass that satisfies

$$M_{\rm sg} > \frac{4}{3}\pi\rho_c r_{\rm th}^3 = 2.2\times 10^{46}\,{\rm GeV}\left(\frac{m}{\rm GeV}\right)^{-3/2}. \quad (6)$$

On the other hand, BEC formation takes place once the WIMP number density is

$$n_{\rm BEC} \simeq 4.7\times 10^{28}\,{\rm cm^{-3}}\left(\frac{m}{\rm GeV}\right)^{3/2}\left(\frac{T_c}{10^5{\rm K}}\right)^{3/2}. \quad (7)$$

One can easily check that for WIMPs roughly lighter than 10 TeV, the accumulated WIMPs within $r_{\rm th}$ meet first the condition for BEC formation. We are going to study these two cases ($m < 10$ TeV and $m > 10$ TeV) separately since events unfold with different order. For WIMPs lighter than 10 TeV, one can estimate that the total number of WIMPs needed to form a BEC is $N_{\rm BEC} \simeq 2\times 10^{36}$. Any accumulated WIMPs on top of this number go directly to the ground state of the BEC state. The radius of the BEC state is

$$r_{\rm BEC} = \left(\frac{8\pi}{3}G\rho_c m^2\right)^{-1/4} \simeq 1.6\times 10^{-4}\left(\frac{\rm GeV}{m}\right)^{1/2}{\rm cm}. \quad (8)$$

As it can be seen, $r_{\rm BEC} \ll r_{\rm th}$ and therefore WIMPs in the ground state can become self-gravitating much faster than what (6) predicts. In fact we can appreciate this if we substitute $r_{\rm th}$ by $r_{\rm BEC}$ in (6). This leads to the condition

$$M > 8\times 10^{27}\,{\rm GeV}\left(\frac{m}{\rm GeV}\right)^{-3/2}. \quad (9)$$

If (2), (7), and (9) are satisfied, a black hole is going to be formed. Once the black hole is formed, its fate is determined by its initial mass $M_{\rm crit}$. On the one hand, the black hole is accreting dark matter and nuclear matter from the core of the star. This tends to increase the black hole mass. On the other hand, emission of photons and particles in general via Hawking radiation tends to reduce the mass of the black hole. The black hole mass evolution is determined by

$$\frac{dM}{dt} = \frac{4\pi\rho_c G^2M^2}{c_s^3} - \frac{f}{G^2M^2}, \quad (10)$$

where c_s is the sound speed at the core of the star and f is a dimensionless number that in general depends on the number of particle species emitted and the rate of rotation of the black hole. We have used a spherically symmetric Bondi accretion of matter into the black hole. By inspection of (10) it is apparent that there is a critical value of the black hole mass M above which accretion always wins, while below, Hawking radiation reduces the mass of the black hole which in turn increases even further the rate of Hawking radiation leading eventually to the evaporation of the black hole. This critical mass has been estimated if one considers only photons in [6] as follows:

$$M > 5.7\times 10^{36}\,{\rm GeV}. \quad (11)$$

The mass becomes slightly larger [10] if one includes also other species that can be emitted (e.g., gravitons, neutrinos,

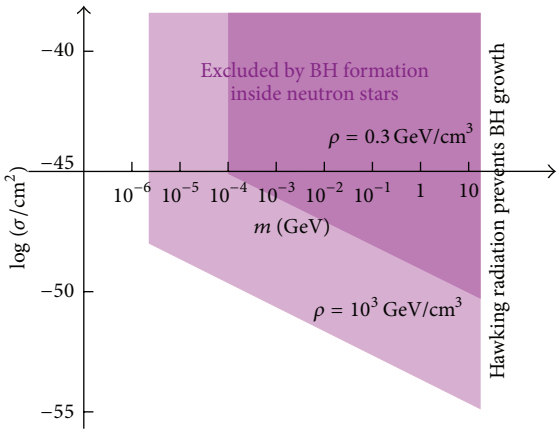

Figure 1: Exclusion regions of the asymmetric bosonic dark matter as a function of the WIMP mass and the WIMP-nucleon cross section for an isolated neutron star at local DM density $\rho_{\mathrm{dm}} = 0.3\,\mathrm{GeV/cm^3}$ (such as J0437-4715 and J0108-1431) and for a neutron star in the core of a globular cluster with $\rho_{\mathrm{dm}} = 10^3\,\mathrm{GeV/cm^3}$.

quarks, leptons, etc.). Comparison of (2) (with $\lambda = 0$) to (11) shows that WIMP masses larger than 16 GeV lead to black hole masses below the limit of (11). This means that, for masses larger than 16 GeV, black holes evaporate and their effect is to heat up the star as they evaporate. However this does not lead to a dramatic effect like the destruction of the star. This 16 GeV mass limit becomes slightly smaller if more Hawking radiation modes are included.

Finally there is one last constraint that should be satisfied. WIMP masses cannot be arbitrarily small because for small WIMP masses, after WIMPs have thermalized, those in the tail of the Maxwell-Boltzmann distribution have large enough velocities to escape from the star. This evaporation effect can be ignored for WIMP masses $m > 2\,\mathrm{keV}$ [6]. If the accreted dark matter mass within a billion years M_{acc} is larger than M_{crit} of (2), and (7), (9), and (11) are satisfied, the WIMPs form a black hole that can destroy the star. There are some subtle issues regarding how fast the black hole consumes the star that have been addressed to some extent in [6]. The constraints on asymmetric bosonic dark matter are depicted in Figure 1. As can be seen, depending on the WIMP-nucleon cross section, WIMP candidates from 100 keV up to roughly 16 GeV are severely constrained by the existence of nearby old neutron stars. The constrained region is bound at 100 keV due to the fact that below that mass accretion it is not sufficient to acquire M_{crit} from (2). These constraints can be enlarged down to 2 keV (the limit from WIMP evaporation we mentioned before) as long as we consider old neutron stars in globular clusters with $\rho_{\mathrm{dm}} \gtrsim 30\,\mathrm{GeV/cm^3}$.

Now we can consider the case where the WIMP mass is larger than 10 TeV and therefore self-gravitation of the WIMP sphere happens before BEC formation. As we mentioned above, black holes of critical mass (2) with WIMP masses roughly larger than ~16 GeV do not survive due to Hawking radiation. Therefore one should expect that black holes of M_{crit} (of (2)) formed out of 10 TeV WIMPs (or heavier) would evaporate quite fast. However, since self-gravitation takes place before BEC and the self-gravitating mass of (6) for $m > 10\,\mathrm{TeV}$ is much larger than the crucial mass for the survival of the black hole of (11), there were speculations in the literature [7, 9, 10] that constraints can be imposed also for $m > 10\,\mathrm{TeV}$. The claim was that, instead of forming a black hole of M_{crit} that is below the surviving threshold for Hawking radiation, a much larger black hole coming from the collapse of the self-gravitating WIMP sphere M_{sg} forms, which due to its larger mass can grow and destroy the star, thus imposing constraints on this part of the parameter space of asymmetric bosonic dark matter. However we review here the argument that was put forward in [22] that demonstrates that the formation of smaller (nonsurviving) black holes of mass M_{crit} is unavoidable and therefore the M_{sg}, instead of collapsing to a single large black hole, forms a series of black holes of M_{crit} that evaporate one after the other, thus resulting in no constraint for WIMP masses with $m > 10\,\mathrm{TeV}$.

In order for the WIMP sphere to collapse, the whole mass should be confined within the Schwarzschild radius $r_s = 2GM$ of the black hole. The density of WIMPs just before forming the black hole would be $n_{\mathrm{BH}} \sim 3(32\pi G^3 M_{\mathrm{sg}}^2 m)^{-1} \sim 10^{74}\,\mathrm{cm^{-3}}(\mathrm{GeV}/m)(M_{\mathrm{sg}}/10^{40}\,\mathrm{GeV})^{-2}$. It is easy to see that this density is higher than the density required for BEC formation of (7). This means that unless the WIMP sphere collapses violently and rapidly, it should pass through the density at which BEC is formed. As the self-gravitating WIMP sphere of mass M_{sg} contracts, at some point it will reach the density where BEC is formed. Any further contraction of the WIMP sphere will not lead to an increase in the density of the sphere. The density remains as that of BEC. The formation of BEC happens on time scales of order [23] $t_{\mathrm{BEC}} \sim \hbar/k_B T \sim 10^{-16}$ s, that is, practically instantaneously. Further shrinking of the WIMP sphere results in increasing the mass of the condensate rather than the density of noncondensed WIMPs. This process happens at a time scale which is determined by the cooling time of the WIMP sphere as discussed below. As we will show, this cooling time is the relevant time scale for the BEC formation. As in the previous case, the ground state will start being populated with WIMPs which at some point will become self-gravitating themselves. This of course will happen not when (9) is satisfied. Equation (9) was derived as the WIMP ground state becomes denser than the surrounding nuclear matter (since the dark matter that is not in the ground state of the BEC is less dense). Here, the condition is that the density of the ground state of the BEC should be larger than the density of the surrounding dark matter (i.e., already denser than the nuclear matter at this point). The condition reads as follows:

$$M_{\mathrm{BEC,sg}} = \frac{4\pi}{3} n_{\mathrm{BEC}} m r_{\mathrm{BEC}}^3 = 9.6 \times 10^{21}\,\mathrm{GeV}\left(\frac{m}{10\,\mathrm{TeV}}\right)^{-7/8}. \tag{12}$$

Once the BEC ground state obtains this mass, the ground state starts collapsing within the collapsing WIMP sphere. Any contraction of the WIMP sphere does not change the density of the sphere but only the density of the ground state. $M_{\mathrm{BEC,sg}}$ is smaller than M_{crit} and therefore the BEC ground

state cannot form a black hole yet. However as the ground state gets populated at some point it reaches the point where its mass is $M_{\rm crit}$ and this leads to the formation of a black hole of mass $M_{\rm crit}$ and not $M_{\rm sg}$. The evaporation time for such a black hole of $M_{\rm crit}$ (composed of WIMPs of mass m) is

$$\tau = 5 \times 10^3 \,\mathrm{s} \left(\frac{10\,\mathrm{TeV}}{m} \right)^3. \tag{13}$$

The only way that such a black hole can be maintained in life is by adding fast new matter inside in a rate that is higher than the Hawking radiation. As we showed earlier accretion of nuclear matter from the core of the star is not sufficient for m larger than roughly 16 GeV. Accretion of dark matter from the rest of the WIMP sphere is also not sufficient. The accretion of noninteracting collisionless particles in the nonrelativistic limit onto a black hole is given by [24]

$$F = \frac{16\pi G^2 M_{\rm BH}^2 \rho_{\rm dm}}{v_\infty}, \tag{14}$$

where $\rho_{\rm dm}$ is $mn_{\rm BEC}$ and v_∞ is the average WIMP velocity far away from the black hole. Using the virial theorem, we take $v_\infty = \sqrt{GM/r}$, M being the total mass of the WIMP sphere and r being the radius of the WIMP sphere. For the first black hole $M = M_{\rm sg}$ and $r = r_0$, where r_0 is the radius of the WIMP sphere when it reaches the BEC density; that is,

$$r_0 = \left(\frac{3M_{\rm sg}}{4\pi m n_{\rm BEC}} \right)^{1/3} = 2.2\,\mathrm{cm} \left(\frac{10\,\mathrm{TeV}}{m} \right)^{4/3}. \tag{15}$$

For WIMP sphere masses ranging from (2) to (6) the Hawking radiation dominates overwhelmingly over the WIMP accretion despite the large WIMP density, and therefore the black hole evaporation time is given accurately by (13).

There are another two ways where the black hole can be maintained in life, that is, if the WIMP capture time scale and/or the cooling time scale are smaller than τ. The capture time scale is defined as the time it takes for the star to capture a number of WIMPs with a total mass of $M_{\rm crit}$. If this time is smaller than τ, a new black hole of $M_{\rm crit}$ will form before the extinction of the previous one. Therefore it is possible that gradually the mass of the black hole could increase after successive black holes form before previous ones have evaporated. However, using (2) and (3) we get the following capture time scale:

$$t_{\rm cap} = 7.6 \times 10^4 \,\mathrm{s} \left(\frac{m}{10\,\mathrm{TeV}} \right)^{-1} \left(\frac{\rho_{\rm dm}}{10^3\,\mathrm{GeV/cm^3}} \right)^{-1}, \tag{16}$$

which is larger than τ for $m > 10$ TeV even for neutron stars located in high dark matter density globular cluster cores. Capture rates of new WIMPs cannot replenish the black hole mass rate loss to Hawking radiation.

Finally one should estimate the cooling time scale for the WIMP sphere. Once self-gravitating, the WIMP sphere does not collapse to a black hole just because WIMPs still have a lot of energy. This energy can be lost via collisions with nucleons. This way the WIMPs lower their energy and the WIMP sphere contracts. Let us assume that a black hole of mass $M_{\rm crit}$ has been formed and it is going to evaporate in τ. Once formed the black hole is doomed to evaporate unless the WIMP sphere contracts fast enough, so it replenishes the BEC ground state with another $M_{\rm crit}$ mass that collapses and forms a second black hole, before the first one has evaporated. In that case, the mass of the black hole would be reinforced with new mass making it possible for the black hole to grow. As we will show the time scale it takes for the WIMP sphere to populate again, the BEC ground state is larger than the evaporation time and therefore the black hole cannot survive. The energy that the WIMP sphere has to lose in order to admit $M_{\rm crit}$ in the BEC ground state is

$$\delta E = \frac{1}{2} \frac{GMM_{\rm crit}}{r}, \tag{17}$$

where M is the total WIMP mass and r is the radius of the WIMP-sphere. For the first black hole $M = M_{\rm sg}$ and $r = r_0$. This energy must be lost by WIMP-nucleon collisions. The time it takes on average for a WIMP-nucleon collision (taking into account the Pauli blocking effect for the degenerate nucleons) is

$$\tau_{\rm col} = \frac{1}{n\sigma v} \frac{4p_F}{3m_N v} = \frac{2p_F m}{3\rho_c \sigma \epsilon}, \tag{18}$$

where $p_F \simeq 1\,\mathrm{GeV}$ is the nucleon Fermi momentum at the core of the star, n the number density of nucleons, m_N the nucleon mass, σ the WIMP-nucleon cross section, and ϵ the kinetic energy of the WIMP. ϵ can be estimated by the use of the virial theorem as follows:

$$\epsilon \sim \frac{GMm}{2r_0}. \tag{19}$$

One should keep in mind that each WIMP-nucleon collision leads to a loss of energy $\delta\epsilon = 2(m_N/m)\epsilon$. Therefore in order for $N = M/m$ WIMPs to lose the excess δE energy colliding in $\tau_{\rm col}$ time scales with nucleons losing each time on average energy $\delta\epsilon$, it takes

$$t_{\rm cool} = \tau_{\rm col} \frac{\delta E}{N\delta\epsilon} = \tau_{\rm col} \frac{m\delta E}{M\delta\epsilon} = \frac{4}{3\pi} \frac{p_F}{m_N} \frac{r_0 M_{\rm pl}^4}{\rho_c \sigma M^2}. \tag{20}$$

One can see that this time is shorter for larger mass M. Substituting $M = M_{\rm sg}$ into (20) one gets

$$t_{\rm cool} \simeq 1.5 \times 10^3 \,\mathrm{s} \times \left(\frac{m}{10\,\mathrm{TeV}} \right)^{5/3} \left(\frac{T}{10^5\,\mathrm{K}} \right)^{-3} \left(\frac{\sigma}{10^{-43}\,\mathrm{cm^2}} \right)^{-1}. \tag{21}$$

This time is shorter by a factor of a few than the black hole evaporation time of (13). Note, however, the strong dependence of both quantities on the WIMP mass m. Already for masses $m > 13$ TeV the black hole evaporation time becomes shorter. The cooling time derived above refers to the formation of the first black hole. Subsequent black holes require progressively longer times. This is easily seen from (20) because $t_{\rm cool}$ scales as $1/M^{5/3}$ (recall that r_0 scales as $M^{1/3}$ from (15)). Thus, the more the black holes have formed and evaporated, the smaller is the remaining WIMP mass M and the longer the time needed to form the next one.

3. Conclusions

We reviewed the current status of constraints on non-self-interacting asymmetric bosonic dark matter based on observations of old neutron stars. We showed that severe constraints can be imposed for these candidates from the keV to the GeV range, excluding all candidates with WIMP-nucleon cross sections like the ones favorited by the DAMA experiment within this mass range. We also reviewed the arguments why these constraints cannot be extended to candidates with masses in the TeV range or higher.

References

[1] C. Kouvaris, "WIMP annihilation and cooling of neutron stars," *Physical Review D*, vol. 77, no. 2, Article ID 023006, 9 pages, 2008.

[2] G. Bertone and M. Fairbairn, "Compact stars as dark matter probes," *Physical Review D*, vol. 77, no. 4, Article ID 043515, 9 pages, 2008.

[3] C. Kouvaris and P. Tinyakov, "Can neutron stars constrain dark matter?" *Physical Review D*, vol. 82, no. 6, Article ID 063531, 2010.

[4] A. de Lavallaz and M. Fairbairn, "Neutron stars as dark matter probes," *Physical Review D*, vol. 81, no. 12, Article ID 123521, 10 pages, 2010.

[5] I. Goldman and S. Nussinov, "Weakly interacting massive particles and neutron stars," *Physical Review D*, vol. 40, no. 10, pp. 3221–3230, 1989.

[6] C. Kouvaris and P. Tinyakov, "Excluding light asymmetric bosonic dark matter," *Physical Review Letters*, vol. 107, no. 9, Article ID 091301, 4 pages, 2011.

[7] S. D. McDermott, H. B. Yu, and K. M. Zurek, "Constraints on scalar asymmetric dark matter from black hole formation in neutron stars," *Physical Review D*, vol. 85, no. 2, Article ID 023519, 12 pages, 2012.

[8] C. Kouvaris, "Limits on self-interacting dark matter from neutron stars," *Physical Review Letters*, vol. 108, no. 19, Article ID 191301, 5 pages, 2012.

[9] T. Guver, A. E. Erkoca, M. H. Reno, and I. Sarcevic, "On the capture ofdark matter by neutron stars," http://arxiv.org/abs/1201.2400.

[10] Y. Z. Fan, R. Z. Yang, and J. Chang, "Constraining asymmetric bosonic non-interacting dark matter with neutron stars," http://arxiv.org/abs/1204.2564.

[11] N. F. Bell, A. Melatos, and K. Petraki, "Realistic neutron star constraints on bosonic asymmetric dark matter," *Physical Review D*, vol. 87, no. 12, Article ID 123507, 15 pages, 2013.

[12] A. O. Jamison, "Effects of gravitational confinement on bosonic asymmetric dark matter in stars," *Physical Review D*, vol. 88, no. 3, Article ID 035004, 2 pages, 2013.

[13] K. Petraki and R. R. Volkas, "Review of asymmetric dark matter," *International Journal of Modern Physics A*, vol. 28, no. 19, Article ID 1330028, 66 pages, 2013.

[14] K. M. Zurek, "Asymmetric dark matter: theories, signatures, and constraints," http://arxiv.org/abs/1308.0338.

[15] I. Lopes and J. Silk, "Solar constraints on asymmetric dark matter," *The Astrophysical Journal*, vol. 757, no. 2, article 130, 9 pages, 2012.

[16] J. Casanellas and I. Lopes, "First asteroseismic limits on the nature of dark matter," *The Astrophysical Journal*, vol. 765, no. 1, article L21, 5 pages, 2013.

[17] J. Casanellas and I. d. Lopes, "Constraints on asymmetric dark matter from asteroseismology," http://arxiv.org/abs/1307.6519.

[18] C. J. Horowitz, "Dark matter transport properties and rapidly rotating neutron stars," http://arxiv.org/abs/1205.3541.

[19] S. C. Leung, M. C. Chu, L. M. Lin, and K. W. Wong, "Dark-matter admixed white dwarfs," *Physical Review D*, vol. 87, no. 12, Article ID 123506, 8 pages, 2013.

[20] I. Goldman, R. N. Mohapatra, S. Nussinov, D. Rosenbaum, and V. Teplitz, "Possible implications of asymmetric fermionic dark matter for neutron stars," *Physics Letters B*, vol. 725, no. 4-5, pp. 200–207, 2013.

[21] E. W. Mielke and F. E. Schunck, "Boson stars: alternatives to primordial black holes?" *Nuclear Physics B*, vol. 564, no. 1-2, pp. 185–203, 2000.

[22] C. Kouvaris and P. Tinyakov, "(Not)-constraining heavy asymmetric bosonic dark matter," *Physical Review D*, vol. 87, no. 12, Article ID 123537, 5 pages, 2013.

[23] H. T. C. Stoof, "Nucleation of Bose-Einstein condensation," *Physical Review A*, vol. 45, no. 12, pp. 8398–8406, 1992.

[24] B. Ya. Zeldovich and I. D. Novikov, *Relativistic Astrophysics*, vol. 1, The University of Chicago Press, Chicago, Ill, USA, 1972.

Hindawi Publishing Corporation
Advances in High Energy Physics
Volume 2013, Article ID 746894, 13 pages
http://dx.doi.org/10.1155/2013/746894

Research Article

Graviatoms with de Sitter Interior

Irina Dymnikova[1,2] and Michael Fil'chenkov[3]

[1] *Department of Mathematics and Computer Science, University of Warmia and Mazury, Słoneczna 54, 10-710 Olsztyn, Poland*
[2] *A. F. Ioffe Physico-Technical Institute, Politekhnicheskaja 26, St. Petersburg 194021, Russia*
[3] *Institute of Gravitation and Cosmology, Peoples' Friendship University of Russia, 6 Miklukho-Maklay Street, Moscow 117198, Russia*

Correspondence should be addressed to Irina Dymnikova; irina@uwm.edu.pl

Received 25 July 2013; Accepted 18 September 2013

Academic Editor: Maxim Khlopov

We present a graviatom with de Sitter interior as a new candidate to atomic dark matter generically related to a vacuum dark energy through its de Sitter vacuum interior. It is a gravitationally bound quantum system consisting of a nucleus represented by a regular primordial black hole (RPBH), its remnant or gravitational vacuum soliton G-lump, and a charged particle. We estimate probability of formation of RPBHs and G-lumps in the early Universe and evaluate energy spectrum and electromagnetic radiation of graviatom which can in principle bear information about a fundamental symmetry scale responsible for de Sitter interior and serve as its observational signatures.

1. Introduction

Nonluminous atomic dark matter includes a wide range of candidates starting from the historically first mirror dark matter [1–3]. Presented here is graviatom, a gravitationally bound quantum system consisting of a regular black hole or gravitational soliton G-lump and a captured charged particle, which can be formally classified as atomic dark matter with an additional intrinsic dark feature presented by dark energy interior of a certain fundamental scale of de Sitter vacuum. Electromagnetic radiation of a graviatom bearing information on this scale fits in the ultrahigh gamma range and can be regarded as its independent observational signature.

The idea of an atom with a black hole as a nucleus goes back to 1971 when Hawking put forward the idea that primordial charged black holes could capture free charged particle forming neutral and nonrelativistic ultraheavy *black hole atoms* [4]. The minimal mass of a primordial black hole that would not have evaporated entirely by now is $M \sim 5 \times 10^{14}$ g [5]. The term *gravitational atom* was introduced in [6] for gravitationally bound neutral black hole and a charged particle. Similar quantum system called a *hypothesized gravitational atom* was considered in [7] by solving the Schrödinger equation with the Newtonian gravitational potential of a point-like mass modified by the presence of extra compactified dimensions and a captured neutron [7].

Quantum levels in the field of a black hole have been studied in detail starting from 1987 [8–10]. The gravitational analogue of the hydrogen atom orbitals was considered in [11] where the spectrum of normalizable fermion bound states was calculated in the Schwarzschild background. Perturbative modification of electronic orbitals around charged black holes was proposed in [12]. It is clear that a particle undergoing transitions between quantum levels should radiate. However, this question has been much less studied in the literature than the question of quantum spectrum of a black hole.

Quantum radiation of a charged nonrelativistic particle in the Schwarzschild field was first studied in 1990 in [13] with taking into account the DeWitt conservative self-force whose origin is interaction of an electrostatic field of a charged particle with a gravitational field of a source [14]. It was shown that in this case the DeWitt self-force always exceeds the nonconservative radiation damping force; the energy spectrum and intensity of the electric dipole radiation were calculated for the case of black hole with masses ranging from 10^{-5} g to 10^{14} g [13] (see also [15]). The conditions of existence

of a gravitationally bound quantum system with a neutral black hole as a nucleus were formulated in [16, 17] where it was called *graviatom*.

In this paper we study graviatoms with regular black holes with de Sitter interior [18], their remnants [19, 20], and vacuum gravitational solitons G-lumps [19, 21] as nuclei.

Primordial black hole remnants left after the Hawking evaporation have been considered as a source of dark matter for more than two decades [22–29] (for a review see [30–32]). They could also be a source of additional information about the primordial power spectrum [29, 33, 34] and about their effect on big bang nucleosynthesis [29, 35]. However, the question whether some remnants leave after the Hawking evaporation of a singular black hole still remains open. The generalized uncertainty principle requires existence of a black hole remnant as a Planck size black hole [25]. On the other hand, no evident symmetry or quantum number was found which would prevent a complete evaporation [36]. Another question in the case of a singular black hole is how to evaporate a singularity? The complete evaporation would involve a serious and unclear change in spacetime structure which would have to evolve from a singularity to a maximally symmetric Minkowski (or de Sitter) space [37].

These problems do not arise in the case of a regular black hole with de Sitter centre instead of a singularity which leaves behind a thermodynamically stable double-horizon remnant [20] and does not involve a dramatic change in spacetime structure [37].

The idea of de Sitter interior goes back to the heuristic hypothesis that de Sitter vacuum could be a final state in a collapse [38], to the idea of a self-regulatory behavior of space-time geometry at achieving the Planckian densities [39], and to the idea of the existence of the limiting curvature of the Planck scale [40]. Second-order phase transition during evaporation of a black hole with de Sitter interior [19, 20] suggests possibility for a phase transition to de Sitter vacuum in the origin [41].

Arguments in favour of a regular black hole are provided by a loop quantum gravity [42, 43]. The "renormalization group improving" approach based on the running Newton constant, applied to the Schwarzschild spacetime, predicts an appearance of a smooth de Sitter core replacing a singularity [44]. The noncommutative geometry approach (for a review see [45]) applied to the Schwarzschild black hole leads to a regular de Sitter core at short distances from the origin [46]. Appearance of de Sitter core was found also for a cosmological noncommutative black hole of positive mass with the Gaussian density profile [47].

The Einstein equations admit the class of regular spherically symmetric solutions asymptotically de Sitter as $r \to 0$ with $\Lambda = 8\pi G\rho_{\rm int}$, $\rho_{\rm int} = \rho(r \to 0)$ of a certain fundamental scale and at infinity [21, 48, 49]. A source term for this class is specified by $T_0^0 = T_1^1$ and provides a unified model-independent description of dark ingredients in the Universe by a vacuum dark fluid [50, 51]. In this approach a vacuum dark energy is described by a time evolving and spatially inhomogeneous cosmological term [48], while dark matter is represented by compact objects generically related to vacuum dark energy through de Sitter vacuum interior. They include regular black holes [18, 52, 53], their remnants [20], and gravitationally bound vacuum structures without black hole horizon (dark particles or dark stars, dependently on a mass) [19, 21], called G-lumps, since they hold themselves together by their own gravity [21]. For this class a static metric is described by the line element:

$$ds^2 = g(r)\,dt^2 - \frac{dr^2}{g(r)} - r^2 d\Omega^2. \tag{1}$$

In the asymptotically flat case to be studied in this paper, the metric function reads

$$g(r) = 1 - \frac{\mathcal{R}_g(r)}{r}, \quad \mathcal{R}_g(r) = 2G\mathcal{M}(r), \qquad \mathcal{M}(r) = 4\pi \int_0^r \rho(x)\, x^2 dx. \tag{2}$$

A metric function $g(r)$ is asymptotically Schwarzschild at $r \gg r_*$, where $r_* = (r_{\rm int}^2 r_g)^{1/3}$ is the characteristic length of de Sitter-Schwarzschild spacetime [18, 19], $r_g = 2GMc^{-2}$, and $r_{\rm int}$ is characteristic scale for the interior de Sitter vacuum related to its density by $r_{\rm int}^2 = 3c^2/8\pi G\rho_{\rm int}$. (Characteristic length scales essential for graviatom are summarized in the Appendix.) The scale r_* comes as the radius of the direct matching of the de Sitter and Schwarzschild metrics, $g_{\rm deS} = g_{\rm Schw}$; that is, $1 - r_*^2/r_{\rm int}^2 = 1 - r_g/r_*$ [39]. It is also the scale at which the scalar curvature R changes sign [19]. The mass $M = 4\pi \int_0^\infty \rho(r) r^2\, dr$ is related to interior de Sitter vacuum and to breaking of spacetime symmetry from the de Sitter group at $r = 0$ [21, 54, 55].

Regular black hole with de Sitter centre has two horizons [19, 21] which coalesce in the course of evaporation at a certain mass $M_{\rm cr}$ corresponding to a thermodynamically stable double-horizon remnant [19–21, 46, 56, 57]. For $M < M_{\rm cr}$, the metric (1)-(2) describe G-lumps. The typical behaviour of the metric function [21] is shown in Figure 1.

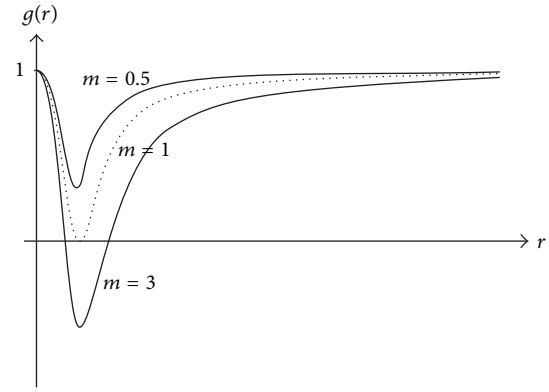

Figure 1: The metric function $g(r)$ for de Sitter-Schwarzschild spacetime; $m = M/M_{\rm crit}$.

Primordial black holes can be formed by various mechanisms (for a review see [35, 58]). Most general possibility involves primordial density inhomogeneities forming overdense regions which can stop expanding and collapse [4, 59].

The particular origin of inhomogeneities can be quantum fluctuations arising in various inflationary scenarios [35]. PBH formation would be enhanced if inflation is followed by a dust-like stage dominated by nonrelativistic particles [58]. This point is of special interest in the context of graviatoms. As we will see below, the case of graviatom with RPBH remnant or G-lump and captured GUT particles, $M \sim 10^{14}$ – 10^{16} GeV, which are considered as superheavy dark matter, is the most promising [60–64].

In the literature two mechanisms of producing such particles have been considered. One is gravitational production towards the end of inflation [60–62, 65, 66]. The other is decay of the inflationary de Sitter vacuum during symmetry-breaking phase transitions at the GUT scale: statistical mechanics approach with model-independent description of cosmological background shows that appearance of GUT particles from the GUT scale de Sitter vacuum looks like evaporation of Bose-condensate: particles satisfy the equation of state of an ideal quantum degenerate Bose gas with the Gibbons-Hawking temperature related to the de Sitter Horizon [67–71]. GUT particles could be captured by RPBH remnants or G-lumps and survive to the present epoch as constituents of graviatoms.

The main goal of this paper is to study typical features of graviatoms radiation which could result in their observational signatures as dark matter candidates.

In Section 2 we estimate the probability of formation of a RPBH and G-lump in a quantum collapse of a primordial fluctuation. In Section 3 we introduce the Schrödinger equation for graviatom and study typical behaviour of its potential. Section 4 is devoted to quantum spectra and mechanisms of graviatom radiation. In Section 5 we summarize the results.

2. Formation of the Regular Primordial Black Holes and G-Lumps with de Sitter Interior

In the classical approach geometry of a collapsing body in the comoving coordinates can be presented by the FRW spacetime with the positive curvature [72]. In quantum cosmology the wave function is defined on a superspace which is the space of all 3-dimensional geometries $g_{ij}(\vec{x})$ and matter field configuration $\varphi_m(\vec{x})$, $\Psi = \Psi[g_{ij}(\vec{x}), \varphi_m(\vec{x})]$. It satisfies the Wheeler-DeWitt equation $\widehat{H}\Psi = 0$. In the case of the FRW cosmology with the only dynamical variable, the scale factor $a(t)$, the Wheeler-DeWitt equation reduces to the simple case called minisuperspace model. For the Friedmann closed model it reads [73]

$$\frac{d^2\Psi}{da^2} - V(a)\,\Psi = 0, \tag{3}$$

where

$$V(a) = \frac{1}{l_{pl}^4}\left(ka^2 - \frac{8\pi G}{3c^4}\varepsilon a^4\right), \quad k = 1. \tag{4}$$

In general case a collapsing quantum fluctuation can be described as a superposition of partial energy densities of possible matter contributions [74]:

$$\varepsilon = \varepsilon_{pl}\sum_{0}^{6} A_n\left(\frac{l_{pl}}{a}\right)^n. \tag{5}$$

The parameter n is related to the parameter w in the equation of state $p = w\varepsilon$, as $n = 3(1 + w)$. Contributions to density (5) include an inflationary vacuum ($n = 0$), ensembles of domain walls ($n = 1$) and strings ($n = 2$), nonrelativistic matter (dust with $n = 3$), ultrarelativistic gas ($n = 4$), perfect gas ($n = 5$), and ultrastiff matter ($n = 6$).

The Wheeler-DeWitt equation (3) reduces to

$$-\frac{\hbar^2}{2m_{pl}}\frac{d^2\Psi}{da^2} + (U(a) - E)\,\Psi = 0, \tag{6}$$

where the potential $U(a)$ expressed in terms of the dimensionless variable $\gamma \equiv a/l_{pl}$ has the form [75]

$$U(\gamma) = \frac{E_{pl}}{2}\left(k\gamma^2 - B_0\gamma^4 - B_1\gamma^3 - B_2\gamma^2 - B_3\gamma - \frac{B_5}{\gamma} - \frac{B_6}{\gamma^2}\right). \tag{7}$$

Energy of a fluctuation in (6) is

$$E = \frac{E_{pl}}{2}B_4. \tag{8}$$

Coefficients B_n are related to the coefficients A_n in (5) by $B_n = (8\pi G/3c^2)A_n$.

To model a collapse to a compact object with the de Sitter interior, we modify the potential (7) by introducing a cutoff related to characteristic scale for an interior de Sitter vacuum γ_{int} in the terms of the negative powers of γ corresponding to high density contributions to (5), in accordance with the underlying hypothesis [38–40] that transition to interior de Sitter vacuum may occur at achieving a certain high density during contraction. Modified potential has the form

$$U(\gamma) = \frac{E_{pl}}{2}\left(k\gamma^2 - B_0\gamma^4 - B_1\gamma^3 - B_2\gamma^2 - B_3\gamma - \frac{B_5}{(\gamma - \gamma_{\text{int}})} - \frac{B_6}{(\gamma - \gamma_{\text{int}})^2}\right). \tag{9}$$

The potential (9) tends to minus infinity for $\gamma \to \infty$ and $\gamma \to \gamma_{\text{int}}$. Near $\gamma > \gamma_{\text{int}}$, the potential (9) has a maximum $U_m > 0$, and the process of a quantum collapse involves tunnelling through the potential barrier.

For big values of the variable γ, in the limit $\gamma \gg |B_4|^{1/4}$, the Schrödinger equation (6) reduces to

$$\frac{d^2\Psi}{d\gamma^2} + B_0\gamma^4\Psi = 0, \tag{10}$$

which has the solution [76]:

$$\Psi = \sqrt{\gamma}Z_{1/6}\left(\frac{\sqrt{B_0}}{3}\gamma^3\right), \tag{11}$$

with the asymptotics [75]:

$$\Psi = C_1 \exp\left(\frac{iB_0\gamma^3}{3}\right) + C_2 \exp\left(-\frac{iB_0\gamma^3}{3}\right). \quad (12)$$

Choosing integration constant proper for a collapse, we get the WKB wave function corresponding to deflation. Indeed, in the limits $B_0\gamma^4 \gg B_4$ and $\gamma \gg \gamma_{\text{int}}$, the action $S = \int L\,da \propto \pm a^3$, where $L = (da/d\eta)^2 + H^2a^4/c^2 - ka^2$, $ad\eta = cdt$, and $H = \pm\dot{a}/a$ [75]. The classical solutions are $a \propto e^{Ht}$ (inflation) and $a \propto e^{-Ht}$ (deflation).

For γ very close to γ_{int}, $0 < \gamma - \gamma_{\text{int}} \ll \sqrt{B_6/B_4}$, the Schrödinger equation takes the form

$$\frac{d^2\Psi}{d\gamma^2} + \frac{B_6}{(\gamma-\gamma_{\text{int}})^2}\Psi = 0. \quad (13)$$

Its solution, satisfying the boundary condition $\Psi(\gamma_{\text{int}}) = 0$, is given by

$$\Psi = \sqrt{\gamma-\gamma_{\text{int}}}\left(C_1(\gamma-\gamma_{\text{int}})^b + C_2(\gamma-\gamma_{\text{int}})^{-b}\right), \quad b^2 = \frac{1}{4} - B_6 > 0. \quad (14)$$

After tunnelling through the barrier, a collapsing object appears in the potential well. In this region, for $\gamma - \gamma_{\text{int}} \ll 1$ the Schrödinger equation (6) reduces to [75]

$$\frac{d^2\Psi}{d\gamma^2} + \left(B_0\gamma_{\text{int}}^4 + \frac{B_5}{(\gamma-\gamma_{\text{int}})} + \frac{B_6}{(\gamma-\gamma_{\text{int}})^2} + \frac{2E}{E_{pl}}\right)\Psi = 0, \quad (15)$$

whose solution, satisfying the boundary condition $\Psi(\gamma_{\text{int}}) = 0$, reads

$$\Psi = C\rho^{s+1}e^{-\rho/2}F\left(-p, 2s+2, \rho\right), \quad (16)$$

where $F(-p, 2s+2, \rho)$ is the degenerate hypergeometric function, $s = -(1/2) + \sqrt{(1/4) - B_6}$, $\rho = 2(\gamma - \gamma_{\text{int}})\sqrt{-B_0\gamma_{\text{int}}^4 - 2E/E_{pl}}$, $p = n - s - 1$, $n = B_5/\sqrt{-B_0\gamma_{\text{int}}^4 - 2E/E_{pl}}$, and $p = 0, 1, 2, \ldots$.

The energy spectrum is given by

$$E_p = -\frac{B_5^2}{8\left(p + 1/2 + \sqrt{1/4 - B_6}\right)^2}E_{pl} - \frac{1}{2}B_0\gamma_{\text{int}}^4E_{pl}. \quad (17)$$

The discrete spectrum does exist only if the following condition is satisfied:

$$\frac{2|E|}{E_{pl}} = |B_4| \geq B_0\gamma_{\text{int}}^4. \quad (18)$$

This allows one to estimate the probability of tunnelling through the barrier and range of masses M of a collapsing object. The tunnelling probability is determined by the WKB penetration factor:

$$D = \exp\left(-\frac{2l_{pl}}{\hbar}\int_{\gamma_1}^{\gamma_2}\sqrt{2m_{pl}(U-E)}\,d\gamma\right) = \exp(-2\Gamma), \quad (19)$$

where $\gamma_1 \approx (|B_4|/B_0)^{1/4}$, $\gamma_2 \approx \gamma_{\text{int}} + \sqrt{B_6/(|B_4| - B_0\gamma_{\text{int}}^4)}$, and $\gamma_2 < \gamma_1$.

The factor Γ is estimated as $\Gamma < 2|B_4|^{3/4}B_0^{-1/4}$, which gives $D > \exp(-4|B_4|^{3/4}B_0^{-1/4})$.

The Schrödinger equation (6) describes the planckeon on the energy level given by (17); $E = -(|B_4|/2)E_{pl}$. Its total energy includes the rest mass, $Mc^2 + E = E_{pl}$, so the mass of an object is given by $M/m_{pl} = 1 + |B_4|/2$. Taking into account $|B_4| < M/m_{pl}$ and $B_0 = \varepsilon_0/\varepsilon_{pl} = (E_0/E_{pl})^4$, we estimate the probability of the tunnelling for the compact object with the mass M:

$$D > \exp\left[-4\left(\frac{M}{m_{pl}}\right)^{3/4}\left(\frac{E_{pl}}{E_0}\right)\right]. \quad (20)$$

It seems for the first sight that smaller objects collapse with bigger probability. However, this estimate does not involve the scale for de Sitter interior E_{int}. General constraint on the mass involving E_{int} is obtained from (18). It gives $M/m_{pl} > |B_4| > B_0\gamma_{\text{int}}^4$ where $\gamma_{\text{int}} = r_{\text{int}}/l_{pl} = (E_{pl}/E_{\text{int}})^2$. Ultimately we get

$$\frac{M}{m_{pl}} > \left(\frac{E_0}{E_{pl}}\right)^4\left(\frac{E_{pl}}{E_{\text{int}}}\right)^8. \quad (21)$$

As we see, possibilities of formation of compact objects with the de Sitter interior depend on the scales of the interior vacuum E_{int} and of the inflationary vacuum E_0. The scale of inflationary vacuum can be adopted as the GUT scale $E_0 \simeq 10^{15}$ GeV. In the frame of the hypothesis of arising of interior de Sitter vacuum due to the phase transition at the GUT scale [41], constraint on the mass is $M > 10^{11}$ g. In this case only regular primordial black holes can be formed in a collapse of primordial fluctuations. In the frame of hypothesis of self-regulation of geometry near the Planck scale [39] or existence of limiting curvature of the Planck scale [40], mass range for collapsing objects admits G-lumps and RPBH including those with masses sufficiently small to evaporate and produce remnants to the end of inflation. Objects with small masses are produced with the bigger probability (20).

One more possibility for a wide range of masses is related to production of compact objects with de Sitter interior during later stages of the early Universe. The standard model of particle physics predicts a phase transition at the QCD scale of 100–200 MeV (see [77] and references therein) which can lead to a second inflationary stage with duration of about 7–10 e-foldings [78–80]. In this case the formation constraint (21) admits any mass.

We conclude that regular primordial black holes, their remnants, and G-lumps can arise in the early Universe during first and second inflationary stages, so that they can capture available particles and form graviatoms.

3. The Schrödinger Equation for Graviatom and Conditions of Its Existence

The problem of a motion of a nonrelativistic charged particle in a curved spherically symmetric spacetime reduces to the Schrödinger equation [81]:

$$-\frac{\hbar^2}{2m}\Delta\psi + U(r)\psi = E\psi, \tag{22}$$

where m is the mass of a particle. The potential $U(r)$ includes contribution of gravity and of the DeWitt conservative self-force acting on a charged particle with the mass m and the charge q. It is given by [14]

$$f_s = mc^2\frac{r_q r_g}{2r^3}, \tag{23}$$

and directed outward the field centre. Here $r_q = q^2/mc^2$ is a classical electromagnetic radius of a particle. In a weak gravitational field the conservative self-force f_s always exceeds the nonconservative radiation damping force $f_r = 2q^2\ddot{v}/3c^3$, where v is the particle velocity [13]. In this approximation the gravitational part of the potential is given by $m\varphi(r) = (mc^2/2)[g_{tt}(r) - 1]$. For a metric of the class (1) the gravitational potential reads $m\varphi = -(mc^2/2)(\mathscr{R}_g(r)/r)$.

This approach corresponds to the Pauli approximation to the Dirac equation [16, 17]. As we will see below, characteristic orbits of particles in the field of graviatom are in most cases located far from the characteristic Schwarzschild-de Sitter radius $r_* = (r_{\text{int}}^2 r_g)^{1/3}$ which justifies application of the Pauli approximation for analysis of basic properties of graviatom. In what follows we will consider the range of frequencies $\hbar\omega < mc^2$ relevant for this approximation.

With taking into account the DeWitt self-force we have for the potential

$$U(r) = \frac{mc^2}{2}\left(-\frac{\mathscr{R}_g(r)}{r} + \frac{r_g r_q}{2r^2}\right). \tag{24}$$

The behaviour of the potential (24) is determined by typical behaviour of the metric function $g(r)$: in the asymptotically flat case it has not more than two zeros, one maximum at $r = 0$ where $g(r) = 1$ and one minimum [21]. This follows directly from the Einstein equation for the metric (1) which reads

$$g'' + \frac{2g'}{r} = 16\pi G p_\perp. \tag{25}$$

The pressures are given by

$$p_r = -\rho, \qquad p_\perp = -\rho - \frac{r}{2}\rho'. \tag{26}$$

For the solutions satisfying the weak energy condition (nonnegative density for an observer on a timelike curve), $\rho' \le 0$ [21]. In the extremum of the metric function, $g' = 0$, and the type of extremum is determined by the sign of the tangential pressure $p_\perp$. In the asymptotically flat spacetime with de Sitter centre there is one scale of a vacuum energy, $p_r = p_\perp = -\rho_{\text{int}}$ at $r = 0$, and at this point $g(r)$ has a maximum. The next extremum is a minimum [21], in the region where $p_\perp$ is already positive (since $g'' > 0$ and $g' = 0$ there). In an extremum of the potential (24) the condition $U'(r_m) = 0$ gives

$$g'(r_m) = \frac{r_g r_q}{r_m^3}. \tag{27}$$

It follows that $U(r)$ has an extremum in the region where $g'(r) > 0$ and the metric function is growing. In particular, the extremum of $U(r)$ is always outside the double horizon on which $g' = 0$. The second derivative is given by, with taking into account (25) and (27),

$$U'' = \frac{mc^2}{2}\left(g'' + \frac{3r_g r_q}{r^4}\right) = 16\pi G p_\perp + \frac{g'(r_m)}{r_m}. \tag{28}$$

According to (27), $g' > 0$ at the extremum of $U(r)$, and also $p_\perp > 0$ there; hence, the second derivative of the potential $U(r)$ is always positive in its extremum and the potential $U(r)$ can thus have only one minimum. For $r \to 0$, the potential $U(r)$ goes to infinity. For $r \to \infty$, the metric function $g(r)$ goes asymptotically to the Schwarzschild metric, so that the potential for $r \to \infty$ goes to

$$U(r) \longrightarrow \frac{mc^2}{2}\left(-\frac{r_g}{r} + \frac{r_g r_q}{2r^2}\right), \tag{29}$$

and therefore $U(r) \to -0$ as $r \to \infty$. The only minimum, $U(r_m)$, is thus always negative.

The radial wave function $R(r)$ in (22) satisfies the equation

$$\frac{1}{r^2}\frac{d}{dr}\left(r^2\left(\frac{dR}{dr}\right)\right) - \frac{l(l+1)}{r^2}R + \frac{2m}{\hbar^2}(E - U(r))R = 0. \tag{30}$$

The potential $U(r)$ can be presented as

$$U(r) = -\frac{GMmc^2}{r}\left(1 - f_g(r)\right) + \frac{mc^2}{2}\frac{r_q r_g}{2r^2},$$
$$f_g(r) = \frac{8\pi G}{r_g c^2}\int_r^\infty \rho(x)\, x^2 dx < 1. \tag{31}$$

Equation (30) describes a captured particle in the effective potential:

$$U_{\text{eff}} = -\frac{GMmc^2}{r}\left(1 - f_g(r)\right) + \frac{mc^2}{2}\frac{r_q r_g}{2r^2} + \frac{\hbar^2 l(l+1)}{2mr^2}. \tag{32}$$

In the Schwarzschild limit,

$$U_{\text{eff}} = -\frac{GMmc^2}{r} + \frac{mc^2}{2}\frac{r_q r_g}{2r^2} + \frac{\hbar^2 l(l+1)}{2mr^2}. \tag{33}$$

In this limit we see clearly that in the case of a graviatom the fine structure constant is replaced with the effective gravitational fine structure constant [13]:

$$\alpha_G = \frac{GMm}{\hbar c}. \tag{34}$$

The corresponding Bohr radius for the graviatom with the potential (33) is given by [16, 17]

$$r_b = \frac{\hbar^2}{GMm^2} = \frac{2\lambda\!\!\!^{-2}}{r_g}, \tag{35}$$

where $\lambda\!\!\!^{-} = \hbar/mc$ is the Compton wavelength of a captured particle.

The condition $r_g < r_b$ (the Bohr orbit in the R-region outside the horizon) gives

$$r_g < r_b \longrightarrow r_g^2 < 2\lambda\!\!\!^{-2}. \tag{36}$$

Equation (36) gives the constraint on the mass of the graviatom nucleus:

$$M < 2 \times 10^{17} \left(\frac{m_e}{m}\right) \text{grams}, \tag{37}$$

where m_e is the mass of the electron.

The main condition for the existence of a graviatom is the geometrical condition:

$$L > r_n + r_p. \tag{38}$$

Here L is the characteristic size of a graviatom, r_n is the size of its nucleus, and r_p of a captured particle. For a hydrogen-like graviatom, it reads $r_b > r_n + \lambda\!\!\!^{-}$.

For the metric function (2), the black hole horizon, $r_+ = 2G\mathcal{M}(r_+)$, satisfies $r_+ < r_g$ since, for any density profile satisfying the weak energy condition $\rho'(r) \leq 0$, $\mathcal{M}(r)$ is monotonically growing, and $\mathcal{M}(r_+) < M$. The restriction following from $r_g < r_b$ will also hold for r_+ to guarantee $r_b > r_+$, so we can take $r_n = r_g$. The condition (38) in this case, $r_b > r_g + \lambda\!\!\!^{-}$, with taking into account (35), gives $r_g^2 + r_g\lambda\!\!\!^{-} - 2\lambda\!\!\!^{-2} = (r_g - \lambda\!\!\!^{-})(r_g + 2\lambda\!\!\!^{-}) < 0$ which follows in the constraint:

$$r_g < \lambda\!\!\!^{-}. \tag{39}$$

Fulfillment of the conditions (39) guarantees fulfillment of the constraint (36).

In the case of G-lump, its characteristic size is of the order of r_* [19, 21], and the condition of the existence of the hydrogen-like graviatom reads

$$r_b > r_* + \lambda\!\!\!^{-}. \tag{40}$$

Introducing the dimensionless quantities $x_g = r_g/r_{\text{int}}$ and $\eta = \lambda\!\!\!^{-}/r_{\text{int}}$, we get the inequality $x_g^{4/3} + \eta x_g - 2\eta^2 < 0$. With the new variable $x = x_g^{1/3}$, it reduces to $x^4 + \eta x^3 - 2\eta = (x - x_1)(x - x_2)(x - x_3)(x - x_4) < 0$. This is the 4th order polynomial; complex conjugate roots come in pairs and make this polynomial positive, so that it can be negative only if real roots exist. The condition of their existence, $\eta \geq 0.124$, results in the following constraint:

$$\lambda\!\!\!^{-} > 0.124 r_{\text{int}}. \tag{41}$$

This is the important constraint; only when (41) is satisfied, the geometric condition (40) holds. In this case the above polynomial has three negative and one positive root. The only possibility to satisfy (40) results in the second constraint:

$$r_g < 1.66\lambda\!\!\!^{-}. \tag{42}$$

With these two constraints we estimate

$$\frac{r_b}{r_*} > 1.21. \tag{43}$$

For further analysis we adopt some slowly falling density profile $\rho(r)$ which should vanish for large r faster than r^{-3} to guarantee finiteness of the mass M [21]. If we choose $\rho(r) = \rho_{\text{int}}(r_{\text{int}}/r)^4$, we obtain

$$f_g(r) = \frac{3r_{\text{int}}^2}{r_g r}. \tag{44}$$

The requirement for the Bohr orbit (35) to be outside the horizon, $r_\pm < r_g < r_b$, results in

$$f_g(r_b) < f_g(r_g), \quad \frac{3r_{\text{int}}^2}{2\lambda\!\!\!^{-2}} < f_g(r_g) < \frac{3r_{\text{int}}^2}{r_\pm^2}, \tag{45}$$

where $r_\pm$ is the double horizon radius. It is calculated from $g(r_\pm) = 0$, $g'(r_\pm) = 0$ which gives

$$r_\pm = 2G\mathcal{M}(r_\pm), \qquad r_\pm^2 = \frac{c^2}{8\pi G\rho(r_\pm)}. \tag{46}$$

The first inequality in (45) gives, with taking into account (31), the constraint

$$\frac{3}{2}\left(\frac{l_{pl}}{\lambda\!\!\!^{-}_e}\right)^2\left(\frac{E_{pl}}{E_{\text{int}}}\right)^4\left(\frac{m}{m_e}\right)^2 < f_g(r_g), \tag{47}$$

where m_e is the mass of the electron and $\lambda\!\!\!^{-}_e$ is its Compton wavelength.

For the GUT scale interior $E_{\text{int}} \simeq 10^{15}$ GeV, this gives for the mass of the captured particle $m < 10^{11}$ GeV and for the Planck scale interior $m < m_{pl}$.

The second inequality in (45) gives, with taking into account (46), the constraint

$$f_g(r_g) < 9\frac{\rho_\pm}{\rho_{\text{int}}} = \frac{9c^2}{32\pi G^3\mathcal{M}^2(r_\pm)} < 1. \tag{48}$$

It follows that the more the mass contained under the double horizon is, the better graviatom with a regular black hole can be approximated by the Schwarzschild potential (33). It suggests also that more quickly falling density profile would be more favorable for the existence of the Bohr orbits in the R-region outside the horizon.

For detailed estimates we adopt the density profile [18]:

$$\begin{aligned} &\rho(r) = \rho_{\text{int}} e^{-r^3/r_*^3}, \quad r_* = \sqrt[3]{r_{\text{int}}^2 r_g}, \\ &r_{\text{int}}^2 = \frac{3}{8\pi G\rho_{\text{int}}}, \quad \rho_{\text{int}} = \rho(r \longrightarrow 0), \end{aligned} \tag{49}$$

which describes vacuum polarization effects leading to de Sitter interior [39] in the semiclassical model for vacuum polarization in the gravitational field [19]. The metric function is given by

$$g(r) = 1 - \frac{r_g}{r}\left(1 - \exp\left(-\frac{r^3}{r_*^3}\right)\right). \quad (50)$$

A black hole exists for $r_g \geq r_{g(\mathrm{cr})} = 1.7576 r_{\mathrm{int}}$ [19]. The boundary value corresponds to the mass $M_{\mathrm{cr}} \simeq 10^3 (E_{\mathrm{GUT}}/E_{\mathrm{int}})^2$ g. With using (50) we get for the horizon r_+

$$\frac{r_g}{r_+}\left(1 - \exp\left(-\frac{r_+^3}{r_*^3}\right)\right) = 1. \quad (51)$$

The most essential difference between a graviatom and the hydrogen atom is that, in the graviatom, due to the presence of the DeWitt force and modification of the Coulomb-like part of the potential, the effective potential has the minimum. This leads to an appearance of oscillatory spectrum and radiation from oscillatory levels.

With the density profile (49) the effective potential (32) takes the form

$$U_{\mathrm{eff}} = -\frac{GMmc^2}{r}\left(1 - \exp\left(-\frac{r^3}{r_*^3}\right)\right) + \frac{mc^2 r_g r_q}{4r^2} + \frac{\hbar^2 l(l+1)}{2mr^2}. \quad (52)$$

The condition for a minimum of the function (52), $U'(r_m) = 0$, gives the relation

$$e^{-x} = \left(1 - \frac{\widetilde{r}_q}{r_* \sqrt[3]{x}}\right)(1+3x)^{-1}, \quad (53)$$

where $x = r_m^3/r_*^3$ and

$$\widetilde{r}_q = r_q + \frac{2\lambda\!\!\!^{-2}}{r_g} l(l+1). \quad (54)$$

Equation (53) can be written as

$$\frac{\widetilde{r}_q}{r_*} = \left[1 - (1+3x)\, e^{-x}\right] \sqrt[3]{x}. \quad (55)$$

For $\widetilde{r}_q/r_* \gg 1$ we have $\sqrt[3]{x} = r_q/\sqrt[3]{r_{\mathrm{int}}^2 r_g}$ and $r_m = \widetilde{r}_q$. For $r_q r_g \gg 2\lambda\!\!\!^{-2}$, $\widetilde{r}_q = r_q$, oscillatory levels are determined by the effective classical electromagnetic radius r_q, and the second term in (54) would provide quantum corrections to oscillatory levels.

For $\widetilde{r}_q/r_* \ll 1$ we have $x = 1.9$ and

$$r_m = \sqrt[3]{1.9 r_{\mathrm{int}}^2 r_g}. \quad (56)$$

This is the most promising case since quantum radiation which we present in the next section carries information about de Sitter interior of the graviatom nucleus.

In the general case the position of the minimum r_m is determined by the interpolation formula:

$$r_m = \widetilde{r}_q\left(1 - \exp\left(-\frac{\widetilde{r}_q}{\sqrt[3]{1.9 r_{\mathrm{int}}^2 r_g}}\right)\right)^{-1}. \quad (57)$$

The hydrogen-like radiation dominates when the effect of the DeWitt contribution is less that of the Coulomb-like term in (33), $r_g r_q \ll \lambda\!\!\!^{-2}$. Radiation from the oscillatory levels dominates in the opposite case, $r_g r_q \gg \lambda\!\!\!^{-2}$.

4. Graviatom Radiation

4.1. Hydrogen-Like Spectrum and Radiation. The constraint (38) leads, with taking (35) into account, to $r_b^3/r_*^3 > 8 r_g^2/r_{\mathrm{int}}^2$.

For the density profile (49) $8 r_{g(\mathrm{cr})}^2/r_{\mathrm{int}}^2 \simeq 24.7 (E_{\mathrm{int}}/E_{\mathrm{GUT}})^4$; as a result $f_g(r_b) \ll 1$ for the graviatom with a regular black hole and its remnant, and spectrum of radiation can be approximated with the high accuracy by that for the Schwarzschild potential.

In this case the energy spectrum is given by [16, 17]

$$E = -2\alpha_G^2 mc^2 \frac{1}{\left[2p + 1 + \sqrt{(2l+1)^2 + \dfrac{8mA}{\hbar^2}}\right]^2}, \quad (58)$$

where

$$A = \frac{mc^2 r_q r_g}{4}, \qquad p = n - s - 1, \qquad s(s+1) = \frac{2mA}{\hbar^2} + l(l+1), \quad (59)$$

$p = 0, 1, 2, \ldots$, $l \leq n$, $n = 1, 2, 3, \ldots$. Here n and l are the principal and orbital quantum numbers, respectively. This is general formula including both the Bohr levels and oscillatory levels.

The radiation from transitions between the Bohr levels dominates when $8mA/\hbar^2 \ll (2l+1)^2$. The condition of its domination,

$$\left(l + \frac{1}{2}\right)^2 \lambda\!\!\!^{-2} \gg r_g r_q, \quad (60)$$

gives the constraint $M \ll 3 \times 10^{19} (m_e/m)$ g.

In the case of a black hole, the requirement $r_g \geq r_{g(\mathrm{cr})}$ ($M \geq M_{\mathrm{cr}}$) results in the estimate:

$$r_b^3 > 8 r_{g(\mathrm{cr})}^2 r_g. \quad (61)$$

In the limit (60) the energy spectrum reduces to

$$E_B = -\frac{mc^2}{2n^2}\alpha_G^2. \quad (62)$$

In this case we have the dipole electromagnetic radiation of graviatom (dominating for the Bohr levels) similar to that

for a hydrogen-like atom. Frequencies for the transitions $2p \to 1s$ and $3p \to 1s$ are given by

$$\hbar\omega_{21} = \frac{3}{8}\alpha_G^2 mc^2, \qquad \hbar\omega_{31} = \frac{4}{9}\alpha_G^2 mc^2, \tag{63}$$

and intensities are related by $I_{21}/I_{31} = 3.161$ [16, 17].

For the case of a black hole there is the natural stability condition [16, 17]: $\tau_{gr} < \tau_H$ and $\tau_{gr} < \tau_p$ where τ_{gr} is the graviatom lifetime, τ_H is the black hole lifetime, and τ_p is the particle lifetime. The condition of indestructibility, $E_d < E_b$, where E_d is the destructive energy (due to tidal forces, the Hawking radiation and "ionization"-eventual removing of a charged captured particle) and E_b is the binding energy, was thoroughly studied in [16, 17]. For the case of the hydrogen-like graviatom with the Schwarzschild potential ($f(g) \ll 1$), conditions of stability and indestructibility constrain the gravitational fine structure constant within the narrow range [16, 17] $0.512 < \alpha_G < 0.625$. For this range of the coupling α_G the applied Pauli approximation holds for the frequencies of the hydrogen-like radiation (63).

In the case of G-lump the estimate (43) restricts the correction to the potential for the density profile (49),

$$f_g(r_b) = \exp\left(-\frac{r_b^3}{r_*^3}\right) < 0.17. \tag{64}$$

However, we cannot approximate the radiation spectrum by that for the Schwarzschild case with this accuracy since the energy is proportional to α_G^2 and thus to M^2.

In the case of G-lump we should have to solve a separate problem with the potential (32). Preliminary consideration can be made by replacing the mass M in (62) with $M(1 - \exp(-r^3/r_*^3))$. The rough estimate with

$$\begin{aligned} E_B &= -\frac{mc^2}{2n^2}\alpha_G^2\left(1 - 2\exp\left(-\frac{r_b^3}{r_*^3}\right)\right) \\ &= -\frac{mc^2}{2n^2}\alpha_G^2\left(1 - 2\exp\left[\left(-\frac{r_b^3}{r_g}\right)\left(\frac{8\pi G\rho_{\text{int}}}{3}\right)\right]\right) \end{aligned} \tag{65}$$

gives the correction of the order of 0.34. This estimate is relevant also for a remnant since its characteristic size, $r_\pm = 1.414 r_{\text{int}}$, is close to $r_* = 1.207 r_{\text{int}}$. This allows us to conclude that radiation from the Bohr levels in the case of G-lump and remnant will depend on the density of the interior de Sitter vacuum ρ_{int} and would result in observational signatures for them as dark matter candidates.

4.2. Oscillatory Spectrum and Radiation. In the case when

$$\left(l + \frac{1}{2}\right)^2 \lambda\!\!\!^{-2} \ll r_g r_q, \tag{66}$$

the DeWitt force is dominating, and we deal with an oscillatory spectrum and radiation.

Near the minimum, the potential reduces to

$$U_{\text{eff}}(r) \simeq U_{\text{eff}}(r_m) + \frac{1}{2}\frac{d^2 U_{\text{eff}}}{dr^2}\Big|_{r=r_m}(r - r_m)^2. \tag{67}$$

Introducing in (30) with the effective potential (67) the new variables

$$\chi(r) = R(r)\, r, \qquad y = r - r_m, \tag{68}$$

we obtain the equation of a harmonic oscillator in one dimension:

$$\frac{d^2\chi}{dy^2} + \frac{2m}{\hbar^2}\left(E - \frac{m\omega^2 y^2}{2}\right)\chi = 0, \tag{69}$$

The energy spectrum is given by

$$\begin{aligned} E_p &= -U(r_m) + \hbar\omega\left(p + \frac{1}{2}\right), \\ p &= 0, 1, 2, \ldots; \quad \omega = \sqrt{\frac{1}{m}\frac{d^2U}{dr^2}\Big|_{r=r_m}}. \end{aligned} \tag{70}$$

The wave function being a solution to (69) has the form [82]:

$$\chi_n(y) = \left(\frac{m\omega}{\pi\hbar}\right)^{1/4}\frac{1}{\sqrt{2^n n!}}\exp\left(-\frac{m\omega}{2\hbar^2}y^2\right)H_n\left(y\sqrt{\frac{m\omega}{\hbar}}\right) \tag{71}$$

and satisfies the normalization condition:

$$\int_{-\infty}^{\infty}\chi_n^2(y)\, dy = 1. \tag{72}$$

Matrix elements of the coordinate y are

$$y_{n,n-1} = \int_{-\infty}^{\infty}\chi_n\chi_{n-1}\, y\, dy = \sqrt{\frac{n\hbar}{2m\omega}}. \tag{73}$$

The intensity of an electric dipole radiation has the form [83]:

$$P_{if} = \frac{4q^2\omega_{if}^4}{3c^3}\left|y_{if}\right|^2, \tag{74}$$

where $\omega_{if} = (1/\hbar)(E_i - E_f)$ is the frequency of a transition $i \to f$ and y_{if} are the matrix elements of the charge coordinate y in the transition from the state i to the state f.

Using (73), we obtain, for $i = n$ and $f = n - 1$, the expression

$$P_{n,n-1} = \frac{2q^2\omega^3 n\hbar}{3mc^3}. \tag{75}$$

For the graviatom with the de Sitter interior in the limit (66), there are two possibilities. For $r_q/r_* \gg 1$, the correction to the Coulomb part potential in (32) satisfies $f_g(r_m) \ll 3r_{\text{int}}^2/\lambda\!\!\!^{2}$ by virtue of $r_g r_q \gg \lambda\!\!\!^{2}$. The graviatom can be described with the high accuracy by the Schwarzschild potential (33) which does not provide information about internal structure of the graviatom nucleus. The minimum of the potential (33) is located at $r_m = r_q$. The series in $\lambda\!\!\!^{-}/\sqrt{r_q r_g} \ll 1$ gives the oscillatory spectrum:

$$E = -\frac{mc^2 r_g}{4r_q} + \frac{\hbar c}{r_q}\left(p + \frac{1}{2}\right)\sqrt{\frac{r_g}{2r_q}}, \tag{76}$$

where $p = 0, 1, 2, \ldots$.

For a black hole as a nucleus, the condition for the minimum outside of horizon, $r_q > r_g$, leads to the constrain $M < 2 \times 10^{15}(m_e/m)$ g. The condition (66) gives the restriction $\lambda\!\!\!^{-} \ll r_q$ which results in $Z \gg 11$ for particles captured by a black hole. Only atomic nuclei can be captured with $Z \gg \sqrt{\hbar c/e^2}$ [13]. However, the captured nuclei with $Z \gg 11$ are quickly destroyed by the Hawking radiation from the black hole horizon. The condition for existence of such a graviatom, $kT_H < E_b$ where E_b is a binding energy, is not satisfied for $Z \gg 11$ [16, 17].

In the case of a G-lump or remnant as a graviatom nucleus, the condition (66) of capture of a particle on a level near the minimum $r_m = r_q$ leads to the constraint $r_g \gg \lambda\!\!\!^{-2}/r_q$ which excludes a nucleus with $M \leq M_{\rm cr}$. This is not a big disaster since a spectrum in this case does not carry information about an internal structure. From this point of view, the most interesting is the case (56) when r_m and thus frequency depend on the interior vacuum scale $\rho_{\rm int}$.

The second possibility is specified by

$$\frac{r_q}{r_*} \ll 1. \tag{77}$$

For the case of the density profile (49) the minimum of the effective potential (52) in the limit (66) is given by (56), and the oscillatory spectrum

$$E = \simeq -\frac{0.425mc^2 r_g}{\left(1.9r_{\rm int}^2 r_g\right)^{1/3}} + \frac{0.678\hbar c}{r_{\rm int}}\left(p + \frac{1}{2}\right), \quad p = 0, 1, 2, \ldots, \tag{78}$$

the intensity of the dipole radiation

$$P_{n,n-1} = \frac{0.416q^2 n\hbar}{mr_{\rm int}^3}, \tag{79}$$

and the frequency

$$\hbar\omega = \frac{0.678\hbar c}{r_{\rm int}} \tag{80}$$

depend on $r_{\rm int}$ and hence on $\rho_{\rm int}$.

The geometrical condition requires $\lambda\!\!\!^{-} < r_m$. It gives us the upper limit for the intensity

$$P_{10} < \xi\left(\frac{l_{pl}}{r_{\rm int}}\right)^2 \sqrt[3]{\frac{r_g}{r_{\rm int}}}\frac{c^5}{G}, \tag{81}$$

where $\xi = 0.111(e^2/\hbar c)$ and $c^5/G = 3.63 \cdot 10^{59}\,\mathrm{erg\,s^{-1}}$. In the case of G-lump with $r_g \sim r_{\rm int} \sim 10^{-25}$ cm we have $P_{10} < 4 \cdot 10^{40}\,\mathrm{erg\,s^{-1}}$, and for a remnant and near extremal black hole P_{10} is bigger. Formula (81) is valid for particles with the mass $m > \hbar/cr_{\rm int}$ which follows from the restriction $\hbar\omega < mc^2$ of applicability of nonrelativistic quantum mechanics.

The energy of radiated quanta exceeds the average energy $kT_H = \hbar c^3/8\pi GM$ of the quantum radiation from the Schwarzschild black hole and the average energy $kT_H = \hbar c/4\pi r_{\rm int}$ from the de Sitter horizon of the interior scale $\rho_{\rm vac}$.

The ratio of the intensity of radiated quanta in our case to the Hawking radiation of the Schwarzschild black hole is estimated as

$$\frac{P_{10}}{P_{H(\rm Sch)}} \leq 960 \times 4\pi \times \beta \times \left(\frac{r_g}{r_{\rm int}}\right)^{7/3} \simeq 9.68\left(\frac{r_g}{r_{\rm int}}\right)^{7/3}. \tag{82}$$

The ratio of our intensity to intensity of the Hawking radiation of the de Sitter horizon is

$$\frac{P_{10}}{P_{H(\text{de Sitter})}} \leq 960\pi\beta\left(\frac{r_g}{r_{\rm int}}\right)^{1/3} \simeq 38.7\left(\frac{r_g}{r_{\rm int}}\right)^{1/3}. \tag{83}$$

4.3. Availability of Information on Graviatom Interior. The most promising case is when the frequency of oscillatory transitions (80) depends on the scale of the interior de Sitter vacuum. It could be an observational signature of a graviatom with de Sitter interior as a dark matter candidate. In this case we can estimate frequency as

$$\hbar\omega = \frac{0.678\hbar c}{r_{\rm int}} = 0.678 \times 10^{11}\,\mathrm{GeV}\left(\frac{E_{\rm int}}{E_{\rm GUT}}\right)^2. \tag{84}$$

Photons with frequencies of order 10^{11} GeV were first observed in ultra-high-energy cosmic rays in 1962 [84]. Current experiments allow detection of photons up to $10^{11.5}$ GeV (see [85] and references therein). Present observational possibilities prefer thus graviatoms with the GUT scale interior although those with the Planck scale interior can exist in principle, and probabilities of their production in a collapse are bigger, but their typical frequency, $\hbar\omega \simeq 0.7 \times 10^{19}$ GeV, is far from the today observational range.

The most promising case can be realized when two conditions are satisfied: the condition (66) of dominance of the oscillatory levels and the condition (77) defining appropriate location of the minimum of the effective potential.

To tell something about a graviatom nucleus, we can take roughly $r_+ = r_g$ and apply the requirement that the minimum of potential must be located in the R-region outside the event horizon. The requirement $r_g < r_m$ leads for the density profile (49) to $x_g < 1.38$. This means that the most favorite situation can take place for G-lump.

Precise estimate gives $x_g = 1.7576$, $x_m = 2.284$, $x_\pm = 1.414$ for a double-horizon remnant with the density profile (49). The minimum of the potential is outside of the double horizon. The Hawking temperature is zero, so that it does not disturb the oscillatory radiation of the graviatom. The case of almost extremal black hole is also possible, until $r_m > r_+$, in such a case temperature is quickly going to zero, and oscillatory spectrum cannot be destroyed by the Hawking radiation.

Our predictions concerning captured particles are restricted here by the applied approach. The basic requirement of applicability of the Pauli approximation

$$\hbar\omega < mc^2 \longrightarrow m > \frac{\hbar}{cr_{\rm int}} \tag{85}$$

gives immediately in (84) the constraint on the mass of a captured particle $m > 5 \times 10^{10}$ GeV for the GUT scale of the interior de Sitter vacuum, so we can trust the above conclusions made in the frame of nonrelativistic quantum mechanics but cannot exclude that a more precise approach would open additional possibilities.

To evaluate which particle can be a captured, we apply the constraint $x_g \leq 1.7576$. The condition of the proper location of the minimum (77) requires $r_q \ll (1.7576)^{1/3} r_{\rm int}$. This gives $r_q \ll \simeq 1.21 \times 10^{-25}$ cm for the GUT scale of the interior de Sitter vacuum. What a particle it can be? From $r_q = e^2/Nm_e c^2 = r_e/N \ll 1.21 \times 10^{-25}$ cm, we get $N \gg 2 \times 10^{12}$ which means $m = Nm_e \gg 10^9$ GeV.

This range admits GUT particles with masses 10^{14} GeV $< E_{\rm GUT} < 10^{16}$ GeV which could be captured by RPBH at the end of inflation. However, here the problem arises. Formation constraint restricts masses of RPBH with GUT scale interior by $M > 10^{11}$ g. For such a black hole, even with very quickly falling density profile (49), proper for the frequency (84), minimum (56) is located deeply inside T-region, so a particle would not be captured on an orbit but would be swallowed by a black hole. G-lumps and remnants which do not encounter this problem can be formed at the first inflationary stage only with Planck scale interior. They can capture GUT particles, but their radiation would be then in the range unavailable for near future observations.

Question arises where regular black hole remnants with GUT scale interior produced in evaporation, as well as remnants and G-lumps produced at the second inflationary stage, can capture particles with masses of the order of the GUT mass.

Speaking about RPBH produced during first inflation, one can imagine a situation when it would capture a GUT particle on some higher oscillatory level. Simple estimate $r - r_m > r_g$ with the spectrum (78) shows that it is possible, but lifetime of such a level should have to be comparable to the evaporation time $\tau \simeq (M/m_{pl})^3 \tau_{pl}$ [35]. In our case it gives $\tau > 6.75 \times 10^3$ s.

Such a case could be realized if some metastable level(s) with appropriate quantum number(s) p would exist in the oscillatory spectrum, which cannot be excluded *a priori*.

Good news is that the level with energy $E_p > 0.678 \times 10^{11}$ GeV would not be destroyed by the Hawking radiation. Spherically symmetric regular black hole with de Sitter interior evolves during evaporation to the double-horizon remnant with zero temperature, while its maximal temperature is given by $kT_{\rm max} = 0.2 \times 10^{11}$ GeV [19, 37, 41].

Another channel is related to leptoquarks which can survive in galactic halos [86]. The leptoquarks arising at the GUT epoch are decayed into quarks and leptons. The quarks form nucleons in three minutes after the Big Bang. However, a part of leptoquarks survives and is accumulated in the galactic halos contributing to a dark matter [86]. The leptoquarks in the galactic halos can be captured by any of the considered here objects with de Sitter interior: by near extreme primordial black holes, by remnants, and by G-lumps.

5. Summary

General constraint on formation of a compact object with the de Sitter interior results in the following options: at the first inflationary stage at the GUT scale, regular black holes with masses $M > 10^{11}$ g can be formed with the GUT scale interior and any objects with the Planck scale interior including G-lumps. There are no constraints on formation of RPBH and G-lumps during the second inflationary stage at the QCD scale.

Spectra and radiation of graviatoms are studied in the Pauli approximation to the Dirac equation. The gravitational coupling $\alpha_G \sim 0.5$ is much bigger than the fine structure constant $\alpha = e^2/\hbar c = 1/137$. The energy levels in a graviatom are determined by α_G, and relativistic correction which would allow for a particle spin is of the order of $\alpha/\alpha_G \ll 1$. The condition of the particle localization dimension exceeding the Compton wavelength is valid all over the paper. This means that the problem is solvable in the framework of nonrelativistic quantum mechanics, although it gives the restriction on the mass of a captured particle, $m > \hbar\omega/c^2$.

The electromagnetic radiation of charged particles in the field of a regular black hole exceeds the Hawking radiation from Schwarzschild black hole of the same mass. The essential difference is that a graviatom emits spectral lines which can bear information on its de Sitter interior.

Hydrogen-like spectrum and radiation of graviatom with RPBH as a nucleus is described with the high accuracy by those for the Schwarzschild black hole. Requirements of stability of graviatom with respect to tidal forces and Hawking radiation constraint the gravitational coupling within the narrow range $0.512 < \alpha_G < 0.625$. Dominating is the dipole radiation which does not carry information about de Sitter interior of graviatom. In the case of G-lump and RPBH remnant, approximation of the potential by the corrected Schwarzschild potential suggests that hydrogen-like radiation will depend on the density of the interior de Sitter vacuum $\rho_{\rm int}$ and result in observational signatures for G-lump and remnant as dark matter candidates. This case needs further detailed investigation.

The oscillatory radiation can depend essentially on the interior vacuum scale and gets in the range of ultrahigh cosmic ray energies.

Typical features of graviatoms radiation can result in observational signatures for G-lumps and RPBH remnants as dark matter candidates, as well as provide information about their interior de Sitter vacuum.

Let us note that regular primordial black holes, their remnants, and G-lumps can also serve as a very sensitive universal probe for a scale of inhomogeneities in the very early Universe being in this context the most elusive among dark matter candidates [87].

Appendix

Characteristic Length Scales of Graviatoms

Graviatoms have rich internal structure, characterized by several essential length scales which we summarize below.

Characteristic size of a graviatom L satisfies the geometrical condition $L > r_n + r_p$ where r_n is the size of the nucleus and r_p is the size of a captured particle.

The characteristic length of any de Sitter-Schwarzschild spacetime $r_* = (r_{\rm int}^2 r_g)^{1/3}$ comes as the radius of the direct matching of the de Sitter and Schwarzschild metrics, $1 - r_*^2/r_{\rm int}^2 = 1 - r_g/r_*$. It depends on both gravitational radius $r_g = 2GMc^{-2}$ and characteristic scale of the interior de Sitter vacuum $r_{\rm int}$ related to its density by $r_{\rm int}^2 = 3c^2/8\pi G\rho_{\rm int}$. For the GUT scale $\simeq 10^{15}$ GeV interior, $r_{\rm int} \simeq 2.4 \times 10^{-25}$ cm. For the Planck scale, $r_{\rm int} = r_{pl}$. Characteristic scale r_* gives rough estimate for the size of a G-lump. More precise estimate involves critical gravitational radius $r_{g(\rm cr)}$, related to critical mass $M_{\rm cr}$, actually mass of the remnant which gives the boundary between black holes ($M > M_{\rm cr}$) and G-lumps ($M < M_{\rm cr}$). It is given by $M_{\rm cr} = \beta m_{pl}\sqrt{\rho_{pl}/\rho_{\rm int}}$ where the numerical coefficient β depends on the model. For the density profile (49), $M_{\rm cr} \simeq 0.3 m_{pl}\sqrt{\rho_{pl}/\rho_{\rm int}}$ and $r_{g(\rm cr)} = 1.7576 r_{\rm int}$. In this case, $r_* > 0.69 r_g$ for a G-lump, and $r_* < 0.69 r_g$ for a black hole.

The black hole horizon $r_+ = 2G\mathcal{M}(r_+)$ satisfies always $r_+ < r_g$. Double horizon $r_\pm = 2G\mathcal{M}(r_\pm)$ gives roughly a size of RBH remnant. Masses of remnants ($r_g = r_{g(\rm cr)}$) range from m_{pl} for the Planck scale interior, through $\sim 10^3$ g for the GUT scale interior, up to $\sim 10^{32}$ g ($r_g \sim 10^4$ cm) for the QCD scale interior. Regular remnants are stable, and their population includes all remnants of RPBH evaporated till now.

The gravitational analogue of the Bohr radius is given by $r_b = \hbar^2/GMm^2 = 2\lambda\!\!\!^{-2}/r_g$, where $\lambda\!\!\!^{-} = \hbar/mc$ is the Compton wavelength of a captured particle. The hydrogen-like radiation dominates in the case when $r_g r_q \ll \lambda\!\!\!^{-2}$, where $r_q = q^2/mc^2$ is electromagnetic radius of a captured particle.

In the case $r_g r_q \gg \lambda\!\!\!^{-2}$, the oscillatory radiation is dominating. Minimum of the graviatom potential r_m, responsible for its existence, is always outside the double horizon. For the case $r_q \gg r_*$, oscillatory levels are determined by r_q, with quantum corrections depending on r_g; in this case, $r_m = r_q + 2\lambda\!\!\!^{-2} l(l+1)/r_g$. In the most promising for the observational manifestations case, when $r_q \ll r_*$, location of the minimum r_m depends directly on $r_{\rm int}$ and thus on the interior vacuum density, $r_m = \sqrt[3]{1.9 r_{\rm int}^2 r_g}$ for the density profile (49). For a remnant with the density profile (49), $r_g = 1.7576 r_{\rm int}$, $r_m = 2.284 r_{\rm int}$, $r_\pm = 1.414 r_{\rm int}$, and $r_* = 1.207 r_{\rm int}$.

Acknowledgments

This work was supported by the Polish Ministry of Science and Education for the research project "Globally Regular Configurations in General Relativity Including Classical and Quantum Cosmological Models, Black Holes and Particle-Like Structures (solitons)" in the frame of the "Polish-Russian Agreement for collaboration in the Field of Science and Technology" and by the Polish National Science Center through the Grant 5828/B/H03/2011/40.

References

[1] S. Blinnikov and M. Y. Khlopov, "On possible effects of mirror particles," *Soviet Journal of Nuclear Physics*, vol. 36, p. 472, 1982.

[2] S. Blinnikov and M. Y. Khlopov, "Possible astronomical effects of mirror particles," *Soviet Astronomy*, vol. 27, pp. 371–375, 1983.

[3] M. Y. Khlopov, G. Beskin, N. Bochkarev, L. Pustylnik, and S. Pustylnik, "Observational physics of mirror Word," *Soviet Astronomy*, vol. 35, p. 21, 1991.

[4] S. Hawking, "Gravitationally collapsed objects of very low mass," *Monthly Notices of the Royal Astronomical Society*, vol. 152, p. 75, 1971.

[5] C. W. Misner, "Relativistic fluids in cosmology," in *Batelle Recontres in Mathematics and Physics*, M. de Witt and J. Wheeler, Eds., p. 117, 1967.

[6] V. V. Flambaum and J. C. Berengut, "Atom made from charged elementary black hole," *Physical Review D*, vol. 63, no. 8, Article ID 084010, 2001.

[7] E. G. Floratos, G. K. Leontaris, and N. D. Vlachos, "Gravitational atom in compactified extra dimensions," *Physics Letters B*, vol. 694, no. 4-5, pp. 410–416, 2011.

[8] A. B. Gaina and F. G. Kochorbé, "S matrix and resonance states in the Kerr-Newman geometry," *Journal of Experimental and Theoretical Physics*, vol. 65, pp. 211–215, 1987.

[9] I. M. Ternov and A. B. Gaina, "Energy spectrum of the Dirac equation for the Scharzschild and Kerr fields," *Soviet Physics Journal*, vol. 31, no. 2, pp. 157–163, 1988.

[10] A. B. Gaina and O. B. Zaslavskii, "On quasilevels in the gravitational field of a black hole," *Classical and Quantum Gravity*, vol. 9, no. 3, pp. 667–676, 1992.

[11] A. Lasenby, C. Doran, J. Pritchard, A. Caceres, and S. Dolan, "Bound states and decay times of fermions in a Schwarzschild black hole background," *Physical Review D*, vol. 72, no. 10, Article ID 105014, 2005.

[12] M. S. Pindzola, "Inelastic scattering of electrons by black hole atoms," *Journal of Physics B*, vol. 42, Article ID 095202, 2009.

[13] M. L. Fil'chenkov, "Quantum radiation of a charged particle in a Schwarzschild field," *Astronomische Nachrichten*, vol. 311, pp. 223–226, 1990.

[14] C. M. DeWitt and B. S. DeWitt, "Falling charges," *Physica*, vol. 1, p. 3, 1964.

[15] M. L. Fil'chenkov, "Behavior of a charged particle in a Schwarzschild field," *Izvestiya Vysshikh Uchebnykh Zavedenii Fizika*, no. 7, pp. 75–82, 1998.

[16] Y. P. Laptev and M. L. Filchenkov, "Electromagnetic and gravitational radiation of graviatoms," *Astronomical and Astrophysical Transactions*, vol. 25, pp. 33–42, 2006.

[17] M. L. Filchenkov and Y. P. Laptev, "Graviatom dipole radiation," *Gravitation and Cosmology*, vol. 12, pp. 65–68, 2006.

[18] I. G. Dymnikova, "Vacuum nonsingular black hole," *General Relativity and Gravitation*, vol. 24, pp. 232–242, 1992.

[19] I. G. Dymnikova, "De Sitter-Schwarzschild black hole: its particlelike core and thermodynamical properties," *International Journal of Modern Physics D*, vol. 5, no. 5, pp. 529–540, 1996.

[20] I. Dymnikova and M. Korpusik, "Regular black hole remnants in de Sitter space," *Physics Letters B*, vol. 685, no. 1, pp. 12–18, 2010.

[21] I. Dymnikova, "The cosmological term as a source of mass," *Classical and Quantum Gravity*, vol. 19, no. 4, pp. 725–739, 2002.

[22] J. H. MacGibbon, "Can Planck-mass relics of evaporating black holes close the Universe?" *Nature*, vol. 329, pp. 308–309, 1987.

[23] K. Rajagopal, M. S. Turner, and F. Wilczek, "Cosmological implications of axinos," *Nuclear Physics B*, vol. 358, no. 2, pp. 447–470, 1991.

[24] B. J. Carr, J. H. Gilbert, and J. E. Lidsey, "Black hole relics and inflation: limits on blue perturbation spectra," *Physical Review D*, vol. 50, no. 8, pp. 4853–4867, 1994.

[25] R. J. Adler, P. Chen, and D. I. Santiago, "The generalized uncertainty principle and black hole remnants," *General Relativity and Gravitation*, vol. 33, no. 12, pp. 2101–2108, 2001.

[26] P. Chen and R. J. Adler, "Black hole remnants and dark matter," *Nuclear Physics B*, vol. 124, pp. 103–106, 2003.

[27] E. Bugaev and P. Klimai, "Constraints on amplitudes of curvature perturbations from primordial black holes," *Physical Review D*, vol. 79, no. 10, Article ID 103511, 2009.

[28] M. Kesden and S. Hanasoge, "Transient solar oscillations driven by primordial black holes," *Physical Review Letters*, vol. 107, no. 11, Article ID 111101, 2011.

[29] F. S. N. Lobo, G. J. Olmo, and D. Rubiera-Farcia, "Semiclassical geons as solitonic black hole remnants," *Journal of Cosmology and Astroparticle Physics*, vol. 2013, 2013.

[30] B. J. Carr, "Primordial black holes—recent developments," ECONFCO41213, 0204, 2004, http://arxiv.org/abs/astro-ph/0504034.

[31] B. J. Carr, "Primordial black holes as a probe of cosmology and high energy physics," *Lecture Notes in Physics*, vol. 631, pp. 301–321, 2003.

[32] M. Y. Khlopov and S. G. Rubin, *Cosmological Pattern of Microphysics in Inflationary Universe*, Kluwer Academic, Dordrecht, The Netherlands, 2004.

[33] A. M. Green and A. R. Liddle, "Constraints on the density perturbation spectrum from primordial black holes," *Physical Review D*, vol. 56, no. 10, pp. 6166–6174, 1997.

[34] M. Drees and E. Erfani, "Primordial black holes in single-field inflation models," *Journal of Cosmology and Astroparticle Physics*, vol. 1201, article 035, 2012.

[35] B. J. Carr, K. Kohri, Y. Sendouda, and J. Yokoyama, "New cosmological constraints on primordial black holes," *Physical Review D*, vol. 81, no. 10, Article ID 104019, 2010.

[36] L. Susskind, "The world as a hologram," *Journal of Mathematical Physics*, vol. 36, no. 11, pp. 6377–6399, 1995.

[37] I. Dymnikova, "Regular black hole remnants," in *Proceedings of the Invisible Universe International Conference*, Paris, France, June-July 2009, AIP: New York, NY, USA, 50, 2010.

[38] E. B. Gliner, "Algebraic properties of the energy-momentum tensor and vacuum-like states of matter," *Journal of Experimental and Theoretical Physics*, vol. 22, p. 378, 1966.

[39] E. Poisson and W. Israel, "Structure of the black hole nucleus," *Classical and Quantum Gravity*, vol. 5, no. 12, pp. L201–L205, 1988.

[40] V. P. Frolov, M. A. Markov, and V. F. Mukhanov, "Black holes as possible sources of closed and semiclosed worlds," *Physical Review D*, vol. 41, no. 2, pp. 383–394, 1990.

[41] I. Dymnikova, "Internal structure of nonsingular spherical black holes," in *Internal Sructure of Black Holes and Spacetime Singularities*, M. Burko and A. Ori, Eds., p. 422, Bristol In-t of Physics and the Israel Physical Society, 1997.

[42] A. Perez, "Spin foam models for quantum gravity," *Classical and Quantum Gravity*, vol. 20, no. 6, pp. R43–R104, 2003.

[43] C. Rovelli, *Quantum Gravity*, Cambridge University Press, Cambridge, UK, 2004.

[44] A. Bonanno and M. Reuter, "Renormalization group improved black hole spacetimes," *Physical Review D*, vol. 62, Article ID 043008, 21 pages, 2000.

[45] P. Nicolini, "Noncommutative black holes, the final appeal to quantum gravity: a review," *International Journal of Modern Physics A*, vol. 24, no. 7, pp. 1229–1308, 2009.

[46] P. Nicolini, A. Smailagic, and E. Spallucci, "Noncommutative geometry inspired Schwarzschild black hole," *Physics Letters B*, vol. 632, no. 4, pp. 547–551, 2006.

[47] R. B. Mann and P. Nicolini, "Cosmological production of noncommutative black holes," *Physical Review D*, vol. 84, Article ID 064014, 13 pages, 2011.

[48] I. G. Dymnikova, "The algebraic structure of a cosmological term in spherically symmetric solutions," *Physics Letters B*, vol. 472, no. 1-2, pp. 33–38, 2000.

[49] I. Dymnikova, "Spherically symmetric space-time with regular de Sitter center," *International Journal of Modern Physics D*, vol. 12, no. 6, pp. 1015–1034, 2003.

[50] I. Dymnikova and E. Galaktionov, "Vacuum dark fluid," *Physics Letters B*, vol. 645, no. 4, pp. 358–364, 2007.

[51] I. Dymnikova and E. Galaktionov, "Dark ingredients in one drop," *Central European Journal of Physics*, vol. 9, no. 3, pp. 644–653, 2011.

[52] I. Dymnikova and B. Sołtysek, "Spherically symmetric space-time with two cosmological constants," *General Relativity and Gravitation*, vol. 30, pp. 1775–1793, 1998.

[53] I. Dymnikova and B. Sołtysek, "Nonsingular cosmological black hole," in *Particles, Fields and Gravitation*, J. Rembielinsky, Ed., p. 460, AIP, New York, NY, USA, 1998.

[54] I. Dymnikova, "Cosmological term, mass, and space-time symmetry," in *Beyond the Desert: Proceedings of the 4th Tegernsee International Conference on Particle Physics Beyond the Standard Model, Germany, June 2003*, H. V. Klapdor-Kleinhaus, Ed., p. 485, Springer, Berlin, Germany, 2004.

[55] I. Dymnikova, "Spacetime symmetry and mass of a lepton," *Journal of Physics A*, vol. 41, Article ID 304033, 2008.

[56] A. Bonanno and M. Reuter, "Spacetime structure of an evaporating black hole in quantum gravity," *Physical Review D*, vol. 73, no. 8, Article ID 083005, 2006.

[57] Y. S. Myung, Y.-W. Kim, and Y.-J. Park, "Quantum cooling evaporation process in regular black holes," *Physics Letters B*, vol. 656, no. 4-5, pp. 221–225, 2007.

[58] M. Y. Khlopov, "Primordial black holes," *Research in Astronomy and Astrophysics*, vol. 10, no. 6, p. 495, 2010.

[59] Y. B. Zeldovich and I. D. Novikov, *Soviet Astronomy*, vol. 10, p. 602, 1967.

[60] V. A. Kuzmin and I. I. Tkachev, "Ultrahigh-energy cosmic rays, superheavy long-lived particles, and matter creation after inflation," *JETP Letters*, vol. 68, pp. 271–275, 1998.

[61] V. A. Kuzmin and I. I. Tkachev, "Ultra-high-energy cosmic rays and inflation relics," *Physics Reports*, vol. 320, pp. 199–221, 1999.

[62] V. A. Kuzmin and I. I. Tkachev, "Matter creation via vacuum fluctuations in the early Universe and observed ultrahigh energy cosmic ray events," *Physical Review D*, vol. 59, Article ID 123006, 8 pages, 1999.

[63] L. Hui and E. D. Stewart, "Superheavy dark matter from thermal inflation," *Physical Review D*, vol. 60, Article ID 023518, 6 pages, 1999.

[64] A. E. Faraggi, K. A. Olive, and M. Prospelov, "Probing the desert with ultra-energetic neutrinos from the sun and the earth," *Astroparticle Physics*, vol. 13, pp. 31–43, 2000.

[65] A. A. Grib and V. Y. Dorofeev, "Creation of particles and entropy in the early friedmann universe," *International Journal of Modern Physics D*, vol. 3, p. 731, 1994.

[66] I. F. M. Albuquerque, L. Hui, and E. W. Kolb, "High energy neutrinos from superheavy dark matter annihilation," *Physical Review D*, vol. 64, Article ID 083504, 10 pages, 2001.

[67] I. Dymnikova and M. Krawczyk, "First post-inflationary particles equation of state," in *Birth of the Universe*, F. Occhionero, Ed., Springer, New York, NY, USA, 1994.

[68] I. Dymnikova and M. Krawczyk, "Equation of state and temperature of massive nonrelativistic bosons arising in the universe at the first stage of reheating ," *Modern Physics Letters A*, vol. 10, p. 3069, 1995.

[69] S. Capozziello, R. de Ritis, I. Dymnikova, C. Rubano, and P. Scudellaro, "Inflationary cosmology without slow rolling," *Physics Letters A*, vol. 203, no. 1, pp. 18–22, 1995.

[70] S. Capozziello, R. de Ritis, I. Dymnikova, C. Rubano, and P. Scudellaro, "Temperature at the first stage ofreheating in in flationary cosmology without slow rolling," *Nuovo Cimento B*, vol. 111, pp. 623–630, 1996.

[71] I. Dymnikova and M. Khlopov, "Decay of cosmological constant as bose condensate evaporation," *Modern Physics Letters A*, vol. 15, no. 38-39, pp. 2305–2314, 2000.

[72] B. K. Harrison, K. S. Thorne, M. Wakano, and J. A. Wheeler, *Gravitational Theory and Gravitational Collapse*, University of Chicago Press, 1965.

[73] A. V. Vilenkin, "Quantum creation of universes," *Physical Review D*, vol. 30, no. 2, pp. 509–511, 1984.

[74] M. L. Fil'chenkov, "The pre-de Sitter universe in terms of quantum mechanics," *Physics Letters B*, vol. 354, no. 3-4, pp. 208–212, 1995.

[75] M. L. Fil'chenkov, "Quantum collapse and the birth of a new universe," *Physics Letters B*, vol. 441, pp. 34–39, 1998.

[76] E. Kamke, *Differentialgleichungen. Lösungmethoden und Lösungen. I. Gewöhnliche Differentialgleichungen*, Chelsea Publishing Company, Leipzig, Germany, 1959.

[77] D. Boyanovsky, H. J. de Vega, and D. J. Schwarz, "Phase transitions in the early and present universe," *Annual Review of Nuclear and Particle Science*, vol. 56, pp. 441–500, 2006.

[78] T. Boeckel and J. Schaffner-Bielich, "A little inflation in the early universe at the QCD phase transition," *Physical Review Letters*, vol. 105, Article ID 041301, 2010.

[79] D. H. Lyth and E. D. Stewart, "Cosmology with a TeV mass Higgs field breaking the grand-unified-theory gauge symmetry," *Physical Review Letters*, vol. 75, no. 2, pp. 201–204, 1995.

[80] N. Borghini, W. N. Cottingham, and R. V. Mau, "Possible cosmological implications of the quark-hadron phase transition," *Journal of Physics G*, vol. 26, p. 771, 2000.

[81] K. Kuchař, "Gravitation, geometry, and nonrelativistic quantum theory," *Physical Review D*, vol. 22, no. 6, pp. 1285–1299, 1980.

[82] L. D. Landau and E. M. Lifshitz, *Quantum Mechanics*, Fizmatgiz, Moscow, Russia, 1963.

[83] H. A. Bethe and E. E. Salpeter, *Quantum Mechanics of One- and Two-Electron Atoms*, Springer, Berlin, Germany, 1957.

[84] J. Linsley, "Evidence for a primary cosmic-ray particle with energy 1020 eV," *Physical Review Letters*, vol. 10, no. 4, pp. 146–148, 1963.

[85] O. E. Kalashev, G. I. Rubtsov, and S. V. Troitsky, "Sensitivity of cosmic-ray experiments to ultrahigh-energy photons: reconstruction of the spectrum and limits on the superheavy dark matter," *Physical Review D*, vol. 80, no. 10, Article ID 103006, 2009.

[86] A. A. Grib and Y. V. Pavlov, "Do active galactic nuclei convert dark matter into visible particles?" *Modern Physics Letters A*, vol. 23, no. 16, pp. 1151–1159, 2008.

[87] I. Dymnikova and M. Khlopov, "Regular black hole remnants with de Sitter interior as a universal probe of inhomogeneity of early Universe," In press.